

**Modelling spatial patterns of erosion
in the West Usambara Mountains of Tanzania**

Promotor: Prof. Dr. Ir. L. Stroosnijder
Hoogleraar Erosie en Bodem & Waterconservering

Co-promotor: Dr. Ir. G. Sterk
Universitair docent bij de leerstoelgroep Erosie en Bodem &
Waterconservering

Promotiecommissie:
Prof. Dr. Ir. J. Bouma Wageningen Universiteit
Dr. Ir. J.C. van Dam Wageningen Universiteit
Dr. V.G. Jetten Universiteit Utrecht
Prof. Dr. K.J. Beven Lancaster University, U.K.

Dit onderzoek is uitgevoerd binnen the C.T. de Wit onderzoekschool PE & RC

Modelling spatial patterns of erosion in the West Usambara Mountains of Tanzania

Olga Vigiak

Proefschrift

ter verkrijging van de graad van doctor
op gezag van de rector magnificus
van Wageningen Universiteit
Prof. Dr. Ir. L. Speelman
in het openbaar te verdedigen
op 26 april 2005
des namiddags te half twee in de aula

Wageningen University, ISBN 90-8504-169-4

Also published as Tropical Resource Management Papers, No. 64 (2005), ISBN 90-6754-908-8

Vigiak, O., 2005

Modelling spatial patterns of erosion in the West Usambara Mountains of Tanzania

Doctoral Thesis Wageningen University – with ref. – with summary in Dutch

Key words: erosion modelling; spatial patterns; overland flow distribution; dynamic Hortonian hydrologic regime; farmers' knowledge; catchment scale

EROAHI Report 3

The work reported in this book has been carried out as part of the project ‘Development of an improved method for soil and water conservation planning at catchment scale in the East African Highlands’ (EROAHI). This project was funded through the Dutch/Swiss ‘Fund for Methodological Support to Ecoregional Programmes’, and the Dutch ‘Partners for Water Programme’.

EROAHI was carried out by the following institutions:

Agricultural Research Institute-Mlingano
P.O. Box 5088
Tanga
Tanzania

Kenya Agricultural Research Institute-Embu
P.O. Box 27
Embu
Kenya

Lushoto District Agriculture and Food Security Office
P.O. Box 22
Lushoto
Tanzania

Kenyan Ministry of Agriculture
Soil Water Conservation Branch
P.O. Box 30028
Nairobi
Kenya

Wageningen University
Department of Environmental Sciences
Erosion and Soil Water Conservation Group
Nieuwe Kanaal 11
6709 PA Wageningen
The Netherlands

Alterra Green World Research
Soil and Land Use Department
P.O. Box 47
6700 AC Wageningen
The Netherlands

Al clan, le mie radici
(To my 'clan', my roots, wherever)

Acknowledgements

The day I had received the official approval of my PhD proposal, I wrote a letter to my friends telling how excited I was of the opportunity and how much I was looking forward to put myself at work. As an afterthought, I added a postscript where I pleaded them to keep the letter so they could send it back to me when the tough moments would arrive and I would wonder why I had accepted the task. They never had to. The difficult moments, though present at times, never wiped away the excitement of the work. I must thank many people for making my PhD such an enjoyable experience.

First, I would like to acknowledge the constant scientific, logistic and human support I got from the Erosion and Soil & Water Conservation Group of Wageningen University. In particular, Prof. Leo Stroosnijder, beside providing scientific supervision, made sure that I got all the help I needed for living in The Netherlands as an Italian with a Tanzanian partner. I only regret I never got to learn Dutch as much as he would have liked. Dr Geert Sterk has been my supervisor since the time of the MSc studies. I owe him my scientific growth, several beers in good company, and many hours of discussing and arguing, which I hope he enjoyed as much as I did. Geert, I will miss working with you very much. Dr. Jan de Graaff and his wife made me dream of far, far away countries with a mixture of nostalgia and enthusiasm. Ir. Dirk Meindertsma, Jolanda Hendriks, Bram Kuyper, Magda de Bie-Meurs, and the personnel at De Haaff library solved many of my troubles on bureaucracy, computer issues and bibliographic work, all with a smile. The PhD fellows of the third floor at De Nieuwlanden gave me a lot of ideas, energy, and good mood in grim times: thanks a lot to all of you.

I wish to thank the Agricultural Research Institute of Tanzania ARI-Mlingano and African Highland Initiative personnel in Mlingano and Lushoto, in particular Dr George Ley and Dr Jeremias G. Mowo, for the logistic support during the fieldwork. The extension officers Matosho and Selungato, and the field assistant Antoni helped throughout the data collection campaign. The farmers of Kwalei welcomed my incursions in their fields with kind curiosity. In Lushoto, Boka, Jamali, and Toni spent with me many hours listening reggae and discussing Rastafarianism.

This study built a lot upon the findings of my two PhD fellow colleagues, Dr (I can say that now!) Barrack O. Okoba and Dr. Albino J. Tenge. Working with you has been my honour and my good luck: asante sana, I wish you a successful academic carrier and happiness in your personal life. MSc Sokhon Phem at the International Institute for Geo-information Science and Earth Observations (ITC, Enschede, the Netherlands) offered his expertise to create the Digital Terrain Model of Kwalei catchment. The collaboration of Alterra has been essential to the research: particularly, my thanks go to Dr Rudi Hessel, who shared data and ideas on many modelling issues; to Dr Simone van Dijck, who coordinated much of the project and participated in untangling some difficult datasets; and to Ir. (H.) Rik van den Bosch, who, together with Dr Sterk, formulated the research proposal and tirelessly managed the project.

The hydrologic modelling had been the most difficult part of the study. I am indebted with the Environmental Sciences Department of Lancaster University, U.K., and in particular with Prof. Keith J. Beven, who inspired much of the modelling approach and contributed a lot in translating my few, scattered ideas of the Kwalei catchment hydrology into a conceptual model of scientific interest. A special word of thanks goes to Dr Renata J. Romanowicz (Lancaster University) and Dr E. Emiel van Loon (Institute of Biodiversity and Ecosystem Dynamics, University of Amsterdam), who have been an irreplaceable source of knowledge and practical help. Their dedication and

enthusiasm in taking on ever-arising problems and giving them the best of their time, scientific understanding and skills set the example of academic attitude I wish to follow in the future. More personally, I am grateful of the kindness and friendship they always reserved me.

“Partire vuol dire morire” (To leave is a bit like to die) - my grandfather used to sing me - and indeed every time I say goodbye it’s a small, big pain I cannot grow accustomed to. The conclusion of my PhD experience puts an end to the almost seven years I spent in The Netherlands. I take this opportunity to thank all the friends who helped me to discover and appreciate the ‘Dutch-abilities’ of living ‘under the low sky’: Sander (the fisherman) at Hoevestein, Maria, Henk-Jan, Noortje, Erik and Suzanne at Haarweg 43, Yvette, Instructor Morão and the group of Capoeira Brasil, Margi (Lulú) in Amsterdam. During my staying in Wageningen, I have been honoured to meet exceptional people, with whom I share a lasting friendship: Sarah, Jennifer and Martin, Raul (el matador) and his family, Cesare and Marta, Claudia and Riccardo, Federico and Laura, Raul (Mandingo) and Jolanda, Attilio and Antonella, Lorenzo, Jeroen, Edoardo, Michiel, Antonella (Antons), Claudio and Francesca, Lorenzo and small Teresa. Maria José Villalon shared much of the PhD daily joys and frustrations. The friendship of Hassan, Urszula (Ula) – and recently little Hannah – Taweel has been like a beacon that guided me throughout my studies. Andy left his home to be with me in the times to come, and teaches me every day of love and respect for life. My family, the ‘clan’, and especially my brother Andrea, endured my long – and not yet about to finish - absence from home with begrudgingly acceptance, and constant support. My parents, Lorenzina and Dusan, bore most of the emotional load of these years and much of the financial ‘recessions’ of their hare-brained daughter.

All this, I can never repay, I can only be grateful for. So now I shall better be quite and ‘*stare in the sun, let the rays shine in my eyes*’ [Bob Marley; Talkin’ blues].

Wageningen, April 2005

Table of contents

Chapter 1	Introduction	1
Chapter 2	Modelling catchment-scale erosion patterns in the East African Highlands	13
Chapter 3	Matching hydrologic response to measured effective hydraulic conductivity	37
Chapter 4	A disaggregating approach to describe overland flow occurrence within a catchment	63
Chapter 5	A semi-empirical model to assess uncertainty of spatial patterns of erosion	91
Chapter 6	Water erosion assessment using farmers' indicators in the West Usambara Mountains, Tanzania	119
Chapter 7	Modelling spatial scale of water erosion in the West Usambara Mountains	137
Chapter 8	Summary and conclusions	165
	Samenvatting en conclusies	171
	<i>Curriculum vitae</i>	176
	<i>PE&RC PhD education statement form</i>	177

Chapter 1

INTRODUCTION

INTRODUCTION

In developing countries, where rural population is often more than 80 %, assessment of erosion focuses mainly towards on-site effects of erosion. This on-site erosion strongly affects crop yields, undermines the long term sustainability of farming systems, and represents a major threat to the livelihood of farmers and rural communities. In the industrialized countries, more attention is being paid to assess off-site effects of erosion, which are of interest for the society at large, e.g. in flood prevention, water reservoir preservation and water pollution control (Garen *et al.*, 1999). Whether the main concern of Soil and Water Conservation (SWC) planning is toward prevention of on-site or off-site effects of erosion, there is a growing need for tools that enable to define the spatial distribution of erosion within a catchment or a water basin, i.e. to locate sources of soil sediment where to invest most SWC efforts (Ritchie *et al.*, 2003). Indeed, the location of sediment sources and sinks can be more important than the quantification of soil losses, as it is more cost effective to over-dimension erosion control measures than to locate them in the wrong place (Jetten and de Roo, 2001; Jetten *et al.*, 2003). In this context, the appropriate scale for erosion assessment is the catchment, i. e. the natural geomorphologic unit where sources of soil losses and surface runoff are topographically linked to areas of sedimentation, and where therefore both on-site and off-site effects of erosion can be appreciated (Morgan, 1995).

Models are vital tools for soil erosion assessment and watershed conservation planning (Garen *et al.*, 1999; Ritchie *et al.*, 2003). They may be used for erosion risk assessment, but also for evaluating the possible effects of changes in land use or adoption of SWC measures. Extension services and environmental agencies increasingly make use of models for assessing the intensity of erosion before SWC activities are implemented and to estimate the possible outcomes of the SWC plan.

Depending on the approach adopted to represent erosion processes, erosion models can be broadly classified as empirical, physics-based or conceptual (Wheater *et al.*, 1993; Merritt *et al.*, 2003). This classification refers to the main structure of the model and is largely subjective, as in all models a certain degree of empiricism can not be avoided (Merritt *et al.*, 2003). Empirical models consists of regression equations that relate the rate of erosion to its determining factors, like climate, topography, vegetation and soil characteristics. Empirical models, of which the Universal Soil Loss Equation (USLE; Wischmeier and Smith, 1978) is the most famous example, have long been used for SWC planning purposes. They are simple to use and require limited data. However, the empirical relationships they embed are built from site-specific observations. As the mechanisms of erosion processes are not dealt with explicitly, and the relationships between soil losses and erosion factors are derived from the aggregated response of the natural system, empirical models may not perform well when applied under different conditions.

Physics-based models, instead, represent flow and sediment processes and their interactions on the basis of physics laws of mass and momentum conservation. Physics-based models include the state-of-the-art knowledge of the system and provide good tools to understand the interactions occurring between erosion processes. However, they also suffer from some main drawbacks. Physics-based models are composed of a large number of sub-processes, the solution of whose describing equations

requires huge amounts of input data and computational power. These describing equations often refer to physics laws that were originally formulated at a scale different from the model scale. Moreover, erosion models are highly nonlinear, thus errors in any part of the model may propagate to the final results in ways that are difficult to foresee. Because of these shortcomings, model parameters need to be locally calibrated and validated (Jetten *et al.*, 1999). However, the parameters to be calibrated often outnumber the data available, so that unequivocal identification of the parameters can not be achieved (over-parameterisation). In practice, error propagation and uncertainties in the estimation of input data often more than compensate for the theoretically more accurate description of the system (Jetten *et al.*, 2003).

Placed somewhere in between these two opposite approaches, conceptual (or semi-empirical) models incorporate transfer mechanisms of sediment and overland flow generation, but do not include specific details of process interactions (Merritt *et al.*, 2003). Conceptual models aim at reflecting the physical processes governing the system, but describe them with empirical relationships. They thus combine a physical interpretability of modelling results with a simple structure. Conceptual models tend to suffer less of parameters identifiability and over-parameterisation problems, but may suffer of aggregation problems (Merritt *et al.*, 2003). They generally require calibration and validation, and a good number of observations. However, their limited number of parameters and processes reduces computational requirements, simplifies the assessment of model prediction uncertainties, and facilitates the implementation by user agencies and in data poor environments (Garen *et al.*, 1999; Merritt *et al.*, 2003; Jetten *et al.*, 2003).

In hydrology, a fourth type of models can be distinguished: the hybrid-metric models, which rely on robust statistical techniques to characterise the dominant processes at work in the system (Wheater *et al.*, 1993; Young, 1998). Hybrid-metric models adopt an inferring approach: they identify the modal response of a system and interpret it according to physics paradigms. However, they require long time-series data to extract the dominant response information, and no equivalent in erosion modelling was found in the literature.

With the advent and spread of Geographic Information Systems (GIS), erosion modelling increasingly aimed at providing spatially distributed predictions. GIS tools enhanced exponentially the possibilities of handling spatial information such as topography, soil and land use, thus simplifying the implementation of spatially distributed models, sometimes so much that scaling considerations would be overlooked. However, the capabilities of gathering information on the spatial distribution (spatial pattern) of environmental data evolved less quickly than the capabilities to manipulate the spatial information (Grayson and Blöschl, 2000). Probably because of this, the reliability of erosion model predictions in depicting the spatial patterns of erosion and deposition within a catchment has not been questioned until recently. Unfortunately, recent assessments showed that erosion models performances in this respect are generally poor (Jetten *et al.*, 1999; Jetten *et al.*, 2003; Merritt *et al.*, 2003). As in other environmental modelling areas, difficulties in distributed erosion modelling arises from the natural complexity of the landscape system, spatial heterogeneity and lack of available data (Merritt *et al.*, 2003).

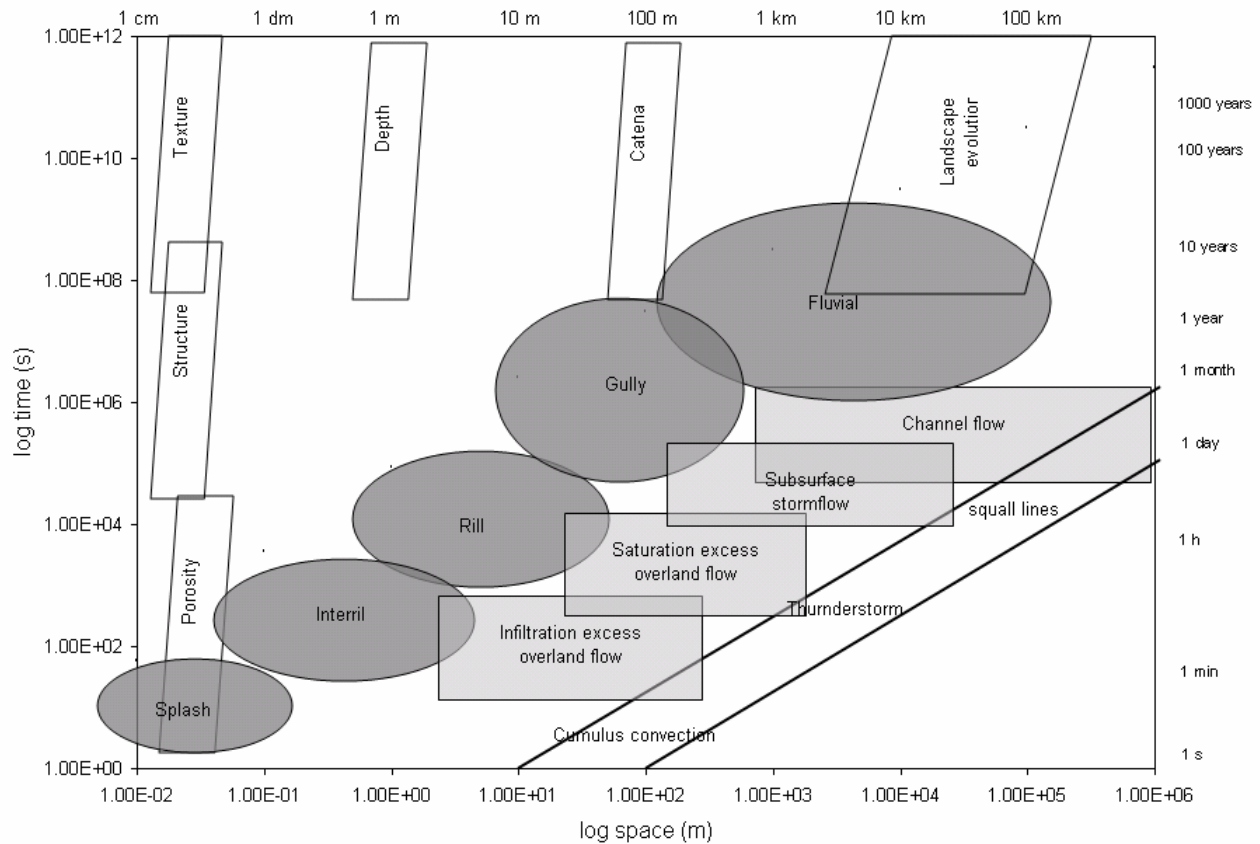


Figure 1. Characteristics space-time scales for some hydrological and erosion processes and relevant soil properties. Adapted from Blöschl and Sivapalan (1995) and Renschler and Harbor (2002).

Erosion processes consist of complex ecological interactions that are strongly scale-dependent. Fig. 1 shows the characteristic lengths of some important hydrologic and erosion processes in the space and time dimensions. The scale for erosion modelling aiming at SWC planning can be roughly positioned at the event-annual time range (from less than one hour to 10 year) and the hillslope-catchment space range (from 100 m to 10 km). This scale frame encompasses different mechanisms of water flow, from infiltration excess overland flow to channel flow, and erosion mechanisms, from splash detachment by raindrops to soil transport and deposition in shallow water and channels, to bank erosion. Even though all ecologic processes interact at any moment and at any place, their relative importance changes with the time-scale frame adopted to describe them. As a consequence, the relative importance of forces and resistances applied to the system change, and the factors required to describe the processes change with them.

The time-space scale dimension is also crucial to observe erosion processes and their factors. Unfortunately, measurement techniques seldom match the optimal modelling time-space scale frame (i.e. the event and the catchment). Often, the temporal and spatial support of measurements, i.e. the size on which measurements are conducted, is small in comparison to model requirements (Blöschl and Sivapalan, 1995; Grayson and Blöschl, 2000). Moreover, erosion processes proved to be extremely

variable even under controlled conditions. Studies conducted on ‘homogeneous’ plots reported a natural (or unexplained) variability of overland flow depth and soil loss that resulted in coefficient of variations per rainfall event larger than 65 %. This variability was spatially inconsistent among plots during different events and was larger for the smaller events (Hjelmfelt and Burwell, 1984; Wendt *et al.*, 1986; Nearing *et al.*, 1999).

In the face of the spatial and temporal heterogeneity of the erosion processes, measurement strategies may point at increasing the extent of the monitoring scheme (i.e. the overall coverage of the data; Grayson and Blöschl, 2000), by repeating measurements either in time or in space. Time and capital constrains seldom allow for both large and long (if any) monitoring campaigns. It follows that in virtually all situations, the data available for erosion modelling is usually much below the requirements for adequate calibration and validation of complex models (e.g. Quinton, 1997). This is especially true for applications of erosion models aiming at SWC planning, for which data consist mainly of general databases created at national or regional level instead of well-equipped experimental catchments (Renschler and Harbor, 2002). The problem is particularly crucial in developing countries, where erosion data are seldom available (e.g. Dregne, 1989).

In practice, the environmental data that are usually available contain information to characterize only the dominant processes active in a given system, which may then be described effectively by conceptual approaches (Young, 1998). Indeed, conceptual (semi-empirical) models offer a compromise between the need to explicitly deal with the main processes and the limited data availability, and may therefore be appropriate in characterizing the distribution of erosion within a catchment (Viney and Sivapalan, 1999; Jetten *et al.*, 2003). For example, Desmet and Govers (1995) obtained some encouraging results with a simple transport-limited erosion model whose main driving factor was topography.

Because of the largely unknown interactions between parts of the natural system, the simplifications necessarily assumed by any model, and the limited availability of data, model predictive errors may be large. In SWC planning, model outputs guide important decisions. Therefore, the uncertainties of model predictions should be made explicit to policy and decision makers (Garen *et al.*, 1999; Merritt *et al.*, 2003), in the form, for example, of output bands (Quinton, 1997) or maps showing where model predictions are most uncertain.

The inherent structure of GIS favoured the mathematical processing of spatial information and the handling of quantitative (hard) data, thus the development of spatially distributed models have so far mainly concentrated on quantitative approaches. However, opportunities for the improvement of spatially distributed predictions may lay in less explored sources of information. One of these sources is represented by the analysis of landscape spatial patterns (Grayson and Blöschl, 2000). Spatial patterns reveal, very much like a picture of landscape processes, the spatial organization of environmental processes and can be considered the integrated response of the system to its main drivers. Spatial patterns therefore represent a source of information for landscape research that is largely unexploited, also because tools to analyse them are still very much under development (Grayson and Blöschl, 2000; Jetten *et al.*, 2003).

Another potential source of information is the qualitative (soft) information offered by farmers' and experts' knowledge. Farmers' knowledge of their environment is linked to land management experience and land use history (Payton *et al.*, 2003; Murage *et al.*, 2000; Habarurema and Steiner, 1997; Warren *et al.*, 2003). Though acknowledged as scientifically valid, soft information has often been overlooked, probably because it is difficult to integrate it into the existing landscape analysis systems and methodology studies that focus on integrating local and scientific knowledge are still few (Niemeijer and Mazzuccato, 2003; Payton *et al.*, 2003).

Aim

The study reported in this thesis aimed at developing a semi-empirical, spatially distributed erosion model to locate sources of sediment within a catchment in data scarce environments. Three specific objectives were defined: (i) identifying the main physical processes affecting the distribution of erosion, (ii) by describing them with simple equations, enabling the estimation of the spatial uncertainties of model predictions, and (iii) exploring the potential use of alternative sources of information, such as observed spatial patterns of erosion and overland flow and farmers' indicators of erosion, for the improvement of spatially distributed erosion modelling.

Research area

Most of the data reported in the thesis were collected during four fieldwork periods conducted from 2001 till 2003 in Kwalei catchment, located in the humid-warm agro-ecological zone of the West Usambara Mountains, in North-east Tanzania.

The West Usambara Mountains lay between latitude 4°24'-5°00' S and longitude 38°10'-38°36' E and are an important zone of agricultural production, comprising staple food, cash crops and timber. The farming system is mixed: farmers are involved in rain-fed agriculture, traditional irrigation in valley bottoms, livestock keeping and off-farm activities (Tenge *et al.*, 2004). Tea, coffee and vegetables are the main cash crops; whereas banana, maize, bean, and round potato are the main food crops. Intercropping is a common farming practice. Major cropping systems are coffee-banana intercrop with other tree species, e.g. temperate fruits and yam below the coffee, maize and bean, and patches of sweet potatoes, cassava and sugarcane (Tenge *et al.*, 2004). Tea, instead, is cultivated as monocrop by both smallholder farmers and large-scale estates.

Population density ranges from 200 to 400 inhabitants per km² (Kaoneka *et al.*, 2000). People live in villages consisting of clusters of homesteads (hamlets) with about 60-80 households. Hamlets are often placed on the ridge shoulders, and the fields run downhill (Mbaga-Semgalawe, 1998). The main ethnic group is the Sambaa tribe, which accounts for 79% of the population, followed by Pare (14%), Mbugu (8%) and Taita. Traditionally, Sambaa are mainly smallholder farmers, while Pare are agropastoralists and Mbugu are pastoralists (Kaoneka *et al.*, 2000). Smallholder farm size varies between 0.7 and 4.1 ha per household, fragmented in several small plots at average walking distance of around 40 minutes from the homestead (Mbaga-Semgalawe and Folmer, 2000).

The West Usambara Mountains have been inhabited since at least 2000 years. Until the end of the 19th century most of them were covered by mountain rain forest (Kaoneka et al., 2000). Agriculture practice consisted of shifting cultivation, whereby after two years of cultivation the land was left for long fallow periods, and agroforestry techniques, whereby the multi-storey cultivation of selected species reproduced the structure of the forest. Land management changed drastically under the rule of the German colonial government. The new government established large plantations of coffee and tea, demarcated forest reserves, and reallocated land to the new European settlers. At the same time, the local population started to grow at a very fast rate. Land availability decreased quickly. The trend did not change under the British administration, and by 1936 all arable land was under cultivation.

Population adapted to land scarcity by reducing and abandoning shifting cultivation and fallow practices, by cultivating food crops in the low-lands or on steep slopes, and by encroaching forests, valley bottoms and wetlands. The intensification of agriculture led to accelerated soil erosion, reduced water availability and decreased soil chemical fertility, ultimately reducing land productivity and triggering a vicious circle of land degradation (Mbaga-Semgalawe and Folmer, 2000).

At the end of the 1940s, the British colonial government, concerned with the consequences of accelerated soil erosion, enforced soil conservation plans aiming to intensify the agricultural production systems while rehabilitating the degraded natural resources. Farmers, however, experienced the coercive conservation activities as heavy duties that were devoid of any tangible benefit. Population reacted with passive resistance and anger, which at times exploded into open riot and alimanted the opposition to the colonial government. Quite naturally, with the independence the soil conservation plans were abandoned and for around ten years land degradation disappeared from the political agenda. In the 1970s, however, the severe degradation of natural resources became evident in the reduction of forest cover, the appearance of denuded patches of land, and the drying up of springs and rivers. Almost 10000 ha, roughly equal to six per cent of arable land, were estimated to be affected by severe erosion (TIRDEP, 1977). In answer to the crisis, the government engaged in several conservation programs planned in collaboration with international donor agencies. Project approaches changed over time, moving from top-down schemes to more participatory planning (Johansson, 2001). While these programmes have certainly had an impact in improving the awareness and perception of the erosion problem among farmers (Johansson, 2001), the adoption rate of SWC measures has remained below expectations and the resources available for intervention are still critically below the needs for proper SWC implementation.

Study outline

Environmental data of the study area at the beginning of the research were limited and scattered. The first fieldwork period (March-May 2001) was mainly devoted to the collection of basic bio-physical information and secondary data, and to the identification of the main erosion processes at work. The most substantial climatic information consisted of 75 years of monthly rainfall records from Sakarani Mission, located at about five km from the catchment. A set of false colour aero photos (approx. scales 1:27000 dating September 1996) was used to derive a Digital Terrain Model (DTM) of the catchment

by aerophotogrammetric techniques. From the DTM, a 20 m pixel size Digital Elevation Model (DEM) and a one m pixel size orthophoto image, which constituted the base of the land use map, were derived. At the same time, a rectangular flume was built at the catchment outlet, and equipped with an automatic recording station for continuous measurement of water level and for sampling sediment concentrations during rainfall events. The team of scientists of the Agricultural Research Institute of Tanzania (ARI-Mlingano) provided the soil map of the catchment (Meliyo *et al.*, 2001) and conducted a Participatory Rural Appraisal focused on erosion problems. In the following short rainy season (Oct-Nov 2001) an erosion assessment survey that covered one fifth of the catchment was carried out to complete the appraisal of basic information of the Kwalei catchment. These data were used to test the capability of an empirical erosion model, the Morgan, Morgan and Finney model (MMF, Morgan, 2001), to locate erosion in Kwalei. The analysis was expanded by including another experimental area, Gikuuri catchment in Kenya, where a parallel research had provided a similar dataset (chapter 2).

One of the main problems of erosion modelling is to model correctly the distribution of overland flow in space and time. The fieldwork period of March-May 2002 focused on overland flow processes, monitoring the spatial pattern of overland flow occurrence and exploring whether field measurements of infiltration could help to model it (chapter 3).

These observations allowed to formulate hypotheses on the catchment hydrology that needed confirmation; at the same time the focus had to shift once again from the hydrologic to the erosion processes. The last fieldwork period (Dec 2002-May 2003) was devoted to (i) verify and enlarge the observations of overland flow occurrence in other areas of the catchment, (ii) quantify erosion within the catchment, and (iii) re-assess and enlarge the spatial distribution of erosion in the catchment. Intensive observations concentrated along two longitudinal transects in the lower and middle slopes of the catchment, where overland flow occurrence and depth, soil losses, presence and intensity of erosion features were monitored. At the catchment scale, the erosion assessment survey was repeated and expanded, recording also the presence of farmers' indicators of erosion and presence and coverage of soil surface crusts.

The observations of overland flow occurrence at the hillslope scale were linked to the rainfall-discharge relationship observed at the catchment outlet to build a hybrid-metric, semi-distributed hydrologic model to predict overland flow distribution within the catchment (chapter 4). This model was then coupled with the sediment phase of the MMF model to simulate the distribution of soil erosion within a catchment. The uncertainty of model predictions due to the choice of sediment transport parameters was estimated with a Monte Carlo simulation experiment (chapter 5).

The limited improvements in the erosion distribution achieved by the better hydrologic characterisation called for a critical reflection on erosion modelling, especially in the light of similar problems experienced by other models in the same area (Hessel *et al.*, 2005). Farmers' knowledge showed to be a promising alternative source of information, as the presence of farmers' indicators of erosion matched well the observed pattern of erosion (chapter 6). The analysis of spatial patterns of observations and model simulations, together with farmers' indicators of erosion and other data collected during the fieldwork shed a new light on scale issues that erosion modelling research should address in the future (chapter 7).

References

- Blöschl G, Sivapalan M. 1995. Scale issues in hydrological modelling: a review. *Scale issues in hydrological modelling*, J. D. Kalma and M. Sivapalan, Eds., John Wiley and Sons, 9-48.
- Dregne HE. 1989. Informed opinion: filling the soil erosion data gap. *Journal of Soil and Water Conservation* **44**: 303-305.
- Garen G, Woodward D, Geter F. 1999. A user agency's view of hydrologic, soil erosion and water quality modelling. *Catena* **37**: 277-289.
- Grayson R, Blöschl G. 2000. Spatial processes, organisation and patterns. *Spatial patterns in catchment hydrology*, R. Grayson and G. Blöschl, Eds., Cambridge University Press, 3-16.
- Habarurema E, Steiner KG. 1997. Soil suitability classification by farmers in southern Rwanda. *Geoderma* **75**: 75-87.
- Hessel R, van den Bosch R, Vigiak O. 2005. Evaluation of the LISEM soil erosion model in two catchments in the East African Highlands. *Earth Surface Processes and Landforms* **subm.**
- Hjelmfelt AT, Burwell RE. 1984. Spatial variability of runoff. *Journal of Irrigation and Drainage Engineering* **110**: 46-54.
- Jetten V, de Roo APJ, Favis-Mortlock D. 1999. Evaluation of field-scale and catchment-scale soil erosion models. *Catena* **37**: 521-541.
- Jetten V, de Roo APJ. 2001. Spatial analysis of erosion conservation measures with LISEM. *Landscape erosion and evolution modelling*, W. W. Doe, Ed., Kluwer Academic, 429-445.
- Jetten V, Govers G, Hessel R. 2003. Erosion models: quality of spatial predictions. *Hydrological Processes* **17**: 887-900.
- Johansson L. 2001. *Ten million trees later*. GTZ, 163 pp.
- Kaoneka ARS, Ngaga YM, Monela GC. 2000. Case study: forests of the Usambara Mountains: historical perspectives and future prospects. *Forests in sustainable mountain development: a state of knowledge report for 2000*, Price M.F. and B. M., Eds., CABI Publishing, 97-103.
- Mbaga-Semgalawe Z. 1998. Household adoption behaviour and agricultural sustainability in the Northeastern Mountains of Tanzania. The case of soil conservation in the North Pare Mountains and West Usambara Mountains, General Economics, Wageningen University, 189.
- Mbaga-Semgalawe Z, Folmer H. 2000. Household behaviour of improved soil conservation: the case of North Pare and West Usambara Mountains of Tanzania. *Land Use Policy* **17**: 321-336.

- Meliyo JL, Kabushemera JW, Tenge AJM. 2001. Characterization and mapping soils of Kwalei subcatchment, Lushoto District. Mlingano Agricultural Research Institute. Tanga, Tanzania.
- Merritt WS, Letcher RA, Jakeman AJ. 2003. A review of erosion and sediment transport model. *Environmental modelling & software* **18**: 761-799.
- Morgan RPC. 1995. *Soil erosion and conservation*. Second ed. Longman Group UK, 198 pp.
- Morgan RPC. 2001. A simple approach to soil loss prediction: a revised Morgan-Morgan-Finney model. *Catena* **44**: 305-322.
- Murage EW, Karanja NK, Smithson PC, Woome PL. 2000. Diagnostic indicators of soil quality in productive and non-productive small holders' fields of Kenya's Central highlands. *Agriculture, Ecosystems and Environments* **79**: 1-8.
- Nearing MA, Govers G, Darrell Norton L. 1999. Variability in soil erosion data from replicated plots. *Soil Science Society of America Journal* **63**: 1829-1835.
- Niemeijer D, Mazzuccato V. 2003. Moving beyond indigenous soil taxonomies: local theories of soils for sustainable development. *Geoderma* **111**: 403-424.
- Payton RW, Barr JJF, Martin A, Sillitoe P, Deckers JF, Gowing JW, Hatibu N, Naseem SB, Tenywa M, Zuberi MI. 2003. Contrasting approaches to integrating indigenous knowledge about soils and scientific soil survey in East Africa and Bangladesh. *Geoderma* **111**: 355-386.
- Quinton JN. 1997. Reducing predictive uncertainty in model simulations: a comparison of two methods using the European Soil Erosion Model (EUROSEM). *Catena* **30**: 101-117.
- Renschler CS, Harbor J. 2002. Soil erosion assessment tools from point to regional scales - the role of geomorphologists in land management research and implementation. *Geoderma* **47**: 189-209.
- Ritchie JC, Walling DE, Peters J. 2003. Application of geographic information systems and remote sensing for quality patterns of erosion and water quality. *Hydrological Processes* **17**: 885-886.
- Tenge AJM, de Graaff J, Hella JP. 2004. Social and economic factors for adoption of soil and water conservation in West usambara highlands, Tanzania. *Land degradation and development* **15**: 99-114.
- TIRDEP. 1977. Tanga Water Master Plan - Land Use Atlas. Regional Development Director. Tanga, Tanzania. VOL. VI.
- Viney NR, Sivapalan M. 1999. A conceptual model of sediment transport: application to the Avon River Basin in Western Australia. *Hydrological Processes* **13**: 727-743.
- Warren A, Osbahr H, S. B, Chappell A. 2003. Indigenous views of soil erosion at Fandou Beri, southwestern Niger. *Geoderma* **111**: 439-456.

Wendt RC, Alberts EE, Hjelmfelt AT. 1986. Variability of runoff and soil loss from fallow experimental plots. *Soil Science Society of America Journal* **50**: 730-736.

Wheater HS, Jakeman AJ, Beven KJ. 1993. Progress and directions in rainfall-runoff modelling. *Modelling change in environmental systems*, A. J. Jakeman, M. B. Beck, and M. J. McAleer, Eds., John Wiley & Sons, 101-132.

Wischmeier WH, Smith DD. 1978. Predicting rainfall erosion losses - a guide to conservation planning. USDA. Washington DC, U.S. USDA Agricultural Handbook 537, 58 pp.

Young PC. 1998. Data-based mechanistic modelling of environmental, ecological, economic and engineering systems. *Environmental modelling & software* **13**: 105-122.

Chapter 2

MODELLING CATCHMENT-SCALE EROSION PATTERNS IN THE EAST AFRICAN HIGHLANDS

Olga Vigiak, Barrack O. Okoba, Geert Sterk and Sander Groenenberg

Earth Surface Processes and Landforms 30: 183-196 (2005).

MODELLING CATCHMENT-SCALE EROSION PATTERNS IN THE EAST AFRICAN HIGHLANDS

Abstract

Prompt location of areas exposed to high erosion is of the utmost importance for soil and water conservation planning. Erosion models can be useful tools to locate sources of sediment and areas of deposition within a catchment, but the reliability of model predictions of spatial patterns of erosion at catchment scale has seldom been validated against observations. This study aimed to evaluate the performance of a simple empirical model (Morgan, Morgan and Finney model, MMF) in predicting spatial patterns of erosion at two small catchments in the East African Highlands: Kwalei (Tanzania) and Gikuuri (Kenya). Erosion maps predicted by the MMF model were compared with erosion maps obtained by direct survey. In Kwalei, erosion features were especially frequent in fields of annual crops. In Gikuuri, slope was the critical erosion factor, with estimated erosion rates $> 10 \text{ kg m}^{-2} \text{ y}^{-1}$ on slopes $> 18\%$. Predicted erosion rates were mainly transport-limited and ranged from < 0.01 to $13.50 \text{ kg m}^{-2} \text{ y}^{-1}$ in Kwalei and $9.29 \text{ kg m}^{-2} \text{ y}^{-1}$ in Gikuuri. The performance of the MMF model in predicting the spatial patterns of erosion was acceptable in Kwalei, but poor in Gikuuri. However, by excluding the elements at the valley bottoms in Gikuuri Catchment, the performance of the model improved dramatically. The spatial pattern of erosion predicted by the MMF model was driven by the accumulation of surface runoff, which did not consider the possibility of re-infiltration along the slope. As a result, the MMF erosion patterns predicted by the model increased invariably from the ridges to the valley bottoms, hampering the model suitability for locating areas subjected to high and very high erosion. It is concluded that the model predictions could be substantially improved by introducing a more realistic hydrological component for the prediction of surface runoff along the hillslope.

Keywords: *spatial pattern of erosion; empirical modelling; Morgan, Morgan and Finney model; erosion assessment; East African Highlands.*

Introduction

The East African Highlands constitute more than 76 % of the Highland ecosystems of Tropical Africa (Pfeiffer, 1990). Thanks to a favourable climate and fertile soils, these areas have a high potential for crop production, and are very important sources of staple food, forest products and export crops (Lundgren, 1980). However, population densities are generally > 100 persons per km^2 . Because of this heavy pressure on land resources, soil erosion is widespread and a major cause of land degradation (Tiffen *et al.*, 1994). Reported soil losses from runoff plots ranged from $4.3 \text{ kg m}^{-2} \text{ y}^{-1}$ in coffee

plantations in Tanzanian Highlands (Mitchell, 1965) to $25.5 \text{ kg m}^{-2} \text{ y}^{-1}$ under tea plantations in Kenya (Othieno, 1975).

Soil and Water Conservation (SWC) projects are active in these areas since the colonial period, experiencing various degrees of success. Past experiences showed that SWC planning should be approached at catchment level, instead of at individual farm or administrative districts (Pretty *et al.*, 1995). The catchment has the advantage of being a natural geomorphologic unit, in which sources of soil losses and surface runoff are topographically linked to areas of sedimentation, and therefore both on-site and off-site effects of erosion can be appreciated (Morgan, 1995). The catchment is at the core of the SWC planning method introduced by the Government of Kenya and now adopted by six East African Countries: the so-called Catchment Approach (Pretty *et al.*, 1995; Kamar, 1998). The method consists of a participatory community planning process, with actual planning of SWC measures at farm level. At the beginning, the catchment scale was selected in order to efficiently use the limited available sources of capital and labour, but it eventually evolved into a focal area where a community is willing to work towards a more conservative utilisation of natural resources. Since its introduction in the 1980s, the Catchment Approach gave positive results in the improvement of soil productivity, together with reduced resource degradation (Pretty *et al.*, 1995; Kizunguto and Shelukindo, 2002). However, capital, technical skills and labour availability are still limited in comparison with the needs (Pretty *et al.*, 1995).

Therefore, a method that would allow quick assessment of major sediment sources and sinks within catchments would help to prioritise the most affected areas. Tools for locating soil erosion sources and areas of deposition are, however, still lacking. An ideal SWC planning tool should be reliable and reproducible, able to predict the post-intervention situation, but simple in use and with limited data requirements. Field surveys may give the actual erosion status of an area, but surveys are time consuming and resource demanding. Moreover, they refer to a situation at a given time and area: their results are not reproducible elsewhere, neither can they predict changes after SWC planning. On the other hand, erosion models can potentially be used to predict areas within the catchment exposed to high erosion. Most catchment-scale erosion models are deterministic models, created since the 1960s to evaluate off-sites risks of soil erosion and surface runoff (Morgan, 1995). Even though they are based on physical laws, they retain a high level of empiricism in their equations and require much data for input, calibration and validation (Morgan, 1995). Their usefulness in quick SWC planning is therefore questionable. This explains the popularity and wide use of empirical models, such as the Universal Soil Loss Equation (USLE, Wischmeier and Smith, 1978). These empirical models have long been used for SWC planning purposes. They are simple to use and require limited data. On the other hand, empirical models have been derived using site-specific data and may not perform well if applied under different conditions. Moreover, they were usually created for erosion prediction at the field scale, and even if they are increasingly used at catchment level, their reliability in depicting soil erosion patterns at this scale has seldom been tested. In general, only recently the ability of erosion models in predicting spatial patterns of erosion has been explored. Deterministic models proved generally ineffective in reproducing spatial patterns of erosion unless a high level of detail in the input data was provided (e.g. Takken *et al.*, 1999). On the other hand, Desmet and Govers (1995) obtained some encouraging results

with a simple transport-limited erosion model whose main driving factor was topography. A simulation of 60 years of erosion with their model matched quite closely the erosion data derived from a soil map, showing that patterns of soil redistribution could be represented even with a crude process description. More recently, van Rompaey *et al.* (2001) developed an empirical but spatially distributed model for the calculation of sediment delivery to river channels (SEDEM). The model predicted erosion at the catchment outlet well, but the reliability of the model predictions of the spatial pattern of erosion was not assessed.

Among the empirical models, the Morgan, Morgan and Finney (MMF) model (Morgan *et al.*, 1984) was created for tropical conditions, where it performed well (Morgan *et al.*, 1982a). The model was recently revised and adapted for applications at the catchment scale (Morgan, 2001). The aim of this paper is to evaluate the performance of the revised MMF model for SWC planning at the catchment-scale in the East African Highlands. The spatial patterns of erosion predicted by the MMF model were compared with erosion maps obtained from field surveys for two small catchments representative of the East African Highlands: Kwalei Catchment in the West Usambara Mountains (Tanzania) and Gikuuri Catchment in Embu District (Kenya).

Materials and methods

The Morgan, Morgan and Finney Model

The Morgan, Morgan and Finney model is an empirical model developed to estimate mean annual soil loss from field-sized areas on hillslopes (Morgan *et al.*, 1984). The model was selected in our study for several reasons. First, the model retains a strong physical base, but is easy to understand and requires few parameters. Moreover, the model had been applied successfully over many tropical locations and had already been tested in the East African Highlands (West Usambara Mountains, Tanzania; Morgan *et al.*, 1984).

The model is structured into two phases: a water phase (where energy of rainfall and volume of surface runoff are calculated), and a sediment phase (where soil detachment and soil transport rates are calculated). The lowest of the last two values is taken as the soil loss at a particular location, indicating the erosion-limiting factor. The model was recently revised and described in detail (Morgan, 2001). The new version presented an improved physical basis by incorporating a more accurate description of erosion processes and by enlarging the guidelines for model inputs. Examples with the model applied at catchment scale were also included. In our study, this new version of the model was used; in what follows only the equations relevant for the application in the East African Highlands are given.

The rainfall kinetic energy (KE , $J\ m^{-2}$) is a function of the effective rainfall (ER , mm), i.e. the fraction of mean annual rainfall (R , mm) that is not intercepted by the vegetation canopy (INT , fraction between 0 and 1). The effective rainfall (ER) is split into direct throughfall (DT), which directly reaches the soil, and leaf drainage (LD), which is intercepted by the canopy and reaches the surface by stemflow or dripping from leaves. The division is a function of the canopy cover (CC , fraction between 0 and 1). The kinetic energy of the direct throughfall DT (KE_{DT} , $J\ m^{-2}$) is a function of rainfall intensity.

The kinetic energy of the leaf drainage (KE_{LD} , J m⁻²) is a function of canopy height (PH , m). The total kinetic energy KE (J m⁻²) is given by the sum of the two fractions:

$$KE = KE_{DT} + KE_{LD} \quad (1)$$

Rainfall kinetic energy KE determines the soil detachment by raindrop impact F (kg m⁻² y⁻¹), which is defined as:

$$F = 10^{-3} K KE \quad (2)$$

where K = soil detachability index (g J⁻¹), defined after Quansah (1981).

In each field, the volume of surface runoff Q_i (expressed in mm of runoff depth) is calculated in terms of saturation excess runoff: surface runoff is generated when daily rainfall exceeds the soil moisture storage capacity. The annual surface runoff is obtained from:

$$Q_i = R \exp(-R_c/R_0) \quad (3)$$

where R = mean annual rainfall (mm), R_c = soil moisture storage capacity, and R_0 = mean rainfall per rainy day (i.e. mean annual rainfall R divided by the number of rainy days per year, n). The soil moisture storage capacity (R_c) is estimated as:

$$R_c = 1000 MS BD EHD (ET_a/ET_p)^{0.5} \quad (4)$$

where MS = soil moisture at field capacity (weight %), BD = soil bulk density (Mg m⁻³), EHD = soil effective hydrological depth (m), and ET_a/ET_p = ratio of actual and potential evapotranspiration. The soil effective hydrological depth (EHD) indicates the depth of soil within which the moisture storage capacity controls runoff generation and depends on root density and depth, or on the presence of an impermeable soil layer (i.e. shallow soils or presence of a crust) that limits water storage capacity (Morgan, 2001).

The application of the model to areas larger than a field requires the introduction of some mechanism for accumulation of surface runoff along the slope. Morgan (2001) suggested subdividing the catchment into elements of homogeneous land characteristics, i.e. homogeneous slope, soil and land use, and arranging them in a cascading sequence of surface runoff accumulation. However, the author did not mention how to take into consideration the relative importance of the area of the different elements, and how this would affect the accumulation of surface runoff along the slope.

In our case, the total surface runoff of the element i (Q_{ti}) is considered as the sum of the surface runoff generated within the element i , Q_i (eq. 3), plus the surface runoff received from the immediate upslope area (Q_{up}) weighted by the ratio between the upslope element area (A_{up}) and the area of the element i (A_i):

$$Q_{ti} = Q_i + Q_{up} (A_{up} / A_i) \quad (5)$$

Eq. 5 takes account of slope divergence and convergence, and for the element surface.

The total surface runoff Q_{ti} is then used to calculate the detachment rate by surface runoff H_i and the transport capacity TC_i of the element i . Soil detachment by surface runoff H_i ($\text{kg m}^{-2} \text{y}^{-1}$) is estimated as:

$$H_i = 10^{-3} (0.5COH)^{-1} Q_{ti}^{1.5} \sin\beta (1-GC) \quad (6)$$

where COH = soil cohesion (kPa), Q = volume of surface runoff, $\sin\beta$ = sine of the slope and GC = fraction of vegetation ground cover (0-1).

The transport capacity TC_i ($\text{kg m}^{-2} \text{y}^{-1}$) is equal to:

$$TC_i = 10^{-3} CP Q_{ti}^2 \sin\beta \quad (7)$$

where CP = crop cover factor, given by the product of the Universal Soil Loss eq. C and P factors (Wishmeier and Smith, 1978).

Finally, the mean annual soil loss rate of the element i (E_i , $\text{kg m}^{-2} \text{y}^{-1}$) is estimated as the minimum of sediment available and transport capacity:

$$E_i = \min [(F + H_i + E_{up}), TC_i] \quad (8)$$

where E_{up} = influx of material from the immediate upslope area.

Sedimentation occurs where the influx of material from upslope E_{up} is larger than the transport capacity out of the element TC_i , with a net sedimentation SED_i equal to:

$$SED_i = E_{up} - TC_i \quad (9)$$

The study areas

Two experimental catchments were selected as representative of the East African Highlands for morphology, land use and socio-economic conditions: Kwalei Catchment in the West Usambara Mountains (Tanzania) and Gikuuri Catchment at Embu District (Kenya) (Fig. 1).

Kwalei ($4^\circ 48' \text{ S}$, $38^\circ 26' \text{ E}$) is situated in Lushoto District, in the West Usambara Mountains, North-East Tanzania. This catchment has an area of *c.* 2 km^2 , and is roughly triangular in shape. Elevation ranges from 1337 to 1820 m, and the terrain is rough and highly dissected, with one half of hillslopes $> 20\%$. Drainage comprises four permanent streams running from Northwest to Southeast (Fig. 1). Mean annual rainfall is *c.* 1000 mm, almost half of which falls during the long rainy season that stretches from late February until late May. A shorter and less predictable rainy season occurs from October to January. Average daily temperature is 18°C , with diurnal temperature ranges ($12\text{--}25^\circ \text{C}$) greater than annual ranges ($16\text{--}20^\circ \text{C}$). Five soil types occur in the catchment (FAO-Unesco legend, FAO, 1990):

Humic Acrisols at the summits, Haplic Lixisols at the summit footslopes, Haplic Acrisols on the ridges, Eutric Fluvisols and Umbric Gleysols in the river valley (Meliyo *et al.*, 2001). In general, topsoils are porous and sandy, with medium to high organic carbon contents. Subsoils are clayey and less well-drained. Poor drainage occurs only in the valley bottom Gleysols (Meliyo *et al.*, 2001). The highest part of the catchment is covered by mountain rain forest, whereas the middle and lower slopes are used for agriculture. Due to the intense land use and small field sizes, the vegetation cover is complex: annual crops are intercropped with perennials, and interspersed with fodder and fruit trees, or fuel and timber woodlots. However, cultivation of annual crops concentrates close to the compounds, along the ridge shoulders: maize is the most cultivated crop, often intercropped with bean, banana, cassava and sugarcane. The two-layer cultivation of banana and coffee is frequent on the steeper slopes along the stream incisions. Valley bottoms are intensively cultivated with vegetables, which represent the major local cash crops.

Gikuuri Catchment (00°25' N, 37° 00' E) is situated in Embu District, Central Kenya. It covers an area of *c.* 5 km² and presents an elongated stream system that comprises three main permanent streams running North-South. Convex-concave slopes, with flat summits, steep midslopes and V-shaped valleys, form the landscape (Fig. 1). Slope gradient is from 2 to 55 %, with a mean of 18 %. Mean annual rainfall is *c.* 1100 mm, distributed over the long rainy season (650 mm), from mid-March until June, and the short rainy season, from mid-October until December (450 mm). Diurnal temperature fluctuates between 10 and 25 °C. Three major soil types (FAO-Unesco legend, FAO, 1990) occur in the catchment: Rhodic Nitisols on the ridge summits and on moderate and steep slopes, Chromic Cambisols and Chromic Luvisols on the very steep slopes along the drainage system. Soils are clayey, deep, and well-drained, but of poor chemical fertility. Minor soil types comprise Haplic Acrisols in the Northern and Western slopes, and Dystric Fluvisols and Gleysols along valley bottoms (Wanjogu, 2001). The farm system is composed of coffee-dairy enterprises (Jaetzold and Schmidt, 1983). The land use is patchy, but coffee, maize and bean fields cover > 70% of the catchment. Major cash crops are coffee, banana, mango and miraa (*Cathy edulis* L.; a stimulant that forms an excellent cash crop for farmers), whereas main food crops are maize, bean, cassava and vegetables. Fodder trees, bushes and timber woodlots are also frequent in the area.

In both catchments, cultivation and clearance of steep slopes expose bare and loose soil to the first rainstorms, and intense erosion may occur especially at the onset of the rainy seasons, before vegetation cover can protect the soil. Erosion mainly occurs in the form of interrill and rill erosion from annual fields.

Data collection

During the long rainy season (March-June) of 2002 intensive fieldwork took place in the two catchments with the double purpose of collecting input data for the MMF model and assessing the actual erosion in both catchments. Data collection strategy was different for the two catchments, as they differed both in the pre-existing information and geographical characteristics.

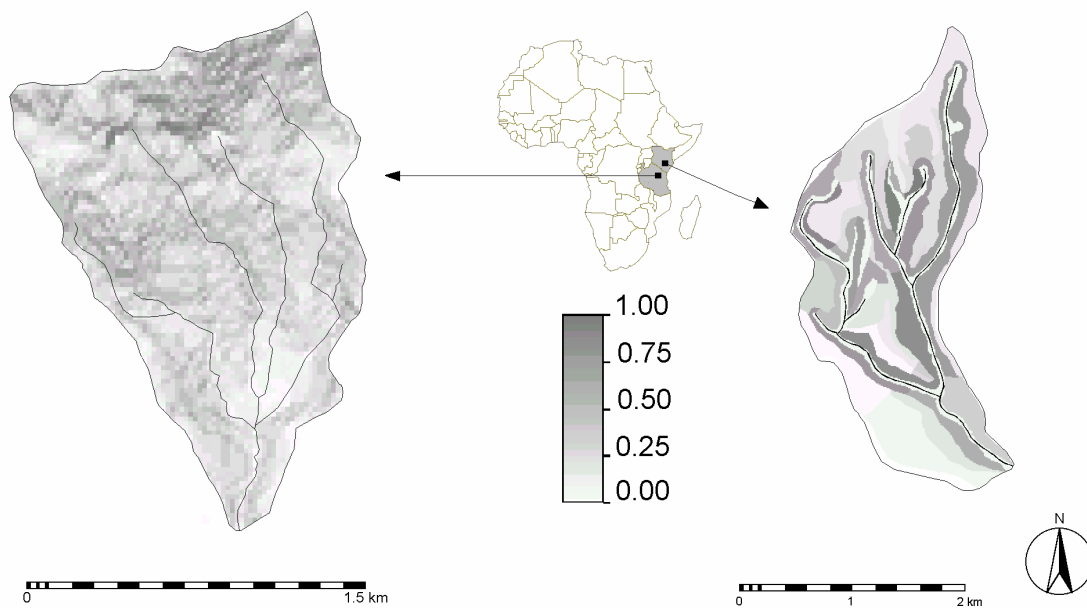


Figure 1. Location and topography of the study areas: on the left Kwalei Catchment (Tanzania), on the right Gikuuri Catchment (Kenya). Shading represents the sine of local slope ($\sin\beta$).

Cartographic environment

In order to represent the spatial distribution of MMF inputs, outputs and field observation, data were organised in a Geographical Information System (ILWIS 3.1, ITC, 2002). For each catchment, four basic maps were created for MMF inputs (soil, land use, slope and element map).

Soil maps were available for both catchments (Meliyo *et al.*, 2001; Wanjogu, 2001). The land use map of Kwalei was produced by surveying and on the basis of an orthophotomap. The land use map of Gikuuri was created on the basis of a cadastral map. The slope map of Kwalei was derived from a Digital Terrain Model (DTM), with a pixel size of 20 m, produced by the aerophototriangulation method with Socet Set software (BAE SYSTEMS, 2003). No DTM was available for Gikuuri, therefore slope was estimated in the fields using an inclinometer (Fig. 1).

The element maps represented elements of homogenous landscape and formed the basis for application of the model at catchment scale. In Kwalei, elements represented fields (i.e. areas with homogeneous land use and soil type). Mean element size was 0.30 ha. In Gikuuri, elements represented portions of hillslope homogeneous per slope direction and gradient: from the water divide to the stream, hillslopes were divided in upper, middle, lower slope and valley bottoms. Elements were in this case large (mean size = 1.52 ha) and comprised more than one soil and land use type.

Mean surface runoff Q_i and mean detachment rate by raindrops F were calculated per element. The elements were then arranged in a cascading sequence of surface runoff accumulation (eq. 5). The accumulation of surface runoff proceeded from elements along the slope ridges to the streams. However, the actual accumulation of surface runoff along the slopes was checked in the field. Where ditches or other obstacles that removed the run-on were present, like roads or well-maintained SWC measures, the cascading sequence was adjusted for. If the obstacle were in good working conditions,

the surface runoff had reached the drainage system and was removed from the accumulation sequence; the elements downstream the obstacle received neither surface runoff nor sediment from the elements upstream the obstacle. If the obstacle were badly maintained, surface runoff and sediment were re-directed toward the element where the obstacle drained.

Soil erosion assessment

The element maps defined the maximum level of accuracy of the MMF model predictions at the catchment scale, therefore these maps were used as the basis for erosion assessment by direct survey. Assessment of actual erosion was conducted with the Assessment of Current Erosion Damage method (ACED, Herweg, 1996). The method consisted of surveying erosion features, together with major causes of erosion, such as land management, surface characteristics, and runoff patterns (Herweg, 1996).

In Kwalei, rills were often removed by frequent weeding operations, which hampered the semi-quantitative erosion assessment. The ACED method was then applied to assess qualitative classes of erosion. Five classes of erosion were defined, from very low to very high, on the basis of erosion features presence and intensity, without attaching a quantitative value to the erosion classes. The survey took place during the short rainy season (Oct-Nov) 2001, when signs of erosion could be considered representative of the past year of rains. The survey did not cover the whole catchment, but only a subcatchment of 47.5 ha (Fig. 2).

In Gikuuri, the ACED method was applied along four longitudinal transects of 2.5 m width. For each transect, four segments were identified: upper, middle, lower slope and valley bottom. For each segment, rill number, mean depth, mean width and length were monitored during the long rainy season (March-June) 2002. Volumes of soil losses from each segment were estimated from these features, and multiplied by topsoil bulk density to estimate soil losses in weight. Sets of erosion pins were placed in each segment to monitor sheet erosion and re-deposition of soil particles. The ACED erosion map of Gikuuri was obtained by extrapolating the transect observations to the element map by using soil type, slope and land use. Five classes of erosion, from very low to very high, were defined according to the assessed amounts of soil losses from the transect observations. The map was checked in the field, where it was verified that it reproduced the actual situation.

MMF input data: rainfall, soil and land use

Daily rainfall records of at least 10 years were available from pluviometer stations close to both catchments.

Soil detachability index K was estimated from literature data of comparable soils of Kenya and Tanzania (Morgan *et al.*, 1982b), using topsoil texture. In the case of clayey soils, however, observation of soil detachment in splash cups (Vigiak, unpublished data) indicated that the suggested value of 0.02 was too low and raised to 0.05. Soil moisture at field capacity MS and topsoil bulk density BD were measured in the laboratory with standard methods (Meliyo *et al.*, 2001; Wanjogu,

2001). Cohesion COH was measured on saturated topsoil with a torvane in the fields and averaged per soil type.

Vegetation-related inputs were monitored during the long rainy season 2002 on the major land uses in Gikuuri. Vegetation interception INT of maize and bean, coffee, and woodlot was measured by splash cups (Morgan, 1981). Canopy cover CC , Plant height PH and ground cover GC were monitored every two weeks in 16 fields cultivated with maize and bean, coffee and banana, woodlot and mixtures of these crops. In Kwalei, INT , CC , PH , and GC were estimated in the fields, monitoring them twice in the long rainy season. Literature values were employed in both catchments for minor land uses (Morgan, 1995; Morgan *et al.*, 1982b). No limiting horizons were detected in any soil profile, therefore the effective hydrological depth (EHD) was considered a land use dependent input, and set according to the model guidelines (Morgan, 2001). The ratio of actual to potential evapotranspiration ET_a/ET_p was estimated as the crop coefficient K_c of the FAO procedure for calculation of crop water requirements (Allen *et al.*, 1998). The crop cover factor C was derived from literature (Morgan, 1995).

In Kwalei, SWC measures were negligible. In Gikuuri, SWC measures consisted of *fanja juu* terraces (i.e. narrow embankments built by digging a ditch on the contour and throwing the soil upslope; Thomas and Biamah, 1991) and grass strips in maize and bean fields, and bench terraces in coffee stands. The protection factor P was estimated from measurements of soil losses in Gerlach troughs (Gerlach, 1967) and splash cups (Morgan, 1981) placed in 12 fields under maize and bean, coffee, and fallow.

Comparison of spatial erosion patterns

For the comparison of erosion patterns at catchment scale, MMF predictions were reclassified into five classes of erosion, from very low to very high. As the purpose of the evaluation was to prove whether the model could locate areas subject to high erosion without regards to quantitative erosion assessment, model predictions were classified on a qualitative criterion. Instead of establishing limits among classes *a priori*, these limits were chosen so to obtain a number of elements per class comparable to the corresponding number of elements per class of the ACED erosion map. For example, if in the ACED erosion map x elements were classified in very low erosion class, then the x element with the lowest erosion rates predicted by the model were classified as very low erosion class, and so forth.

The degree of agreement between the (classified) MMF erosion map with the ACED map was assessed by the weighted Kappa coefficient of the error matrix (Cohen, 1968). To limit the influence of the classification system and to account for uncertainties in the ACED map, one class difference (e.g. very low class in the ACED erosion map predicted as low erosion in the MMF erosion map) was considered acceptable. In these cases, the weight factors were set = 1. For larger disagreements between the two maps (e.g. very low class in the ACED erosion map predicted as moderate erosion in the MMF erosion map or worst), the weights were linearly dependent on the distance between classes (Table 3a). Kappa coefficients were calculated with kappa.exe software (Bonnardel, 1995).

Results and Discussion

Soil erosion assessment

In Kwalei, pedestals, tree mounds, rock and tree roots exposure, together with deposition of soil at the footslopes and along the roads and paths were frequently observed. Erosion features were especially frequent in annual crop fields (cassava, maize and bean). Rills, however, were often removed by weeding operations, and gullies were present only close to major roads, where surface runoff accumulated and entered as concentrated flow into the fields. The ACED erosion map (Fig. 2a) showed that 38 elements out of the 92 surveyed (*c.* 34 % of the area) could be classified as affected by high or very high erosion. Most parts of the forest, the coffee and banana fields and the flat area of the valley bottom were classified as low or very low erosion.

Along the four transects of Gikuuri, soil losses by rill erosion were estimated at between 0.12 – 27.12 kg m⁻² y⁻¹. Surface lowering measured with erosion pins ranged from 0.4 to 4.0 mm. At the footslopes, deposition was always observed. Five classes of erosion were defined according to the slope of the transect segments: very low erosion (< 2 kg m⁻² y⁻¹) on flat areas (< 5% gradient, e.g. valley bottoms); low erosion (2 - 7.5 kg m⁻² y⁻¹) on very gentle slopes (5–9 %); moderate erosion (7.5 -10 kg m⁻² y⁻¹) on gentle slopes (9-18 %); high erosion (10 - 20 kg m⁻² y⁻¹) on steep slopes (18-30 %); and very high erosion (> 20 kg m⁻² y⁻¹) on very steep slopes (> 30 %). According to the ACED erosion map (Fig. 3a), all the valley bottoms and some flat hill summits were classified as subject to very low erosion, whereas *c.* 33 % of the area was affected by high or very high erosion.

Years 2001 and 2002 were dry in Kwalei Catchment. Rainfall totalled 603 mm in 2001 and 202 mm in the long rainy season (March-May) 2002. The probability of non-exceedence of such low rainfall amounts is < 10 % according to rainfall records. On the contrary, the long rainy season of Gikuuri Catchment was wet: in the period April- June 2002 it rained 624 mm, roughly equal to half of mean annual rain. Such a wet season was not exceeded in three out of four years in the last 25 years of records. Soil erosion assessment was therefore likely to underestimate the mean situation in Kwalei and slightly overestimate it in Gikuuri. However, as rainfall is homogeneously distributed within each catchment, the erosion patterns depicted by the ACED maps were considered representative of the average situation.

MMF model results

In Kwalei, mean annual rainfall R was 967.4 mm y⁻¹, with a mean number of rainy days per year n of 89.5. In Gikuuri, mean annual rainfall was 1270 mm y⁻¹ and the mean number of rainy days per year n was 107.

Soil input data are summarized in Table 1. Soil bulk densities BD were low in both catchments, but in the range of tropical soils (1-1.5 Mg m⁻³, Zoon, 1986). Topsoil bulk densities < 1 Mg m⁻³ may be due to high organic carbon content (Meliyo *et al.*, 2001). Soil cohesion COH generally resulted in high values. In the case of Kwalei, the values were however in the range of reported literature (2-12 kPa, Morgan, 2001). In the case of Gikuuri, cohesion was unusually high and indicated very high soil resistance to

Table 1. Distribution of soil types and soil input data for MMF model.

	Soil type	Area (%)	Topsoil texture	K (gJ^{-1})	MS (%w/w)	BD (Mg m^{-3})	COH (kPa)
Kwalei	Humic Acrisol	47.9	Sandy clay loam	0.35	0.27	0.95	8.06
	Haplic Lixisol	15.4	Sandy clay loam	0.35	0.28	1.05	6.61
	Haplic Acrisol	29.4	Sandy clay	0.30	0.31	1.04	7.06
	Eutric Fluvisol	6.4	Sandy clay loam	0.35	0.26	1.32	8.99
	Umbric Gleysol	0.9	Clay	0.05	0.45	1.06	9.51
Gikuuri	Rhodic Nitisol	36.4	Clay	0.05	0.45	0.94	20.1
	Haplic Acrisol	13.9	Clay	0.05	0.45	0.89	15.3
	Chromic Luvisols	8.2	Sandy clay loam	0.35	0.27	0.99	20.2
	Chromic Luvis./Camb.	29.1	Sandy clay loam	0.35	0.27	0.93	20.3
	Dystic Fluvis./Gleys.	6.4	Clay	0.05	0.45	1.03	17.9
	Dystic Fluvisols	6.1	Clay	0.05	0.45	1.02	23.1

K is the soil detachability index, MS is soil moisture at field capacity, BD is bulk density of topsoil and COH is cohesion of topsoil.

shear stress. The high organic matter content and cohesion values of topsoils indicated high resistance to soil particle detachment. However, due to a lack of more detailed information, the detachability indices K derived from literature were not changed.

Land use inputs are reported in Table 2. In general, the land use assured a good cover of soil, with interception of rainfall INT ranging from 0.12 to 0.34, canopy cover CC from 0.25 to 0.86 and ground cover GC from 0.14 to 0.94. Model inputs of annual crops (maize and bean, vegetables, cassava) reflected conditions of low soil protection: rainfall interception $INT < 0.20$, canopy cover CC and ground cover $GC < 0.50$, crop protection factor $C > 0.30$. Most protective land uses were forest, woodlot and grassland, which ensured good rainfall interception and soil cover. In the case of forest and woodlot, however, plant height PH was high, enough for leaf drainage to significantly contribute to total rainfall kinetic energy. Among SWC measures, *fanja juu* terraces were the most effective (P factor = 0.19), followed by bench terraces and grass strips.

In Kwalei, the detachment rate by raindrops (F in eq. 2) ranged from $2.32 \text{ kg m}^{-2} \text{ y}^{-1}$ for grassland to $7.79 \text{ kg m}^{-2} \text{ y}^{-1}$ under forest, with a mean of $4.44 \text{ kg m}^{-2} \text{ y}^{-1}$ for the whole catchment. Detachment rate by raindrops F in Gikuuri ranged from $1.00 \text{ kg m}^{-2} \text{ y}^{-1}$ on clay soils to $7.00 \text{ kg m}^{-2} \text{ y}^{-1}$ on Chromic Luvisols and Cambisols, with little variation due to land use. The detachment rate by raindrops F depends upon two parameters: soil detachability K and rainfall kinetic energy KE . In the case of clay soils, the very low detachability index K (0.05, Table 1) was the most sensitive parameter. On other soil types, differences in the kinetic energy of rainfall KE among land uses became important. By consequence, in Kwalei, where clay soils occupy only a small part of the catchment ($< 1\%$, Table 1), the spatial pattern of the detachment rate by raindrop F reflected more the land use, via the kinetic

Table 2. Land use input data for MMF model

Land use type		<i>EHD</i> (m)	<i>INT</i>	<i>CC</i>	<i>PH</i> (m)	<i>GC</i>	<i>ET_a/ET_p</i>	<i>C</i>	<i>P#</i>
Maize and beans		0.12	0.17	0.26	0.67	0.44	0.78	0.30	FJ=0.19; GS=0.50
Banana and maize		0.12	0.16	0.38	1.24	0.30	0.98	0.25	
Bush/fallow		0.15	0.20	0.63	0.60	0.67	0.73	0.05	
Vegetables		0.12	0.15	0.25	0.28	0.50	0.90	0.35	
Woodlot		0.20	0.28	0.45	9.33	0.45	0.95	0.05	
Kwalei	Cassava	0.12	0.12	0.40	0.80	0.49	0.70	0.40	
	Coffee and banana	0.15	0.30	0.78	1.75	0.79	1.10	0.20	
	Forest	0.20	0.30	0.86	6.43	0.94	0.95	0.01	
	Grassland	0.12	0.30	0.62	0.24	0.75	0.80	0.01	
	Sugarcane	0.12	0.25	0.30	1.32	0.49	0.90	0.15	
	Tea	0.12	0.30	0.45	0.47	0.67	0.92	0.20	
Gikuuri	Banana	0.18	0.23	0.31	1.38	0.16	1.10	0.40	
	Coffee	0.12	0.34	0.29	1.04	0.23	1.08	0.42	BT=0.25
	Coffee and maize	0.12	0.23	0.37	0.95	0.14	1.04	0.42	BT=0.25
	Miraa	0.12	0.34	0.25	0.81	0.23	0.86	0.32	

#Soil and water conservation measures: FJ = fanja juu terraces, GS = Grass strips, BT= bench terraces. EHD is effective root depth, INT is interception factor, CC is canopy cover fraction, PH is plant height, GC is ground cover fraction, ET_a/ET_p is actual to potential evapotranspiration ratio, C and P are the USLE crop and protection parameters.

energy *KE*. The area mean rainfall kinetic energy *KE* amounted to *c.*14700 J m⁻², being least on grassland (7140 J m⁻²) and largest under woodlot (22750 J m⁻²). In Gikuuri, instead, clay soils cover > 60 % of the area (Table 1), therefore detachment rates were lower than in Kwalei, notwithstanding the rainfall kinetic energy was higher (area mean = 20000 J m⁻²) and ranged from 13400 J m⁻² (under long term fallow) to 29900 J m⁻² (under woodlot).

Soil detachment by surface runoff (*H_i* in eq. 6) ranged from 0.00 to 1.07 kg m⁻² y⁻¹ (mean = 0.06 kg m⁻² y⁻¹) in Kwalei and was even lower in Gikuuri, where it ranged from 0.00 to 0.44 kg m⁻² y⁻¹ per element (mean = 0.02 kg m⁻² y⁻¹). The contribution of soil detachment by surface runoff *H_i* increased along the slope due to runoff accumulation, but it was far less important than soil detachment by raindrops. Total detachment rates (*F + H_i*) therefore changed little along the slope, and averaged *c.* 4.50 kg m⁻² y⁻¹ in Kwalei and 2.66 kg m⁻² y⁻¹ in Gikuuri.

Transport capacity rates (*TC_i* in eq. 7) ranged from < 0.01 to 43.77 kg m⁻² y⁻¹ in Kwalei (mean = 1.90 kg m⁻² y⁻¹) and from < 0.01 to 78.06 kg m⁻² y⁻¹ in Gikuuri (mean = 2.28 kg m⁻² y⁻¹).

Erosion rates (*E_i* in eq. 8) ranged from < 0.01 to 13.50 kg m⁻² y⁻¹ in Kwalei, with a mean of 1.07 kg m⁻² y⁻¹. The erosion rates were reclassified into five erosion classes: very low erosion (*E_i* < 0.025 kg m⁻² y⁻¹), low erosion (0.025–0.065), moderate erosion (0.065–0.350), high erosion (0.350–1.750), and very

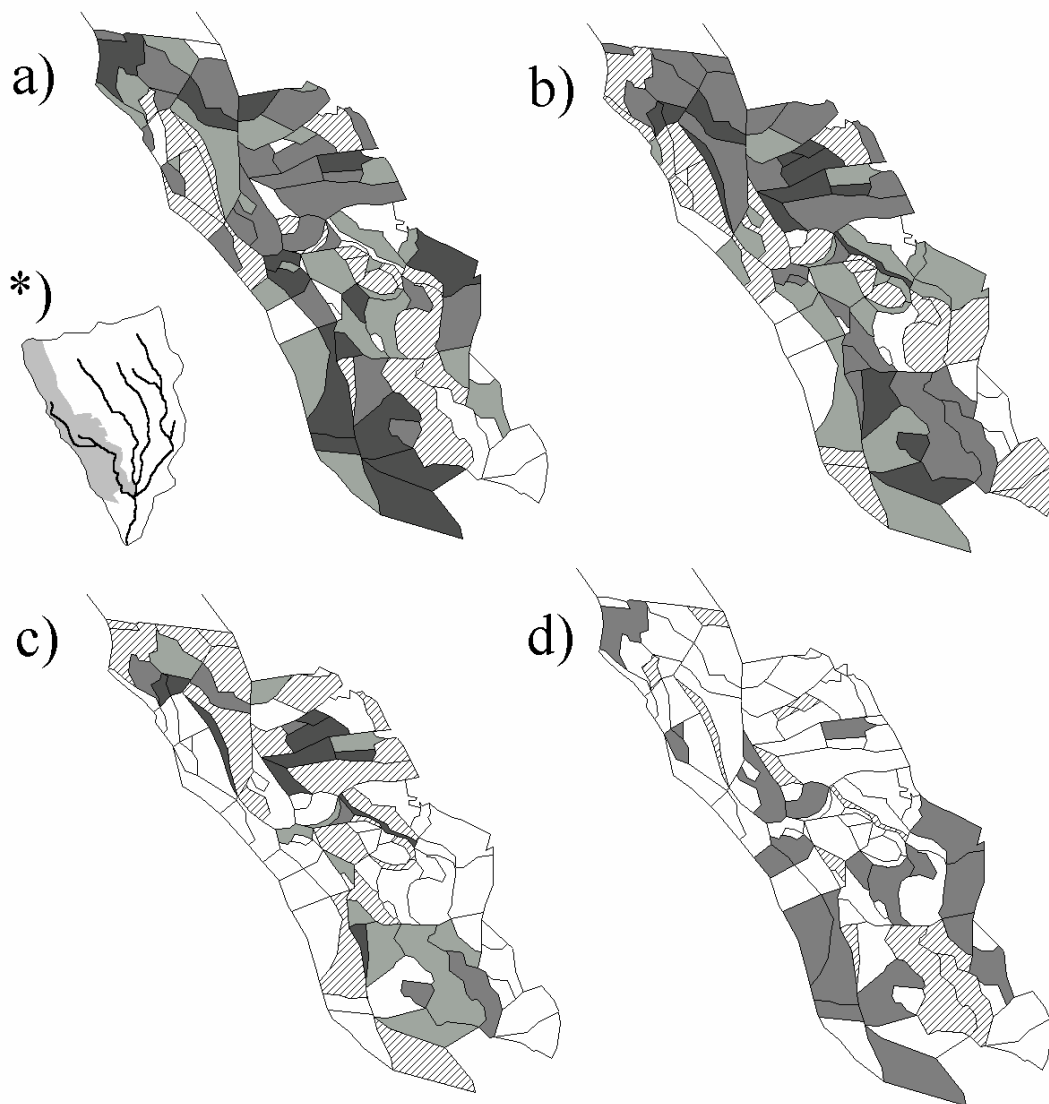


Figure 2. Spatial patterns of erosion at Kwalei Catchment: asterisk indicates surveyed subcatchment; (a) ACED erosion map (white = very low; hatched = low, light grey = moderate, grey = high, dark grey = very high); (b) MMF erosion map (legend as above); (c) MMF distribution of surface runoff (legend as above); (d) location and type of errors of MMF model predictions (hatched = overestimates; grey = underestimates)

high erosion ($> 1.750 \text{ kg m}^{-2} \text{ y}^{-1}$). The resulting MMF erosion map (Fig. 2b) showed that, according to the MMF model, areas subjected to high erosion were especially located in the downslope elements of hills covered by annual crops, and along the streams, i.e. where surface runoff accumulated.

In Gikuuri, erosion rates E_i ranged from 0.02 to $9.29 \text{ kg m}^{-2} \text{ y}^{-1}$, with a mean of $0.75 \text{ kg m}^{-2} \text{ y}^{-1}$. Model erosion rates were similar to figures reported in literature (Mitchell, 1965; Othieno, 1975), but lower than observations along Gikuuri transects. However, observations in Gikuuri were limited to one rainy season, which was wetter than the average year. Moreover, ACED method allows only semi-quantitative assessment of erosion and, while it can give the order of magnitude of the problem, is not

meant to give accurate quantification of soil losses. Therefore, no conclusion could be drawn on the reliability of model quantitative assessment of erosion soil losses. The model erosion rates were reclassified into five erosion classes: very low erosion ($E_i < 0.050 \text{ kg m}^{-2} \text{ y}^{-1}$), low erosion (0.050-0.125), moderate (0.125-0.600), high (0.600-1.000), and very high ($> 1.000 \text{ kg m}^{-2} \text{ y}^{-1}$). The MMF erosion map of Gikuuri (Fig. 3b) showed again that, according to the model, erosion increased along the slope, from ridges to valley bottoms, with especially high erosion rates on the Chromic Luvisols and Cambisols of the steep slopes of the Southern hillslopes.

In $> 90 \%$ of elements of both catchments, transport capacity was the erosion-limiting factor and erosion was detachment-limited only on a few elements at the valley bottoms. Transport capacity depends on the second power of surface runoff (eq. 7). Therefore, MMF model predictions of erosion were driven by the accumulation of surface runoff along the slopes. Low erosion rates were predicted on the ridges, while high erosion rates occurred along the streamlines (Figs. 2b and 3b).

Surface runoff generated within the elements (Q_i in eq. 3) was low and similar in the two catchments, *c.* 35 mm. In Kwalei, where soils are rather homogeneous, the model simulation of surface runoff reflected differences in land use. The highest rates of runoff were recorded in the annual crop fields on the Haplic Acrisols and Lixisols of the ridges, whereas the lowest surface runoff was generated under forest and coffee and banana fields. On the contrary, in Gikuuri because of the difference in soil moisture at field capacity MS among soil types (Table 1), surface runoff was much higher in Chromic Luvisols and Cambisols than elsewhere. However, due to the accumulation sequence (eq. 5), the total surface runoff Q_{ti} per element increased systematically along the slopes. In Kwalei, where the element map depicted relatively small elements and where slopes were rather short, the surface runoff generated within the element Q_i was generally more important than incoming runoff Q_{up} (A_{up} / A_i). The total surface runoff Q_{ti} ranged from 6 to 550 mm, with a mean of 92 mm. Fig. 2c shows the distribution of total surface runoff Q_{ti} in the catchment. Surface runoff generally increased along the slope, but the elements in the cascading sequence retained their own characteristics and therefore some elements at the footslopes maintained very low or low surface runoff. In Gikuuri, where element size were larger and comprised different land uses, the incoming surface runoff Q_{up} (A_{up} / A_i) had a greater impact on the total surface runoff Q_{ti} than the surface runoff generated within the element Q_i . As a result, the total surface runoff was larger than for Kwalei, ranging from 16 to > 3000 mm (mean = 177 mm) and increased invariably from the ridges to the valley bottoms (Fig. 3c). The influence of soil type, very important on the surface runoff generated within the element Q_i , i.e. at the element scale, was completely lost at the catchment scale. As surface runoff simulation is of saturation-excess type and no mechanism for reinfiltration along the slope could be taken into account, all the footslopes and valley bottoms resulted in having high and very high surface runoff.

Finally, in Kwalei sedimentation rates (SED_i in eq. 9) occurred on 17 % of the elements, and ranged from $0.005\text{-}10.83 \text{ kg m}^{-2} \text{ y}^{-1}$, with a mean of $0.65 \text{ kg m}^{-2} \text{ y}^{-1}$. In Gikuuri, sedimentation occurred on 47 % of the elements, and ranged from $0.005\text{-}3.16 \text{ kg m}^{-2} \text{ y}^{-1}$, with a mean of $0.46 \text{ kg m}^{-2} \text{ y}^{-1}$. Sedimentation occurred where the influx of material from upslope E_{up} was consistent and where sudden

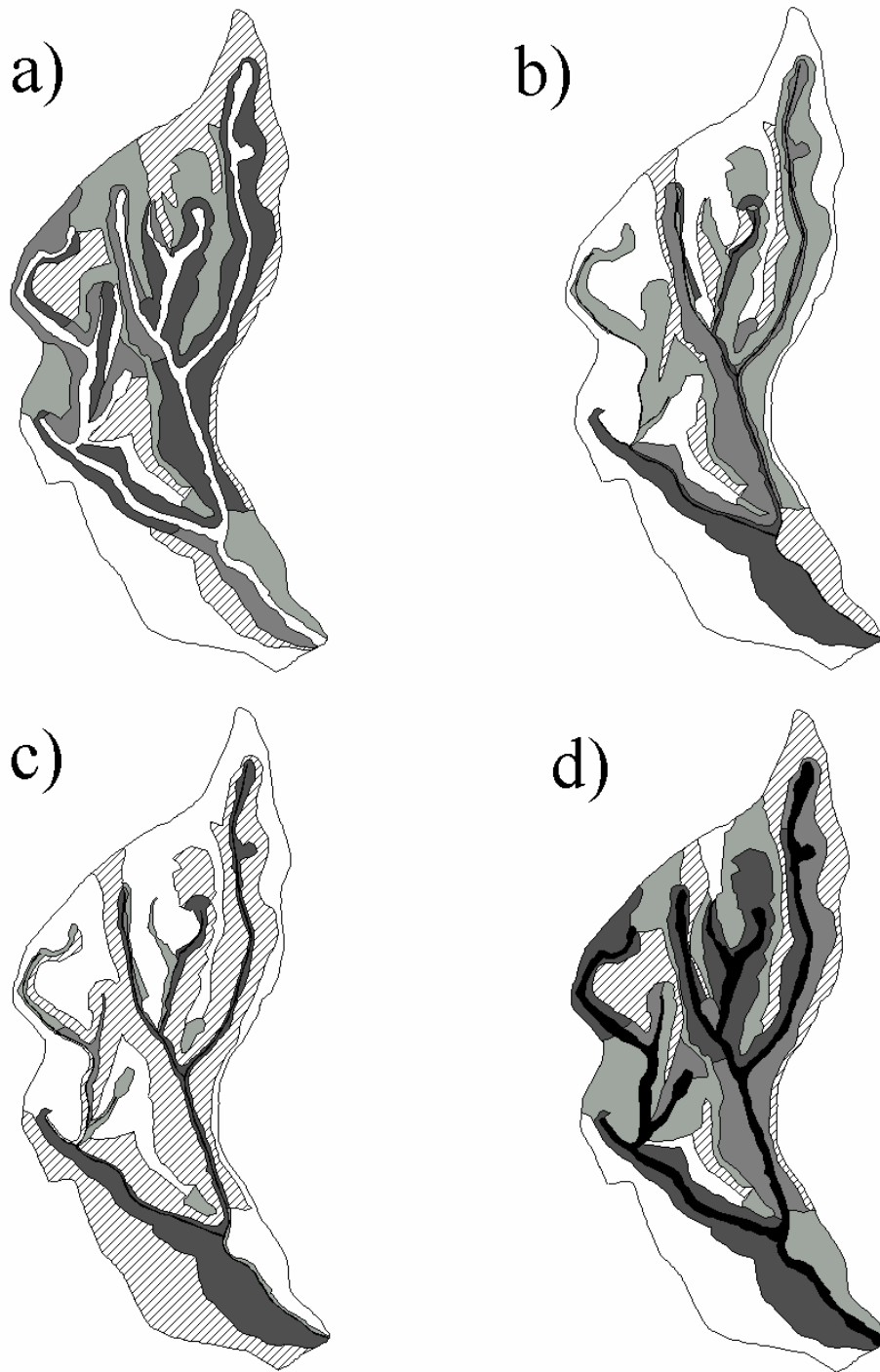


Figure 3. Spatial patterns of erosion at Gikuuri Catchment. (a) ACED erosion map (white = very low; hatched = low, light grey = moderate, grey = high, dark grey = very high); (b) MMF erosion map (legend as above); (c) MMF distribution of surface runoff (legend as above); (d) MMF erosion map with the exclusion of valley bottoms (legend as above; in black the excluded area).

changes in vegetation cover or slope reduced drastically the transport capacity TC_i of surface runoff (eq. 7). The vegetation cover control on the sedimentation pattern was dominant in Kwalei, where sedimentation occurred mainly on the steep coffee and banana stands along the streamlines. The topography control was instead dominant in Gikuuri, where sedimentation occurred mainly at the footslope elements.

Comparison of erosion maps

The comparison of the MMF erosion map with the ACED erosion map in Kwalei showed that out of 92 elements of the ACED erosion map, 30 were correctly classified, 30 were acceptably classified (i.e. one class difference) and few major misclassification errors occurred (Table 3b). The weighted Kappa coefficient of the error matrix was 0.241, which, according to Landis and Koch (1977), indicates fair agreement between the two maps. Fig. 2d showed the location and type of error in the model predictions. The model performed better in the upper part of the sub-catchment; errors of model predictions consisted of overestimates of erosion along streamlines, and underestimates on ridges.

In Gikuuri, the spatial pattern of model predictions differed significantly from the ACED classification. Out of 65 elements, only 11 were correctly classified and 22 were acceptably classified; 14 elements were completely misclassified (more than 2 classes of difference, Table 3c). The weighted Kappa coefficient in this case was 0.047, indicating very poor agreement between the two maps. Besides some ridges that were correctly classified as subject to low erosion, the erosion pattern depicted by the model was wrong (Figs. 3a and 3b). In the valley bottoms erosion was highly overestimated; along the steep and very steep slopes, erosion was instead generally underestimated. Therefore, the pattern of model prediction errors was similar in both catchments and consisted of underestimates of erosion on the ridges and overestimates along the streamlines and at the valley bottoms. This associated combination of overestimates in the lower parts and underestimates in the upper parts was considered to be independent from the classification system adopted for MMF predictions. By setting qualitative limits to classify the model erosion rates, possible overestimates of erosion rates at the end of the accumulation sequence should exert only little influence on underestimates at the beginning of the sequence.

More probably, the errors of model predictions depended on the model structure. MMF model simulates surface runoff in terms of saturation excess. The occurrence of infiltration excess surface runoff on the annual crop fields at the onset of the rainy season cannot be accounted for. This might explain the underestimates in the upper parts of the ridges, where the cultivation of annual crops is more intense. Moreover, in both catchments, reinfiltration along the slopes and sedimentation at the footslopes was observed. However, the mechanism of surface runoff accumulation (eq. 5) did not account for reinfiltration. As a result, the model structure resulted in exaggerated flow accumulation along the slope, which almost completely drove the simulation of spatial patterns of erosion: the erosion patterns predicted by the model increased invariably from the ridges to the valley bottoms. This was more dramatic at Gikuuri, where elements of cascading sequences were large and comprised different land uses.

Table 3. Error matrixes for the comparison of ACED and MMF erosion maps: a) Kappa coefficient weights; b) Kwalei error matrix; c) Gikuuri error matrix; and d) Gikuuri error matrix after excluding the elements of valley bottoms. n indicates the number of elements per erosion class.

		ACED erosion map					
		Very low	Low	Moderate	High	Very high	
a) Weights	Very low	1	1	0.5	0.25	0	
	Low	1	1	1	0.5	0.25	
	Moderate	0.5	1	1	1	0.5	
	High	0.25	0.5	1	1	1	
	Very high	0	0.25	0.5	1	1	
		Very low	Low	Moderate	High	Very high	n
b) Kwalei MMF map	Very low	5	2	6			13
	Low	4	8	2	5	2	21
	Moderate		3	7	4	7	21
	High	3	3	6	8	3	23
	Very high	3	2	1	6	2	14
	n	15	18	22	23	14	92
c) Gikuuri MMF map	Very low	4	6	7	2	1	20
	Low	2	1	3		2	8
	Moderate	6	1	3	3	5	17
	High	3		3	1	2	9
	Very high	6			2	2	11
	n	21	8	16	8	12	65
d) Gikuuri MMF map No valley bottom	Very low	3	1				4
	Low	1	3	3			7
	Moderate		3	12	1	1	16
	High				2	3	5
	Very high		1	1	5	8	14
	n	4	8	16	8	12	48

To verify that the mechanism of accumulation was at the origin of the errors in the model predictions, the comparison of the two maps was repeated in Gikuuri catchment after excluding the valley bottom elements from the analysis. The resulting MMF erosion map (Fig. 3d) was much closer to the ACED erosion map (Table 3c), and the weighted Kappa coefficient increased dramatically (0.868), indicating almost perfect agreement between the two maps.

At the scale of the single element, the MMF retained a good balance between rainfall kinetic energy KE and surface runoff Q , the two driving forces behind erosion. However, at the catchment scale,

surface runoff became the only important erosive force of the model simulation. The application of field models at catchment scale requires careful consideration of scale issues. Topography, which may play a relative role at field scale, becomes a major factor controlling erosion at catchment scale (Desmet and Govers, 1995). The introduction of a topographic factor that considers the three-dimensionality of a catchment is crucial for capturing the spatial pattern of erosion at catchment scale (Desmet and Govers, 1997; van Rompaey *et al.*, 2001). Successful algorithms incorporate usually the upslope draining area and the local slope (Moore *et al.*, 1993). These two parameters are represented in the MMF model by the upslope area A_{up} and the sine of the slope $\sin\beta$, but their role in the model appears to be unbalanced (eqs. 5 and 7). Similar scaling problems had been already observed in other empirical erosion models. For example, the original LS factor of the USLE model has long been substituted with more appropriate algorithms for application at hillslope or catchment scale (Desmet and Govers, 1997). Notwithstanding the improvements, the USLE model cannot account yet for infiltration and sedimentation along the slope and failed in reproducing erosion patterns in a catchment in Southern Spain (Vigiak and Sterk, 2001). Only recently, Warren and Mitsova (2003) were able to improve the prediction of erosion patterns of a USLE-derived model by introducing a sedimentation mechanism.

In this respect, the structure of MMF model offers an advantage. In eq. 9 both the influx material E_{up} and the transport capacity TC_i were affected in a similar way by the accumulation of surface runoff, so that their difference was more realistic. Indeed, the patterns of soil sedimentation in the two catchments were close to the observations: the model simulated the occurrence of sedimentation in the coffee and banana stands along the steep streamlines in Kwalei and at the footslopes in Gikuuri, exactly as it was observed in the fields.

Conclusions

The assessment of erosion showed that areas affected by high and very high erosion covered around one third of both catchments. In Kwalei, erosion features were especially frequent in fields of annual crops, like cassava, maize and bean. In Gikuuri, soil losses by rill erosion were estimated between $0.12 - 27.12 \text{ kg m}^{-2} \text{ y}^{-1}$ and surface lowering as measured with erosion pins ranged from 0.4 to 4.0 mm in the 2002 long rainy season only.

MMF predictions of erosion indicated that erosion was mainly transport-limited, and erosion rates ranged from < 0.01 to $13.50 \text{ kg m}^{-2} \text{ y}^{-1}$ in Kwalei catchment and from 0.02 to $9.29 \text{ kg m}^{-2} \text{ y}^{-1}$ in Gikuuri. The model erosion rates were close to figures reported in literature, but lower than the observations at Gikuuri. However, the transect observations were of limited accuracy and duration, so no conclusion of the quantitative erosion rates of MMF model could be drawn.

The performance of the MMF model in reproducing spatial pattern of erosion was fair in Kwalei (weighted Kappa coefficient 0.241), but poor in Gikuuri (weighted Kappa coefficient 0.047). However, by excluding the elements at the valley bottoms in Gikuuri, the performance of the model increased dramatically (weighted Kappa coefficient 0.868). Most of model errors consisted of overestimates of

erosion rates along the streamlines and underestimates on the ridges. The pattern of sedimentation was instead closer to reality: the model simulated sedimentation occurrence in the coffee and banana stands along the steep streamlines in Kwalei and at the footslopes in Gikuuri, exactly as it was observed in the fields.

The major cause of model errors was identified in the mechanism of surface runoff accumulation, which could not account for the reinfiltration along slopes or footslopes that was instead observed in the field. At the scale of the single element, the MMF retained a good balance between rainfall kinetic energy and surface runoff, the two driving forces behind erosion. Because of the accumulation along the slope, at the catchment scale the importance of surface runoff volume increased in the model structure, until it drove almost completely the simulation of spatial patterns of erosion rates.

At field scale, considering the limited number of model inputs and its simplicity of application, the MMF model is well suited for SWC planning purposes. At the catchment scale, the accumulation procedure of surface runoff should be applied critically, or even excluded in catchments where reinfiltration is frequent. More generally, by introducing a more realistic hydrological component for the prediction of surface runoff along the hillslope, the model performance at catchment scale could improve substantially and the model could become a very useful tool for SWC planning in the East African Highlands catchments.

Acknowledgements

The authors wish to thank A. Tenge and all the colleagues collaborating in the EROAHI project “*Development of an improved method for soil and water conservation planning at catchment scale in the East African Highlands*”, within which this research was conducted. The financial support from the Ecoregional Fund is gratefully acknowledged. We like to thank ITC Enschede for their help with the construction of the DEM for Kwalei Catchment and the two anonymous reviewers for their useful comments and suggestions.

References

Allen RG, Pereira LS, Raes D, Smith M. 1998. *Crop evapotranspiration. Guidelines for computing crop water requirements. Irrigation and Drainage paper 56*, FAO.

BAE-SYSTEMS. 2003. Socet Set.[Available online from <http://socetset.com/trademarks/index.ht>, 18 November 2003.]

Bonnardel P. 1995. Kappa.exe.[Available online from http://kappa.chez.tiscali.fr/Kappa_cohen.htm 17 November 2003.]

- Cohen J. 1968. Weighted Kappa: nominal scale agreement with provision for scaled disagreement or partial credit. *Psychological Bulletin* **70**: 213-220.
- Desmet PJJ, Govers G. 1995. GIS-based simulation of erosion and deposition in an agricultural landscape. *Catena* **25**: 389-401.
- Desmet PJJ, Govers G. 1997. A GIS procedure for automatically calculating the USLE-LS factor on topographically complex landscape units. *Journal of Soil and Water Conservation* **51**: 427-433.
- FAO. 1990. *Guidelines for soil description*. 3rd edition (revised) ed. *Soil Resource Management and Conservation Service, Land and Water Division*, FAO.
- Gerlach T. 1967. Hillslope troughs for measuring soil movement. *Revue de geomorphologie dynamique* **17**: 173.
- Herweg K. 1996. *Assessment of Current Erosion Damage*. Centre for Development and Environment Institute of Geography, University of Berne.
- ITC. 2002. Ilwis 3.1 Academic
- Jaetzold R, Schmidt H. 1983. *Farm management handbook for Kenya*. Vol. IIC, Ministry of Agriculture and GTZ.
- Kamar MJ. 1998. Soil conservation implementation approaches in Kenya. *Advances in Geoecology* **31**: 1051-1064.
- Kizunguto TM, Shelukindo HB. 2002. Guidelines to mobilize and support community-based Catchment Approach Watershed Management. SECAP. Lushoto, Tanzania.
- Landis J, Koch GG. 1977. The measurement of observer agreement for categorical data. *Biometrics* **33**: 159-174.
- Lundgren L. 1980. Comparison of surface runoff and soil loss from runoff plots in the forest and small scale agriculture in the Usambara Mts., Tanzania. *Geografiska Annaler* **62A**: 113-148.
- Meliyo JL, Kabushemera JW, Tenge AJM. 2001. Characterization and mapping soils of Kwalei subcatchment, Lushoto District. ARI Mlingano. Tanga, Tanzania.
- Mitchell HW. 1965. Soil erosion losses in coffee. *Tanganyika Coffee News* **April-June**: 135-155.
- Moore ID, Turner K, Wilson JP, Jenson SK, Band LE. 1993. GIS and land surface-subsurface process modelling. *Environmental modeling with GIS*, M. F. Goodchild, B. O. Parks, and L. T. Steyaert, Eds., Oxford University Press, 196-230.
- Morgan RPC. 1981. Field measurements of splash erosion. *International Association of Scientific Hydrology Publication* **133**: 373-382.

-
- Morgan RPC, Hatch T, Sulaiman W, Harun W. 1982a. A simple procedure for assessing soil erosion risk: a case study for Malaysia. *Zeitschrift für Geomorphologie Supplement Bulletin* **44**: 69-89.
- Morgan RPC, Morgan DDV, Finney HJ. 1982b. Stability of agricultural ecosystems: documentation of a simple model for erosion assessment. International Institute for Applied System Analysis. Laxenburg, Austria. CP-82-50, 20 pp.
- Morgan RPC, Morgan DDV, Finney HJ. 1984. A predictive model for assessment of erosion risk. *Journal of Agricultural Engineering Research* **30**: 245-253.
- Morgan RPC. 1995. *Soil erosion and conservation*. Second edition ed. Longman, 198 pp.
- Morgan RPC. 2001. A simple approach to soil loss prediction: a revised Morgan-Morgan-Finney model. *Catena* **44**: 305-322.
- Othieno CO. 1975. Surface run-off and soil erosion on fields of young tea. *Tropical agriculture (Trinidad)* **52**: 299-308.
- Pfeiffer R. 1990. Sustainable agriculture in practice - The production potential and environmental effects of macro-contour lines in West Usambara Mountains, Tanzania, Hohenheim University.
- Pretty TN, Thompson J, Kiara JK. 1995. Agricultural regeneration in Kenya: the catchment approach to soil and water conservation. *Ambio* **24**: 7-15.
- Quansah C. 1981. The effect of soil type, slope, rain intensity and their interactions on splash detachment and transport. *Soil Science* **32**: 215-224.
- Takken I, Beuselinck B, Nachtergaele J, Govers G, Poesen J, Degraer G. 1999. Spatial evaluation of a physically based distributed erosion model (LISEM). *Catena* **37**: 431-447.
- Thomas DB, Biamah EK. 1991. Origin, application and design of fanya juu terrace. *Development of conservation farming on hillslopes*, W. C. Moldenhauer, N. W. Hudson, T. C. Sheng, and S. W. Lee, Eds., Ankeny I.A., Soil and Water Conservation Society, 185-194.
- Tiffen DB, Mortimore M, Gitchuki F. 1994. *More people, less erosion: environmental recovery in Kenya*. John Wiley & Sons.
- van Rompaey AJ, Verstraeten G, van Oost K, Govers G, Poesen J. 2001. Modelling mean annual sediment yield using a distributed approach. *Earth Surface Processes and Landforms* **26**: 1221-1236.
- Vigiak O, Sterk G. 2001. Empirical water erosion modeling for soil and water conservation planning at catchment-scale. *Ecosystems and sustainable development III*, Y. Villacampa, C. A. Brebbia, and J.-L. Usó, Eds., WIT Press, 219-228.

Wanjogu SM. 2001. Detailed soil survey report of the EROAHI project site, Runyenjes, Embu District. KARI. Embu, Kenya. KARI Soil Survey Reports 21.

Warren SD, Mitsova H. 2003. Validation and application of a 3-D erosion/deposition model based on the Universal Soil Loss Equation. *In: Proceedings of the International Symposium 25 Years of Assessment of Erosion, 22-26 September 2003*, Ghent, Belgium, D. Gabriels and W. Cornelis (Eds).

Wishmeier WH, Smith DD. 1978. Predicting rainfall erosion losses. USDA Agricultural Research.

Zoon SV. 1986. *Tropical and subtropical soil science*. MIR Publisher.

Chapter 3

MATCHING HYDROLOGIC RESPONSE TO MEASURED EFFECTIVE HYDRAULIC CONDUCTIVITY

Olga Vigiak, Simone J.E. van Dijck, E. Emiel van Loon and Leo Stroosnijder

Hydrological Processes. Accepted for publication.

MATCHING HYDROLOGIC RESPONSE TO MEASURED EFFECTIVE HYDRAULIC CONDUCTIVITY

Abstract

The objective of this study was to test the practicability of defining hydrologic response units as combinations of soil, land use and topography for modelling infiltration at the hillslope and catchment scales. In an experimental catchment in the East African Highlands (Kwalei, Tanzania), three methods of measuring infiltration were compared for their ability to capture the spatial variability of effective hydraulic conductivity: the constant head method (CH); the tension infiltration method (TI); and the mini-rainfall simulation method (RS). The three methods yielded different probability distributions of effective hydraulic conductivity and suggested different types of hydrologic response units. Independently from these measurements, the occurrence of infiltration-excess overland flow was monitored over an area of six hectares by means of overland flow detectors. The observed pattern of overland flow occurrence did not match any of the patterns suggested by the infiltration measurements. Instead, clusters of spots with overland flow were practically independent from field borders. Geostatistical analysis of the overland flow confirmed the absence of spatial correlation for distances over 40 m. The RS method yielded the pattern closest to the observations, probably because the method simulated better the processes that trigger infiltration-excess overland flow, i.e. soil sealing and infiltration through macroporosity. The RS hydrologic response unit correlated significantly with observed overland flow frequency. However, the location of clusters and “hot spots” of overland flow remained largely unexplained by land use, soil and topographic variables. It is concluded that using such landscape variables to define hydrologic units may create artificial boundaries that do not correspond to physical realities, especially if the stochastic component within hydrologic units is neglected.

Keywords: *overland flow pattern; overland flow detectors; effective hydraulic conductivity measurement; hydrologic response units.*

Introduction

Characterization of infiltration is of the utmost importance to understand the occurrence and movement of overland flow at the field, hillslope and catchment scales. Infiltration rates are generally high at the beginning of the process, and decline gradually until a constant rate is reached, i.e. the so-called effective hydraulic conductivity of the soil surface. During a rainfall event, the infiltration rate may fall below the rainfall intensity; at this moment ponding starts and overland flow may begin. This mechanism of generation of overland flow from excess infiltration is termed Hortonian (Horton, 1933).

There are many methods for measuring infiltration experimentally (e.g. Klute and Dirksen, 1986). They differ in equipment and technical skill required, and in the accuracy and reproducibility of the results. Some require soil cores to be taken for laboratory analysis. Others measure infiltration of water in situ. The area of the soil surface on which measurements are taken, i.e. the spatial support of the measurement, may be a few square centimetres to several square meters. More importantly, measurement methods reproduce the process of infiltration differently: e.g. some methods measure infiltration at ponding conditions; others measure infiltration through non-saturated surfaces or under simulated rainfall. Not surprisingly, the final steady rates of infiltration measured with different methods may differ substantially. This final infiltration capacity can be termed effective hydraulic conductivity, but its physical meaning changes with the measurement method, so that methods are incommensurable with each other (Beven, 2001). Indeed, comparative studies have generally reported a lack of consistency among measurement methods (Clothier and Smettem, 1990; Reynolds *et al.*, 2000; Bagarello *et al.*, 2004; Paige and Stone, 2003).

Infiltration and Hortonian overland flow vary greatly in space and time. Most measurement methods estimate point-scale steady rate of infiltration. For most practical applications, however, the quantification of infiltration is needed at field, hillslope and watershed scales instead of at points. In integrated watershed planning in particular, the issue is frequently to locate where (or how often) infiltration will be exceeded and where (or how often) the overland flow could be triggered. Hydrological modelling at catchment scale requires strategies to simulate infiltration in space notwithstanding the limited knowledge of the phenomena and the limited availability of data in both space and time (Beven, 1992; Blöschl and Sivapalan, 1995; Karssenberg, 2002). A frequent strategy adopted in hydrologic modelling has been to define hydrologic response units, with the idea that infiltration (as well as other hydrological processes) will be more similar within the unit than between units (Blöschl and Sivapalan, 1995). Effective parameters for each unit can be defined deterministically (i.e. single parameter values) or stochastically (i.e. by assuming probability distribution functions of the parameters; e.g. Vertessy and Elsenbeer, 1999; Seguis *et al.*, 2002). Either way, effective parameters are usually obtained by calibration against measurements; this accounts for the scale of the model simulations and compensates for the model's conceptual and structural limitations.

An operative definition of the hydrologic response units must rely on data whose spatial patterns, and possibly their temporal changes, are available. The spatial information consists usually of topographic, soil, and land use maps. As soil porosity and soil surface characteristics are major factors affecting infiltration, soil maps are often taken as the basis for the definition of hydrologic response units. However, the use of pedo-transfer functions to derive infiltration parameters from soil map data has generally yielded very poor results (Jarvis *et al.*, 2002; Tietje and Hennings, 1996; Wösten *et al.*, 1999). On the other hand, due to the high variability of infiltration within short distances, the application of geostatistical approaches requires systematic measurements at very short distances and may even result in no spatial correlation (Loague and Gander, 1990; Al-Jabri *et al.*, 2002). Common sense suggests then that the available spatial information may guide the identification of the hydrologic response units and the design of experimental infiltration measurements aimed to characterize their hydrologic behaviour.

For subsequent up-scaling, the spatial and temporal supports of the experimental measurements should be as close as possible to the modelling scale and to the processes to be simulated (Karssenberg, 2002). However, large spatial and temporal supports often conflict with the possible number of replications. Quick experimental methods yielding many observations in a given time may result more informative than methods whose experimental conditions may be closest to the modelling purposes but use cumbersome equipment, take more time, and are more expensive (e.g. Bagarello *et al.*, 2004). Moreover, once the idea of incommensurability between measurement data and model parameters and the consequent need for re-calibration of model parameters has been accepted, a measurement method should better focus on correctly identifying the hydrologic response units rather than on quantifying the infiltration parameters. Following this reasoning, the “best” measurement method will (1) identify correctly the hydrologic units and (2) provide statistical information on infiltration variability within and between the hydrologic units, with limited resource investment in terms of money, people, and equipment.

Few studies have tested the reliability of the identification of hydrologic units for modelling spatial patterns of infiltration over a hillslope or a catchment. This is probably because observations of infiltration or, more practically, of Hortonian overland flow, are difficult to obtain (van Loon, 2002). The spatial pattern of overland flow can be observed after rainfall events through the patterns of erosion features, like rills and gullies, provided the rainfall event has been erosive (Takken *et al.*, 1999). However, this type of observation remains quite subjective. Alternatively, the occurrence of overland flow can be observed by means of unbounded devices, such as Gerlach troughs (Morgan, 1995) or overland flow detectors of various design (Kirkby *et al.*, 1976; Gascuel-Odoux *et al.*, 1996; Elsenbeer and Vertessy, 2000; van Loon, 2002). The figures for volumes of overland flow and for runoff coefficients obtained using such devices are uncertain as the contributing area is unknown (Gascuel-Odoux *et al.*, 1996). However, as they are cheap and can be made locally, overland flow detectors are useful in locating overland flow occurrence in quite large areas.

The objective of our study is to test the common practice of defining hydrologic response units as combinations of soil, land use and topography for modelling infiltration and Hortonian overland flow distribution at hillslope and catchment scale.

Materials and methods

Study area – Kwalei catchment

Kwalei catchment (4°48' S, 38° 26' E) is situated in the West Usambara Mountains, North-East Tanzania (Fig. 1). The catchment size is around 2 km² and the altitude ranges from 1337 to 1820 m. The terrain is very dissected, with more than half of the hillslopes steeper than 20 %. Average annual rainfall is approximately 1000 mm, with a bimodal distribution: a long rainy season from March through May and a short rainy season from October to January. Average daily temperature is 18 °C, with diurnal temperature ranges (12-25 °C) greater than annual ranges (16-20 °C). Five soil types occur

in the catchment (FAO, 1990): Humic Acrisols on the summits (48 % of the catchment), Haplic Lixisols on the summit footslopes (15 %), Haplic Acrisols on the ridges (29 %), Eutric Fluvisols (6 %) and Umbric Gleysols in the river valleys (1 %) (Meliyo *et al.*, 2001). The soils on the slopes are clayey and deep; the topsoils are porous and sandy and overlie clayey, deep, and well-drained horizons. Saturation conditions may occur only in the Umbric Gleysols in the valley bottoms. The highest part of the catchment is covered by mountain rain forest, whereas the middle and lower slopes are farmed. The vegetation cover is complex: annual crops are intercropped with perennials, fodder and fruit trees or timber woodlots. Annual crops are concentrated on the ridge shoulders: maize is the most cultivated crop, intercropped with bean, banana, cassava, and sugarcane. Soil preparation and weed control is done by hand-hoeing. The two-layer cultivation of banana and coffee is frequent on the steeper slopes along the incised streams. Irrigation is limited to the vegetable fields of the valley bottoms. The cartographic information comprised a soil map (Meliyo *et al.*, 2001); a land use map, and a Digital Elevation Model (DEM) of 20 m pixel size (Vigiak *et al.*, 2005). Rainfall was measured with a tipping bucket rain gauge recording at two minutes interval and placed at the catchment outlet.

Point measurement of effective hydraulic conductivity

Surface effective hydraulic conductivity was measured with three point infiltration methods: constant head method (CH, infiltrating surface *c.* 20 cm²), tension infiltrometer (TI, infiltrating surface *c.* 254 cm²) and mini-rainfall simulation (RS, infiltrating surface *c.* 525 cm²). The methods were selected because they require easily transportable equipment, use limited amounts of water, consist of relatively quick tests, but simulate infiltration in completely different ways. The measurements were done on ten fields (Fig. 1), selected to cover all the soil types, different landscape positions, and the main land use types occurring in the catchment (Table 1). All the measurements were done during the long rainy season of March-May 2002, using stream water for the field tests.

CONSTANT HEAD METHOD (CH). Effective hydraulic conductivity of soil cores was measured in the laboratory with the constant head method (Klute and Dirksen, 1986). Ten samples of five cm depth of soil were taken for each field, five at 0-5 cm depth and five at 5-10 cm of depth. The cores were pre-saturated for 24 hours. The constant head was set to five cm. The dataset was extended with core samples taken in five more locations (two replicates each) at 0-10 cm depth during the period March-May 2003, after verifying the homogeneity of the samples.

TENSION INFILTRMETER METHOD (TI). Apparent field-saturated hydraulic conductivity was estimated from observations of near-saturated hydraulic conductivity measured with a disk infiltrometer (Perroux and White, 1988). To maximize the number of observations per site, the experiment was conducted with the single test method, using one disk radius ($r = 9$ cm) and one tension ($h_0 = -30$ mm). Sites were pre-wetted to limit the influence of initial soil moisture conditions, and a sand layer was interposed to ensure good contact between the soil surface and the disk. Soil moisture before and after the disk application was measured by the gravimetric method. At least three measurements were repeated in each site. Near-saturated hydraulic conductivity K_h at the imposed pressure head h_0 was estimated according to the Improved White and Sully method proposed by Vandervaere *et al.* (2000a; 2000b).

Apparent field-saturated hydraulic conductivity was estimated from K_h by assuming an exponential function between hydraulic conductivity and water tension (Gardner, 1958), with the alpha parameter α_G taken constant between soil types and equal to the average exponent of eight water-retention curves ($\alpha_G = 0.467 \text{ cm}^{-1}$).

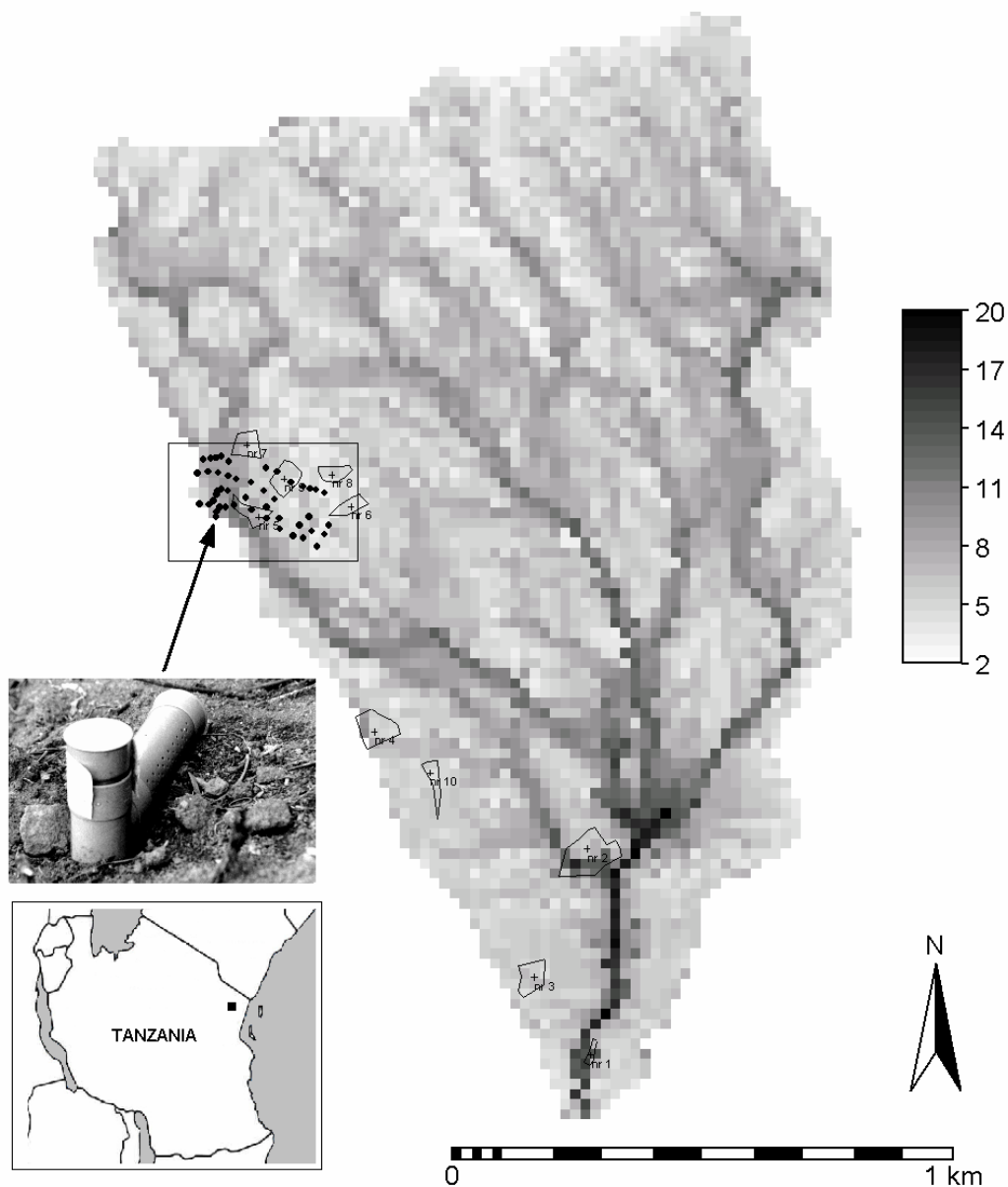


Figure 1. Kwalei catchment: location of the ten fields for infiltration measurement and of the subcatchment monitored for occurrence of overland flow (boxed area with dots indicating detectors). Shading represents the topography index of the catchment.

Table 1. Characteristics of the effective hydraulic conductivity measurement sites, Kwalei, Tanzania.

Site	Soil type FAO classification	Land use type	Topography			
			Slope (%)	Slope class ^a	Topography index	Top. index class ^b
1	Umbric Gleysols	Vegetables: tomato	2	1	11.28	3
2	Eutric Fluvisols	Maize and beans	7	1	10.28	3
3	Haplic Acrisols	Maize and beans	27	2	5.72	2
4	Haplic Acrisols	Coffee and banana	8	1	6.73	2
5	Haplic Lixisols	Coffee and banana	15	2	8.38	3
6	Humic Acrisols	Cassava (mixed with sugarcane)	37	3	4.66	1
7	Humic Acrisols	Forest	48	3	5.89	2
8	Humic Acrisols	Grazing	28	2	5.40	1
9	Humic Acrisols	Tea	38	3	4.89	1
10	Haplic Acrisols	Wattle	17	2	5.30	1

^a The slope classes were: class 1 ($\leq 10\%$), 2 ($10 < \text{slope} \leq 30\%$), and 3 ($> 30\%$).

^b The topography index classes were: class 1 (≤ 5.5), 2 ($5.5 < \text{topography index} \leq 8$), and 3 (> 8).

MINI-RAINFALL SIMULATION METHOD (RS). Effective hydraulic conductivity was measured in terms of effective steady-state infiltration rates measured during rainfall simulations. A portable rainfall simulator (Kamphorst, 1987) was used on rectangular plots of 0.0525 m^2 , bounded on three sides by metal strips and by a gutter on the fourth side where runoff was collected. Constant rainfall intensity was applied at 300 mm h^{-1} . The high rainfall intensity was not meant to reproduce steady-state infiltration under natural rainfall, but to induce runoff in all cases to allow comparisons between fields and to assure that the whole surface contributed to runoff (Paige and Stone, 2003). Runoff was measured every two minutes until a constant rate was measured; two rainfall simulation tests were repeated per site.

STATISTICAL ANALYSIS. The landscape variables for which consistent cartographic data was available were soil type, land use type, and topography. Two topographic variables were taken into consideration: maximum slope and topography index, defined as $\ln(a/\tan\beta)$, where a is the upslope contributing area, and $\tan\beta$ is the local slope (Beven and Kirkby, 1979). Maximum slope was estimated with an inclinometer in the fields. The topography index was calculated from the DEM by applying a multiple direction flow algorithm (Quinn *et al.*, 1995), and averaged across fields. The two topographic variables were employed as continuous variables and as ordinal classes (Table 1).

Surface effective hydraulic conductivity is usually log-normally distributed (Angulo-Jaramillo *et al.*, 2000). Original and log-transformed data distributions were tested for normality with the non-parametric Kolmogorov-Smirnov test. Variance of the log-transformed distributions of effective hydraulic conductivity was tested against the landscape variables at probability level $p = 0.05$. Analysis of variance were tested with classic ANOVA, if Levene test verified that variance among groups was homogeneous, and with Kruskal-Wallis test otherwise.

The significant landscape variables were employed to identify the hydrologic response units. However, landscape variables were correlated. By definition, the two topographic variables were correlated, so analysis of variance was conducted on both, but only the most important variable was employed to define the hydrologic units. The soil types were strongly correlated with topography (correlation coefficients $ETA > 0.90$). This reflected the real soil and land use distribution in the catchment: Umbric Gleysols and Eutric Fluvisols have developed on the central valley bottom, whereas Acrisols and Lixisols are concentrated along the slopes. Only two combinations of soil and land use types were present in the field sample (Table 1). Because of the high correlation between landscape variables, it was not possible to estimate interactions between factors. The classification of effective conductivity into hydrologic units was therefore based on the estimated marginal means for each independent variable of the univariate general linear model. The noncentrality parameters of the univariate tests were used to measure the observed power of the independent variables and to establish the hierarchy of classifiers: the main classifier was the variable that resulted in the largest differences among groups, and so on. Land use, soil types or topography classes that resulted in no significant mean difference in pair wise comparison were merged. In this way, all the possible combination of hydrologic response units, i.e. 9 land use types (8 tested + 'Others') \times 6 soil types \times 3 topography classes = 162 theoretical combinations, could be related to the cases for which measurements were available.

Overland flow observations

Overland flow occurrence was monitored per rainfall event by means of 50 overland flow detectors made locally to a slightly modified design of Vertessy *et al.* (2000). The detectors consisted of 30 cm long PVC tubes connected to a T-junction provided with a removable lid. About 50 holes of 2 mm diameter were drilled along one third of the PVC tube surfaces. The detectors were placed on the soil surface, with the drilled side facing upslope in order to catch any overland flow from the area immediately above (detail in Fig. 1). The overland flow monitoring was concentrated in a small subcatchment of around six hectares located in the upper, north-western corner of Kwalei catchment (box in Fig. 1). The area is representative for erosive slopes and is subject to frequent overland flow incidents. It has seven annual and perennial land use types: vegetables, fallow, tea, cassava, maize and bean, sugarcane, and coffee and banana. The area straddles two different soil types (Humic Acrisols on the shoulder slopes and Haplic Lixisols on the footslopes). Both soil types have thick, sandy clay loam to sandy and well structured topsoils, but Humic Acrisols are generally more gravelly than Haplic Lixisols (Meliyo *et al.*, 2001). However, no sensitive difference in gravel cover was evident in the area,

whose soil properties were therefore considered homogeneous. The slopes were convexo-linear, and steep (10-30 %). The 50 detectors were placed in four lines 250 m long along the 1580, 1560, 1545 and 1530 m contours, and crossing slopes 100 m long. During the period March-May 2002, after each rainfall event, the presence of water in the PVC tubes was recorded and interpreted in terms of overland flow occurrence (presence or absence).

The data were analyzed considering time-aggregated frequency, i.e. the number of times per spot when overland flow occurred divided by the total number of rainfall events. Time-aggregated frequency was analyzed in terms of landscape variables, i.e. land use type, slope and topography index. Soil type was excluded because of the apparent homogeneity of soil properties and because the available soil map was insufficiently detailed to place exactly the boundary between the Humic Acrisols and Haplic Lixisols in relation to the positions of the detectors. Besides classic ANOVA, data were analyzed with geostatistical tools. Hierarchical cluster analysis was carried on the original binary (present or absent) data for all events, using square Euclidean distance to measure between-group linkages. The statistical analysis was done using SPSS 11.5 software (SPSS, 2002), the geo-statistical analysis with GSTAT software (Pebesma, 2004), and the geographic analysis with ILWIS 3.1 (ITC, 2002).

Results and discussion

Point measurement of effective hydraulic conductivity

Some measurements of CH effective hydraulic conductivity were discarded because the soil cores had not been properly saturated. Also, some TI measurements were rejected because they yielded negative steady-state hydraulic conductivity K_h . The effective hydraulic conductivity was log-normally distributed for both CH and TI measurements; and normally distributed for RS. However, to keep the analysis homogeneous, the RS distribution was also log-transformed.

The three methods yielded different values of effective hydraulic conductivities (Table 2). The geometric means were all statistically different: CH yielded the highest geometric mean, followed by RS. TI resulted in the lowest effective hydraulic conductivity values (one order of magnitude lower than the other two methods) and in the largest variance and range of the log-transformed distributions. Site-wise correlation among the methods could only be established between CH and TI (Pearson correlation coefficient = 0.37) and between CH and RS (Pearson c.c. = 0.66), but not between RS and TI. These results are similar to those reported by Reynolds *et al.* (2000), who found both lack of consistency among effective conductivities estimated with different methods and lower values for TI in very permeable soils.

All the effective conductivity distributions fell within the ranges that can be estimated with pedo-transfer functions for similar soil conditions (Tietje and Hennings, 1996; Wösten *et al.*, 1999), and agreed well with the equation of Brakensiek *et al.* (1984). The CH and RS effective conductivities fell in

Table 2. Statistical results of effective hydraulic conductivity estimated by the three methods: constant head method (CH), tension infiltration (TI) and rainfall simulations (RS).

			CH	TI	RS
Sample number	n		100	37	20
Geometric mean	m h ⁻¹		0.3687	0.0397	0.1865
Harmonic mean	m h ⁻¹		0.2744	0.0276	0.1448
Kolmogorov-Smirnov test of original data	Z		1.488*	2.598*	0.609
Kolmogorov-Smirnov test of log-transformed data	Z		0.825	0.887	0.738
Log-transformed statistical moments	Mean	ln(m h ⁻¹)	-0.99767	-3.22562	-1.67955
	Min	ln(m h ⁻¹)	-3.32871	-5.09762	-3.25166
	Max	ln(m h ⁻¹)	+0.69099	0.10781	-0.95410
	St deviation	ln(m h ⁻¹)	0.71240	0.91117	0.65834
	Variance	[ln(m h ⁻¹)] ²	0.508	0.830	0.433
Analysis of variance	Soil type (d.f. 4)	F, χ^2 ¹	20.989*, ¹ (55.34)	1.354	3.725 ¹
	Land use type (d.f. 7)	F, χ^2 ¹	14.134* (100.01)	14.971*, ¹	16.745*, ¹ (244.65)
	Slope class (d.f. 3)	F, χ^2 ¹	8.292*	0.850	2.366 ¹
	Topographic index class (d.f. 3)	F, χ^2 ¹	15.267*, ¹ (32.58)	0.366	3.717* (78.15)

Effective 10-minutes rainfall peak intensity ranged from 3.6 to 85.2 mm h⁻¹ in the observation period.

* the value is significant at $p = 0.05$

¹ for the cases of non-homogeneous variance the value refers to the χ^2 of Kruskal-Wallis test, otherwise it is the F value of classic 1-way ANOVA. Values in brackets indicate the noncentrality parameter of the variable in the univariate general linear model.

the higher part of this range, while the TI conductivities fell in the lower tail of the range. In RS measurements, the high intensities applied, and possibly the use of stream water instead of distilled water (Assouline, 2004), induced accelerated sealing of the soil surface. Though at a slower rate, surface sealing was observed to develop also under natural rainfall conditions. Therefore, RS measurements are likely to overestimate effective infiltration under natural conditions. However, the variability among sites, i.e. differences among hydrologic units, should be well represented, as high rainfall intensities assured that all the plot surface contributed to runoff (Paige and Stone, 2003). Among the three cases, TI estimates of effective hydraulic conductivity were the most uncertain. The assumption of a Gardner exponential model with the alpha parameter constant for all soil types and equal to the water retention curve exponent, used to extrapolate the effective hydraulic conductivity from near-saturated measurements, may have introduced estimation errors. Infiltration tests at two or

more head pressures might have yielded higher confidence for the alpha parameter estimation, but would have reduced the number of spatial replications. However, the TI distribution of effective hydraulic conductivity was consistent with the other soil parameters estimated by the TI method, i.e. sorptivity, steady-state infiltration flux, and near-saturated hydraulic conductivity (results not shown here). The use of effective hydraulic conductivity, preferred for the sake of comparison with the other methods, was therefore considered reliable for defining the TI hydrologic response units.

Identification of hydrologic response units

The analysis of variance in terms of landscape variables revealed even more differences between the three distributions (Table 2).

All the landscape variables significantly affected the CH effective hydraulic conductivity. Land use type was the most powerful classifier, followed by soil type and topography index classes. Pair wise comparison allowed us to merge the land use types into 3 groups: forest + coffee and banana + cassava + tea (0.55 m h^{-1} on average); maize and bean + vegetables + grassland (0.25 m h^{-1}); and wattle (0.04 m h^{-1}). The soil types could be aggregated into two groups: upper and lower catchment soils. The upper-catchment soils (Humic Acrisols + Haplic Lixisols) were found to have a high mean effective hydraulic conductivity (0.46 m h^{-1}). The lower catchment soils (Umbric Gleysols + Eutric Fluvisols + Haplic Acrisols) covered the lower hillslopes and the valley bottom of the catchment and had mean effective conductivity of 0.29 m h^{-1} , i.e. half of that of the upper-catchment soils. Topography was the least important classifier.

The TI tests yielded opposite results. The only landscape variable affecting the variance of effective hydraulic conductivity was the land use. The original land use types could be merged into six final classes: tea (0.25 m h^{-1}), grassland + cassava (0.07 m h^{-1}), maize and bean + vegetables (0.04 m h^{-1}), coffee and banana (0.03 m h^{-1}), forest (0.02 m h^{-1}), and wattle (0.01 m h^{-1}). The very high values for the tea field should be treated with caution, as of the three replicates on the tea field, one failed and one seemed an outlier of the TI distribution, but was not rejected because it was in the median range of the entire set of effective hydraulic conductivity data.

RS tests revealed a significant effect due to land use and topography index, but no effect due to soil types. Again, the major classifier was land use. Land use types could be grouped into: forest + tea + coffee and banana (0.31 m h^{-1}), maize and bean + vegetables (0.21 m h^{-1}); and cassava + wattle (0.12 m h^{-1}). After classes 2 and 3 had been merged, slight differences between land units were given by topography index classes.

The three methods agreed about the high conductivity of tea fields, the constant association among maize and bean + vegetables in the median range of effective hydraulic conductivity, and the very low conductivity for wattle. All methods showed a strong effect of land use. Only CH revealed an effect of soil types. This may be because this method had the largest sample size, which may have yielded more information for differentiating between sites. However, even in this case, soil type had a lower classifying power than land use. This is surprising, especially considering that soil type is usually

considered the main landscape variable for defining hydraulic parameters (Tietje and Hennings, 1996; Wösten *et al.*, 1999).

Overland flow observations

From 10 March until 10 May 2002, 12 rainfall events caused overland flow and two resulted in no overland flow. Rainfall depth of effective rain events ranged from 2.8 to 38.5 mm, with recorded 10-minutes peak intensities ranging from 3.6 to 85.2 mm h⁻¹. The proportion of spots per effective rain event where overland flow occurred varied from 11 % to 94 %.

The number of times per spot during the entire rainy season when overland flow was detected, i.e. the time-aggregated overland flow frequency, was normally distributed and varied from 0 to 71 %, with a mean value of 44 %. The ability of overland flow detectors to catch overland flow accurately may be questioned. The T-tubes were quite short, so the microtopography and surface roughness of the spots where the detectors were located may have affected the probability of detecting overland flow once it occurred. To limit this problem, utmost care was taken to place the detectors in small depressions. Moreover, splashes of rain might have entered the small holes in the pipes; if this happens, the presence of water in the T-tube is not related to the occurrence of overland flow. Therefore, the presence of only a few drops of water in the T-tubes was considered evidence of splash water, not of overland flow. In future, sheltering the drilled part of the T-tube could avoid the interference of splashing drops. Notwithstanding the care we took during the experiment, these, and possibly other sources of errors might have occurred, blurring the information about overland flow occurrence. Very few studies have made use of this type of detector. Van Loon (2002) estimated that the observation error of the quantification of overland flow for such devices is around 18 % of RRMSE. However, in terms of presence or absence of overland flow (binary response), the observation error is likely to be much smaller.

Fig. 2 shows the time-aggregated overland flow frequency of the area. The grey background shows the actual soil erosion as assessed during the same period with the Assessment of Current Erosion Damage method (ACED; Herweg, 1996). ACED classes of erosion spanned from very low, i.e. fields with sporadic pedestals and no signs of sheet wash, to very high, i.e. fields with widespread interrills and presence of rills with cross sections larger than ten cm² (Vigiak *et al.*, 2005). Overland flow was more frequently detected in fields prone to severe erosion, while it was detected only at the upper edges of the fields prone to slight erosion. This confirms indirectly that the detectors' information is reliable. Fig. 2 shows that frequency of overland flow was highly variable in space, with large differences occurring within small distances. At one spot overland flow was never detected, whereas at its neighbouring spots less than 40 m away, overland flow was detected with a frequency that varied from 14 % to 64 %. Contrary to our expectations, overland flow was more frequent in the upper part of the subcatchment than in the lower part: mean frequency of runoff occurrence was 50 % at the highest contour lines (1560-1580 m) and 39 % at the lowest ones (1530-1545 m). This confirms that the observed overland flow was Hortonian. In fact, runoff resulting from saturation excess should be more

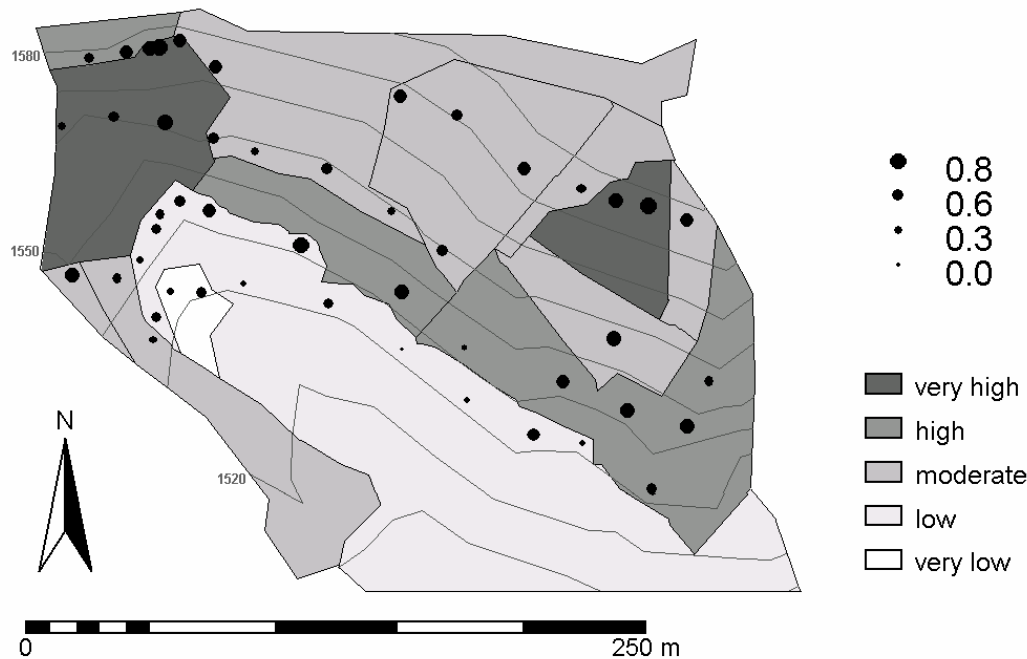


Figure 2. Time-aggregated overland flow frequency during rainy season March-May 2002 at Kwalei, Tanzania. Field grey shades indicate actual erosion of the fields observed in the same period (very low = sporadic pedestals; no signs of sheet wash; very high = widespread interrills; frequent rills with cross sections larger than 10 cm^2). The 10 m-contour lines are shown.

frequent on the lower part of the slopes, where soil moisture accumulates and where there might be a perched water table at or near ground level.

Rainfall variability in the area could not be measured, and spatially variable convective thunderstorms may occur in Kwalei catchment at the onset of the rainy season. Goodrich *et al.* (1995) showed that spatial variability in rainfall depth may be important even in areas as small as the monitored subcatchment. However, overland flow occurrence (not depth) depends more on the rainfall peak intensity than rainfall depth. During the rainfall event, it is the relationship between rainfall intensity and local infiltration characteristics that may trigger or not Hortonian overland flow in a given spot (Woolhiser and Goodrich, 1988). Rainfall variability may be an important component of the scatter of overland flow occurrence during a single rainfall event, especially at low rainfall intensities (Woolhiser and Goodrich, 1988). However, Goodrich *et al.* (1995) reported that measured peak rainfall intensities did not vary across their small experimental catchment and rainfall depths were shown to compensate in time. Moreover, the time-aggregated frequency data indicate a seasonal pattern, for which small variations of rainfall depth that may affect the spatial pattern of single rainfall events should be compensated. Therefore, rainfall variability, which may contribute to the variability of

Table 3. Land cover characteristics in the monitored area (average values per land use type).

	Canopy cover	Ground cover	Plant height
	(%)	(%)	(m)
Cassava	29	41	0.76
Coffee and banana	52	76	1.50
Fallow	48	70	0.80
Maize and bean	26	43	0.67
Sugarcane	38	55	0.91
Tea	27	37	0.55
Vegetables	13	22	0.40

overland flow occurrence at the single rainfall event, should exert negligible influence on the seasonal pattern.

Apart from the altitude gradient, no other pattern could be detected by visual inspection. This was confirmed by the analysis of variance. Overland flow frequency showed no significant relationships with land use types, slope or topography index. Soil type may affect the spatial pattern of overland flow, but this could not be verified in the monitored area. However, borders between soil types are usually gradual and not as abrupt as the observed pattern of overland flow frequency suggests. To search for landscape factors that could explain the observed pattern, we tested other derived topographic variables: the cumulative upslope area (to the watershed divide and of the immediate surroundings), and slope convergence across and along the main direction of slope. None of these variables were statistically related to the overland flow frequency.

The only variable that could significantly explain the variance of overland flow frequency was a reclassified land use variable that separated coffee and banana stands (i.e. the field classified as prone to slight erosion in Fig. 2) from all the other land uses. The average frequency of overland flow was 35 % in the coffee and banana stand and 48 % in the other fields ($F = 4.771$, significant at $p = 0.034$). This reclassification basically reproduced the altitude gradient. The reclassification of land use types, however, might explain why overland flow was more frequent on the slope shoulders than on the footslopes. Coffee and banana stands differ from the other crops both for canopy structure and land management. Table 3 shows the land use characteristics observed in Kwalei catchment during a field survey (Vigiak *et al.*, 2005). Canopy cover and ground cover were not significantly correlated to overland flow frequency. For example, in the fallow fields frequency of overland flow was 48 %, whereas in coffee and banana stands was only 35 %, notwithstanding the canopy cover and ground cover were similar (Table 3). Average plant height was not tested, because it varied a lot among fields, depending on the time of survey, the crop management and the degree of intercropping (coefficient of variation > 100 %). However, these three parameters are insufficient to describe the differences of canopy architecture among land use types. It is intuitive that rainfall interception is larger in the dense canopy of coffee and banana stands and on the large leaves of banana trees than in other crop covers. Rainfall interception plays a crucial role on the redistribution of rainfall that actually hits the ground. Canopy interception is also an extremely variable phenomena both in space and time (Jackson, 1971; Jackson, 2000), but while rainfall variability can be considered spatially random, the effect of canopy is

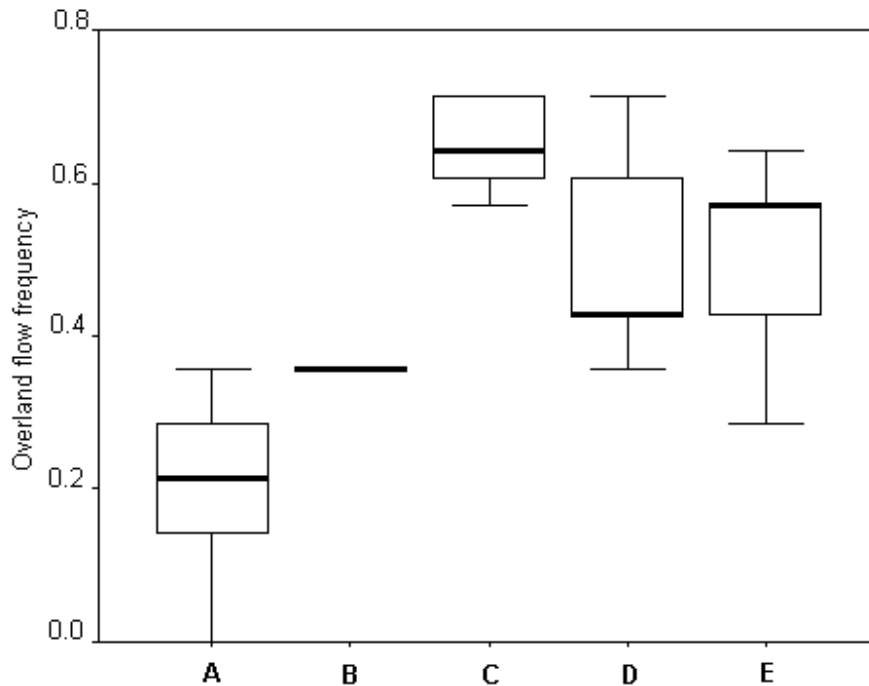


Figure 3. Box plots of time-aggregated overland flow frequency associated to clusters (see Figure 4 for locations). Cluster B comprised only one spot.

more constant in space. The support of overland flow detectors is small in comparison to such heterogeneity: this may explain the presence of spots where overland flow was never detected close to spots with mean overland flow occurrence. A second important difference between coffee and banana stands versus other crops is land management, which affects soil surface conditions. In coffee and banana stands a litter layer a few mm thick usually covers the soil surface. By contrast, the fields on the upper slopes (annual crops, fallow, tea, and sugarcane) are frequently hoed to prepare the soil and control weeds. This cultivation may temporarily increase soil roughness, but it degrades soil structure and removes the litter layer. As a result, the soil surface is more exposed to raindrop impacts and sealing. These conditions may favour the occurrence of overland flow notwithstanding that the vegetation cover may be high.

The original binary data, i.e. presence or absence of overland flow per spot and per event, were classified into hierarchical clusters. Five clusters could be distinguished, which were associated with different frequency distributions (Fig. 3). Cluster A had the lowest frequency and cluster C the highest. Clusters A and B (the latter consisting of only one spot) showed some similarities, and will converge at the next level of aggregation level. Clusters D and E will also converge at the next level of aggregation. Cluster C, however, stood out. It comprised the most “hot spots”, i.e. the points where overland flow occurred most frequently. “Hot spots” also appeared in clusters D and E, however. Eventually, at a higher level hierarchical level, clusters C, D and E will also merge, leading once again to the main pattern of Fig. 2.

Clusters were very scattered over the area (Fig. 4). This was especially true for cluster C (×), i.e. the

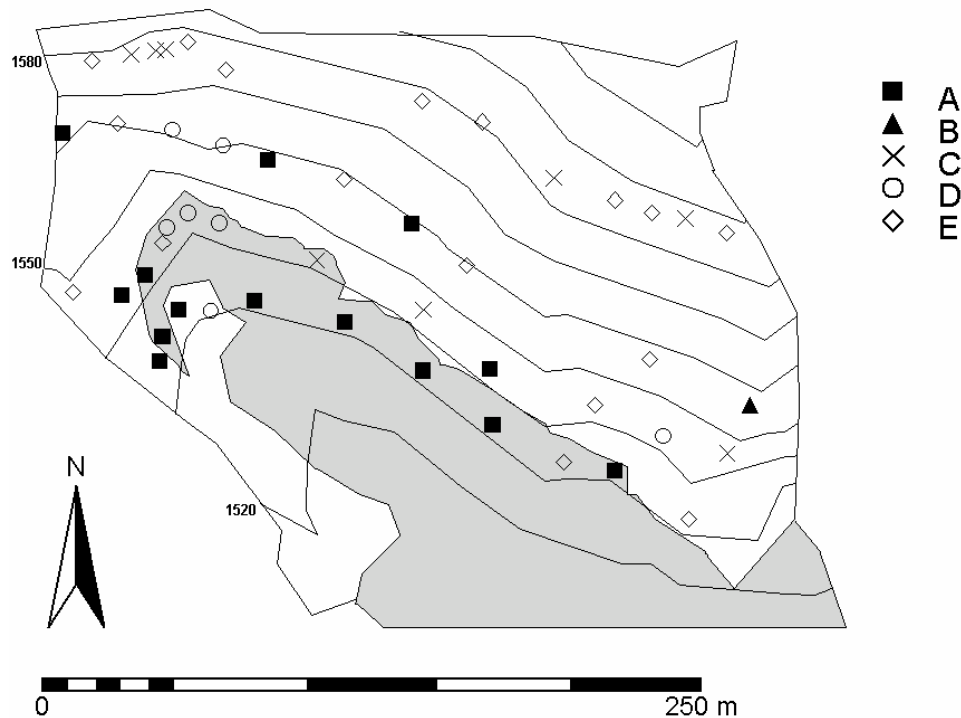


Figure 4. Clusters of overland flow occurrence during rainy season March-May 2002 at Kwalei, Tanzania. The grey background indicates the coffee and banana stand, the other land use types are in white. The 10 m-contour lines are shown.

critical spots, where overland flow occurred more frequently. Some spatial structure was also present. For example, cluster D (○) had a clear spatial aggregation, with all but one spots belonging to one converging slope. The highest spot of Cluster D had a time-aggregated frequency of 71 %, whereas the lowest one had a frequency of 43 %. This suggests that once overland flow was triggered somewhere in the upper part of the slope, it sometimes flowed far enough to cross into the coffee and banana stands on the lower slopes. In a similar way, some spots of cluster A (■), associated with low frequency of overland flow occurrence, were located in diverging slopes. The spots of cluster E (◇) in the right part of the monitored area also belonged to one single convex-linear slope, where overland flow was quite frequent. However, the central part of Fig. 4 is dominated by a mixture of clusters: here spots belonging to clusters A, C and E are scattered along and across slopes without apparent spatial order.

The spatial correlation of overland flow frequency was tested by geostatistical analysis. The best model that fitted the observed semi-variance of overland flow frequency was a spherical semi-variogram (Fig. 5). The semi-variance of the runoff frequency increased with distance up to 40-50 m; thereafter the scatter increased, showing that there was little spatial correlation. Visual inspection of clusters (Fig. 4) suggested that spatial correlation was around 15-20 m across slopes and 50-60 m along the slopes. Unfortunately, the slope direction changed at any spot so that anisotropic geostatistical analysis was not possible.

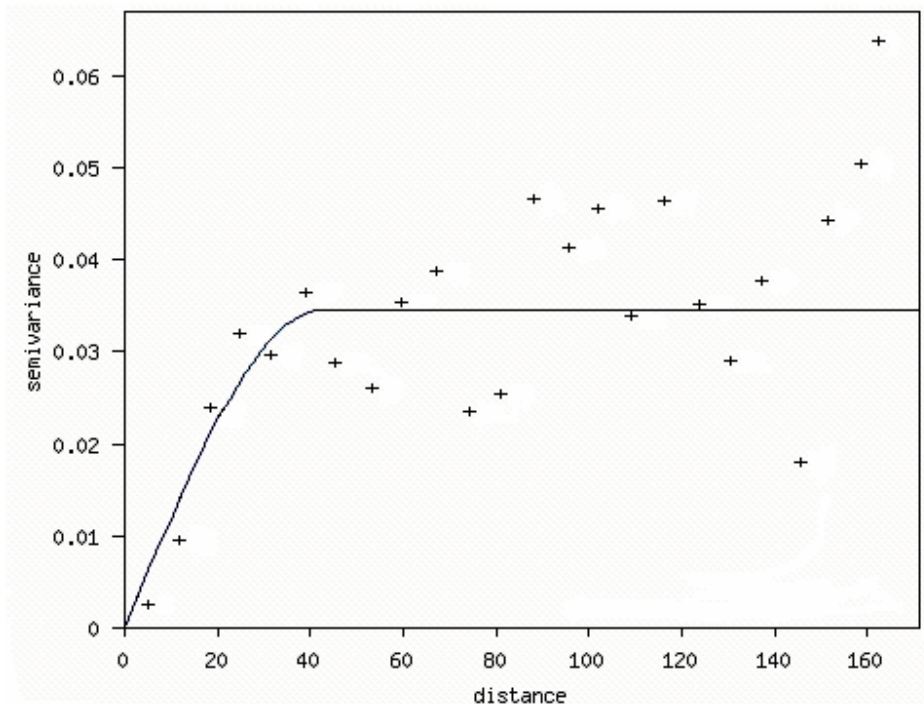


Figure 5. Semi-variogram of time-aggregated overland flow frequency.

Comparison of hydrologic response units and observed overland flow pattern

In Fig. 6a the overland flow clusters are presented in relation to the land use of the monitored area. Figs. 6b-d show the three hydrologic response unit patterns, i.e. the patterns of effective hydraulic conductivity obtained using the average effective conductivity per land use, soil type and topographic index class as defined by the three measurement methods. The darker the shade of grey, the higher the average effective conductivity of the field (note that the ranges vary among the methods). We expected that the higher the effective conductivity, i.e. the more permeable the soil, the less frequent would be the occurrence of Hortonian overland flow. This did not happen. For example, the tea and cassava fields were among the areas with the highest overland flow frequency (50 % and 68 %), whilst tea and cassava scored the highest CH and TI effective conductivities (Figs. 6b and 6c). RS also yielded a very high effective conductivity for the tea field, but at least the cassava field had the lowest effective conductivity (Fig. 6d). On the other hand, the coffee and banana stands should be very permeable, as their overland flow frequency was 35 %. This agreed with the CH and RS hydrologic units, even if in both cases coffee and banana stands were not statistically different from the tea field. The contrast between upper fields and the coffee and banana stands was well recognizable in the CH hydrologic response units, but less marked in the RS pattern, and even reversed in the TI pattern. TI assigned the coffee and banana stands to the least permeable soils. Probably, TI low infiltration rates were caused by the impedance of water infiltration along macropores (e.g. Reynolds *et al.*, 2000). In the coffee and

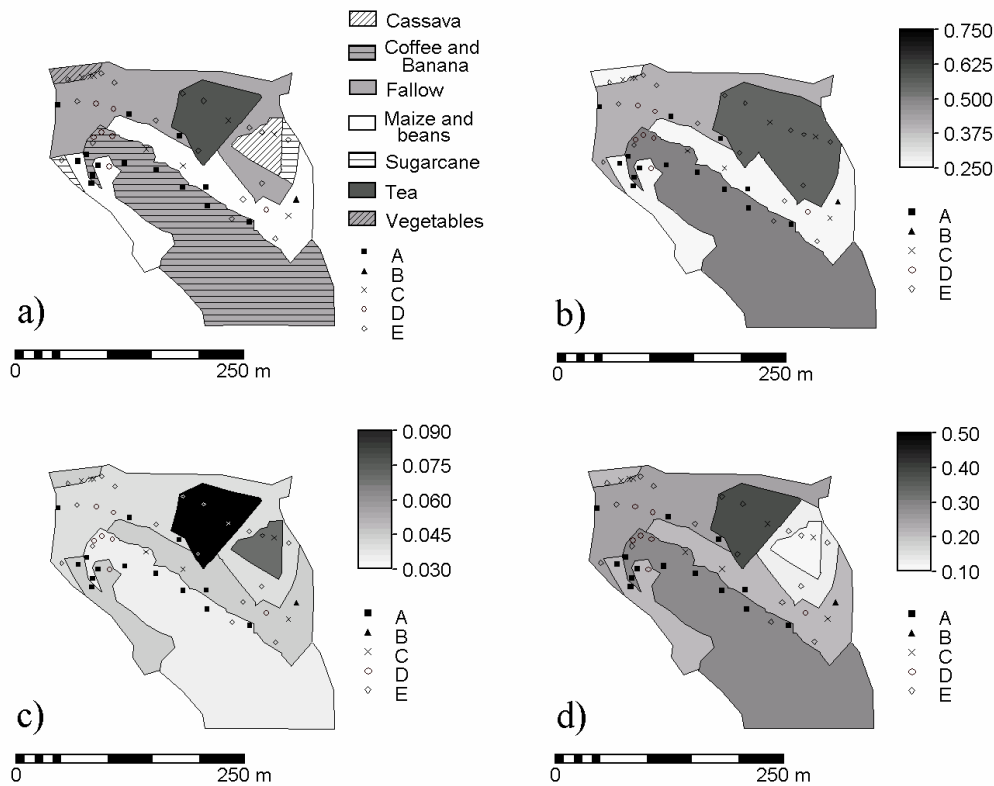
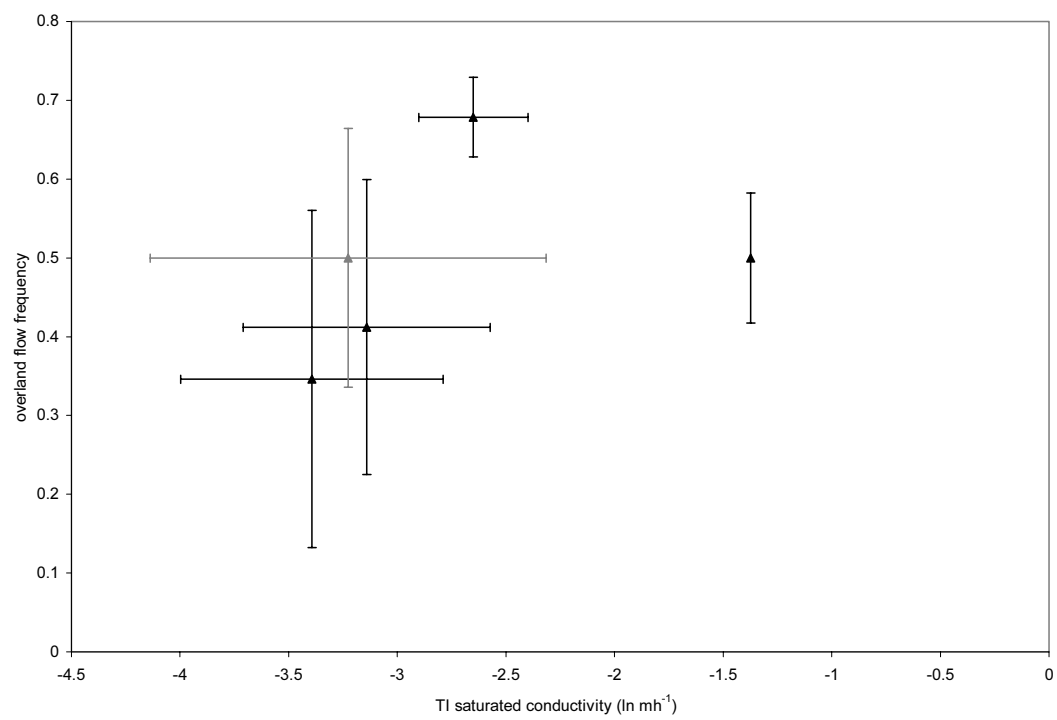
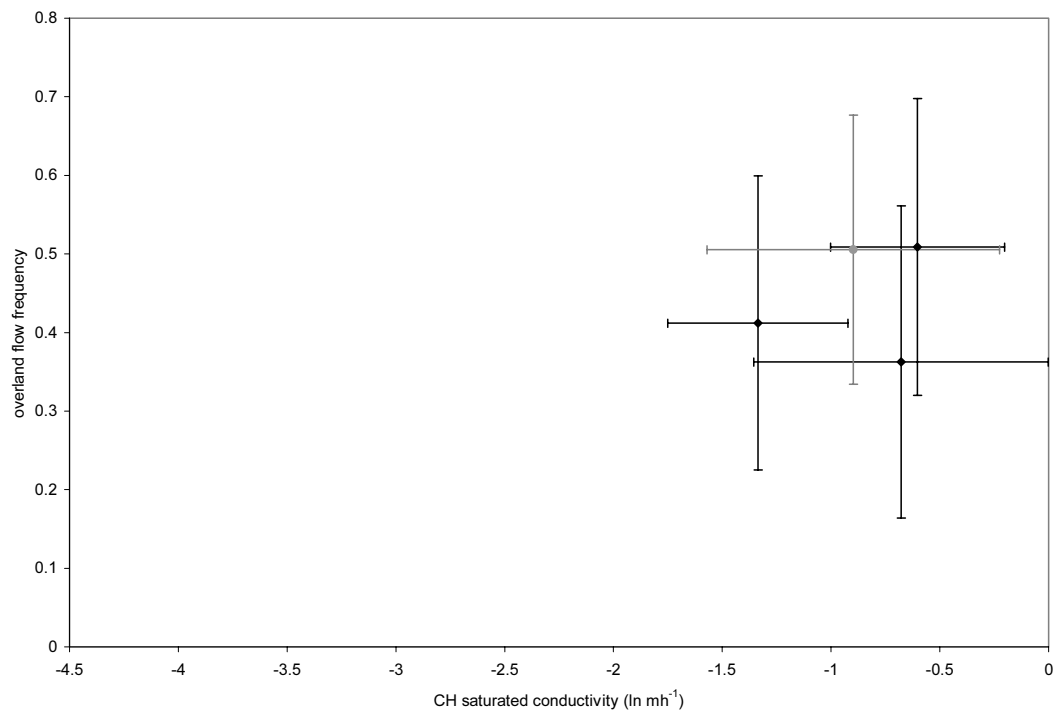


Figure 6. Overland flow cluster pattern in comparison with hydrologic response units: a) overland flow cluster and land use units of the monitored area; b) CH average effective hydraulic conductivity; c) TI average effective hydraulic conductivity; d) RS average effective hydraulic conductivity. Effective conductivity is expressed in m h^{-1} .

banana stands, macroporosity may be important, as biological activity is high and root systems are well developed.

Fig. 7 shows the stochastic component of the hydrologic response units. Each hydrologic unit is represented as a central point given by its average effective conductivity and the average overland flow frequency observed in that unit. The error lines indicate one standard deviation around this central point. The three distributions of effective conductivity are clearly separated, with TI and CH values at the extreme of the range, and RS in the central part. Though the central points of each hydrologic unit were separated, most units overlapped in both effective hydraulic conductivity and overland flow frequency ranges. The subdivision into hydrologic response units did not correspond to real differences in observed overland flow, but was instead mainly an artefact. This was particularly true for CH measurements, where all the units merged together. The TI measurement separated at least 1 unit from all the others (the cassava field, with high overland flow and high effective conductivity). The position of the tea field (the spot at the right) is uncertain, because the standard deviation of its effective conductivity could not be calculated. TI generally showed an increase in overland flow frequency associated with an increase in the mean effective hydraulic conductivity.



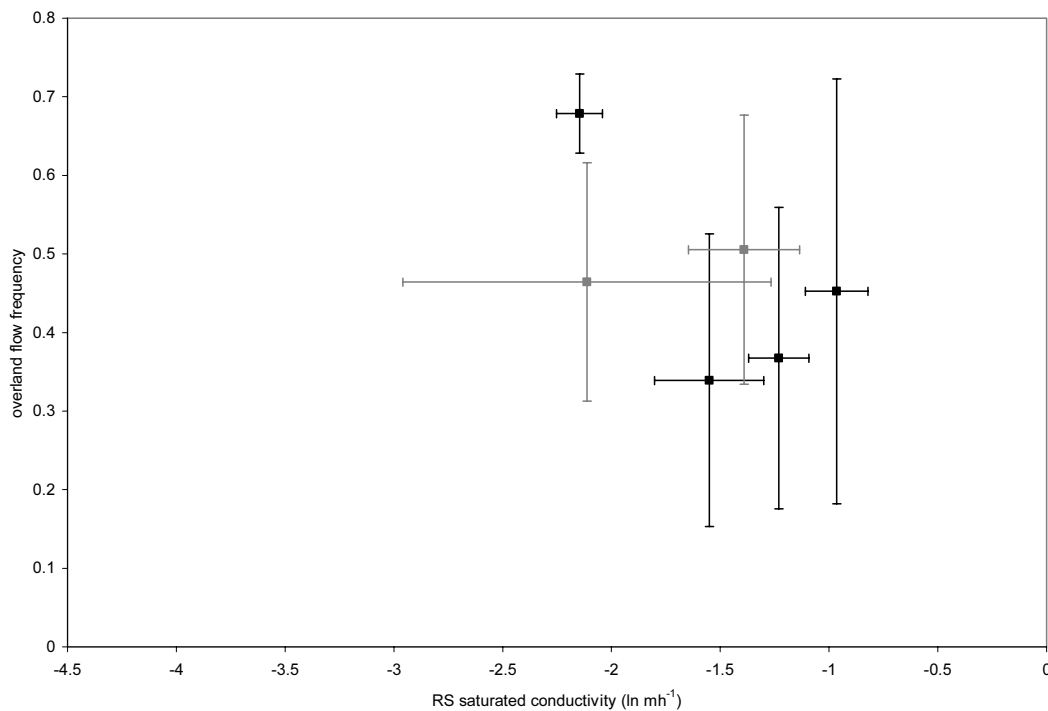


Figure 7. Scatter plot of hydrologic response units and overland flow frequency: CH (●), TI (▲) and RS (■). Central points indicate the average effective conductivity and the average overland flow frequency observed for each hydrologic response unit. Error lines indicate 1 standard deviation range. Black units represent land use types whose effective conductivity was directly measured; grey units represent a “generic” land use type (i.e. not included in the 10 measurement fields).

The RS hydrologic units appeared to be better separated from each other, with an increase of effective conductivity generally associated with a reduction of overland flow frequency. There was a low correlation between average RS effective conductivity and overland flow frequency (Pearson c.c. = -0.262; significant at $p = 0.075$), whereas for the CH and TI hydrologic units there was no correlation, neither linear nor non-parametric (R. Romanowicz, pers.comm., 2003). The RS units also separated the effect of topography: the difference between the two grey spots (a “generic” land use type) reflects a difference in topography index classes, with the left-hand spot for areas with topography index < 5.5 and the right-hand one for areas above this threshold. This separation also corresponded to a slight difference in overland flow frequency.

RS seemed to yield the best results. This was probably because the RS experiment simulated the infiltration process in the most pertinent way, simulating the action of raindrops impact and fast wetting and sealing of the soil surface. TI measurements at near-saturated condition failed to activate the macroporosity that was probably most active in infiltration and re-infiltration processes. The TI method also yielded the most uncertain results and required the longest experimental time; it was therefore the least appropriate method for this research. It is important to note, however, that TI was the only method to provide information on soil infiltration in unsaturated conditions, which is very valuable to

understand the soil hydrology. The CH method yielded large variances within groups and failed to differentiate among very different land use types, i.e. coffee and banana, tea and cassava. Again, measurement support made it impossible to account for large soil pores.

These conclusions are tempting, but may be misleading. The statistical correlation between RS hydrologic units and overland flow frequency was weak, with considerable overlap in overland flow frequency ranges of RS units. Basically, the only spatial pattern of overland flow that could be associated with land use, soil, and topography was the border between the upper fields and the coffee and banana stands on the lower slopes. This border, and the sequence cassava – maize and bean – coffee and banana stands were well captured by the RS units. However, no correlation was found between RS hydrologic units and overland flow clusters, i.e. the location of clusters and especially of “hot spots” remained largely unexplained by the hydrologic units explored in this study.

Conclusions

The spatial pattern of the overland flow occurrence observed in this study was practically independent from the field borders. Overland flow spots more than 40 m apart were not spatially correlated. It was particularly difficult to explain the location of “hot spots” of overland flow (especially cluster C) in terms of soil, land use or topography. This high spatial variability of overland flow is in accordance with reports for both saturation-excess (Elsenbeer and Vertessy, 2000; van Loon, 2002) and infiltration-excess overland flow (Gascuel-Odoux *et al.*, 1996). Overland flow is very variable in space and involves complex non-linear processes that guide the redistribution of overland flow along the slopes in complex patterns. Vegetation interception and local ecological characteristics, e.g. a local slope convergence, or an opening in the canopy cover, or a slightly compacted soil surface due to the passage of an animal, might trigger or not the occurrence of Hortonian overland flow.

The strategy of defining hydrologic response units in terms of landscape variables (soil, land use, and topography) and measuring effective conductivity to characterize their behaviour failed to capture the observed pattern of overland flow.

The causes of the failure are at least twofold. On one side, point infiltration measurements failed to account for infiltration through the soil macroporosity. This was particularly true for TI method, where impedance of water did not activate the macropores, and CH method, where macroporosity was interrupted by the extraction of soil cores. Of the three methods, RS yielded the pattern closest to the observations, probably because it most closely simulates the rainfall event processes that may trigger Hortonian overland flow in this environment, i.e. infiltration in macropores and fast sealing of the surface. These results stress once again the problem of measurement upscaling. Because processes differ at different scales, not only the values of effective hydraulic conductivity should not be directly used without calibration, but also the identification of the hydrologic response units and the estimation of parameter distributions could not be achieved with point-scale measurements.

A second, and probably more important, reason behind the strategy failure was that it neglected the effect of vegetation interception in the distribution of rainfall below the canopy. Rainfall interception

was the main process that could explain the only spatial pattern of overland flow that could be associated with the landscape variables, i.e. the border between cultivated fields on the slope shoulders and the coffee and banana stands at the foot of the slopes. Unfortunately, rainfall interception is also a highly variable phenomenon that is difficult to measure (Jackson, 1971).

In the face of the spatial heterogeneities of rainfall variability, canopy interception, soil sealing and infiltration, and the difficulties of measuring these processes, it is hard to formulate an alternative strategy to identify hydrologic response units. If the final modelling aim is the characterization of overland flow occurrence, then the use of overland flow detectors may be a valid alternative in defining hydrologic response units. Overland flow detectors require little investment and can give the direct picture of overland flow occurrence, without the need to extrapolate this information from indirect sources such as measurements of effective conductivity. The main drawback is that the detectors require occurrence of rainfall, so that observations are needed for a quite long periods (i.e. some rainfall events). However, spatial patterns contain hydrologic information, the exploration of whose potential has only recently been started (Grayson and Blöschl, 2000). Measurements may give new insights to formulate more appropriate modelling approaches (Beven, 2000). It is therefore by observing the spatial pattern of overland flow and gathering enough concurrent information that we may hope to characterize better the hydrological processes involved in Hortonian flow occurrence.

Acknowledgements

We are grateful to Dr R. Romanowicz, who explored the presence of non-parametric relationships in the dataset; to A. Koffeman, who contributed to the data collection and first analysis of effective conductivity measurements; and to the two anonymous reviewers for their useful comments and suggestions. This research was conducted within the EROAHI project “*Development of an improved method for soil and water conservation planning at catchment scale in the East African Highlands*”. The financial support from the Ecoregional Fund, the Partners for Water Programme and the DLO-Research Programme International Co-operation is gratefully acknowledged. Dr J. Burrough advised on the English of the draft manuscript.

References

- Al-Jabri SA, Horton R, Jaynes DB, Gaur A. 2002. Field determination of soil hydraulic and chemical transport properties. *Soil Science* **167**: 353-368.
- Angulo-Jaramillo R, Vandervaere J-P, Roulier S, Thony J-L, Gaudet J-P, Vauclin M. 2000. Field measurement of soil surface hydraulic properties by disc and ring infiltrometers. A review and recent developments. *Soil & Tillage Research* **55**: 1-29.

- Assouline S. 2004. Rainfall-induced soil surface sealing: a critical review of observations, conceptual models and solutions. *Vadose zone Journal* **3**: 570-591.
- Bagarello V, Iovino M, Elrick DE. 2004. A simplified Falling-head technique for rapid determination of field-saturated hydraulic conductivity. *Soil Science Society of America Journal* **68**: 66-73.
- Beven KJ, Kirkby MJ. 1979. A physically-based, variable contributing area model of basin hydrology. *Hydrological Science Bulletin* **24**: 43-69.
- Beven KJ. 1992. Future of distributed modelling. *Hydrological Processes* **6**: 253-254.
- Beven KJ. 2000. Uniqueness of place and process representations in hydrological modelling. *Hydrology and Earth System Sciences* **4**: 203-213.
- Beven KJ. 2001. *Rainfall-runoff modelling. The Primer*. John Wiley & Sons Ltd, 360 pp.
- Blöschl G, Sivapalan M. 1995. Scale issues in hydrological modelling: a review. *Scale issues in hydrological modelling*, J. D. Kalma and M. Sivapalan, Eds., John Wiley and Sons, 9-48.
- Brakensiek DL, Rawls WJ, Stephenson GR. 1984. Modifying SCS hydrologic soil groups and curve numbers for rangeland soils. St. Joseph. PNR-84-203.
- Clothier BE, Smettem KRJ. 1990. Combining Laboratory and Field measurements to define the hydraulic properties of soil. *Soil Science Society of America Journal* **54**: 299-304.
- Elsenbeer H, Vertessy RA. 2000. Stormflow generation and flowpath characteristics in an Amazonian rainforest catchment. *Hydrological Processes* **14**: 2367-2381.
- FAO. 1990. *Guidelines for soil description*. Third ed. Soil Resource management and Conservation Service, Land and Water Development Division, FAO.
- Gardner WR. 1958. Some steady-state solutions of the unsaturated moisture flow equation with application to evaporation from a water table. *Soil Science* **85**: 228-232.
- Gascuel-Oudou C, Cros-Crayot S, Durand P. 1996. Spatial variations of sheet flow and sediment transport on an agricultural field. *Earth Surface Processes and Landforms* **21**: 843-851.
- Goodrich DC, Faures J-M, Woolhiser DA, Lane LJ, Sorooshian S. 1995. Measurement and analysis of small-convective storm rainfall variability. *Journal of Hydrology* **173**: 283-308.
- Grayson R, Blöschl G. 2000. Spatial processes, organisation and patterns. *Spatial patterns in catchment hydrology*, R. Grayson and G. Blöschl, Eds., Cambridge University Press, 3-16.
- Herweg K. 1996. *Assessment of Current Erosion Damage*. Centre for Development and Environment Institute, University of Berne.

Horton RE. 1933. The role of infiltration in the hydrologic cycle. *Transactions of the American Geophysical Union* **14**: 446-460.

ITC. 2002. ILWIS 3.1 Academic

Jackson IJ. 1971. Problems of troughfall and interception assessment under tropical forest. *Journal of Hydrology* **12**: 234-254.

Jackson NA. 2000. Measured and modelled rainfall interception loss from an agroforestry system in Kenya. *Journal of Hydrology* **100**: 323-336.

Jarvis NJ, Zavattaro L, Rajkai K, Reynolds WD, Olsen P-A, McGechan M, Mecke M, Mohanty B, Leeds-Harrison PB, Jacques D. 2002. Indirect estimation of near-saturated hydraulic conductivity from readily available soil information. *Geoderma* **108**: 1-17.

Kamphorst A. 1987. A small rainfall simulator for the determination of soil erodibility. *Netherlands Journal of Agricultural Science* **35**: 407-415.

Karssenbergh D. 2002. Building dynamic spatial environmental models, Facultiet Ruimtelijke Watenschappen, Universiteit Utrecht, 224.

Kirkby MJ, Callan J, Weyman D, Wood J. 1976. Measurement and modeling of dynamic contributing areas in a very small catchment. University of Leeds: School of Geography. Leeds, U.K. Working Paper 167.

Klute A, Dirksen C. 1986. Hydraulic conductivity and diffusivity: Laboratory methods. *Methods of soil analysis*, 2nd ed. A. Klute, Ed., 687-734.

Meliyo JL, Kabushemera JW, Tenge AJM. 2001. Characterization and mapping soils of Kwalei subcatchment, Lushoto District. Mlingano Agricultural Research Institute. Tanga, 34 pp.

Morgan RPC. 1995. *Soil erosion & conservation*. Second ed. Longman, 198 pp.

Paige GB, Stone JJ. 2003. Infiltration and runoff: point and scale. In: *Proceedings of the International Symposium First Interagency Conference on Research in the Watersheds*, 27-30 October, Benson, AZ, K. G. Renard, S. A. McElroy, W. J. Gburek, H. E. Canfield, and R. L. Scott (Eds).

Pebesma EJ. 2004. GStat user's manual.[Available online from <http://www.geog.uu.nl/gstat/>.]

Perroux KM, White I. 1988. Design of disk permeameters. *Soil Science Society of America Journal* **52**: 1205-1215.

Quinn PF, Beven KJ, Lamb R. 1995. the $\ln(a/\tan b)$ index: how to calculate it and how to use it in Topmodel framework. *Hydrological Processes* **9**: 161-182.

Reynolds WD, Bowman BT, R.R B, Drury CF, Tan CS. 2000. Comparison of Tension Infiltrometer, Pressure Infiltrometer, and Soil Core Estimates of Saturated Hydraulic Conductivity. *Soil Science Society of America Journal* **64**: 478-484.

Seguis L, Cappelaere B, Peugeot C, Vieux B. 2002. Impact on Sahelian runoff of stochastic and elevation-induced spatial distributions of soil parameters. *Hydrological Processes* **16**: 313-332.

SPSS. 2002. SPSS

Takken I, Beuselinck L, Nachtergaele J, Govers G, Poesen J, Degraer G. 1999. Spatial evaluation of a physically-based distributed erosion model (LISEM). *Catena* **37**: 431-447.

Tietje O, Hennings V. 1996. Accuracy of the saturated hydraulic conductivity prediction by pedo-transfer functions compared to the variability within FAO textural classes. *Geoderma* **69**: 71-84.

van Loon EE. 2002. Overland flow: interfacing models with measurements, Wageningen University, 171.

Vandervaere J-P, Vauclin M, Elrick DE. 2000a. Transient Flow from Tension Infiltrometers: I. The Two-Parameter Equation. *Soil Science Society of America Journal* **64**.

Vandervaere J-P, Vauclin M, Elrick DE. 2000b. Transient Flow from Tension Infiltrometers: II. Four Methods to Determine Sorptivity and Conductivity. *Soil Science Society of America Journal* **64**: 1272-1284.

Vertessy RA, Elsenbeer H. 1999. Distributed modeling of storm flow generation in an Amazonian rain forest catchment: effects of model parametrization. *Water Resources Research* **35**: 2173-2187.

Vertessy RA, Elsenbeer H, Bessard Y, Lack A. 2000. Storm runoff generation at La Cuenca. *Spatial patterns in catchment hydrology*, R. Grayson and G. Blöschl, Eds., Cambridge University Press, 247-271.

Vigiak O, Okoba BO, Sterk G, Groenenberg S. 2005. Modelling catchment-scale erosion patterns in the East African Highlands. *Earth Surface Processes and Landforms* **30**: 183-196.

Woolhiser DA, Goodrich DC. 1988. Effect of storm rainfall intensity patterns on surface runoff. *Journal of Hydrology* **102**: 335-354.

Wösten JHM, Lilly A, Nemes A, Le Bas C. 1999. Development and use of a database of hydraulic properties of European soils. *Geoderma*: 169-185.

Chapter 4

A DISAGGREGATING APPROACH TO DESCRIBE OVERLAND FLOW OCCURRENCE WITHIN A CATCHMENT

Olga Vigiak, Renata J. Romanowicz, E. Emiel van Loon, Geert Sterk and Keith J. Beven

Journal of Hydrology. Submitted.

A DISAGGREGATING APPROACH TO DESCRIBE OVERLAND FLOW OCCURRENCE WITHIN A CATCHMENT

Abstract

A parametrically parsimonious, data-based model simulating the distribution of overland flow within a catchment was built on observations at hillslope and catchment scale collected in a small East African Highlands catchment (Kwalei, Tanzania). A rainfall-flow Data Based Mechanistic model defined catchment effective rainfall and separated two flow components: the quick flow, interpreted as a combination of overland flow and reinfiltration at the hillslope scale, and the slow flow, interpreted as ground water displacement. Two hydrologic response units (HRUs) were identified: perennial (HRU_1) versus other, mainly annual, crops (HRU_2). Observations of overland flow occurrence at the hillslope scale were used to derive HRU probability distribution functions (pdf) of overland flow occurrence in relation to effective rainfall. The pdfs were employed to disaggregate the catchment quick flow into HRU overland flow depth. Reinfiltration was incorporated in the toposequence by assuming that only the overland flow generated in the lower part of the field would drain out of it. Overland flow pdfs showed that at low effective rainfall, overland flow was more frequent in HRU_2, but at high effective rainfall overland flow in the two HRUs was similar. Comparison of model simulations versus observations in Gerlach troughs indicated that: 1) the effective reinfiltration length was on average 4 m; 2) the reinfiltration length was probably shorter in perennial crops and longer in annual crops; and 3) the model overestimated the effect of large rainfall events and underestimated that of intense rainfall events. Notwithstanding these limitations and in the face of the high variability of overland flow observed at the hillslope scale, model simulations of overland flow distribution within the catchment were considered satisfactory. The disaggregating approach pursued in our study represents a valid alternative to the more common use of infiltration equations to model overland flow within a catchment.

Keywords: DBM modelling; probability distribution functions of overland flow; reinfiltration; overland flow spatial pattern; Tanzania.

Introduction

In humid and wet tropical climates, the mechanisms of runoff generation active in small watersheds are multiple and complex (Dubreuil, 1985). Discharge recordings at the gauged outlet are often interpreted as combinations of base flow, quick flow and slow flow. Streams often carry water all the year around, even when the rainfall season is concentrated in 4-6 months of the year, fed by deep groundwater (base flow). Rapid and intense storms may generate a quick rise of the water level at the outlet within an hour. Infiltration-excess overland flow (Hortonian type), direct rainfall in the streams and saturation

excess overland flow (Dunne type) can all contribute to this rapid discharge (quick flow). Subsurface storm flow and return flow may create a secondary discharge component that is delayed by some hours after the rainfall event (slow flow; Dubreuil, 1985; Beven, 2001).

Rainfall-flow relationships have been the subject of much research work and many well established modelling methodologies exist (for a review see e.g. Beven, 2001). Among the various approaches, data-based mechanistic (DBM) modelling (Young, 1998; Young, 2003) has been developed in the last 20 years and has received much attention in recent literature (Young, 2003; Beven, 2001). DBM modelling rejects deterministic models (upward approach in the terminology of Sivapalan, 2003) as very difficult to identify, estimate and validate, and embraces instead an inductive methodology (downward approach). Arguing that rainfall-flow records usually contain information relative to the one-three main hydrologic mechanisms active in a given catchment, and therefore that complex models are often over parameterised, DBM modelling aims to identify the modal response of catchment rainfall-flow systems through robust statistical analysis tools. Statistical analysis of rainfall-flow time-series is employed to characterize the main hydrologic systems of the catchment, without formulating *a priori* hypotheses that may affect the analysis. In this sense, data analysis is used to suggest an appropriate structure of the hydrologic model (data-based modelling). However, to be acceptable, any model identified with the statistical tools must be interpretable in physical terms (mechanistic modelling). Such an interpretation usually follows established hydrologic paradigms, but sometimes may challenge them (Young, 2003).

DBM modelling has been applied in a wide range of environmental, ecological, economic and engineering systems (Young, 1998). Its application to rainfall-flow processes has been proven in a number of cases in both temperate catchments (Young, 1993; Young and Beven, 1994; Young, 2001a; Young, 2001b; Young and Tomlin, 2000; Young, 2003), and in tropical environments (Mwakalila *et al.*, 2001). The approach is particularly useful where measurements are of poor quality, because the statistical analysis applied to the model identification and estimation allows at the same time an efficient estimation of the uncertainties of model results (e.g. Mwakalila *et al.*, 2001).

The DBM approach therefore offers many advantages for catchment rainfall-flow modelling, thanks to its straightforward, statistically robust methodology, which makes it appropriate for rainfall-flow modelling and flood forecasts of gauged catchments (e.g. Young, 2002). However, it offers little insight into the hydrology at the hillslope scale, which in turn determines the pathways of overland flow and sediment movement within the catchment. The physical interpretation of a DBM model allows us to infer the dominant modes of response in the catchment, but as for any catchment rainfall-flow model, it is difficult to relate the apparent simplicity of the rainfall-flow relationships at the catchment outlet to the hillslope mechanisms of runoff generation (Sivapalan, 2003). Indeed, the complexity and heterogeneity of hillslope hydrology have been the main reasons behind the development of (upward) physics-based distributed models. Sivapalan (2003) argued that a reconciliation of the upward and downward approaches might be achieved through common and scalable features linking the hillslope and catchment scales, such as storage-discharge relationships or probability distribution functions for governing terrain attributes. The topography similarity index used,

for example, in Topmodel (Beven and Kirkby, 1979) offers an example of a linking feature in the case of saturation-excess overland flow.

In the case of infiltration-excess overland flow, however, a similar index has not yet been proposed. This is probably a result of the high variability and complexity of processes driving the occurrence of infiltration-excess overland flow, which are not yet fully understood (Beven, 2001). The occurrence of overland flow is usually modelled through infiltration equations, in which the most sensitive parameter is the effective hydraulic conductivity of the uppermost soil layer that governs the rate at which rainfall infiltrates into the soil. A strategy often adopted to model the spatial distribution of overland flow within a catchment is to assume hydrologic response units (HRU), i.e. areas where infiltration, and thus infiltration-excess overland flow, is more similar within the units than between units (Blöschl and Sivapalan, 1995), and to estimate for each HRU effective infiltration parameters. Unfortunately, infiltration parameters, and particularly the effective hydraulic conductivity, are highly variable in both space and time, and very difficult to measure at the appropriate scale (e.g. Karssenberg, 2002). To account for this variability, infiltration parameters can be defined stochastically through probability distribution functions instead of single deterministic values (e.g. Vertessy and Elsenbeer, 1999; Seguis *et al.*, 2002). In any case, as a consequence of the high variability of infiltration in space and time and because of scale issues, neither the identification of hydrologic response units nor the estimation of effective infiltration parameters can be easily achieved through infiltration measurements (Loague and Gander, 1990; Vigiak *et al.*, 2005a).

Due to the complexities of the hillslope mechanisms, however, an upward approach consisting of adopting an explicit infiltration equation with poorly identified parameters is in our view not appropriate, or required, for capturing the occurrence of overland flow within a catchment. It has been argued that observations of overland flow occurrence at the hillslopes may instead offer more direct information on hillslope scale hydrology (Vigiak *et al.*, 2005a).

The aim of this study was to develop a disaggregating (downward) approach linking catchment and hillslope scale observations to describe the spatial distribution of overland flow within a catchment, without introducing infiltration equations. This paper is the continuation of a study showing the complexity of the spatial patterns of overland flow occurrence observed in a tropical mountain environment (Kwalei catchment, Tanzania; Vigiak *et al.*, 2005a).

Materials and Methods

Study area – Kwalei catchment

The Kwalei catchment (4°48' S, 38° 26'E) is situated in the West Usambara Mountains, North-East Tanzania (Fig. 1). The catchment size is approx. 2 km², and altitude ranges from 1337 to 1820 m. The terrain is rough and highly dissected, with more than half of the hillslopes steeper than 20 %. Drainage comprises four permanent streams running north-west to south-east. Average annual rainfall is approximately 1000 mm, with a bimodal distribution. The long rainy season stretches from the end of

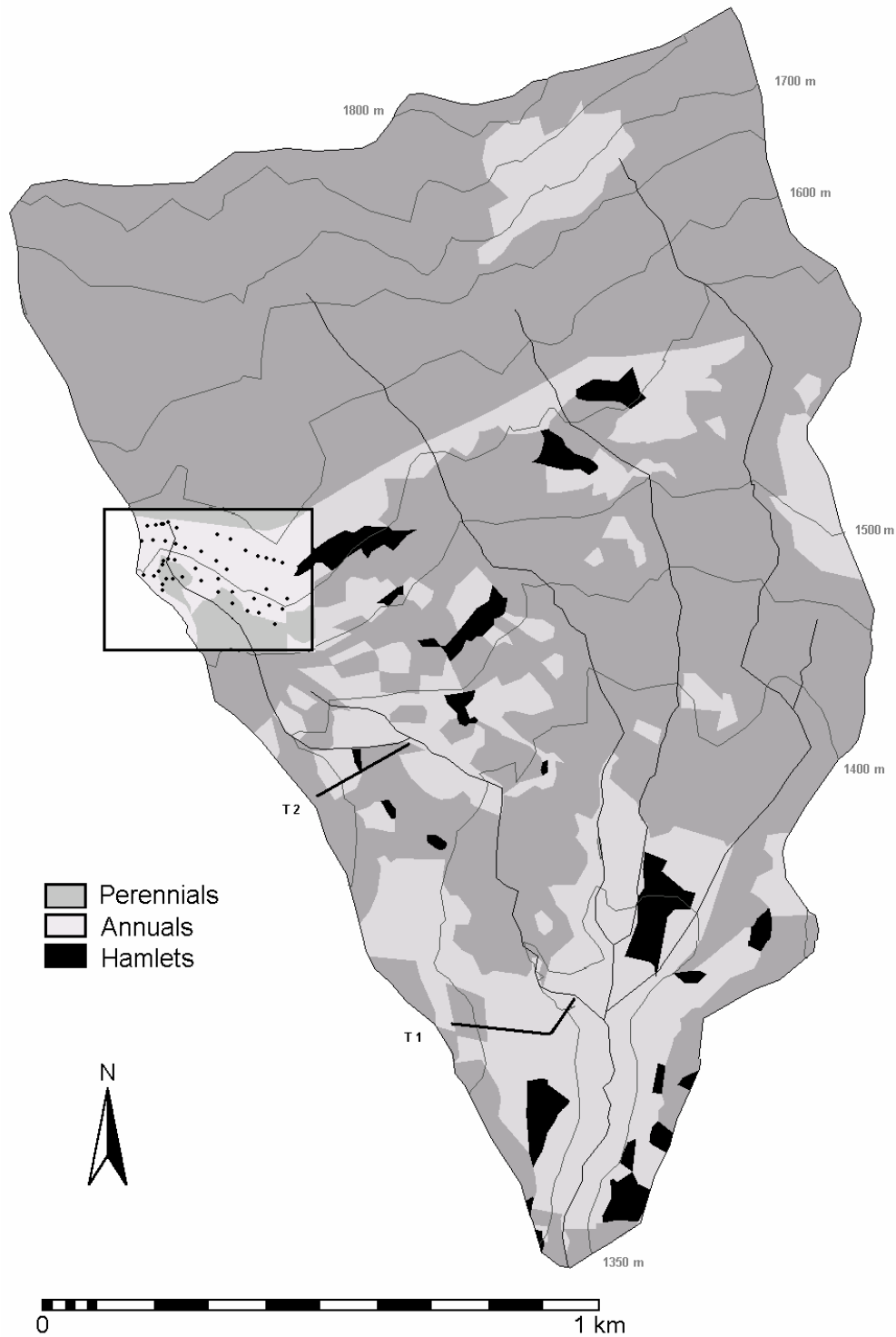


Figure 1. Location of hillslope monitoring areas in Kwalei catchment: the north-western subcatchment set in March-May 2002 (box, dots indicate location of runoff detectors), and the two transects set in March-May 2003 (bold lines). Shading represents the main land use types of the catchment. Grey lines are the 50 m contour lines, black lines indicate the drainage system.

February to the end of May and the short, less reliable rainy season from October to January. The average daily temperature is 20 °C, with diurnal temperature ranges (12-25 °C) greater than annual ranges of mean daily temperatures (16-20 °C) (Vigiak *et al.*, 2005b).

Soils on the slopes consist mainly of Humic and Haplic Acrisols (FAO-Unesco legend, FAO, 1990). They comprise porous, sandy topsoils, and clayey, deep and well-drained subsoils. Saturation may occur in the clayey and vertic Umbric Gleysols in the valley bottoms (Meliyo *et al.*, 2001).

The highest part of the catchment is covered by mountain rain forest, whereas the middle and lower slopes are used for agricultural purposes. Hamlets are located mainly along the ridge shoulders. Cultivation of annual crops is concentrated close to the compounds. Maize is the most commonly cultivated crop, often intercropped with bean, banana, cassava and sugarcane. The two-layer cultivation of banana and coffee is frequent on the steep slopes along the stream incisions. Valley bottoms are intensively planted with vegetables, the major cash crops of the area.

Observations at the catchment scale

Catchment rainfall and discharge were recorded at the catchment outlet in the period August 2001-June 2003. Rainfall was recorded using three tipping bucket rain gauges, one placed at the outlet, one in the middle valley and one in the upper slopes. The catchment outlet was equipped with a rectangular flume where a sonic water level meter recorded the water level at two minute intervals. The flow height-rating curve was derived from observations of flow velocity and water level during a major rainfall event (21-22 May 2003). The data were analysed using a State Dependent Parameter (SDP) method of the Captain Toolbox (Young *et al.*, 2001). The SDP method consisted of a non-parametric signal processing technique that is useful when model parameters change with the state of the input variables. The analysis involves two stages. First, the state dependency of the signal is identified non-parametrically by using a recursive Fixed-Interval Smoothing algorithm (FIS; Young, 2000). Then, the resulting non-parametric (look-up table) relationship is parameterised, so that the final estimation of the parameters that characterise the nonlinearities is statistically efficient (Young, 2001b). In the case of the flume rating curve, the flow and water level relationship was first identified non-parametrically, then parameterised in a power law relationship similar to the theoretical curve for rectangular flumes.

Analysis of the rainfall-flow records indicated that some technical problems occurred during the data collection campaign, critically affecting the quality of the data. The rain gauges positioned far from the outlet malfunctioned: many records were missing, and little correlation was found between their few records and the ones from the rain gauge at the flume. Therefore there was no choice but to rely on rainfall records at the flume station. Rainfall heterogeneity was observed, but could not be quantified.

Moreover, the sonic water level meter apparently failed to compensate for air temperature; as a result, the discharge records showed daily fluctuations that were not related to discharge changes. To limit the influence of poor data quality, rainfall and water level recordings were averaged to one hour time intervals. The use of filtering functions to reduce the noise in the measurements was rejected as it would affect the estimation of model parameters. Instead, the presence of noise, especially during intra-event periods, was taken into consideration during the evaluation of model results.

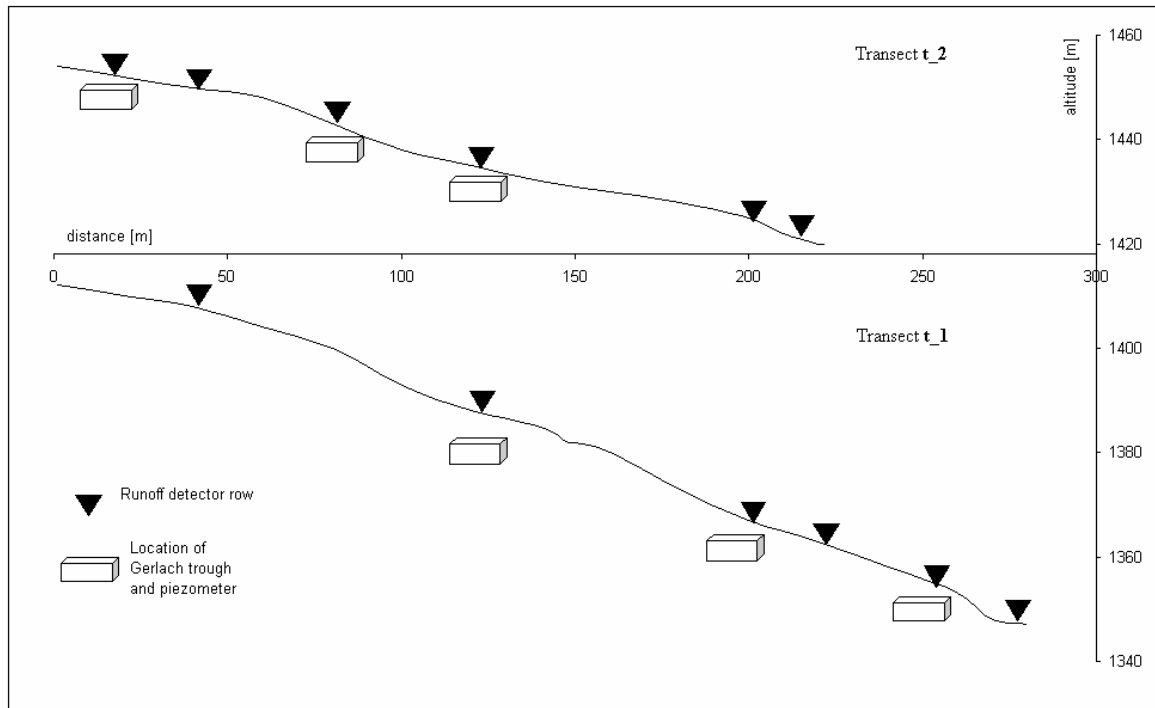


Figure 2. Profiles of the two longitudinal transects set for runoff monitoring during season 2003.

Observations at the hillslope scale

Observations at the hillslope scale in the long rainy season (March-May) 2002 aimed to gain insight into the hydrologic behaviour of the catchment. Overland flow occurrence was monitored by 50 runoff detectors (Vigiak *et al.*, 2005a). The detectors consisted of simple devices (30 cm long PVC-perforated tubes connected to a T-junction provided with a removable lid) able to catch overland flow occurring in their immediate upslope area. The detectors were placed on four, 250-m long contour lines, defining a small subcatchment of around six hectares located in the north-western corner of the catchment (Fig. 1). After each rainfall event, the presence of water in the tubes was recorded and interpreted in terms of overland flow occurrence (presence or absence).

In the long rainy season (March-May) 2003, hillslope scale observations were made to try to validate the perceptual hydrologic model defined on the basis of the year 2002 data. Observations concentrated on 2 longitudinal transects located at the lower (1380 m) and middle (1450 m) slopes of the catchment (Figs. 1 and 2). Transects spanned from the water divide to the drainage line and crossed representative sequences of annual and perennial crops on the most frequent soil type of the catchment (Haplic Acrisols). Transects consisted of six rows of four runoff detectors each, placed at 10 m intervals along the contour line, with a total transect width of around 40 m. Three 0.50 m wide Gerlach troughs (Gerlach, 1967) were installed at different positions along each transect. After each rainfall event, observations consisted of overland flow occurrence in the runoff detectors (presence or absence) and volumes of overland flow collected in the Gerlach troughs.

Rainfall-flow DBM modelling

According to the methodology developed by Young (1993; 2002), the nonlinearity of the rainfall-flow process may be filtered by the transformation of measured rainfall into effective rainfall. The relationship often assumes a simple power-law form that uses gauged flow as a surrogate measure of the soil-water storage in the catchment:

$$u_t = f(y_t)r_t \quad (1)$$

where u_t denotes the effective rainfall and r_t denotes measured rainfall. The scalar function $f(y_t)$ describes the nonlinearity between the effective rainfall and the flow y_t , interpreted as a surrogate of catchment soil moisture. In our study, the function $f(y_t)$ was characterised using again SDP estimation techniques, at first non-parametrically using the recursive FIS algorithm, then parameterised in a power law form (Young, 1993; Young and Beven, 1994). The optimisation procedure of this second stage included the concurrent estimation of the linear Stochastic Transfer Function (STF) model between effective rainfall and flow.

The effective rainfall is the input variable of the Single Input Single Output STF, whose general form is:

$$y_t = \frac{B(z^{-1})}{A(z^{-1})}u_{t-\delta} + \xi_t \quad (2)$$

The polynomials $A(z^{-1})$ and $B(z^{-1})$ are defined by:

$$\begin{aligned} A(z^{-1}) &= 1 + a_1 z^{-1} + \dots + a_n z^{-n} \\ B(z^{-1}) &= b_0 + b_1 z^{-1} + \dots + b_m z^{-m} \end{aligned} \quad (3)$$

where z^{-1} denotes the time shift operator; $b_i, i = 0, 1, 2, \dots, m$ and $a_j, j = 1, 2, \dots, n$ coefficients denote the parameters of the n - m STF polynomial; δ denotes the pure, advective time delay present in the system; and ξ_t denotes the noise (not necessarily white).

The Steady State Gain (SSG) of the model is given by:

$$SSG = \frac{\sum_{i=0}^m b_i}{1 + \sum_{j=1}^n a_j} \quad (4)$$

and describes the portion of rainfall that reaches the catchment outlet, whereas the loss efficiency, i.e. the water lost in the catchment, is equal to $1 - SSG$.

In rainfall-flow modelling the STF is often a second order polynomial that can be decomposed into two parallel components, a quick and a slow component. The quick component is usually interpreted in terms of surface flow, but may include some fast subsurface responses, whereas the slow component is often ascribed to subsurface and groundwater processes (Young and Beven, 1994; Young, 2003). This physical interpretation is similar to other linear transfer function models, such as the Bedford-Ouse

model (Whitehead *et al.*, 1979) and the IAHCRES model (Jakeman *et al.*, 1990), or more generally to their precursor, the unit hydrograph model (Sherman, 1932).

The decomposition of the discharge into the quick and slow components has the form:

$$y_t = y_{1,t} + y_{2,t} + \varepsilon_t \quad (5)$$

where

$$\begin{aligned} y_{1,t} &= \frac{\beta_1}{1 + \alpha_1 z^{-1}} u_{t-\delta} \\ y_{2,t} &= \frac{\beta_2}{1 + \alpha_2 z^{-1}} u_{t-\delta} \end{aligned} \quad (6)$$

$y_{1,t}$ represents the quick flow; $y_{2,t}$ represents the slow flow; $\alpha_1, \alpha_2, \beta_1, \beta_2$ are parameters derived from eq. (2); u_t is the effective rainfall (eq. 1) and ε_t represents the estimation error at the time t . From eq. (6), the discrete equivalents of the Steady State Gain ($SSG = \frac{\beta_\phi}{1 - \alpha_\phi}$) and the time constant ($T_\phi = \frac{-1}{\log(-\alpha_\phi)}$) of the quick ($\phi = 1$) and the slow ($\phi = 2$) flow components can be derived.

The identification and calibration of the DBM rainfall-flow model was performed on November-December 2001 hourly data. Model validation was done for March-May 2003 hourly data.

Disaggregating of overland flow among hydrologic response units (HRUs)

We built a theoretical model to predict HRU overland flow in relation to the catchment outlet discharge. According to the interpretation of the DBM model, we assumed that the quick flow component of the discharge was the aggregated response of the catchment to predominantly surface flow. We further assumed that the contribution of each HRU could be disaggregated by estimating the probability density functions (pdf) of overland flow occurrence in each HRU as a function of the effective rainfall.

The first step of the analysis consisted of a non-linear regression analysis that modelled the observed HRU frequency of overland flow occurrence as a function of the effective rainfall u . The runoff detectors were divided among HRUs. For each observation and HRU, the frequency was given by the number of detectors where overland flow was detected divided by the total number of detectors. The observed presence-absence of overland flow was assumed as resulting from the peak infiltration-excess since the previous observation, and was measured as the maximum (peak) hour effective rainfall u_t of the intra-observation interval (u_{max}). The regression assumed the form:

$$P_k = \Psi_k(u_{max}) \quad (7)$$

P_k linked overland flow occurrence of the k th HRU to the effective rainfall u . At any u , P_k gave the HRU mean overland flow occurrence. The information on the variance of overland flow occurrence, necessary to characterise the probability distribution function of overland flow in u , was contained in the Jacobian matrix associated with the estimated P_k .

In the second step of the analysis, we assumed that the HRU probability distribution functions of the overland flow occurrence $G_k(u)$ were Gaussian at any u . This assumption was justified by the observations of Hjelmfelt and Burwell (1984), who reported that the spatial variability of overland flow was normally distributed. Mean and standard deviation of $G_k(u)$, $\mu_{k,u}$ and $\sigma_{k,u}$, were estimated from P_k and the Jacobian matrix associated to P_k , respectively. The HRU fraction contributing to the overland flow was then considered equal to $G_k(u)$ integrated between 0 (no occurrence, i.e. nowhere) and 1 (complete occurrence, i.e. everywhere).

At any time step, the overland flow generated by the catchment, i.e., the quick flow component $y_{1,t}$ (eq. 6) of the discharge, could then be considered equal to the sum of the fractions contributed by all HRUs:

$$y_{1,t} = \sum_k w_k \int_0^1 G_k(u_t) \quad (8)$$

where w_k is the area of the k th HRU.

From eq. (8), the average overland flow depth $F_{k,t}$ occurring at the k th HRU at any time step could be defined as:

$$F_{k,t} = \frac{y_{1,t}}{A} \left(\frac{w_k \int_0^1 G_k(u_t)}{\sum_k w_k \int_0^1 G_k(u_t)} \right) \quad (9)$$

where A is the total catchment area.

Modelling of reinfiltration along the slopes

The disaggregation of quick flow allowed an estimation of average overland flow depth ($F_{k,t}$) occurring per HRU at each time step. However, the distribution of the overland flow within the catchment depended also on the topographic connectivity of the fields. Therefore, an overland flow accumulation procedure along the slopes was incorporated into the model. The reinfiltration of the overland flow was accounted for by assuming that only the portion of overland flow generated in the lower part of the field could drain out of it (run-off). The maximum field area generating run-off was equal to the length of the lower field border times the characteristic reinfiltration length L , i.e. the average length along which the overland flow travels along the soil surface before reinfiltrating in the soil. If one field drained to more fields, the ratio of the overland flow draining to any receiving field was proportional to the fraction of border length common to the draining and the receiving fields. A field land use map of the catchment was available (Vigiak *et al.*, 2005b). A connectivity matrix linking fields from the upslope (the watershed divide) downwards to the channel streamlines was defined through observations

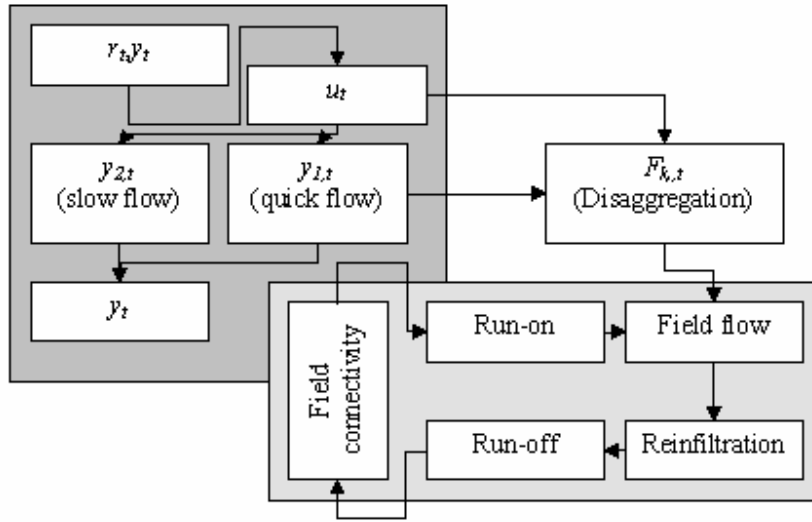


Figure 3. Overview of the hydrologic model: on the left the DBM rainfall-flow model (catchment scale); on the right the disaggregation of quick flow among the hydrologic response units (HRUs; hillslope scale); below, the accumulation of overland flow along the slopes, taking account of reinfiltration (field scale).

of flow direction surveyed in the fields. The stream lines were the final collectors of the overland flow slope accumulation and drained to the outlet.

The complete modelling sequence comprised (Fig. 3): 1) the rainfall-flow DBM model deriving effective rainfall u_t and quick flow $y_{1,t}$; 2) the disaggregation of quick flow $y_{1,t}$ among HRUs, defining $F_{k,i,t}$; and 3) the fields' sequence of run-on and run-off, dependent on the topographic connectivity and the characteristic length of reinfiltration L .

The characteristic reinfiltration length parameter L of the model was assumed equal to the average length of the contributing area of the Gerlach troughs placed along the transects. The Gerlach trough contributing area, given by the Gerlach trough width times the reinfiltration length L , was then estimated by comparison of model simulations against the Gerlach trough observations of overland flow depth.

Results and discussion

The hydrologic perceptual model

In the long rainy season of 2002, 12 events generated overland flow (Table 1), whereas 14 events were recorded in the 2003 season (Table 2). Rainfall events were short, intense and localized at the on-set of the rainy season and became progressively longer, less intense and spatially spread toward the end of the season. Even small rainfall events triggered occurrence of overland flow, but rainfall events with 30-minute peak intensities of less than 3 mm h^{-1} generated overland flow in less than 33% of detectors.

Chapter 4

Table 1. Overland flow occurrence in March-May 2002, Kwalei catchment, Tanzania: rainfall event amount; 30-minute peak intensity and overland flow frequency in runoff detectors (i.e. fraction of runoff detectors where presence of runoff was detected divided by total number of detectors).

Date	Rainfall event		Overland flow frequency in runoff detectors
	Amount (mm)	Peak I (mm h ⁻¹)	
10 March	20.0	35.6	0.94
21 March	4.6	9.2	0.11
27 March	25.0	42.8	0.52
2 April	7.4	11.2	0.37
3 April	7.8	10.8	0.46
5 April	2.0	3.6	0.59
9 April	5.2	10.4	0.74
15 April	1.0	2.0	0.22
18 April	10.6	10.8	0.87
22 April	1.6	2.8	0.24
25 April	3.0	4.8	0.50
1 May	3.0	3.2	0.72

Table 2. Transect observations in March-May 2003, Kwalei catchment, Tanzania: rainfall event amount and the 30-minute peak intensity; overland flow frequency in runoff detectors; and overland flow volumes recorded at the Gerlach sites (number of Gerlach with overland flow, average volume and coefficient of variation).

Date	Rainfall event		Overland flow frequency in runoff detectors	Gerlach troughs		
	Amount (mm)	Peak I (mm h ⁻¹)		n	mean (dm ³)	c.v. (%)
11 March	1.4	2.8	0.29	1	0.085	
23 March	2.0	2.0	0.27			
24 March	29.8	55.6	0.93	4	0.299	170
29 March	6.8	5.2	0.91	2	0.009	42
31 March	15.0	25.2	0.91	6	0.366	119
2 April	14.4	22.8	0.98	6	0.995	148
3 April	20.8	32.8	0.98	5	1.423	98
5 April	10.0	13.2	0.91	1	0.580	
1 May	5.4	7.6	0.38	1	0.125	
7 May	1.8	2.0	0.18			
19 May	16.8	7.6	0.98	3	0.013	141
20 May	65.2	12.6	1.00	4	0.431	151
23 May	57.4	8.8	0.98	4	1.606	63
25 May	2.2	5.4	0.67	4	0.283	100

The frequency of overland flow occurrence increased with rainfall amounts and intensities, but no simple correlation was found between rainfall characteristics and overland flow occurrence. In the 2003 season, with the exception of the first storm, overland flow was recorded in the Gerlach troughs only when rainfall was above 5 mm, and when overland flow occurrence recorded by the detectors was above 50 % (Table 2). Volumes of overland flow were low; the maximum recorded volume was 3.95 dm³, recorded in the lowest field of transect 1 (Gerlach G3). Only in two events all Gerlach troughs recorded overland flow. Hillslope observations indicated that overland flow occurrence was highly variable, both in location and volumes, especially at small rainfall events. This confirms the high variability of hillslope overland flow processes reported in literature (Hjelmfelt and Burwell, 1984; Gascuel-Oudou *et al.*, 1996; Elsenbeer and Vertessy, 2000; van Loon, 2002; Vigiak *et al.*, 2005a).

A more detailed analysis of the hillslope observations was reported elsewhere (Vigiak *et al.*, 2005a). The most important conclusions were: 1) the main mechanism of generation of overland flow in the fields was of infiltration-excess; 2) reinfiltration along the slope was frequently observed and represented an important hillslope hydrological process; 3) no noticeable influence of soil type or topography on overland flow occurrence was detected; 4) two hydrologic response units (HRUs) could be identified: perennial crops (HRU_1: coffee and banana stands, forest and banana and maize fields) versus other crops (HRU_2: mainly annual crops). In HRU_1 overland flow occurrence was observed less frequently than in HRU_2, because of a number of concurrent conditions, i.e. higher canopy interception, presence of litter, better topsoil conditions in HRU_1 than in HRU_2, which were not only related to differences in infiltration as measured in the field (Vigiak *et al.*, 2005a).

The discharge at Kwalei catchment outlet was interpreted as the combined result of different mechanisms of runoff generation: the overland flow generated along the slopes, mainly of Hortonian type, reinfiltrated usually within distances shorter than 20 m (Vigiak *et al.*, 2005a). This reinfiltrated flow and the subsurface flow contributed to the displacement of 'old' water stored in the soils, generating the quick flood wave in response to the rainfall event. Rainfall falling directly on the perennial streams or on the saturation-prone Gleysols in the valley bottom would probably contribute to this first discharge wave, but because of the limited extension of these areas (approximately 1 % of the catchment), their contributions were considered negligible. A large portion (> 90 %) of the rainfall did replenish the catchment storage, to be partly lost either by evapotranspiration or deep leakage, and partly be routed to the outlet (*c.* 11 %, base flow). This interpretation is in agreement with the hydrologic behaviour of many catchments in the wet tropics (Dubreuil, 1985), and implies that the catchment discharge is only indirectly related to the generation of overland flow along the slopes, i.e. reinfiltration and subsurface storm runoff are important components of the quick flow.

The DBM rainfall-flow model

For Kwalei catchment, the nonlinearity between rainfall and flow showed a reasonable power-law form. Eq. (1) was parameterised as:

$$u_t = y_t^x r_t \quad (10)$$

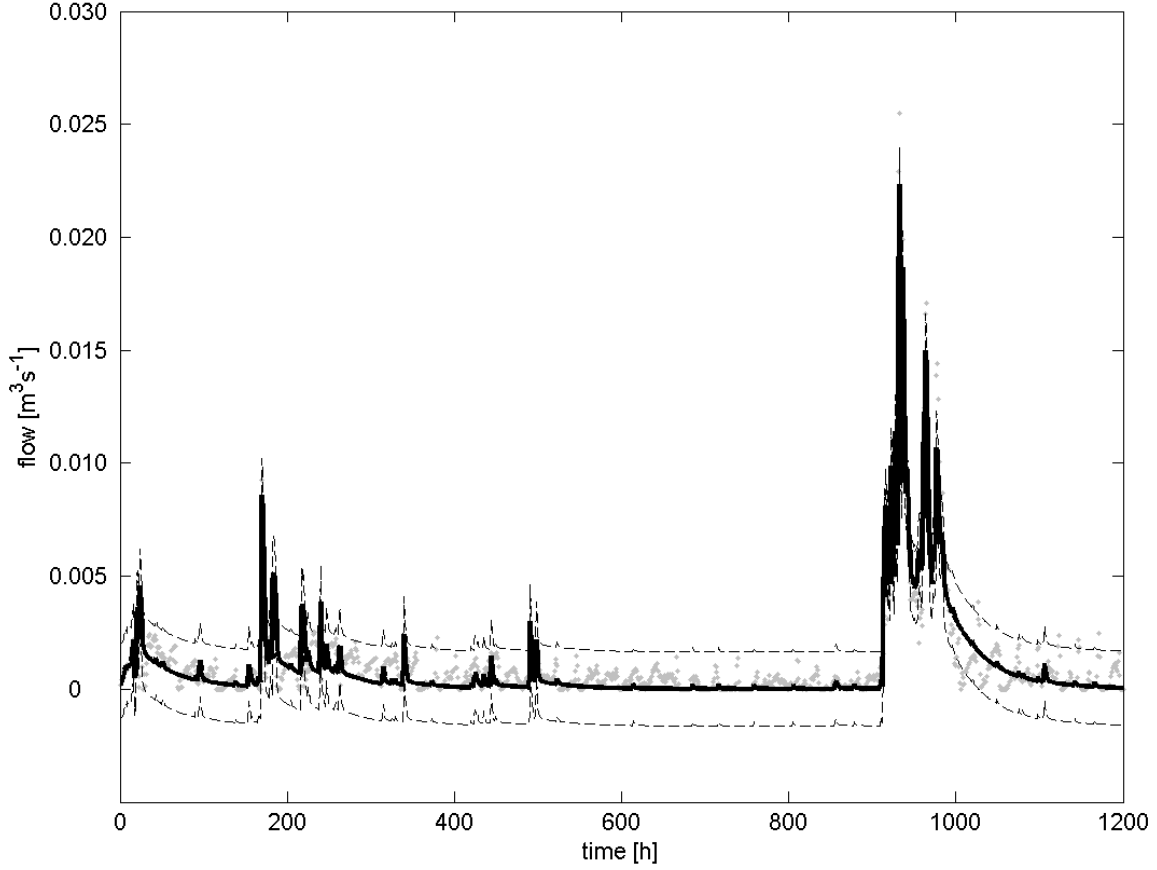


Figure 4. Calibration of rainfall-flow (DBM) model, November-December 2001. Solid black line denotes the estimated flow and thin dashed lines denote 95% confidence limits of the prediction; grey dots denote the measured flow.

with the optimised power-law coefficient parameter $x = 0.6889$. As the flow discharge, expressed in $\text{m}^3 \text{s}^{-1}$, was low and because the power-law coefficient was below 1, the effective rainfall represented only a small fraction (around 5 %) of the measured rainfall. During season 2003, for example, the ratio between effective to measured rainfall, equivalent to the scalar function y_t^x , ranged from 0.029 to 0.181 and was 0.057 on average. Thus, measured rainfall ranged from 0 to 29.2 mm, whereas mean effective rainfall was 0.092 mm, the 75th-percentile was 0.11 mm, the 99th-percentile was 0.75 mm, with maximum effective rainfall of 1 mm.

The best STF model was a second order polynomial that was decomposed into a quick and slow component, with parameters of eq. (6) equal to:

$$\begin{aligned} \frac{B_1}{A_1} &= 0.187 \frac{0.2018}{1 - 0.493z^{-1}} \\ \frac{B_2}{A_2} &= 0.187 \frac{0.0138}{1 - 0.977z^{-1}} \end{aligned} \quad (11)$$

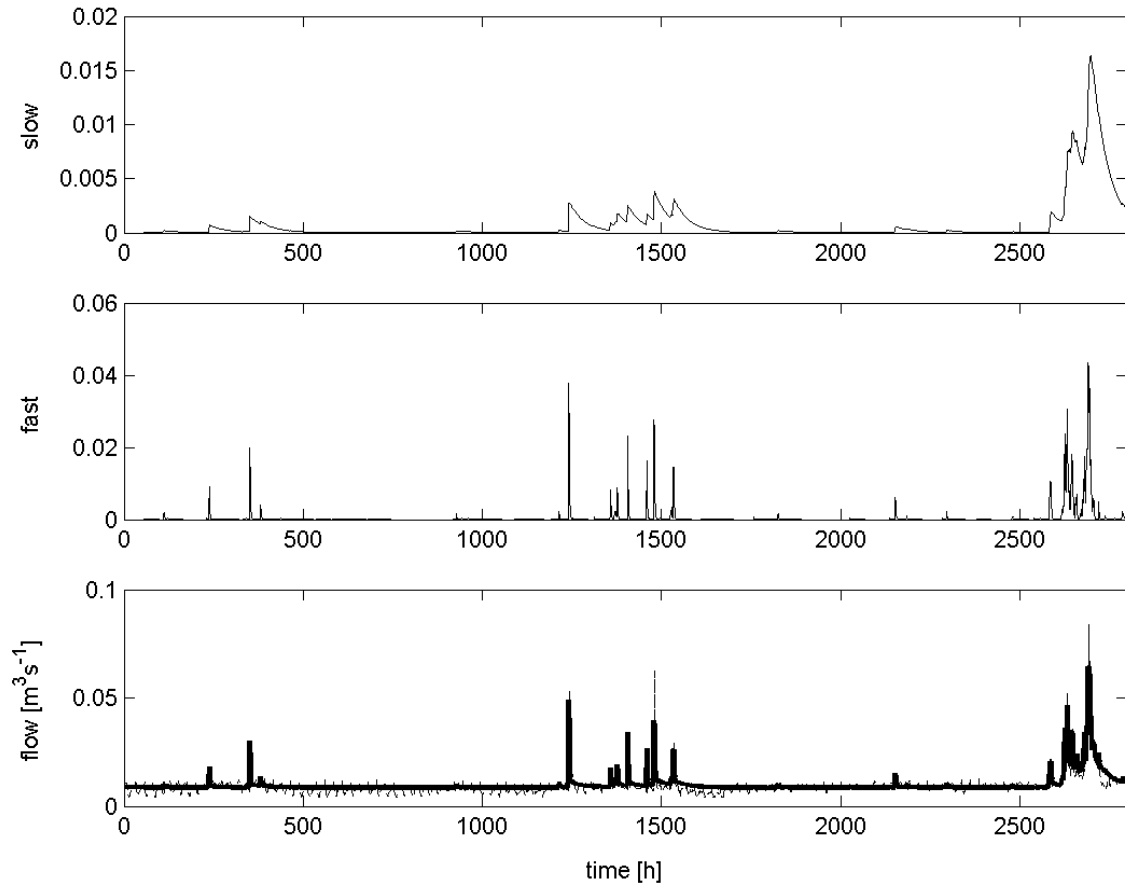


Figure 5. Validation of the DBM model in Feb-May 2003: the upper panel shows slow flow component, the middle panel shows the quick flow component and lower panel shows the total simulated flow (solid line) in comparison with the observed flow (dashed line).

The coefficient 0.187 represents the discrete equivalent of Steady State Gain of the STF model, which when multiplied by the effective rainfall non-linearity y_t^x gives the total runoff component, whereas its complement (1-SSG) gives the catchment water losses, mainly ascribed to evapotranspiration. The quick component had time constant T_1 of around 90 minutes and contributed to 40 % of total flow. The slow component, comprehensive of the base flow, had a time constant T_2 of approx. 43 hours, and contributed the remaining 60% of the flow. The Young information criterion (YIC, Young *et al.*, 2001) of the model was -7.6, indicating that the model was not over parameterised.

The model explained 86 % of the rainfall-flow data, but model efficiency increased to above 90 % during the rainfall event periods, when noise in the data was smaller. Fig. 4 shows the model flow and its 95 % confidence interval for the calibration dataset. The presence of noise in the measurements (solid line) is clear in the intra-event periods. In the validation dataset, the model explained 73% of the

whole dataset and 83% during the rainfall event periods. Fig. 5 shows the flow separation performed by the model for the validation dataset: the upper panel shows the slow component, the middle panel the quick component and the lower panel the total flow in comparison with measurements (dashed line). The model performed badly during the low flow periods, which might indicate that the model did not identify correctly the catchment response during the dry periods. During the intra-rainfall periods, it was difficult to infer the catchment response because the recordings were of poor quality. However, Fig. 5 shows that the model performed well during the rainfall events, which indicates that the relationship between effective rainfall and overland flow generation during the rainfall events was well simulated. Therefore the DBM model was considered appropriate for the further analysis.

Disaggregating of overland flow among HRUs

Eleven runoff detectors were placed in HRU_1 in season 2002 and 16 in season 2003, whereas 34 and 28 detectors were placed in HRU_2 in the two seasons, respectively. The best non-linear regressions P_k of HRU overland flow occurrence in relation to effective rainfall u (eq. 7) were hyperbolic tangents, parameterised as:

$$P_k = h_{1,k} \tanh(h_{2,k} u) \quad (12)$$

where $h_{1,1} = 0.925$ and $h_{2,1} = 10.390$ for HRU_1, and $h_{1,2} = 0.856$ and $h_{2,2} = 16.534$ for HRU_2. The regression functions are presented in Fig. 6, together with the observations. It is interesting to note that the two functions crossed at an effective rainfall u of 0.15 mm: when effective rainfall was small, overland flow was mainly generated in the non-perennial crop fields, whereas when effective rainfall was high, overland flow was active and quite homogeneous throughout the perennial crop fields. The outliers at $u = 0.56$ mm in Fig. 6 belong to the rainfall event recorded on the 27th March 2002, a storm that recorded 25 mm of rainfall in 70 minutes, with a peak 30-minute intensity equal to 42.8 mm h⁻¹ (Table 1). However, on that occasion overland flow was recorded by only 52 % of runoff detectors. The storm event was similar in terms of rainfall intensity, amount, duration and 24h antecedent rainfall to the event of 11th of March 2002, when the recorded overland flow occurrence was 93 %. The area monitored in the season 2002 was quite far from the flume, and at the beginning of the rain season, rainfall events consist mainly of localized and very intense storms. It is probable that the event that was recorded as very intense at the flume was far less intense on the monitored area, which would explain the low occurrence of overland flow observed. This example shows that the spatial distribution of rainfall affected the analysis, enlarging the confidence intervals of P_k , but at the same time, this uncertainty was accounted for in the disaggregating of quick flow among HRUs through the shape of the Gaussian curves, defined by $\sigma_{k,u}$ as estimated from the Jacobian matrix associated with P_k .

Fig. 7 shows an enlargement of the regression curves of Fig. 6 for the interval of effective rainfall u 0 - 0.35 mm and the derived probability density function curves $G_k(u)$ at $u = 0.05$ mm and 0.25 mm as estimated from the Jacobian matrices, multiplied by the HRU areas w_k . The dashed line above the HRU Gaussian curves is the sum of the two curves and represents the totality of the quick component of

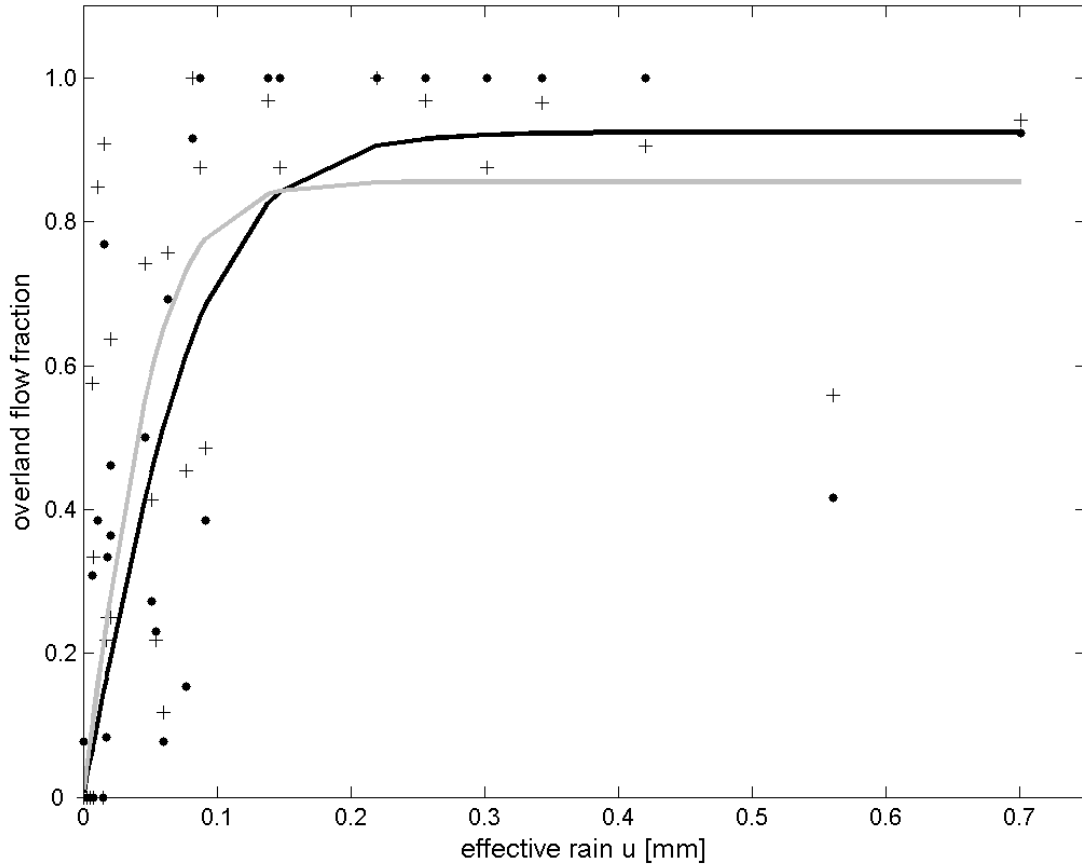


Fig. 6. HRU non-linear regression of overland flow probability of occurrence (P_k) as a function of effective rainfall u (mm). In black the regression for HRU_1 (perennial crops); in grey the regression for HRU_2 (other crops). Dots indicate observations for HRU_1; crosses indicate observations for HRU_2.

discharge $y_{l,t}$ (eq. 8). The ratio between the surface under the HRU Gaussians curves and the total curve gave the fraction of overland flow that was generated by the HRU, which was multiplied by $y_{l,t}$ to estimate the average HRU overland flow depth ($F_{k,t}$, eq. 9).

The characteristic infiltration length

The average HRU overland flow depths were the input for the field run-on run-off accumulation sequence (Fig. 3), to estimate the overland flow accounting for field topographic connectivity. The result consists of the simulation of overland flow depth at any time step at any field.

Table 3 shows the effect of varying the infiltration length L on the overland flow depth as observed in the Gerlach troughs (Gerlach trough volumes divided by contributing area), and as simulated by the model in the six Gerlach trough sites. The range of variation was defined by the hillslope observation analysis (Vigiak *et al.*, 2005a), i.e. from 1 to 20 m. The increase in infiltration length resulted in a larger contributing area of the Gerlach troughs, and therefore in a decrease of the

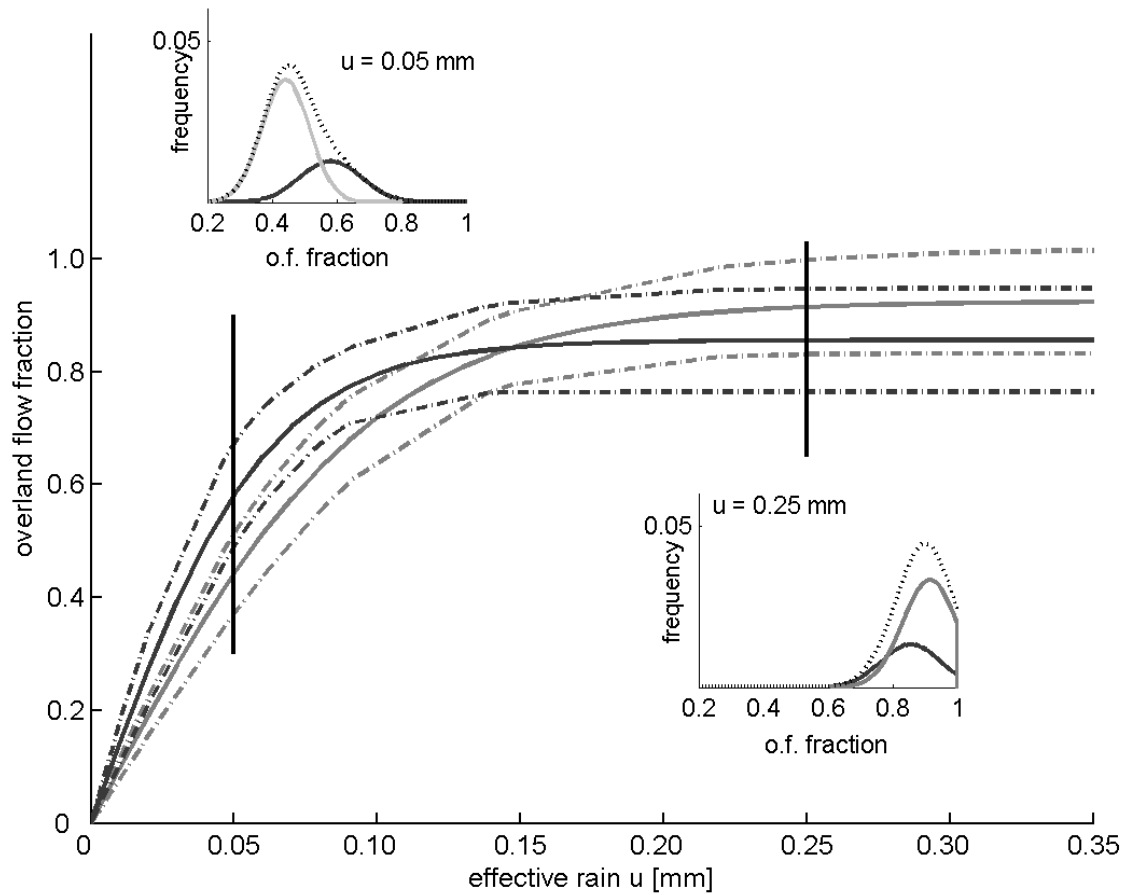


Figure 7. The probability density functions $G_k(u)$ for HRU_1 and HRU_2 at effective rainfall u equal to 0.05 mm (a) and 0.25 mm (b). The dashed line is the sum of the two components and represents the total quick flow at the outlet.

Table 3. Effect of variation of characteristic reinfiltration length L on model simulation in comparison to observation of overland flow depth in the Gerlach troughs. The reinfiltration length determined the accumulation area of the Gerlach troughs and the amount of run-off in the model.

L (m)	Observations		Model simulation	
	mean (mm)	st. deviation (mm)	mean (mm)	st. deviation (mm)
1	0.806	1.631	0.211	0.296
5	0.161	0.326	0.259	0.383
10	0.081	0.163	0.334	0.555
15	0.054	0.109	0.428	0.807
20	0.040	0.082	0.505	1.044

inferred overland flow depths. At the same time, the increase of reinfiltration length increased the proportion of overland flow moving above the surface along the slope. As a result, overland flow simulated in the lower fields received increasingly larger volumes of surface run-on, and both the mean and the variance of overland flow depth simulated by the model increased. The best agreement between mean values of overland flow as inferred from observations and simulated by the model was obtained for reinfiltration lengths around 5 m. For the reinfiltration lengths above 20 m the model was not anymore sensitive to this parameter, as the field lengths were seldom longer than 20 m; in the range 1-10 m model simulations were mainly driven by the disaggregation of overland flow among HRUs.

At 4 m, the distribution of model prediction of overland flow depth overlapped well the distribution of the observations, and therefore this reinfiltration length was considered suitable for Kwalei catchment. A reinfiltration length of 4 m results in the accumulation areas for the Gerlach trough equal to 2 m². This is in good agreement with observations on Gerlach troughs placed in the same area for another experiment, and whose accumulation areas were measured in the field and ranged from 2.5 to 3.5 m² (A. Tenge, pers. comm., 2003). A reinfiltration length L of 4-5 m also indicates that on average only the lower quarter of the fields generated run-off, which was in good agreement with the field observations.

Evaluation of model simulations

Fig. 8 shows the scatter plots of simulated versus observed overland flow depths at the six Gerlach sites, expressed in cubic root of mm to enlarge the differences at smaller values. The reasons behind the scatter between observations and simulations are manifold. In Fig 8a, symbols represent the Gerlach sites. Overland flow appeared to be overestimated in HRU_1 (G4 and G6) and underestimated in HRU_2 (G1-3 and G5). Two Gerlach troughs show this fact more clearly: Gerlach G3, placed at the end of the transect 1, and Gerlach G6, placed at the end of the transect 2. Model simulations of Gerlach G3 greatly underestimated overland flow in three cases out of six: the two outliers in the lower right side of Fig 8a belong to G3. The G3 site is a degraded tea plantation that is seldom cultivated and whose crop cover is less than 50 %. It is also a steep field, with average slope of 30 %. Gerlach G3 always recorded the highest volumes of overland flow. On the other hand, Gerlach G6 at the end of transect 2 hardly showed any overland flow. G6 site consisted of a coffee and banana stand, with crop cover above 90%, a thick layer of litter and of gentle slope (< 15 %). The model simulated occurrence of overland flow in this field, but only in few occasions any volume was collected in the Gerlach. The apparent overestimations for HRU_1 and underestimations for HRU_2 suggests that the reinfiltration length may depend on the HRU types. Indeed, this explanation seems to be logical: in HRU_1 the overland flow occurrence is less frequent, indicating generally higher rainfall infiltration conditions. Consequently overland flow would also quickly reinfiltrate into the soil. Local slope is another important factor affecting reinfiltration: on steeper surfaces, overland flow is likely to travel longer distances before reinfiltrating.

Fig. 8 may also indicate that the disaggregation of overland flow does not separate the two hydrologic units adequately. In Fig. 8b symbols represent the rainfall event observations. Circles

Chapter 4

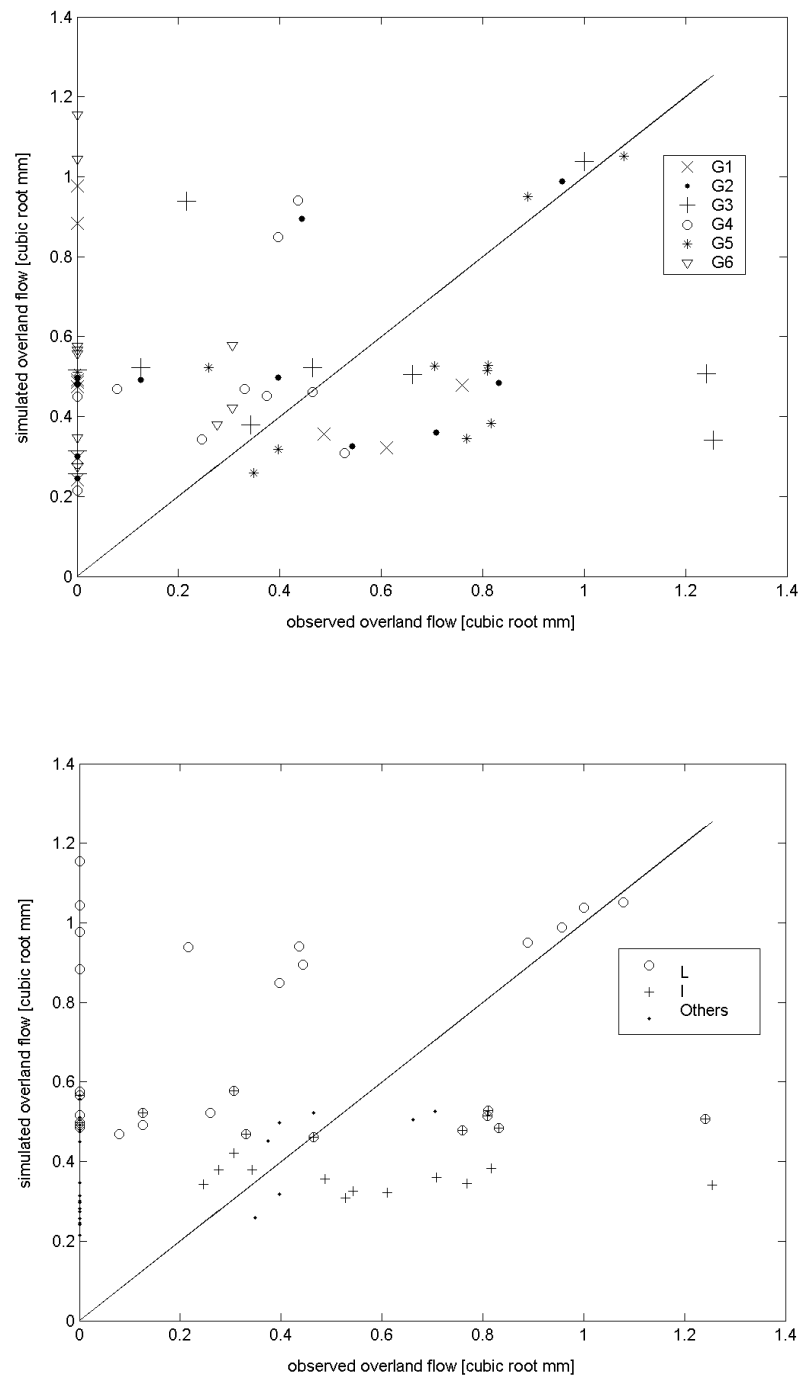


Figure 8. Scatter plot of simulated versus observed overland flow depth at the Gerlach trough sites (data are shown in cubic root of mm of overland flow to enhance the differences in the smaller observations). a) symbols represent the Gerlach trough sites. G4 and G6 were placed in HRU_1 (perennial crops); G1-3 and G5 were in HRU_2 (other crops). b) symbols represent the rainfall event characteristics: circles indicate large rainfall events (L: rainfall amount > 15 mm), crosses indicate intense events (I: 30-minute intensity > 20 mm h⁻¹); dots indicate the other observations.

indicate the observations relative to large rainfall events (i.e. rainfall above 15 mm), whereas crosses indicate intense rainfall events (i.e. 30-minutes peak intensity above 20 mm h⁻¹). Other events are represented by dots. The scatter plot looks in this case “organized”. All large events are simulated with more than 0.4 mm of overland flow and are mostly overestimated, whereas intense rainfall events are mostly underestimated.

Rainfall intensity was not directly used in the regression analysis, whereas it clearly affected the measurements of the overland flow depth in the Gerlach troughs (Table 2). This might be a structural problem of the disaggregation approach. However, its effect could be reduced by using a shorter time step in the rainfall-flow model, e.g. half an hour or 10 minutes. Unfortunately, the available data did not allow a finer resolution of the model. At the catchment level, the poor quality of discharge measurements imposed the limitation of the analysis to 1 hour time step intervals. At the hillslope level, only 26 useful observations per HRU were available for the regression analysis. Furthermore, in season 2002, the distance of the monitored area from the flume introduced more uncertainty in the analysis of overland flow occurrence in relation to effective rainfall (see Fig. 6). As a result, the standard deviations of $G_k(u)$ are quite large.

Points on the y axis of Fig. 8 indicate the overestimations of the model that can be ascribed to the disaggregation of the overland flow, i.e. points where the model predicted overland flow but no volume was collected in the Gerlach troughs. This was expected: the model simulates the occurrence of overland flow as soon as there is a positive effective rainfall, whereas the Gerlach troughs recorded volumes only when rainfall events were above 5 mm (Table 2). This does not unequivocally indicate, however, the model error: at low effective rainfall, the variability of overland flow was much higher than at high effective rainfall (see Fig. 6). It is therefore possible that overland flow was present but did not occur in the upslope area of Gerlach troughs. More Gerlach troughs observations would have been required to check this in the field.

The disaggregation approach models the high variability of overland flow stochastically: the model predicts the average HRU conditions at each time step, taking into account the field position along the slopes only in part because of the infiltration. Local conditions, such as those observed at sites G3 and G6 for example, cannot be included. A perfect match of the model simulation with observations should therefore not be expected. Notwithstanding the high scatter of the points, the order of magnitude of overland flow was well simulated. Furthermore, events that were not too intense or too large (dots in Fig. 8b) were also well simulated.

Fig. 9 shows the simulation of Kwalei catchment at the peak hour of the rainfall event of 24.05.03: overland flow depth varied from 0.075 mm to 0.47 mm. Most of the areas with overland flow depth below 0.15 mm correspond to HRU_1. A sharp difference between HRU_1 and HRU_2 can be noticed especially at the border of the forest area, but also on the western side of the catchment, along the watershed divide, where coffee and banana stands with low overland flow are interspersed with annual crop fields with high overland flow. Overland flow depths above 0.2 mm correspond mainly to areas where incoming run-on is important: e.g. in the north-eastern part of the catchment, below the patch of rock outcrop and burned forest, and in the long central slopes of the catchment. Many of the dark spots

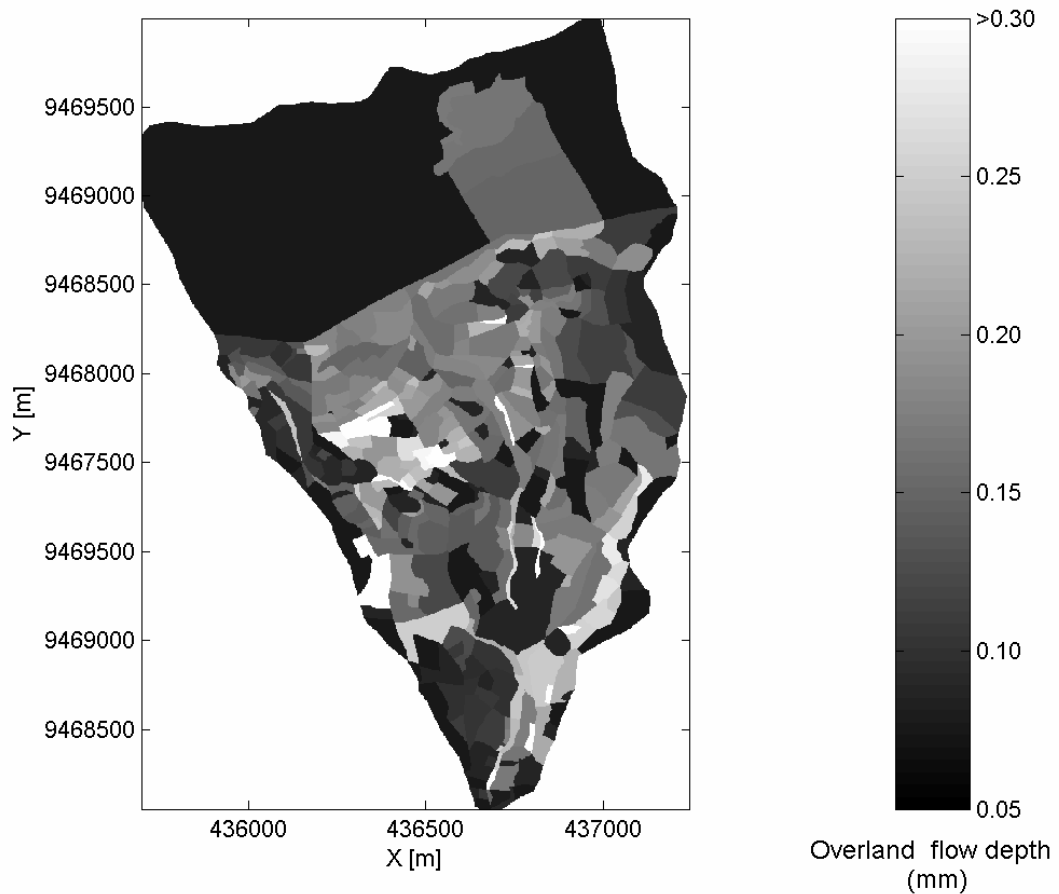


Figure 9. Model simulation of overland flow depth (mm) for Kwalei catchment at 2:00-3:00 of 24.05.03. Overland flow depths above 0.3 mm are shown in white.

scattered around the catchment indicate instead fields that are isolated from the upper slopes by cut-off drains or other features diverting the overland flow.

The effect of field shape on model simulation can be observed in the southern slopes: the western and eastern sides of the river have similar land use, but on the eastern side fields are wider than longer (the main field axis is along the contour line), whereas in the western side fields are longer than wider (the main field axis is along the slope direction) and are generally also larger. The average amount of run-off draining out of a field is proportional to the length of the lower field border length times the infiltration length. The ratio of the field out-draining area to the field total area depends on the field shape: infiltration is more important in long fields than in wide fields, and in big fields than in small fields. As a result, the accumulation of run-off is larger in the eastern side of the catchment than in the western side. In this sense, model simulations depend on the spatial discretization applied to represent the catchment.

The representation of the Kwalei catchment using fields was chosen because the survey of overland flow direction was produced at this level. A different representation, for example by a raster format of homogeneous pixels, would probably result in different simulations. Such an approach would speed up

the model implementation, but would rely heavily on the quality of the DEM available, and on the absence of flow lines cutting through the slope and diverting the surface flow. Field borders often create such discontinuities in the overland flow directions; the use of field border to calculate field runoff adopted in our modelling approach helped taking this into account. Which representation would lead to the best simulation is an issue that will need further investigation in the future. Qualitatively, the distribution of overland flow in Kwalei catchment presented in Fig. 9 seems realistic and was considered satisfactory.

Conclusions

The hydrology of Kwalei catchment comprised many interwoven processes, with a predominance of infiltration-excess overland flow, reinfiltration, and subsurface storm-flow. Observations at the hillslope scale showed that overland flow occurrence was very variable along the catchment slopes and related not only to the differences in soil infiltration, but also to the differences in canopy interception, soil cover conditions and land management (Vigiak *et al.*, 2005a). Moreover, overland flow was only indirectly related to the catchment discharge. Such complex hydrology is frequent in wet tropical environments (Dubreuil, 1985) and poses serious difficulties for hydrologic modelling.

Our disaggregating approach consisted of an unconventional model that rejected the use of any infiltration equation and attempted to reconcile rainfall-flow catchment-scale modelling to hillslope-scale modelling. The variability of overland flow occurrence was incorporated through the use of probability density functions derived from the observations.

The model was built on many assumptions, some of which are questionable: we assumed that overland flow was related to the catchment quick flow through the effective rainfall, and that the overland flow occurrence could be modelled through Gaussian probability density functions. The poor quality of discharge data imposed the use of one hour time step intervals whereas observations of overland flow in the Gerlach troughs showed that rainfall intensities at smaller time step intervals were important. The number of the observations at the hillslope scale was probably too small for a good estimation of model components and a thorough evaluation of the model performance. A larger dataset of hillslope observations would have definitively been useful to improve the reliability of model simulations. Notwithstanding the limits of the analysis and of the available data, the model simulations were in reasonable agreement with overland flow depths observed in Gerlach troughs, and the overall simulation of the spatial distribution of overland flow seemed realistic.

These results were achieved with a rather limited number of parameters, i.e. five parameters for DBM model, three (times two HRUs) for the disaggregation approach, and the reinfiltration length. Even so, the risk of over parameterisation is already evident, for example in the difficult interpretation of the scatter plot of Fig. 8. The advantage of such a parsimonious model is that it may allow the estimation of the uncertainty of model predictions using methodologies that employ Monte Carlo simulations, such as e.g. GLUE (Beven and Binley, 1992).

Model requirements consisted of rainfall-flow time series and observations of overland flow occurrence at the hillslope scale. Such hillslope observations are seldom available, but require rather

simple and inexpensive devices, therefore the methodology could be easily repeated in other catchments. The analysis of overland flow occurrence in relation to catchment discharge through the use of effective rainfall allowed the dependency of hillslope scale overland flow on rainfall amount, catchment antecedent conditions, and rainfall intensity to be explored.

It is our opinion that in the future, the insights gained from analysis of overland flow occurrence and from pursuing downward modelling approaches linking catchment and hillslope processes may improve our understanding of hillslope scale hydrology, and lead eventually to real advances in hydrologic modelling.

References

- Beven KJ, Kirkby MJ. 1979. A physically-based, variable contributing area model of basin hydrology. *Hydrological Science Bulletin* **24**: 43-69.
- Beven KJ, Binley AM. 1992. The future of distributed models - model calibration and uncertainty prediction. *Hydrological Processes* **6**: 279-298.
- Beven KJ. 2001. *Rainfall-runoff modelling - the primer*. John Wiley & Sons, 360 pp.
- Blöschl G, Sivapalan M. 1995. Scale issues in hydrological modelling: a review. *Scale issues in hydrological modelling*, J. D. Kalma and M. Sivapalan, Eds., John Wiley and Sons, 9-48.
- Dubreuil PL. 1985. Review of field observations of runoff generation in the tropics. *Journal of Hydrology* **80**: 237-264.
- Elsenbeer H, Vertessy RA. 2000. Stormflow generation and flowpath characteristics in an Amazonian rainforest catchment. *Hydrological Processes* **14**: 2367-2381.
- FAO. 1990. *Guidelines for soil description*. Third ed. Soil Resource Management and Conservation Service, Land and Water Development Division, FAO.
- Gascuel-Oudou C, Cros-Crayot S, Durand P. 1996. Spatial variations of sheet flow and sediment transport on an agricultural field. *Earth Surface Processes and Landforms* **21**: 843-851.
- Gerlach T. 1967. Hillslope troughs for measuring sediment movement. *Revue de geomorphologie dynamique* **17**: 173.
- Hjelmfelt AT, Burwell RE. 1984. Spatial variability of runoff. *Journal of Irrigation and Drainage Engineering*: 46-54.
- Jakeman AJ, Littlewood IG, Whitehead PG. 1990. Computation of the instantaneous unit hydrograph and identifiable component flows with application to two small upland catchments. *Journal of Hydrology* **117**: 275-300.

Karssen D. 2002. Building dynamic spatial environmental models, Faculteit Ruimtelijke Wetenschappen, Universiteit Utrecht, 224.

Loague K, Gander GA. 1990. R-5 revisited. Spatial variability of infiltration on a small rangeland catchment. *Water Resources Research* **26**: 957-971.

Meliyo JL, Kabushemera JW, Tenge AJM. 2001. Characterization and mapping soils of Kwalei subcatchment, Lushoto District. Mlingano Agricultural Research Institute. Tanga, Tanzania, 34 pp.

Mwakalila S, Campling P, Feyen J, Wyseure G, Beven KJ. 2001. Application of a data-based mechanistic modelling (DBM) approach for predicting runoff generation in semi-arid regions. *Hydrological Processes* **15**: 2281-2295.

Seguis L, Cappelaere B, Peugeot C, Vieux B. 2002. Impact on Sahelian runoff of stochastic and elevation-induced spatial distributions of soil parameters. *Hydrological Processes* **16**: 313-332.

Sivapalan M. 2003. Process complexity at hillslope scale, process simplicity at the watershed scale: is there a connection? *Hydrological Processes* **17**: 1037-1041.

van Loon EE. 2002. Overland flow: interfacing models with measurements, Wageningen University, 171.

Vertessy RA, Elsenbeer H. 1999. Distributed modeling of storm flow generation in an Amazonian rain forest catchment: effects of model parametrization. *Water Resources Research* **35**: 2173-2187.

Vigiak O, van Dijk SJE, van Loon EE, Stroosnijder L. 2005a. Matching hydrologic response with measured effective hydraulic conductivity. *Hydrological Processes* **subm.**

Vigiak O, Okoba BO, Sterk G, Groenenberg S. 2005b. Modelling of catchment-scale erosion patterns in the East African Highlands. *Earth Surface Processes and Landforms* **30**: 183-196.

Whitehead PG, Young PC, Hornberger GM. 1979. A system model of streamflow and water quality in the Bedford-Ouse: 1. Streamflow modelling. *Water Resources Research* **13**: 1155-1169.

Young PC. 1993. Time variable and state dependent modelling of nonstationary and nonlinear time series. *Developments in time series analysis*, T. Subba Rao, Ed., Chapman and Hall, 347-413.

Young PC, Beven KJ. 1994. Data-based mechanistic modelling and the rainfall-flow non-linearity. *Environmetrics* **5**: 335-363.

Young PC. 1998. Data-based mechanistic modelling of environmental, ecological, economic and engineering systems. *Environmental modelling & softwares* **13**: 105-122.

Young PC. 2000. Stochastic, Dynamic Modelling and Signal processing: time variable and state dependent parameter estimation. *Nonlinear and Nonstationary Signal Processing*, W. J. Fitzgerald, A. Walden, R. Smith, and P. C. Young, Eds., Cambridge University Press, 74-114.

Young PC, Tomlin CM. 2000. Data-based mechanistic modelling and adaptive flow forecasting. *Flood forecasting: what does current research offer the practitioner?*, M. J. Lees and P. Walsh, Eds., British Hydrological Society, 26-40.

Young PC. 2001a. Data-based mechanistic modelling and validation of rainfall-flow processes. *Model validation: perspectives in hydrological sciences*, M. G. Anderson and P. D. Bates, Eds., John Wiley & Sons, 117-161.

Young PC. 2001b. The Identification and Estimation of Nonlinear Stochastic Systems. *Nonlinear Dynamics and Statistics*, A. I. Mees, Ed., Birkhäuser, 127-166.

Young PC, McKenna P, Bruun J. 2001. Identification of Nonlinear Stochastic Systems by State Dependent Parameter Estimation. *International Journal of Control* **74**: 1837-1857.

Young PC. 2002. Advances in real time forecasting. *Philosophical transactions of the Royal Society: Mathematical, Physical and Engineering Sciences* **360**: 1433-1450.

Young PC. 2003. Top-down and data-based mechanistic modelling of rainfall-flow dynamics at the catchment scale. *Hydrological Processes* **17**: 2195-2217.

Chapter 5

A SEMI-EMPIRICAL MODEL TO ASSESS UNCERTAINTY OF SPATIAL PATTERNS OF EROSION

Olga Vigiak, Geert Sterk, Renata J. Romanowicz and Keith J. Beven

Catena. Submitted.

A SEMI-EMPIRICAL MODEL TO ASSESS UNCERTAINTY OF SPATIAL PATTERNS OF EROSION

Abstract

Distributed erosion models are potentially good tools for locating soil sediment sources and guiding efficient Soil and Water Conservation (SWC) planning. Together with the potential location of severely eroded areas, decision makers should be informed of the uncertainty of model predictions. In this study, a semi-empirical erosion model was employed to predict the distribution of erosion within a catchment. The model combined a semi-distributed hydrological model with the Morgan, Morgan and Finney (MMF) empirical erosion model. The model was tested in a small catchment of the West Usambara Mountains (Kwalei catchment, Tanzania). Comparison of soil detachability rates measured in splash cups ($0.28\text{--}0.67\text{ g J}^{-1}$) matched well model simulations ($0.30\text{--}0.35\text{ g J}^{-1}$). Net erosion rates measured in Gerlach troughs ($0.01\text{--}1.05\text{ kg m}^{-2}$ per event) were used to calibrate the sediment transport capacity of overland flow. The quality of the predicted pattern of erosion was assessed by comparison with the actual erosion pattern observed in the field. Uncertainties of model simulations due to parameterisation of overland flow sediment transport capacity were assessed with the Generalized Likelihood Uncertainty Estimation (GLUE) methodology. The agreement between simulated and observed erosion patterns was measured by weighted Kappa coefficients. Behavioural parameter sets, i.e. scoring a weighted Kappa above 0.50, were those with short infiltration length ($< 1.5\text{ m}$) and with the ratio of overland flow power α and local topography power γ close to 0.5. In the dynamic Hortonian hydrologic regime and the dissected terrain of Kwalei catchment, topography influenced the distribution of erosion more than overland flow. Simulated erosion rates varied from -4 to $+2\text{ kg m}^{-2}$ per season. Field standard deviation of seasonal erosion rates ranged from 0 to 2.9 kg m^{-2} , and was $< 0.9\text{ kg m}^{-2}$ in more than 95 % of fields. The model simulated correctly around 75 % of erosion pattern; model overestimations of erosion occurred mainly in vegetable plots, whereas underestimations occurred in tea, sugarcane and grassland fields. The uncertainty of model predictions due to sediment transport capacity was high: depending on the transport capacity parameters, around 10 % of the fields were attributed to either slight or severe erosion class. SWC planning should focus on severely eroded fields, but areas whose spatial uncertainty was large should also be carefully checked in the field. The difficult characterisation of effective parameters for sediment transport capacity at the catchment scale introduces large uncertainties in model predictions and poses a major limit to distributed erosion modelling predicting capabilities.

Keywords: *spatial pattern of erosion; Morgan, Morgan and Finney model; catchment erosion assessment; uncertainty estimation; Generalized Likelihood Uncertainty Estimation (GLUE).*

Introduction

Recent assessments of the quality of erosion models showed that these models generally predict poorly the spatial patterns of erosion and deposition within a catchment (Jetten *et al.*, 1999; Jetten *et al.*, 2003; Merritt *et al.*, 2003). As in other environmental modelling areas, difficulties in erosion modelling arise from the natural complexity of the landscape system, spatial heterogeneity and lack of available data (Merritt *et al.*, 2003). The complexity of the natural system has been one driver for the development of physics-based models, with the idea that an accurate description of processes would simulate the system appropriately. However, it is practically impossible to represent adequately the huge spatial and temporal variability of the phenomena for any rainfall event (Quinton, 1997). Moreover, error propagation and uncertainties in the estimation of input data of complex models compromise the theoretically more accurate description of the system (Jetten *et al.*, 2003).

Because of these limits of erosion modelling, model predictions are highly uncertain. Uncertainties in model predictions, usually quite clear in the modeller's perception, should be effectively communicated to policy and decision makers, and made explicit (Beven, 1993; Garen *et al.*, 1999; Merritt *et al.*, 2003). As important decisions may depend on model simulations, model outputs should be provided with an estimation of the predictive errors, like output bands of possible outcomes (e.g. Quinton, 1997; Brazier *et al.*, 2000).

The environmental data that are usually available contain information to characterize only the dominant processes active in a given system, which may then be described more effectively with simpler empirical and conceptual approaches (Young, 1998). Conceptual (or semi-empirical) models offer the advantage of combining the physical interpretability of modelling results with a simple structure, which makes them less prone to over-parameterisation and error propagation problems, even if it exposes them to the risk of aggregation or disaggregation errors (Merritt *et al.*, 2003). A limited number of parameters and processes simplifies model implementation by user agencies and in data poor environments (Garen *et al.*, 1999; Merritt *et al.*, 2003). It also reduces computational requirements, allowing for assessment of model result uncertainties (Merritt *et al.*, 2003; Jetten *et al.*, 2003). Conceptual models may therefore be appropriate in characterizing the distribution of erosion within a catchment (Viney and Sivapalan, 1999). For example, Desmet and Govers (1995) obtained some encouraging results with a simple transport-limited erosion model whose main driving factor was topography. Improved sediment yield predictions were obtained by von Rompaey *et al.* (2001) and Viney and Sivapalan (1999) by coupling empirical erosion models to hydrologic models, however in both studies the quality of the spatially distributed predictions was not assessed. Vigiak *et al.* (2005a) showed that an empirical model, the revised Morgan, Morgan and Finney model (MMF; Morgan, 2001), had good potential to assess the distribution of erosion within a catchment, provided the hydrologic part of the model was improved.

The aim of this study was to evaluate the ability of a simple semi-empirical erosion model to predict the distribution of erosion within a catchment and to assess the uncertainty of model spatially distributed predictions due to the choice of sediment transport capacity parameters.

Materials and methods

The study area: Kwalei catchment

The Kwalei catchment (4°48' S, 38°26' E) is situated in the West Usambara Mountains, North-East Tanzania. The catchment size is approx. 2 km², and altitude ranges from 1337 to 1820 m. The terrain is rough and highly dissected, with more than half of the hillslopes steeper than 20 %. Drainage comprises four permanent streams running north-west to south-east. Average annual rainfall is approximately 1000 mm, with a bimodal distribution. The long rainy season stretches from the end of February to the end of May and the short, less reliable rainy season from October to January (Vigiak *et al.*, 2005a). Soils on the slopes consist mainly of Humic and Haplic Acrisols (FAO-Unesco legend, FAO, 1990). They comprise porous, sandy topsoils, and clayey, deep and well-drained subsoils. Saturation may occur in the clayey and vertic Umbric Gleysols in the valley bottoms (Meliyo *et al.*, 2001). The highest part of the catchment is covered by mountain rain forest, whereas the middle and lower slopes are used for agricultural purposes. Hamlets are located mainly along the ridge shoulders. Cultivation of annual crops is concentrated close to the settlement compounds. Maize is the most commonly cultivated crop, often intercropped with bean, banana, cassava and sugarcane. The two-storey cultivation of banana and coffee is frequent on the steep slopes along the stream incisions. Valley bottoms are intensively planted with vegetables, the major cash crops of the area.

The Kwalei catchment may be considered representative of the East African Highlands environment, and has been already the subject of erosion assessment studies (Vigiak *et al.*, 2005a; Tenge *et al.*, 2004) and hydrologic characterization (Vigiak *et al.*, 2005b; Vigiak *et al.*, 2005c). An erosion assessment survey conducted on part of the catchment showed that areas affected by severe erosion covered around one third of the catchment: erosion features were especially frequent in fields of annual crops, like cassava, maize and bean, and the main erosion processes were sheet and interrill erosion (Vigiak *et al.*, 2005a). The main mechanism of overland flow generation was infiltration-excess, but reinfiltration was important: overland flow reinfiltrated usually at distances shorter than 20 m (Vigiak *et al.*, 2005b). Two main Hydrologic Response Units (HRUs, i.e. areas of homogeneous hydrology; Blöschl and Sivapalan, 1995) could be defined: perennial crops (HRU_1: coffee and banana, forest and banana and maize fields), versus other crops (HRU_2: mainly annual crops) (Fig. 1A).

Assessment of erosion

Assessment of erosion comprised measurements of rainfall detachment rates by splash cups at the plot scale, of net erosion rates by Gerlach troughs placed along two longitudinal transects at the hillslope scale, and surveying the actual status of erosion of fields at the catchment scale.

Splash detachment was monitored in five main land use types (maize and bean, cassava, banana and coffee, tea and vegetables) by means of splash cups (Morgan, 1981). Two fields per land use type were selected with two splash cups each. The splash cups had an inner diameter of ten cm from which the soil was splashed into the surrounding catching tray. Collection of the splashed material was done at monthly intervals, in dry days following at least three days without rain. The soil in the catching tray

was collected and weighed. The dry soil weight was estimated assuming soil moisture content equal to field capacity.

In the long rainy season (March-May) of 2003, six 0.50 m wide Gerlach troughs (Gerlach, 1967) were installed at different positions in the upper, middle and lower part of two longitudinal transects located at the lower (1380 m) and middle (1450 m) slopes of the catchment. The transects spanned from the water divide to the drainage line and crossed representative sequences of annual and perennial crops on the most frequent soil type of the catchment (Haplic Acrisols). After each rainfall event, the total overland flow volume collected in each trough was measured, and a sediment sample was taken to the laboratory to be dried at 105° C for 24 hours and weighed. The sediment load was obtained by multiplying the overland flow volume by the sediment concentration of the sample. The results were referred to the contributing area of the troughs, which was visually estimated in the field to be around 2 m² (Vigiak *et al.*, 2005c).

At the catchment scale, actual erosion was assessed by direct survey using the Assessment of Current Erosion Damage method (ACED; Herweg, 1996). ACED consists of surveying erosion features and main causes of erosion, such as land management, surface characteristics, and run-on and run-off patterns (Herweg, 1996). The method allows semi-quantification of erosion following rainfall events. In order to cover the entire catchment, however, less emphasis was given to the measurements of erosion features and the model was applied to assess erosion qualitatively. Five classes of erosion were defined, from very slight to very severe, on the basis of presence of erosion features and their intensity, without attaching a quantitative value to the erosion classes. The survey took place from December 2002 till May 2003 and was considered representative of the rainy season.

The semi-empirical model

The semi-empirical model proposed in this study superposed the structure of an empirical erosion model, the Morgan, Morgan and Finney model (MMF, Morgan *et al.*, 1984; Morgan, 2001), to a semi-empirical hydrologic model that simulates overland flow depth distribution within the catchment (Vigiak *et al.*, 2005c). The model was formulated in order to be parametrically parsimonious while retaining explicit descriptions of the main erosion processes.

The MMF retains a good physical base in the identification of the soil detachment and transport processes, even if the equations comprise many empirical parameters. The recent version of the model used here incorporates a more accurate description of erosion processes and provides broader guidelines for model inputs (Morgan, 2001). The model is structured in two phases: a water phase (where energy of rainfall and volume of overland flow are calculated), and a sediment phase (where soil detachment and soil transport rates are calculated). Erosion is given by the minimum between soil detachment and transport rate. The application of the model in two catchments of the East African Highlands, one of which was the study area of the present work, showed that the model had good potential for identifying erosion patterns, but that the hydrologic part, unable to account for infiltration along the slopes, was unrealistic for Kwalei catchment (Vigiak *et al.*, 2005a). The same study concluded that better simulations of overland flow would improve the model performances in depicting soil erosion patterns.

Recently, Vigiak *et al.* (2005c) proposed a parametrically parsimonious model simulating the distribution of overland flow within a catchment. The model runs at hourly time step and per field. It simulates average overland flow occurring in the main hydrologic response units as a function of the effective rainfall and accounts for reinfiltration. The model was created to match Kwalei hydrologic conditions and performed well in the catchment (Vigiak *et al.*, 2005c). In the present study, the main structure of the MMF model was retained, but the model of Vigiak *et al.* (2005c) was used to predict overland flow. A detailed description of the original MMF model (Morgan, 2001) and parameters suitable for Kwalei catchment is given in Vigiak *et al.* (2005a), whereas the hydrologic model is described in Vigiak *et al.* (2005c).

The revised MMF model runs at the scale of landscape elements, i.e. for areas with homogeneous soil, land use and topography (Morgan, 2001), whereas the model of Vigiak *et al.* (2005c) runs at the field scale. Therefore, the spatial scale of the semi-empirical erosion model was the field, which can be considered a single landscape element. Fields were arranged in hillslope sequences; a connectivity matrix linking fields from the upslope (the watershed divide) downwards to the channel streamlines was defined through observations of flow direction surveyed in the fields. The stream lines were the final collectors of the overland flow slope accumulation and drained to the outlet.

While the MMF is an average annual model, the hydrologic model is a dynamic model with hourly time steps. Matching the two models raised temporal scale issues that required careful consideration of equations and parameters. In what follows, the equations whose application raises temporal scale issues are addressed.

The MMF method of calculating the rainfall kinetic energy was fully retained. The rainfall kinetic energy (KE , $J m^{-2}$) is a function of the fraction of rainfall (R , mm) that is not intercepted by the vegetation canopy (INT , fraction between 0 and 1). The kinetic-effective rainfall (ER) is split into direct throughfall (DT), which directly reaches the soil, and leaf drainage (LD), which reaches the surface by stemflow or dripping from leaves. The division is a function of the canopy cover (CC , fraction between 0 and 1). The kinetic energy of the direct throughfall DT (KE_{DT} , in $J m^{-2}$) depends on rainfall intensity, which for tropical areas is calculated according to the equation of Hudson (1965), developed for Zimbabwe. The kinetic energy of the leaf drainage (KE_{LD} , in $J m^{-2}$) is a function of the canopy height (PH , m; from Brandt, 1990). Both equations were derived from studies on kinetic energy of storms or intra-storm intervals. The total kinetic energy KE ($J m^{-2}$) is given by the sum of the two fractions ($KE = KE_{DT} + KE_{LD}$), and determines the soil detachment by raindrop impact F ($kg m^{-2}$), which is defined as:

$$F = 10^{-3} K \cdot KE \quad (1)$$

where K is the soil detachability index ($g J^{-1}$), defined after Quansah (1981). Eq. (1) has been shown to be an acceptable definition of detachment rate (Salles *et al.*, 2000). Because the relationship between kinetic energy and rainfall detachment rate (eq. 1) is linear, the application of the detachment rate module at daily or hourly time step does not stretch the use of equations beyond their limits. However,

Table 1. Land use input data for the semi-empirical model: *INT* is interception factor, *CC* is canopy cover fraction, *PH* is plant height, *GC* is ground cover fraction, *CP* is the combination (multiplication) of USLE crop and protection factors, *HRU* is the Hydrologic Response Unit of the hydrologic model.

Land use type	<i>INT</i>	<i>CC</i>	<i>GC</i>	<i>PH</i> (m)	<i>CP</i>	<i>HRU</i>
Banana and maize	0.16	0.27	0.49	1.31	0.25	1
Bush/fallow	0.20	0.67	0.79	1.20	0.05	2
Cassava (and other annuals)	0.12	0.30	0.45	0.60	0.40	2
Coffee and banana	0.30	0.52	0.77	1.50	0.20	1
Forest	0.30	0.67	0.89	3.93	0.01	1
Grassland	0.30	0.20	0.60	0.08	0.01	2
Maize and beans	0.17	0.26	0.43	0.67	0.30	2
Sugarcane	0.25	0.37	0.55	0.91	0.15	2
Tea	0.30	0.27	0.37	0.50	0.20	2
Vegetables	0.15	0.13	0.22	0.43	0.35	2
Wattle	0.28	0.38	0.73	1.55	0.05	2
Woodlot	0.28	0.30	0.73	8.00	0.05	2

seasonal changes in the land use parameters may be important. In perennial crops, such as coffee and banana stands, land use parameters may be assumed constant; but for annual crops this assumption is questionable. In the Kwalei catchment, however, the high rate of intercropping and the lack of well defined crop calendars make changes in land cover characteristics in the season extremely difficult to characterize. Seasonality of land use parameters was therefore not considered further, and constant values were employed for the whole simulation period (Table 1). Similarly, soil detachability changes in time (Rudra *et al.*, 1998), but very little information is available on temporal changes of soil rainfall detachability indexes, which were then kept constant throughout the simulation.

The simulation of overland flow depth as per the original MMF, was substituted by the model of Vigiak *et al.* (2005c). The field overland flow Q_{TOT} (in mm per time step) was modelled as a function of the effective rainfall (u_e , in mm), i.e. the amount of rainfall that generates discharge at the catchment outlet, the Hydrologic Response Unit (HRU: perennial or other crops), and the field topographic connectivity (run-on and run-off). The model accounted for reinfiltration by assuming that only a portion of the total overland flow of the field (Q_{TOT}) would drain out of it (run-off, Q_{OUT} in mm per time step). The maximum field area generating run-off was equal to the length of the lower field border (B_F , in m) times the characteristic reinfiltration length L , i.e. the average length (m) along which the overland flow travels on the soil surface before reinfiltrating in the soil:

$$Q_{OUT} = Q_{TOT} \left[\min \left(1; \frac{B_F L}{A_F} \right) \right] \quad (2)$$

where A_F is the field area (m^2), and min indicates the minimum between the elements in brackets.

The field overland flow Q_{TOT} was used in the original MMF equation to calculate the overland flow detachment rate H (kg m^{-2}):

$$H = 10^{-3} \frac{1}{0.5COH} Q_{TOT}^{1.5} \sin \beta (1 - GC) \quad (3)$$

where COH is the soil cohesion (kPa), $\sin \beta$ is the sine of local slope and GC is the fraction of vegetation ground cover (0-1). Eq. (3) is based on the laboratory experimental work of Quansah (1981), valid at storm basis. Vigiak *et al.* (2005a) showed that in the MMF model overland flow detachment rates account for no more than 2 % of total detachment in this environment. Thus, eq. (3) was retained without changes for use with the daily data available here, since in most events the daily Q_{TOT} will represent the storm overland flow.

The transport capacity rate TC (kg m^{-2}) of the run-off overland flow (Q_{OUT}) was equal to:

$$TC = 10^{-3} CP Q_{OUT}^2 \sin \beta \quad (4)$$

where CP is the crop cover factor, given by the product of the Universal Soil Loss Equation (USLE) C and P factors (Wischmeier and Smith, 1978).

The sediment output (E_{out} , kg m^{-2}) was given by the minimum of sediment available and transport capacity:

$$E_{out} = \min [(F + H + E_{in}), TC] \quad (5)$$

where E_{in} is the influx of sediment transported in the field by the incoming run-on. The net erosion (soil loss rate) E was given by the difference between incoming and outgoing sediment and was negative when sedimentation occurred:

$$E = E_{out} - E_{in} \quad (6)$$

Rainfall and discharge records were available for the period Feb-May 2003; the total erosion of this period gave the erosion rates of the long rainy season 2003.

To choose the model simulation time step the following assumptions were made: (i) most model equations could be considered valid at the event (daily) time scale; (ii) in the hydrologic model, the accumulation of overland flow along the hillslope is linear (i.e. Q_{OUT} is a constant fraction of the Q_{TOT} , eq. 2); and (iii) field observations were conducted on event basis. The event scale is an interesting scale for erosion modelling because most of soil losses occurring in a season are due to few severe erosive events (e.g. Larson *et al.*, 1997); it also represents the upper limit to which most erosion equations established for instantaneous conditions may hold (Morgan, 1995). The event scale (i.e. daily time steps) was therefore chosen as a good compromise between modelling issues, available observations and computing time requirements.

However, the sediment transport capacity TC (eq. 4) is nonlinearly dependent on overland flow and is therefore sensitive to the choice of the temporal scale. Because of this sensitivity and because sediment transport capacity determines the distribution of erosion in the case of transport-limited erosion (eq. 5), the choice of the effective parameters for these equations introduces considerable uncertainty in the model predictions. Effective parameter values may as well compensate for deficiencies of the model representation of the fluxes at the event scale. Thus, effective values might be not commensurate to field measurements.

Uncertainty of sediment transport capacity

In the literature, overland flow sediment transport capacity has been related to different hydraulic variables (shear stress, stream power, effective stream power, and unit stream power). The performance of the equations depends mainly on the overland flow regime (laminar or turbulent; Julien and Simons, 1985). However, where rainfall is spatially uniform, all sediment transport equations can ultimately be defined as (Julien and Simons, 1985):

$$q_{s,TC} = k_{TC} q^{\alpha} \sin \beta^{\gamma} \quad (7)$$

where $q_{s,TC}$ is the sediment transport capacity per unit width of slope, q is the discharge per unit width, $\sin \beta$ is the local topographic gradient, and k_{TC} parameter is a scaling factor that represents soil erodibility and comprises gravitational acceleration, water density, sediment cohesion, density and particle size (Prosser and Rustomji, 2000). According to eq. (7), the distribution of overland flow sediment transport capacity, and thus of erosion, depends ultimately on catchment topography (Desmet and Govers, 1995), and on the spatial pattern of overland flow, which in turn is mainly a function of the land use and soil management (e.g. Takken *et al.*, 1999; Rustomji and Prosser, 2001). The parameters α and γ depend on the hydraulic variable used in the original formulation and on experimental conditions, but express the control that the hydrologic regime and topography exert on the spatial distribution of erosion (Rustomji and Prosser, 2001). Physical conditions affecting the choice of parameters α and γ in eq. (7) change in space and time within a catchment, but catchment-scale effective parameters should capture the dominant sediment transport conditions.

Because of the importance of sediment transport capacity on the spatial distribution of erosion within the catchment, the uncertainty of model predictions due to sediment transport capacity parameters on the distribution of erosion was explored using the Generalized Likelihood Uncertainty Estimation (GLUE) methodology (Beven and Binley, 1992; Beven, 2001). The GLUE methodology assumes that many different parameter sets may result in equally acceptable model performances as measured with given criteria (equifinality thesis). The method is based on Monte Carlo (MC) simulations, with uniform parameter sampling. A likelihood measure, which is chosen according to the purpose of modelling, is used to assess the ‘goodness of fit’ of model output to observed data. Behavioural parameter sets are those that fulfil the minimum threshold set for the appropriate likelihood measure. The behavioural parameter sets can then be used to assess the predictive uncertainty of the model.

In this study, the GLUE methodology was applied to assess the predictive uncertainty associated with the parameterisation of the sediment transport capacity of overland flow. The generic formulation of eq. (7) was embedded in the semi-empirical model by transforming eq. (4) into:

$$TC = k'_{TC} CP Q_{OUT}^{\alpha} \sin \beta^{\gamma} \quad (8)$$

where Q_{OUT} is defined by (eq. 2) and CP is the USLE crop and protection cover factor. The three key parameters of eq. (8) were the reinfiltration length L , which determines the amount of overland flow draining out of the fields (eq. 2), α and γ . A characteristic reinfiltration length L of 4 m was considered suitable for Kwalei catchment (Vigiak *et al.*, 2005c), however some uncertainty in the parameter should be allowed, as the reinfiltration length is likely to vary with rainfall event characteristics, soil conditions, land use, and slope. Rejman (2003) recently reported that effective distances for soil transport in runoff plots varied between two and 13 m. A suitable range of reinfiltration length L was estimated in the interval [2, 10] m for Kwalei catchment. In a recent review, Prosser and Rustomij (2000) showed that the intervals of [1, 1.8] for α and [0.9, 1.8] for γ contain 85 % of the equations proposed in literature. In our study, the range [0.9, 2] was set for α and [0.9, 1.8] for γ , thus slightly enlarging Rustomij and Prosser's (2001) set to include the original MMF equation. The parameters were sampled independently and uniformly in these ranges. The parameter k'_{TC} acted as a pure scaling factor and was calibrated against the Gerlach trough observations, after accounting for the effect of crop management on the distribution of erosion, which was assumed to be realistically represented by the CP factor. Each MC simulation consisted of three steps: first the model was run with the parameter set $\{L \ \alpha \ \gamma \ k'_{TC}\}$ equal to $\{L_n \ \alpha_n \ \gamma_n \ 1\}$, where the subscript n indicates the n th MC random realization of the parameter set; then k'_{TCn} was estimated as the ratio of the median of the sediment load distribution observed in the Gerlach troughs and the median of the sediment load distribution simulated by the model for the same sites; finally the model was run with the $\{L_n \ \alpha_n \ \gamma_n \ k'_{TCn}\}$ for the whole catchment. Eleven thousand MC simulations were performed.

The simulation performance criterion was based on the comparison of simulated erosion patterns against the observed one (ACED map). Model simulations were reclassified into five qualitative erosion classes; thresholds among classes were chosen in such a way that the number of fields per class (regardless of their location) matched that of the ACED map. The measure of agreement between the classified model map with the ACED map was assessed by the weighted Kappa coefficient of the contingency table (Cohen, 1968). Given a contingency table of two classification systems of r classes, in this case the five classes of erosion assessed during erosion survey (i) or predicted by the model (j), the weighted Kappa coefficient (wK) is defined by:

$$wK = \frac{P_{o,w} - P_{e,w}}{1 - P_{e,w}} \quad (9)$$

where

$$P_{o,w} = \sum_{i=1}^r \sum_{j=1}^r w_{ij} P_{ij} \quad (10)$$

Table 2. Weights (w_{ij}) applied to the contingency table to calculate the weighted Kappa to measure of agreement between maps (from Vigiak *et al.*, 2005a).

		ACED map				
		Very low	Low	Moderate	High	Very High
Model map	Very low	1	1	0.5	0.25	0
	Low	1	1	1	0.5	0.25
	Moderate	0.5	1	1	1	0.5
	High	0.25	0.5	1	1	1
	Very high	0	0.25	0.5	1	1

is the weighted observed distribution, and

$$p_{e,w} = \sum_{i=1}^r \sum_{j=1}^r w_{ij} p_{i.} p_{.j} \quad (11)$$

is the weighted chance-expected distribution, with $p_{ij} = \frac{m_{ij}}{m}$, $p_{i.} = \frac{m_i}{m}$, $p_{.j} = \frac{m_j}{m}$, m_{ij} is the number of fields classified in classes i and j ; m_i is the total number of fields classified in the class i ; m_j is the total number of objects classified in the class j and m is the total number of fields (Cohen, 1968).

The weights w_{ij} were set to limit the influence of the classification system and to account for uncertainties in the ACED map. One class difference (e.g. very low class in the ACED erosion map predicted as low erosion in the MMF erosion map) was considered acceptable (weight factors = 1), whereas for larger disagreements between the two maps, the weights were linearly dependent on the distance between classes (Table 2; Vigiak *et al.*, 2005a).

Parameter sets whose simulation scored a weighted Kappa (wK) value equal or larger than a minimal threshold were considered behavioural, whereas parameter sets whose simulation was below the threshold were rejected as non-behavioural.

Results and Discussion

Assessment of erosion

Rainfall detachment

Collection of splashed material was done once in the long rainy season 2002 and twice in the season 2003, after exposing the splash cups to the rainfall for periods of 34–42 days. Rainfall detachment rates were generally high, especially at the beginning of the rainy season, and ranged on average from 14.8 g m⁻² per mm of rain in April 2002 to 6.9 g m⁻² mm⁻¹ in April 2003 and 2.7 g m⁻² mm⁻¹ in May 2003. The splashed dry soil per unit area was divided by the kinetic energy of the observation periods calculated according to the MMF model (eq. 1); Table 3 shows average and standard deviation of the observed

Table 3. Observed rainfall detachment rate measured in splash cups, in Kwalei catchment, Tanzania. The acceptable range for the soil detachability index was given by the average of observed detachment rate minus and plus one standard deviation. The column K shows the MMF detachability index for Kwalei soils (after Vigiak *et al.*, 2005a).

Land use type	Rainfall detachment rate			Acceptable range		MMF K (g J^{-1})
	n	mean (g J^{-1})	st dev (g J^{-1})	min (g J^{-1})	max (g J^{-1})	
Maize and beans	6	0.674	0.344	0.330	1.018	0.3-0.35
Cassava	4	0.281	0.262	0.019	0.544	0.3-0.35
Coffee and Banana	6	0.624	0.581	0.043	1.206	0.3-0.35
Tea	4	0.308	0.515	0.000	0.823	0.3-0.35
Vegetables	5	0.408	0.307	0.100	0.715	0.05

detachment rates per land use type and per Joule of kinetic energy (g J^{-1}). Rainfall detachment was very variable, even within the same field, reflecting the natural variability of erosion processes. Moreover, notwithstanding the good collaboration from the farmers at the field sites, sometimes the splash cups were disturbed by tillage operations (in these cases observations were discarded), and the available number of observations (four to six per land use) was very limited. Figures in Table 3 should therefore be considered only as indicative of the erosion detachment phenomenon in Kwalei catchment.

The high natural variability of erosion must be taken into consideration when comparing model simulations to observations (Nearing, 2000). Similarly to Nearing's approach, the acceptable range of the soil detachability index was considered to be the interval defined by the average of observations ± 1 standard deviation. In Table 3 the acceptable ranges per land use type are shown, together with the MMF soil detachability index (K of eq. 1) suggested for Kwalei soils (Quansah, 1981; Vigiak *et al.*, 2005a). The ranges were wide, especially for the tea fields, but soil detachability indexes were in good agreement with observations and close to 0.3 g J^{-1} , confirming that the MMF calculation of rainfall detachment rate was acceptable, at least in the light of the high variability of measurements. The only exception was given by the vegetable fields, located on the Umbric Gleysols of the valley bottom. In this case, the observed detachment rates were much higher than those estimated from the high clay content of this soil type. As detachment rates did not differ from other soils, the soil detachability index for the Gleysols was raised to 0.3 g J^{-1} .

Erosion rates at the Gerlach trough sites

In Table 4 the event and seasonal (March-June 2003) observations of overland flow depth and sediment load per Gerlach trough are reported. Only in two of the 13 effective rainfall events recorded in Feb-June 2003, did all the Gerlach troughs collect overland flow. The distributions of observed overland flow depth and sediment load were skewed and log-distributed. The median overland flow per event was equal to 0.148 mm, and ranged from 0 to 1.97 mm. The median sediment load was 0.02 kg m^{-2} ,

Table 4. Observations of erosion rates at Gerlach sites, Kwalei catchment.

Gerlach trough	n [#]	Overland flow depth			Sediment load		
		Event mean (mm)	cv (%)	total (mm)	mean (kg m ⁻²)	cv (%)	Total (kg m ⁻²)
G1	3	0.260	63	0.780	0.122	143	0.367
G2	8	0.288	104	2.302	0.017	92	0.136
G3	10	0.675	115	6.744	0.146	165	1.314
G4	10	0.083	118	0.832	0.080	270	0.801
G5	12	0.436	82	5.669	0.058	68	0.759
G6	3	0.026	17	0.079	0.010	133	0.020

[#] number of events during which the trough collected overland flow and sediment.

and ranged from 0.001 to 0.738 kg m⁻². Observed event overland flow and sediment load values compared well with measurements conducted in the same areas with Gerlach troughs located in maize and bean fields (0.16 mm and 0.81 kg m⁻²; A. Tenge, pers. comm.). Variabilities of overland flow and sediment load were high, confirming the extreme spatial and temporal variability of event scale plot measurements (Hjelmfelt and Burwell, 1984; Wendt *et al.*, 1986; Nearing, 2000), especially considering that Gerlach troughs were unbounded and placed at different locations.

The rainfall season was drier than the average year, with 330 mm of rain in Feb-May 2003 against the 510 mm of long term average for the same period (1981-2001 Sakarani mission data). The median observed overland flow depth for the whole season March-June 2003 was 1.57 mm, being generally larger in annual crops (sites G1, G2, and G5) than for perennial crops (sites G4 and G6). The largest amounts of overland flow were recorded in a degraded tea field in the lower part of transect 1 (site G3). Overland flow depths were generally low, but comparable to the 0.6 mm y⁻¹ reported by Lundgren (1980) for the West Usambara Mountains. Observed erosion rates were rather low (Table 4), but close to the estimations of Pfeiffer (1990) of 1.6-2.1 kg m⁻² y⁻¹ for arable land of the West Usambara Mountains.

Catchment scale assessment

The qualitative assessment of current erosion damage (ACED) survey covered 80 % of the catchment area. Of the remaining fifth of the catchment, some fields had been hoed recently before the survey. Their erosion status could not be directly assessed, but was estimated considering other information available, such as land use, slope steepness, and the status of upslope and neighbouring areas. Other fields had been surveyed in the 2002 rainy season, and this information completed the assessment map of the catchment. According to the survey, 39 % of the fields (around 21 % of the catchment area, Fig. 1B) were affected by severe erosion. Except for an area that was burned some years ago, the forest showed little signs of erosion. Most coffee and banana stands also showed little erosion. The survey therefore confirmed the spatial distribution of erosion reported by Vigiak *et al.* (2005a).

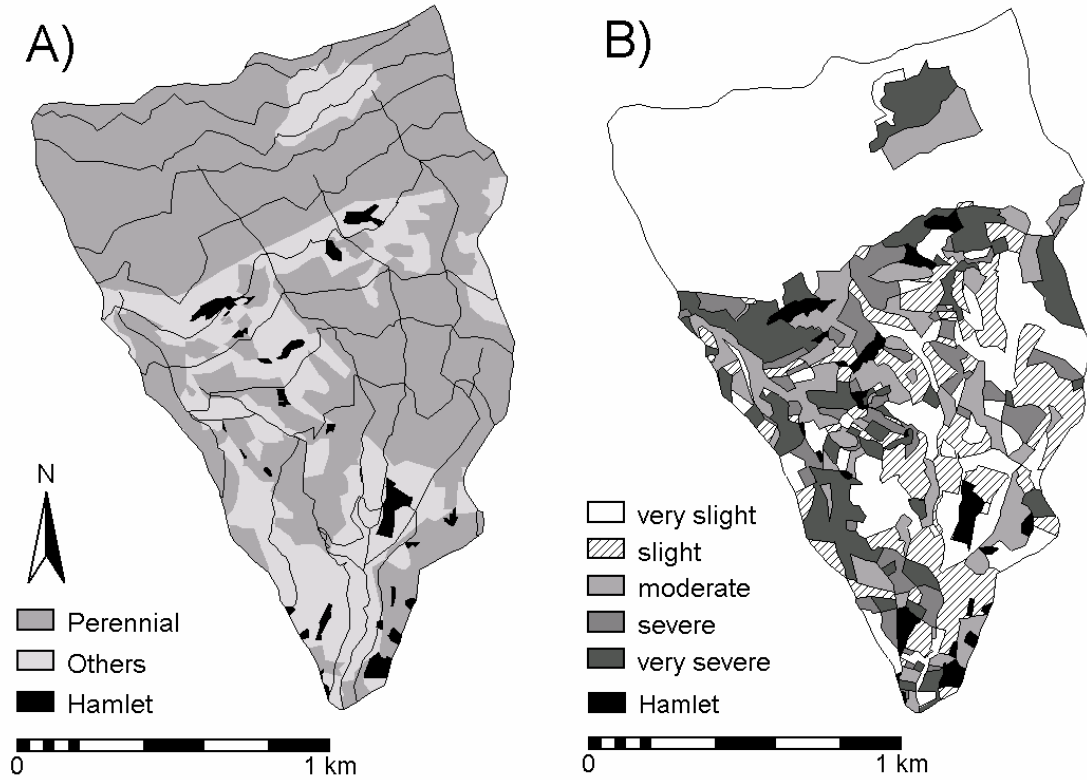
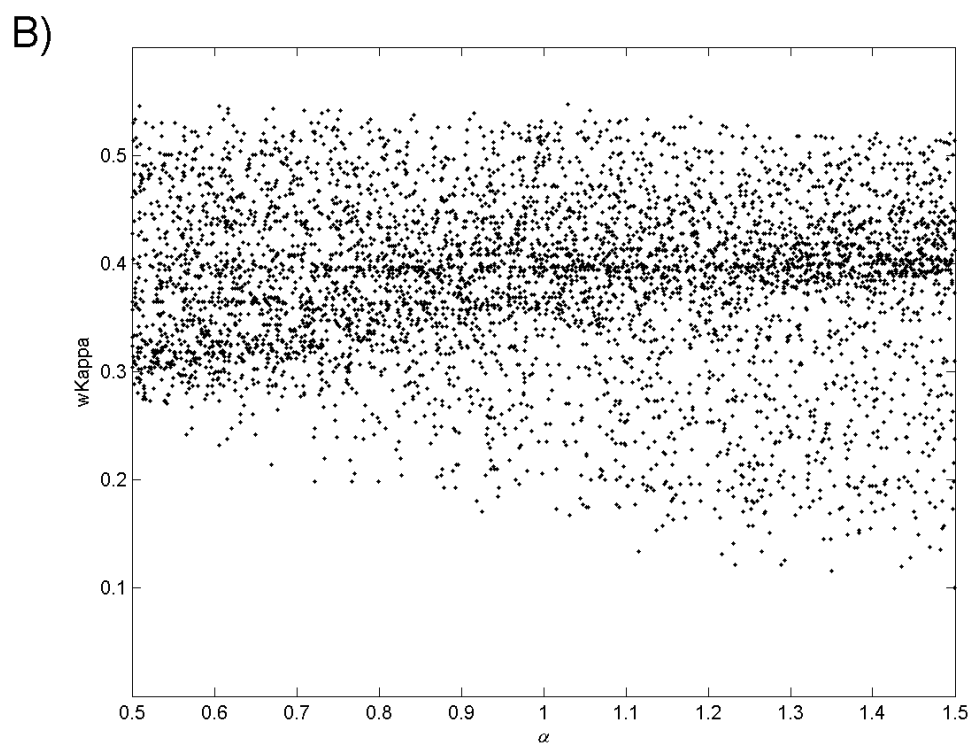
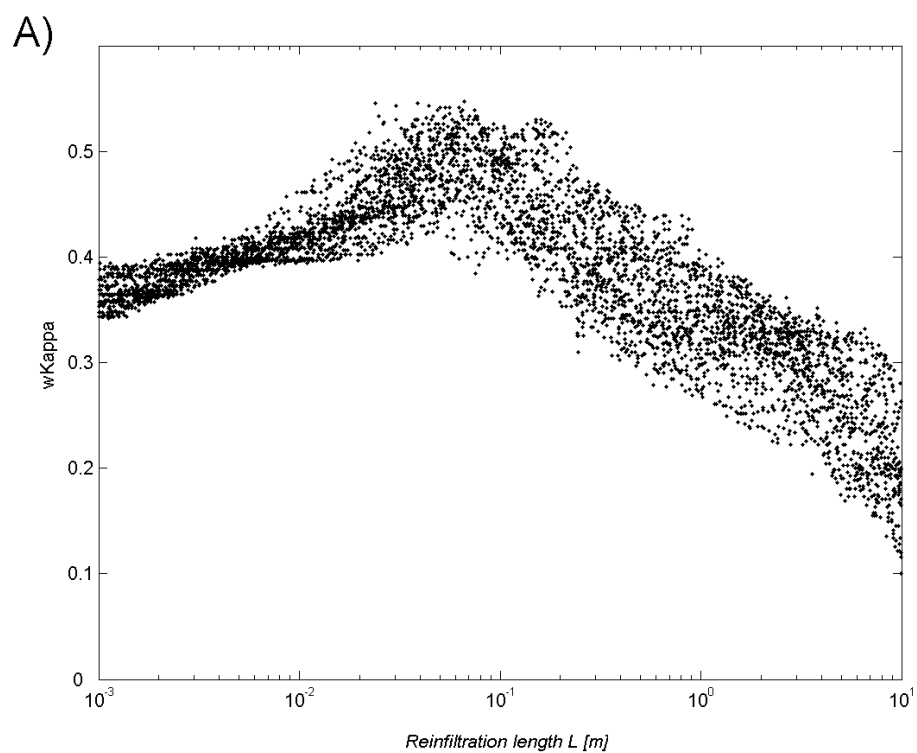


Figure 1. Land characteristics of Kwalei catchment: A) the Hydrologic response units (HRUs), i.e. perennial vs. other crops, in black the hamlets; black lines indicate the perennial streams and 50 m contour lines; B) the assessment of actual erosion map (ACED), from very slight to very severe erosion.

Uncertainty of model simulations

The choice of parameters of eq. (8) strongly affected the estimated distribution of overland flow. The most sensitive parameter affecting the distribution of erosion was the reinfiltration length L . This was expected as L determines the volume of runoff that leaves the fields Q_{OUT} (eq. 2). Most behavioural simulations were at reinfiltration lengths below five meters. The agreement between observed and simulated pattern degraded quickly from a weighted Kappa (wK) above 0.30 at reinfiltration lengths $L = 2$ m to $wK < 0.2$ at $L = 10$ m. A similar trend was depicted for the parameter α , for which, beside few exceptions, best simulations were concentrated at $\alpha < 1.5$. The parameter γ gave an opposite trend, with best simulations concentrated at $\gamma > 1.4$. The parameter k'_{TCn} acted as a scaling factor that was calibrated against the Gerlach observations. Because both overland flow (Q_{OUT}) and local slope ($\sin\beta$) values were below the unity, increases of the powers of α or γ resulted in geometrical increases of k'_{TCn} . The best simulation of the model scored a weighted Kappa of 0.34, which indicates a fair agreement between the two maps at best.

The best simulations were concentrated near the edges of the selected ranges. Therefore, it was decided to enlarge the sampling ranges for other 6.000 new MC simulations, sampling the reinfiltration length L for a logarithmic distribution in the interval $[0, 10]$ m, and sampling the other two parameters



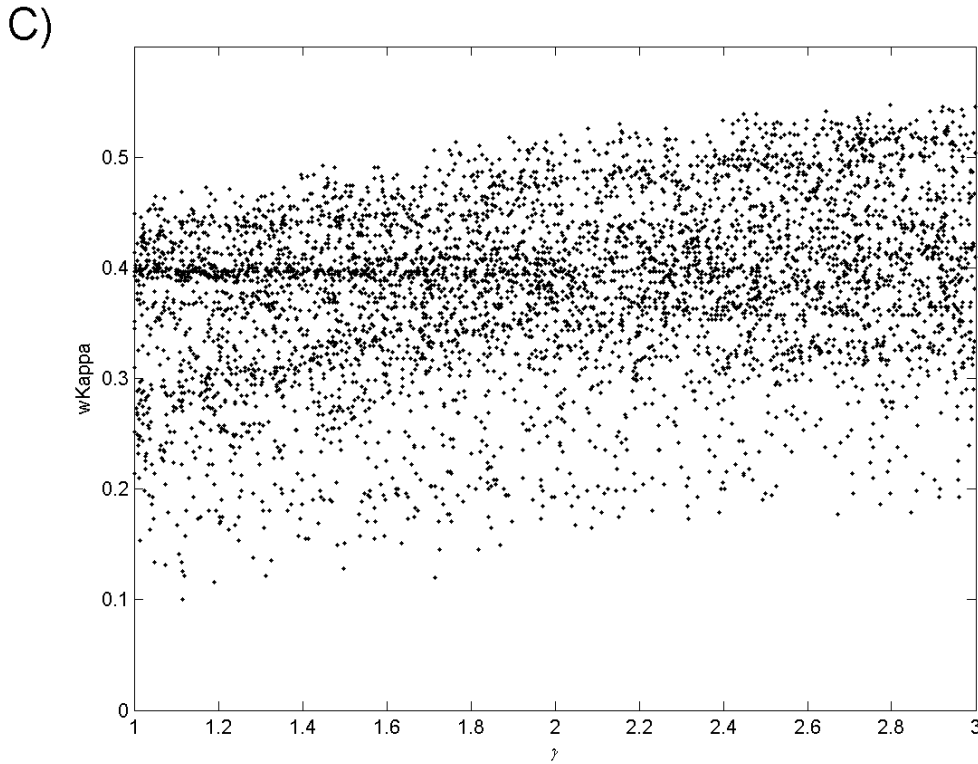


Figure 2. Dotty plots of 6,000 MC simulations ($L = [0, 10]$ m; $\alpha = [0.5, 1.5]$ and $\gamma = [1, 3]$), Kwalei catchment, Tanzania. Weighted Kappa of model simulations are presented in relation to the three parameters selected for the simulation: (A) reinfiltration length L (in logarithmic scale); (B) overland flow power parameter α and C) local slope power parameter γ

uniformly in the intervals $[0.5, 1.5]$ for α and $[1, 3]$ for γ . With the new ranges, weighted Kappa raised above 0.50, which indicates good agreement between the model predictions and the ACED map. The best simulation scored $wK = 0.55$. Fig. 2 shows the dotty plots relating the weighted Kappa values to the three investigated parameters. Dotty plots are scatter plots of the performance measure against the parameter values and represent a projection of sampled goodness of fit response surface of a model onto an individual parameter dimension (Beven, 2001). Fig. 2 shows that the best simulations were at short reinfiltration length L , and relatively high γ values, whereas α gave good simulations along the whole range. The trends observed in the first MC runs were thus confirmed.

Fig. 3 shows the scatter plot of the ratio α/γ versus the reinfiltration length L (in logarithmic scale) at different wK intervals. Increasingly better agreement between the two maps was reached when reinfiltration length L was short and the ratio α/γ was close to 0.5. By defining as behavioural the simulations that yielded a weighted Kappa above 0.50, 277 of the 6,000 (second set) MC simulations were selected. Behavioural parameter sets comprised the following ranges: $[0.002, 1.06]$ m for L , $[0.5, 1.5]$ for α and $[1, 3]$ for γ . The behavioural parameter sets represent an aggregated response of the

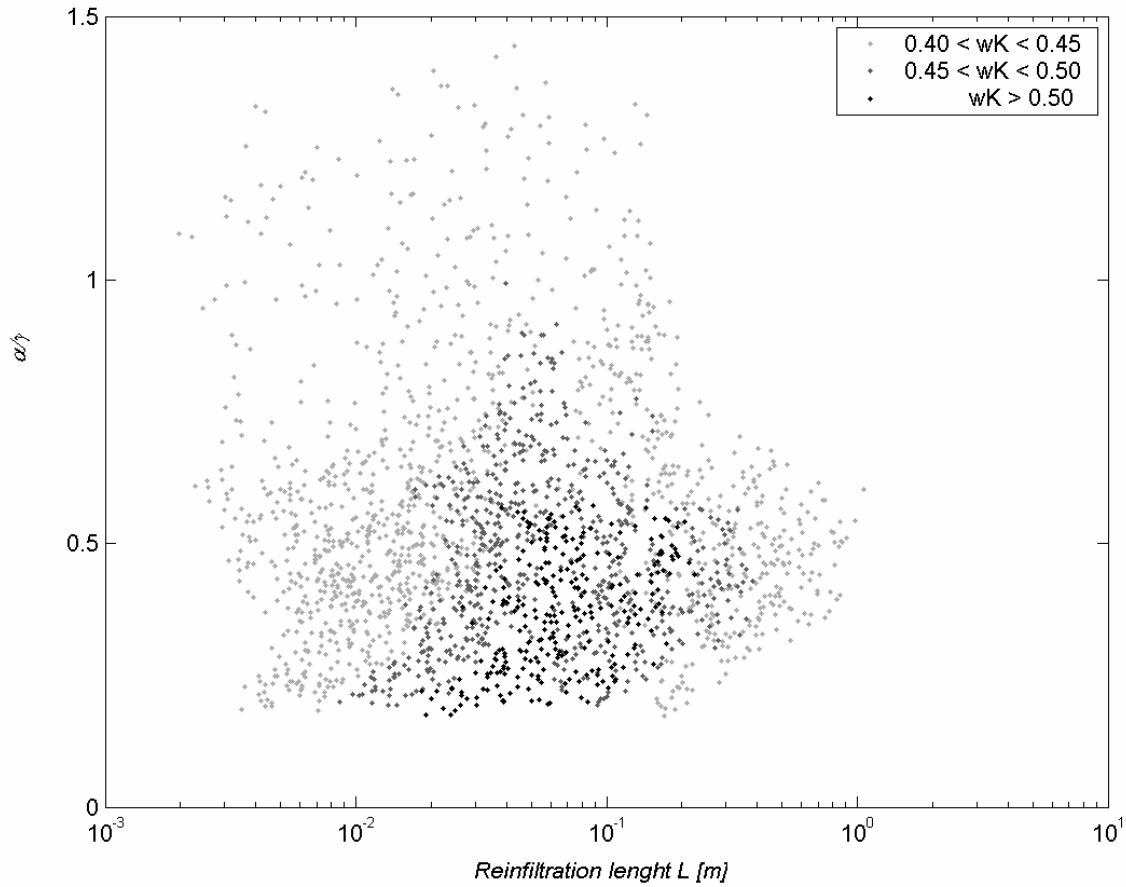


Figure 3. Scatter plot of power α/γ ratio versus reinfiltration length L at different intervals of weighted Kappa. Short reinfiltration length L (in logarithmic scale) in combination with the ratio α/γ close to 0.5 resulted in the best simulations (black dots; $wK > 0.50$).

catchment to the prevailing hydrologic and topographic conditions, but account as well for internal adjustments of the model. Therefore a physical interpretation is always difficult. However, the three parameter trends were consistent with each other and indicated a strong control of local topography above the hydrologic conditions in controlling the pattern of erosion.

The reinfiltration length governs the accumulation of overland flow along the hillslope and accounts for the influence of incoming run-on in the lower fields. Reinfiltration lengths below 5 m resulted also in better simulations of overland flow measurements at the Gerlach sites (Vigiak *et al.*, 2005c) and confirmed the importance of reinfiltration in the hydrology of Kwalei catchment (Vigiak *et al.*, 2005b). The small range for behavioural reinfiltration lengths confirm that there is little movement of overland flow among Hydrologic Response Units. It also indicates that the reinfiltration lengths required by the model are shorter than those measured in the field. This can be a result of the hydrologic model distribution mechanism. The redistribution of overland flow done by the model of Vigiak *et al.* (2005c) is derived from observations of overland flow occurrence, and implicitly accounts in part for the

limited travel distance along the soil surface. The model results, however, are in agreement with Bergkamp (1998), who observed very short reinfiltration lengths (about 0.30 m) in a Mediterranean catchment.

The dynamic Hortonian regime was reinforced by the better agreement of the erosion patterns at low parameter α . Kirkby (1988) showed that when the overland flow longest travel distance is shorter than the hillslope length, not all the upslope area contributes to the field segment overland flow and the parameter α is small. The stronger the reinfiltration, the lower the effective value of the parameter α , approaching zero in the extreme cases when overland flow travel distances are very short (Rustomji and Prosser, 2001). Such scenarios have been reported in some forest and semi-arid environments, and seem extreme for Kwalei conditions. Relatively higher values of parameter γ indicated at the same time that local slope exerted a strong control on sediment transport and on the distribution of erosion. With reference to the values reported by Prosser and Rustomji (2000), low α and high γ parameters correspond generally better to equations that calculate sediment transport in terms of mean stream power of overland flow. However, Figs. 2 and 3 show that more than absolute figures for α and γ , the important factor in depicting the pattern of erosion correctly is the ratio α/γ , which defines the relative importance of overland flow and topography in affecting the distribution of erosion. In the dynamic Hortonian hydrologic regime and in the strongly dissected terrain conditions of Kwalei catchment, it is not surprising that the topography controlled the distribution of erosion.

Field predictions of erosion of the behavioural parameter sets give information on the predictive uncertainty of model simulations. The field average rates of net erosion predicted by the model ranged from -4.2 to $+2.2$ kg m^{-2} for the whole long rainy season (February-May) of 2003. Field estimations varied among fields (Fig. 4). Standard deviation of estimations ranged from 0 to 2.86 kg m^{-2} in behavioural simulations, but was < 0.93 kg m^{-2} in more than 95 % of fields. The scatter of model predictions was large especially at the middle and low values of erosion rates and gradually decreased toward the highest erosion rates. Therefore, the highest uncertainty was in the slightly and moderately eroded fields, where changes in sediment transport capacity parameters may switch the model predictions from conditions of erosion to sedimentation and vice-versa. This is on one side reassuring: model simulations were more consistent in indicating fields where erosion was high than where erosion was low. On the other side, it cannot be excluded that some fields that were on average classified as subject to slight erosion, or even where the model simulated deposition of incoming sediment, might be wrongly classified: a higher uncertainty was linked to these fields.

Fig. 5A shows the average erosion class per field of the behavioural simulations, i.e. the average pattern of erosion predicted by the model. Table 5 shows the contingency table of the average model predictions against the ACED map. By considering acceptable a one class difference, 75 % of fields were correctly classified. Different type of errors could be distinguished: large model overestimations, where the error was larger than two classes (ACED map class – model map class < -1), small overestimations, where there was only one class of difference (-1), correct classification (0), small underestimations ($+1$), and large underestimations ($> +1$). Table 5 shows that both large overestimations, i.e. the model classified a field as subject to very severe erosion when the survey

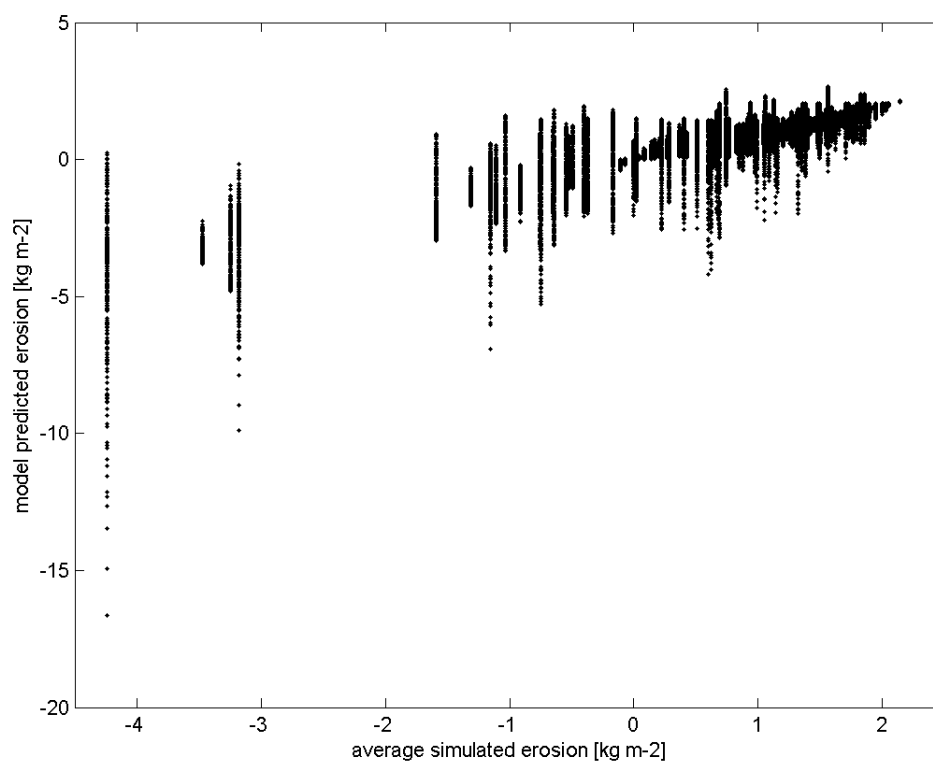


Figure 4. Predictive uncertainty of behavioural model simulations: dots indicate the outcome of field erosion of the behavioural simulations, fields are sorted by the seasonal average erosion rate.

Table 5. Contingency table of ACED map and the average output of model behavioural simulations.

		ACED map				
		Very low	Low	Moderate	High	Very High
Model map	Very low	33	21	8	5	4
	Low	24	19	18	10	11
	Moderate	16	21	30	16	8
	High	4	9	16	14	26
	Very high	2	9	9	22	35

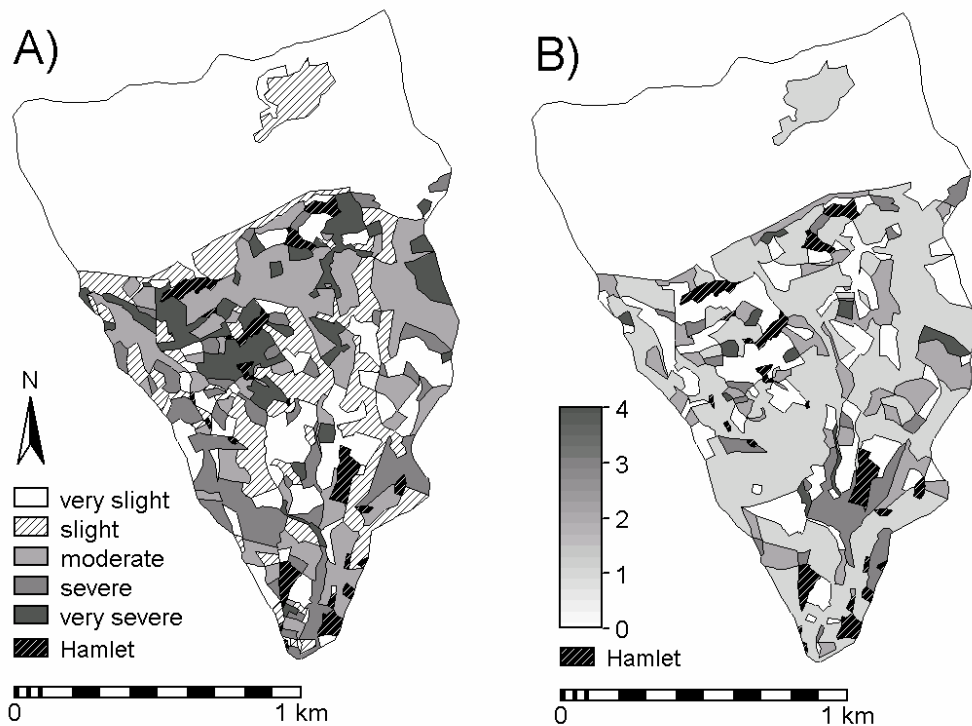


Figure 5. The model outputs. (A) The average classification of behavioural simulations (very slight = class 1; very severe = class 5). (B) The uncertainty of model simulations expressed by the field classification range (= highest class – lowest class attributed to the field by behavioural simulations): a classification range of four means that a given field was classified by some simulations as subject to very low erosion (class 1) and in other behavioural simulations as subject to very severe erosion (class 5).

indicated low or very low erosion, and large underestimations, where the model predicted very low erosion on fields that were actually subject to severe erosion, were present. Still, 64 % of severely and very severely eroded fields were correctly predicted by the model.

The uncertainty of erosion predicted by behavioural parameter sets caused changes in the distribution of erosion within the catchment: depending on the parameter sets, some fields were classified into different classes at each simulation, whereas others were consistently classified into the same class. The consistency of erosion class attribution for the behavioural model simulations can be measured with the classification range, i.e. the difference between the highest class attributed to a given field minus the lowest class attributed to the same field. A classification range of zero indicates that the field was consistently classified into the same class throughout the behavioural simulations, whereas a classification range of four indicates that, depending on the parameter sets, the field was either classified as subject to very slight erosion (class 1), to very severe erosion (class 5), or to any class in between. The classification ranges are shown in Fig. 5B; the classification range was zero in 31 % of fields, whereas 46 % of fields showed one class of difference. Around 10 % of fields resulted in a classification range larger than two. In particular, 3 % of fields had a classification range of four, i.e.

Table 6. Error of model map classification in comparison with model uncertainty (classification range). The type of error is given by the difference between ACED map class and model map class: large overestimation of model (ACED map – model map < -1), small overestimation (-1), correct classification (0), small underestimation (+1), and large underestimations (> +1).

		Difference (ACED map class – Model map class)				
		< -1	-1	0	+1	> +1
Classification range	0	16	27	54	16	7
	1	19	38	53	43	26
	2	7	12	10	13	11
	3	5	3	10	6	2
	4	2	3	4	3	0

model predictions were most uncertain. These areas generally corresponded to the valley bottoms, i.e. the receivers of the run-off coming from the slopes.

It is interesting to verify whether the model prediction errors were consistent, i.e. if the classification ranges of the erroneously classified fields was small (< 2). Table 6 shows the model prediction errors in comparison with the classification range. Around 10 % of all fields were consistently overestimated and 8.5 % of the fields were consistently underestimated. These model errors did not depend on the formulation of sediment transport capacity equation, but were either due to erroneous choice of other model parameters or were structural, i.e. some processes that are important in determining the distribution of erosion were not properly taken into account. The analysis of variance of model prediction error versus the cartographic variables available (i.e. soil type, land use and topography, both in terms of local slope and physiographic position) showed that the only variable significantly related to the model error was the land use. In particular, in vegetable parcels erosion was generally overestimated, whereas in patches of grassland, sugarcane and tea fields erosion was underestimated. Overestimations of erosion in the vegetable parcels are probably due to an incorrect model assumption: vegetable fields are located in the valley bottom, and according to the model they should receive run-on and sediment from the upper slopes. In reality, these fields are irrigated and separated in small parcels of around ten m² by irrigation channels. Incoming run-on and sediment probably drain into these channels and do not damage the vegetables plots. However, this information was not implemented in the model, causing the overestimation of erosion. Underestimations of erosion in tea, sugarcane and grassland were probably due to incorrect estimations of land use parameters. Only two land use parameters were correlated to model errors: *INT* (Pearson correlation coefficient = -0.38) and *CP* (Pearson c. c. = 0.16), which were also correlated (Pearson c.c. = -0.69). Both parameters were retrieved from literature (Morgan, 2001; Morgan, 1995) and apparently overestimated the protective effects of grassland, tea and sugarcane. Unfortunately, for these tropical crops there are not many values reported in the literature.

Conclusions

The semi-empirical erosion model proposed in this study was formulated to predict spatial patterns of erosion within a catchment in data scarce environments. The model included detachment by raindrops and overland flow, and sediment transport by overland flow. The formulation of processes was kept as simple as possible, but the structure of the model was verified to be acceptable for the study area. Soil detachment mechanisms were acceptably predicted and indicated soil detachability rates of 0.3 g J^{-1} .

The uncertainty of model predictions focused on the choice of sediment transport capacity parameters and was assessed with the GLUE methodology. The effects of other sources of uncertainty in model predictions, linked to soil and land use parameters, were considered of more local nature, which may depend on the distribution of soil and land use types, and, though they might be important and add further uncertainty in model predictions, were not addressed here. The parameterisation of the sediment transport capacity was crucial for defining the distribution of erosion within the catchment. The dotted plots revealed that distribution of erosion was well predicted when infiltration length was short ($L < 3 \text{ m}$) and the ratio of the overland flow depth power α and the local topography power γ , was close to 0.5. Our results contrast with the conclusion of Prosser and Rustomji (2000) who suggested to use $\alpha = \gamma = 1.4$ for modelling sediment transport at the catchment scale. However, the optimal α/γ ratio depends on environmental conditions and should not be generalized. In Kwalei conditions, because of the dynamic Hortonian hydrologic regime and the dissected terrain, topography controlled the distribution of erosion more than overland flow distribution.

Erosion rates predicted by behavioural simulations varied from -5.2 to $+2.1 \text{ kg m}^{-2}$ per season. The model simulated well 75 % of the classified pattern of erosion, and 64 % of severely eroded fields were well predicted. Uncertainties due to sediment transport capacity parameters were high; the standard deviation of net erosion rates ranged from 0 to 2.86 kg m^{-2} per season and was below 0.93 kg m^{-2} in more than 95 % of fields. Most uncertain estimations concentrated in the low and middle range of erosion rates, where small changes in sediment transport capacity induced a switch from erosion to sedimentation conditions. As a consequence, the classification of model predictions in classes of erosion varied with the parameter sets and 10 % of the fields showed a classification range larger than two.

SWC planning should focus on fields classified as affected by severe erosion. However, areas whose classification ranges are large should be checked carefully in the field. Still, the model consistently overpredicted erosion rates in around 10 % of fields and underpredicted erosion rates in 8.5 % of the fields. Overestimations of erosion occurred mainly in the vegetable plots, whereas underestimations of erosion were high in sugarcane, tea and grassland fields. The difficult estimation of land use parameters, especially *CP* and *INT*, contributed to the model prediction errors. Model structural errors must also contribute to the prediction errors. Such a simple model was expected to show various shortcomings. However, notwithstanding its simple structure, 65 % of severely eroded fields were well localized.

The application of the MC-based uncertainty estimation methodology showed the importance of sediment transport capacity parameters in defining the distribution of erosion within a catchment.

Notwithstanding the large literature available, the choice of sediment transport capacity parameters is still highly uncertain, and little research has been addressed on defining effective parameters for catchment scale distributed modelling. This is a major issue to be addressed to achieve real improvements of distributed erosion modelling at the catchment scale.

References

- Bergkamp G. 1998. A hierarchical view of the interactions of runoff and infiltration with vegetation and microtopography in semiarid shrublands. *Catena* **33**: 201-220.
- Beven KJ, Binley AM. 1992. The future of distributed models - model calibration and uncertainty prediction. *Hydrological Processes* **6**: 279-298.
- Beven KJ. 1993. Prophecy, reality and uncertainty in distributed hydrological modelling. *Advances in Water Resources* **16**: 41-51.
- Beven KJ. 2001. *Rainfall-Runoff Modelling. The Primer*. John Wiley & Sons Ltd, 360 pp.
- Blöschl G, Sivapalan M. 1995. Scale issues in hydrological modelling: a review. *Scale issues in hydrological modelling*, M. Sivapalan, Ed., John Wiley & Sons, 9-48.
- Brandt CJ. 1990. Simulation of the size distribution and erosivity of raindrops and throughfall. *Earth Surface Processes and Landforms* **15**: 687-698.
- Brazier RE, Beven KJ, Freer J, Rowan JS. 2000. Equifinality and uncertainty in physically based soil erosion models: application of the GLUE methodology to WEPP-the Water Erosion Prediction Project - for site in the UK and USA. *Earth Surface Processes and Landforms* **25**: 825-845.
- Cohen J. 1968. Weighted kappa: nominal scale agreement with provision for scaled disagreement or partial credit. *Psychological Bulletin* **70**: 213-220.
- Desmet PJJ, Govers G. 1995. GIS-based simulation of erosion and deposition patterns in an agricultural landscape: a comparison of model results with soil map information. *Catena* **25**: 389-401.
- FAO. 1990. *Guidelines for soil description*. Third ed. Soil Resource Management and Conservation Service, Land and Water Development Division, FAO.
- Garen G, Woodward D, Geter F. 1999. A user agency's view of hydrologic, soil erosion and water quality modelling. *Catena* **37**: 277-289.
- Gerlach T. 1967. Hillslope troughs for measuring sediment movement. *Revue de Geomorphologie Dynamique* **17**: 173.

-
- Herweg K. 1996. *Assessment of Current Erosion Damage*. Centre for Development and Environment Institute, University of Berne.
- Hjelmfelt AT, Burwell RE. 1984. Spatial variability of runoff. *Journal of Irrigation and Drainage Engineering* **110**: 46-54.
- Hudson NW. 1965. The influence of rainfall on the mechanics of soil erosion with particular reference to Southern Rhodesia, University of Cape Town, University of Cape Town.
- Jetten V, de Roo APJ, Favis-Mortlock D. 1999. Evaluation of field-scale and catchment-scale soil erosion models. *Catena* **37**: 521-541.
- Jetten V, Govers G, Hessel R. 2003. Erosion models: quality of spatial predictions. *Hydrological Processes* **17**: 887-900.
- Julien PY, Simons DB. 1985. Sediment transport capacity of overland flow. *Transactions of the ASAE* **28**: 755-762.
- Kirkby MJ. 1988. Hillslope runoff processes and models. *Journal of Hydrology* **100**: 315-339.
- Larson WE, Lindstrom MJ, Schumacher TE. 1997. The role of severe storms in soil erosion: a problem needing consideration. *Journal of Soil and Water Conservation* **52**: 90-95.
- Lundgren L. 1980. Comparison of surface runoff and soil loss from runoff plots in forest and small scale agriculture in the Usambara Mts., Tanzania. *Geografiska Annaler* **62A**: 113-148.
- Meliyo JL, Kabushemera JW, Tenge AJM. 2001. Characterization and mapping soils of Kwalei subcatchment, Lushoto District. Mlingano Agricultural Research Institute. Tanga, Tanzania.
- Merritt WS, Letcher RA, Jakeman AJ. 2003. A review of erosion and sediment transport model. *Environmental modelling & software* **18**: 761-799.
- Morgan RPC. 1981. Field measurements of splash erosion. *International Association of Scientific Hydrology Publication* **133**: 373-382.
- Morgan RPC, Morgan DDV, Finney HJ. 1984. A predictive model for assessment of erosion risk. *Journal of Agricultural Engineering Research* **30**: 245-253.
- Morgan RPC. 1995. *Soil erosion and conservation*. Second ed. Longman, 198 pp.
- Morgan RPC. 2001. A simple approach to soil loss prediction: a revised Morgan-Morgan-Finney model. *Catena* **44**: 305-322.
- Nearing MA. 2000. Evaluating soil erosion models using measured plot data: accounting for variability in the data. *Earth Surface Processes and Landforms* **25**: 1035-1043.

- Pfeiffer R. 1990. Sustainable Agriculture in Practice - the Production Potential and the Environmental Effects of Macro-contourlines in the West Usambara Mountains of Tanzania, Insitute fur Pflanzenbau und Grundland, Universitaet Hohenheim, 195.
- Prosser IP, Rustomji P. 2000. Sediment transport capacity relations for overland flow. *Progress in Physical Geography*: 179-193.
- Quansah C. 1981. The effect of soil type, slope and rain intensity and their interactions on splash detachment and transport. *Soil Science* **32**: 215-224.
- Quinton JN. 1997. Reducing predictive uncertainty in model simulations: a comparison of two methods using the European Soil Erosion Model (EUROSEM). *Catena* **30**: 101-117.
- Rejman J. 2003. Dynamics of erosion based on studies of different lenght plots. *25 Years of Assessment of Erosion. Proceedings of International Symposium, 22-26 September 2003*, W. Cornelis, Ed., Universiteit Gent, 255.
- Rudra RP, Dickinson WT, Wall GJ. 1998. problems regarding the use of soil erosion models. *Modelling soil erosion by water*, D. Favis-Mortlock, Ed., Springer-Verlag, 175-189.
- Rustomji P, Prosser IP. 2001. Spatial patterns of sediment delivery to valley floors: sensitivity to sediment transport capacity and hillslope hydrology relations. *Hydrological Processes* **15**: 1003-1018.
- Salles C, Poesen J, Govers G. 2000. Statistical and physical analysis of soil detachment by raindrop impact: rain erosivity indices and threshold energy. *Water Resources Research* **36**: 2721-2729.
- Takken I, Beuselinck B, Nachtergaele J, Govers G, Poesen J, Degraer G. 1999. Spatial evaluation of a physically based distributed erosion model (LISEM). *Catena* **37**: 431-447.
- Tenge AJM, de Graaff J, Hella JP. 2004. Social and economic factors for adoption of soil and water conservation in West usambara highlands, Tanzania. *Land degradation and development* **15**: 99-114.
- Vigiak O, Okoba BO, Sterk G, Groenenberg S. 2005a. Modelling catchment-scale erosion patterns in the East African Highlands. *Earth Surface Processes and Landforms* **30**: 183-196.
- Vigiak O, van Dijk SJE, van Loon EE, Stroosnijder L. 2005b. Matching hydrologic response to measured effective hydraulic conductivity. *Hydrological Processes* **subm.**
- Vigiak O, Romanowicz RJ, van Loon EE, Sterk G, Beven KJ. 2005c. A disaggregating approach to describe overland flow occurrence within a catchment. *Journal of Hydrology* **subm.**
- Viney NR, Sivapalan M. 1999. A conceptual model for sediment transport: application to the Avon River Basin in Western Australia. *Hydrological Processes* **13**: 727-743.
- von Rompaey AJJ, Verstraeten G, van Oost K, Govers G, Poesen J. 2001. Modelling mean annual sediment yield using a distributed approach. *Earth Surface Processes and Landforms* **26**: 1221-1236.

Wendt RC, Alberts EE, Hjelmfelt AT. 1986. Variability of runoff and soil loss from fallow experimental plots. *Soil Science Society of American Journal* **50**: 730-736.

Wischmeier WH, Smith DD. 1978. Predicting rainfall erosion losses - a guide to conservation planning. USDA. Washington DC. USDA Agricultural Handbook 537, 58 pp.

Young PC. 1998. Data-based mechanistic modelling of environmental, ecological, economic and engineering systems. *Environmental modelling & software* **13**: 105-122.

Chapter 6

WATER EROSION ASSESSMENT USING FARMERS' INDICATORS IN THE WEST USAMBARA MOUNTAINS, TANZANIA

Olga Vigiak, Barrack O. Okoba, Geert Sterk and Leo Stroosnijder

Catena. Accepted for publication.

WATER EROSION ASSESSMENT USING FARMERS' INDICATORS IN THE WEST USAMBARA MOUNTAINS, TANZANIA

Abstract

The contribution of local knowledge to ecological sciences has not been fully exploited: there is still a gap between the recognition of farmers' knowledge as valid and an effective use of such knowledge in activities aimed at sustainable development. This study explores the use of farmers' indicators of erosion for developing a rapid tool for water erosion assessment at field level in the West Usambara Mountains (Tanzania). Two extensive field surveys were conducted in the research area concurrently. One survey consisted of applying an established erosion assessment method, the Assessment of Current Erosion Damage (ACED). According to the erosion features observed, fields were classified into five erosion classes, from very slightly eroded to very severely eroded. The second survey consisted of recording the type and number of indicators of erosion listed by farmers and present in the fields. The number of farmers' indicators per field increased with erosion intensity, from less than four in slightly eroded fields to more than eight in severely eroded fields. All farmers' indicators were positively correlated to the ACED erosion assessment classes. However, two groups of farmers' indicators could be distinguished in terms of erosion assessment: strong indicators, which were observed in more than 70 % of cases in severely eroded fields, and weak indicators, which were observed more frequently in slightly and moderately eroded fields. Weak indicators appeared to be indicative of other land degradation phenomena, such as chemical fertility decline. Strong indicators and number of indicators were used to create a field erosion assessment tool in the form of a classification tree. The tree was built using one half of the field survey data and validated using the other half. The tree consisted of a hierarchical sequence of questions. Presence of rills and number of farmers' indicators were the most important factors of the tree. The validation yielded a highly significant Spearman rho correlation coefficient (0.81). The contingency table showed that more than 80 % of very severely eroded fields were correctly classified, whereas most misclassification occurred among slightly and moderately eroded fields. Farmers include land degradation phenomena and soil fertility decline in their definition of soil erosion. SWC planning should address this broader farmers' perception by including e.g. soil fertility improvements beside soil conservation. The distinction between strong and weak indicators of erosion is important in recommending the right intervention in the right spot, e.g. by counteracting soil erosion where strong indicators are present and by improving chemical fertility where weak indicators are present. The classification tree is of empirical nature and may need adaptation before being applied to other areas. The proposed methodology can be easily replicated and showed a high potential to provide extensionists with a field tool for erosion assessment. The classification tree was a successful example of integrating different types of knowledge for enhancing the co-operation between stakeholders involved in the erosion-control activities.

Keywords: *indigenous knowledge; farmers' perception; field erosion assessment; erosion indicators; East African Highlands; Tanzania.*

Introduction

In planning erosion control activities prompt and positive interventions are critical to establish a good co-operation between extension workers and farmers. Therefore, soil and water conservation (SWC) planning must take into account farmers needs and priorities and requires information on the effectiveness of SWC practices. The assessment of erosion prior to intervention and the effective location of sites where erosion is most severe should form the basis of any SWC planning.

Soil erosion by water can be assessed through a survey campaign, which is generally time- and resource-demanding. Survey methods usually consist of assessing the presence and intensity of erosion features, as well as recording factors that may cause erosion (Herweg, 1996; Morgan, 1995). Air photo interpretation may guide the sampling of fields or transects, but field work is still the most consistent, yet demanding activity in erosion assessment (Morgan, 1995). Moreover, the timing of the survey is critical: erosion features can be assessed only shortly after erosive events, whereas planning of SWC should be conducted as much in advance as possible before the onset of the critical rainy season.

Data scarcity is, however, a common problem in tropical rural areas. In addition, capital and human resources are usually much below the demand, and extensionists must often cover large areas, that may comprise very different ecological and socio-economic conditions and where their experience may be limited. Integration of the broader experience of the extensionists with the site-specific knowledge of the farmers may then become a key factor for successful interventions.

Local knowledge has been described as experiential, rooted in place, empirical and dynamic (Ellen and Harris, 2000). In particular, farmers' perception and description of their environment are often linked to land management experience and land use history (e.g. Payton *et al.*, 2003). Research has already shown the usefulness of employing farmers' knowledge to assess soil fertility (e.g. Murage *et al.*, 2000). Among others, Habarurema and Steiner (1997), and Murage *et al.* (2000) documented extensive knowledge of farmers on landscape processes, and relations between soil productivity and relief position. Positive experiences have also been reported in the use of indigenous knowledge for erosion assessment (e.g. Warren *et al.*, 2003). As farmers' and scientists' perceptions sometimes mismatch (Kiome and Stocking, 1995; Ostberg, 1995), van Dissel and de Graaff (1998) suggested that the adoption and adaptation of farmers' knowledge into a scientific framework could only be achieved by thorough assessment of farmers' perceptions of ecological degradation.

The importance of the contribution of local knowledge to ecological sciences has been acknowledged (WinklerPrins and Sandor, 2003), but difficulties remains in how to integrate effectively local and scientific knowledge systems. Methodological studies that focus on integrating local and scientific knowledge are few (Payton *et al.*, 2003). Niemeijer and Mazzuccato (2003) argued that the potential of farmers' knowledge has only been partially exploited and they pleaded for a move from the recognition of farmers' knowledge as a source of information to a more effective use of such knowledge for sustainable development. WinklerPrins (1999) stressed that the integration of local and

scientific knowledge would be most beneficial in activities aimed at more sustainable land management.

The incorporation of local knowledge in erosion assessment may offer many advantages for SWC planning. By incorporating local knowledge in a systematic tool for erosion assessment, extensionists would be provided with means to assess erosion, while taking full advantage of the farmers' experiential and dynamic knowledge of their environment. Moreover, the use of farmers' concepts in the description and recognition of erosion phenomena may create a common 'language' among extension workers and farmers that could strengthen farmers' participation in the SWC planning intervention.

The objective of this study was to test the use of farmers' indicators of erosion for developing a rapid tool for water erosion assessment at field level in the East African Highlands.

Material and methods

This research was conducted in the West Usambara Mountains (Tanzania). Thanks to a favourable climate and fertile soils, these areas have a high potential for crop production, and are very important sources of staple foods, forest products and export crops (Lundgren, 1980). Population densities are generally above 100 persons per km². Land scarcity has triggered accelerated soil erosion, which is now a widespread phenomenon and a major cause of land degradation (Mbaga-Semgalawe and Fomer, 2000).

Soil and Water Conservation (SWC) projects have been implemented in these areas since the colonial period, experiencing various degrees of success. In the 1980s, a new SWC planning method was introduced by the Government of Kenya, i.e. the Catchment Approach (Admassie, 1992; Pretty *et al.*, 1995). The method consists of a participatory community planning process, with actual planning of SWC measures at farm level. Since its introduction, the Catchment Approach has given positive results in the improvement of soil productivity together with reduced resource degradation and is now adopted by six East African countries (Kamar, 1998; Kizunguto and Shelukindo, 2002). However, a critical review of the method lamented the low rate of SWC adoption and highlighted the lack of proper tools for soil erosion assessment (Pretty *et al.*, 1995).

Participatory research conducted in two catchments representative of the East African Highlands, Gikuuri in Kenya and Kwalei in Tanzania, resulted in a list of indicators that farmers use to recognize and assess erosion in their fields (Okoba *et al.*, 2003; Tenge *et al.*, 2004). The lists of both areas concurred with each other and with current literature (Barrios *et al.*, 2001; Swete Kelly and Gomez, 1998), indicating good potential for the use of these indicators for East African Highland conditions (Okoba *et al.*, 2003). A preliminary list (indicators with the symbol * in Table 1) was employed to test the usefulness of farmers' indicators for water erosion assessment in the Kwalei catchment.

The Kwalei catchment (4°48' S, 38°26' E) is located in the West Usambara Mountains, at an average altitude of 1500 m a. s. l. Mean annual rainfall is 1100 mm and mainly falls during two rainy seasons, a

Table 1. List of farmer's indicators of soil erosion in Kwalei (Tanzania) and Gikuuri (Kenya) catchments. Symbol \checkmark means that the indicator was mentioned but the local name was not recorded. Symbol * indicates indicators employed in the present assessment survey.

Indicator	LOCAL NAMES [#]		
	Kwalei (Kiswahili)	Gikuuri (Kiambu)	
Soil colour change	Udongo mwekundu [#]	Ithetu itune	*
Absence of topsoil	\checkmark		*
Soil stoniness	Kokoto	Tumathiga	*
Rills	Michirizi	Tumivuko	*
Gullies	Makorongo	Mivuko minene	*
Sheetwash	Mmonyoko tandazo	Muguo	
Bracken fern	Shiuu		*
Poor crop development	Mazao ya rangi njano		*
Root exposure	\checkmark	Kuicirurio tumiri	*
Washing crop / seeds	\checkmark	\checkmark	*
Deposition of soil downslope	Udongo mchanganyiko	Gukunikuo	*
Change in water colour	Rangi ya maji	\checkmark	
Patches of bare land	Tambarare	\checkmark	*
Splash pedestals	Matone	Matata	
Rock exposure	Mawe	Mathiga	*
Slope steepness	Mteremko mkali		*
Breakage of SWC	Kuvunjika kwa hifadhi	Kuomomoka kwa mitaro	
Wind-blown soils		Muthetu muvuthu	
White-soft stones	Mashuhee		*
Poor seed germination	\checkmark		*

[#] Farmers' terms are reported as mentioned, but translated taking into account their practical meanings. For instance, *udongo mwekundu* literally means 'red soil': in Kwalei soil changes to reddish when topsoil is removed by erosion; with this term farmers therefore refer to soil colour change.

long one from March to May and a short one from September to November. The average monthly temperature ranges between 18° and 23 °C with the maximum occurring in March and the minimum in July.

The catchment is intensely populated, with a population density of about 400 persons per km² (Lyamchai *et al.*, 1998). Over 90 % of the catchment population depends on agriculture. The average household land size ranges from 1.2 to 1.6 ha (Tenge *et al.*, 2004). Food crops, mainly maize inter-cropped with banana and bean, are cultivated on the upper slopes. A two-layer cultivation of banana and coffee is frequent on the steeper slopes along the stream incisions. Irrigated vegetables are the main cash crops and are cultivated in the valley bottoms and on the lower slopes. Soil erosion is one of the

major constraints to agricultural production in the area (Meliyo *et al.*, 2001), and occurs especially at the onset of the rainy season, when storms are intense and soil cover poor (Vigiak *et al.*, 2005).

A team of scientists and farmers crossed the study area along two transects to get acquainted with what farmers considered (i) erosion indicators and (ii) an eroded fields. Then, in the period from December to May 2003 an extensive erosion assessment survey was conducted with the Assessment of Current Erosion Damage method (ACED; Herweg, 1996). ACED requires the observations of type and intensity of erosion features, such as pedestals, sheet wash, interrills, rills, gullies, or others features (e.g. tree or rock exposure, build-up areas, re-depositions and so forth), together with presence of factors causing erosion. The method allows the semi-quantification of soil erosion. However, in order to cover the whole catchment, less emphasis was given in the present study to measuring erosion features quantitatively and the method was employed to assess erosion qualitatively. Fields were classified into five qualitative erosion classes, from very low (class 1) to very high (class 5). Concurrently, the surveyor annotated the type and number of the farmers' indicators as observed in the field.

The distribution and frequency of the farmers' indicators were first explored with simple descriptive statistical analysis. Correlation among indicators was assessed by correlation coefficients of the correlation matrix, using SPSS software (2002). Type and number of farmers' indicators present in a field were then cross-tabulated with field erosion class as assessed by the ACED method to explore the relation between farmers' indicators and erosion assessment.

A measure of the strength of the farmers' indicator i in terms of erosion assessment was defined as the empirical probability p_{ij} that the indicator i occurred in an erosion class equal or larger than j :

$$p_{i,j} = 1 - \frac{\sum_{j=0}^{j-1} n_{i,j}}{n_i} \quad (1)$$

where n_{ij} was the number of presence of the indicator i in erosion class j , and n_i was the total number of presences observed for the indicator i . The higher the probability of occurrence in a high erosion class, the stronger was the farmers' indicator in terms of erosion assessment (Okoba *et al.*, 2003).

Farmers' indicators that were shown to be useful for erosion assessment were finally used for developing a simple, in-field erosion assessment tool in the form of a classification tree. The classification tree is a nonparametric type of regression method. It has the advantage that it does not require assumptions of the form of the relationship (linear or otherwise) between the dependent variable (i.e. the field erosion class) and the input data set (i.e. the farmers' indicators). The survey dataset was randomly split in two; one half was used for creating the classification tree; the other half for validating it. The classification tree was built using the guidelines of Breiman (1993) in MATLAB Statistical Toolbox software (The MathWorks, 2002). The validation set was compared with the ACED erosion classification via a contingency table. The degree of agreement between the two classification methods was estimated with the Kappa coefficient (Cohen, 1968), which depends on both the observed and the chance-expected agreement between the two classifications. The Kappa coefficient was calculated with the freeware Kappa.exe (Bonnardel, 1995).

Results and discussion

In total the concurrent surveys covered 336 fields that spanned the whole catchment. The five ACED erosion classes were defined as follows:

- 1) very slightly eroded fields (class 1, very low): sporadic and shallow (average depth < 1.5 mm) pedestals, none or sporadic signs of sheet wash;
- 2) slightly eroded fields (class 2, low): frequent pedestals (average depth = 2 mm), signs of sheet wash, such as interrills, shallow exposure of roots and stones covering part of the field;
- 3) moderately eroded fields (class 3, moderate): intense rain splash signs indicated by frequent pedestals (average depth = 2.5 mm); widespread interrill signs covering the whole field, sporadic rills;
- 4) severely eroded fields (class 4, high): frequent pedestals (average depth = 3 mm); widespread interrill erosion; rills with cross sections of 1-5 cm² and/or covering 10-20 % of the field;
- 5) very severely eroded fields (class 5, very high): frequent pedestals (average depth > 3 mm); widespread interrill erosion; rills with cross sections of 10 cm² or more, and/or covering 30 % or more of the field; presence of gullies.

Fields were equally distributed among the five erosion classes: there were 60 - 80 fields in each class. Two thirds of the fields were surveyed during the short rainy season (December 2002 – February 2003), when most fields were fallow. The remaining third of fields were observed during the long rainy season (March-May 2003), when fields were cultivated and the frequent hoeing hampered the observation of erosion features and farmers indicators. However, the distribution of fields per erosion class was homogeneous in the two periods (one-way analysis of variance test at probability level $\alpha = 0.05$), therefore the sample population was analyzed without distinction between the two seasons.

Farmers' indicators were classified into four groups according to the frequency of observations, i.e. the number of fields where the indicator was present divided by the total number of fields:

- 1) most frequent, observed in more than 25 % of the fields: *Bracken fern* (*Pteridium Aquilinum* L.), *slope steepness* and *white-soft stones* ('*mashuhee*'; Plate 1);
- 2) frequent, observed on the 15-25 % of the fields: *soil colour change*, *absence of topsoil*, *rills*, and *poor crop development*;
- 3) occasional, observed on the 5-15% of the fields: *rock exposure*, *soil stoniness*, *root exposure*, *patches of bare land*, and *deposition of soil downslope*;
- 4) sparsely occurring, observed on less than 5% of the fields: *gullies*, *washing of crops and seeds*, and *poor seed germination*.

Some farmers' indicators could only be observed during a short time, as after an erosive rainfall (e.g. *deposition of soil downslope*) or during early crop cultivation (e.g. *poor seed germination*), while others could be observed at any time (e.g. *slope steepness* or *rock exposure*).

The number of farmers' indicators per field increased with erosion intensity (Fig. 1): no field belonging to very low or low erosion classes in the ACED scheme showed more than four farmers'



Plate 1. *Mashuhee*: farmers of Kwalei consider this white-soft stone a sign of soil erosion.

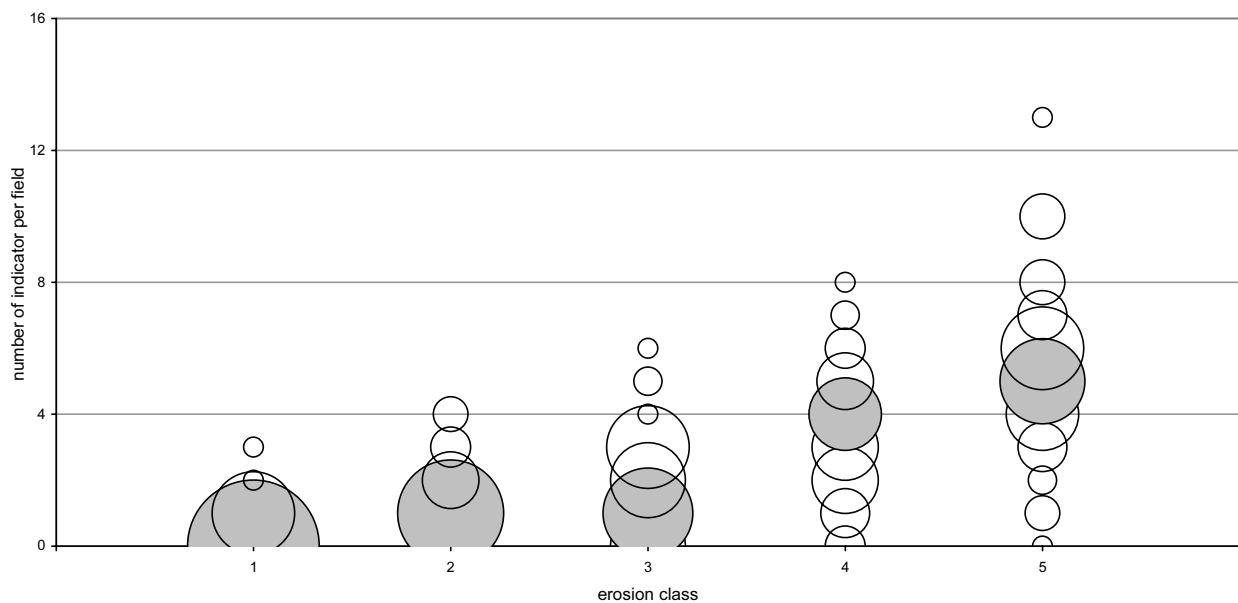


Figure 1. Number of indicators per field and per erosion class (erosion classes: 1 = very low, 5 = very high), in Kwalei, Tanzania. Bubble dimensions are proportional to the frequency of observation for each number of indicators / erosion class combination. The grey bubble indicates the modal combination for each class.

Table 2. Probabilities p_{ij} that an indicator i occurred in a field with erosion class equal or higher than j and total number of presences n_i observed per farmers' indicator.

Indicator i		p_{ij} per erosion class j				n_i
		2	3	4	5	
Most frequent	Slope steepness	0.94	0.79	0.60	0.39	126
	Bracken fern	0.94	0.77	0.56	0.35	124
	White-soft stones	0.99	0.91	0.72	0.40	92
Frequent	Poor crop development	1.00	0.97	0.87	0.58	67
	Rills	1.00	1.00	0.97	0.86	66
	Soil colour change	0.98	0.95	0.79	0.52	66
	Absence of topsoil	1.00	1.00	0.95	0.62	60
Occasional	Patches of bare land	1.00	0.95	0.88	0.59	59
	Root exposure	0.96	0.76	0.60	0.38	45
	Rock exposure	0.95	0.92	0.76	0.58	38
	Deposition soil downslope	1.00	0.97	0.79	0.45	33
	Soil stoniness	0.94	0.84	0.68	0.52	31
Sparsely occurring	Washing crop / seeds	1.00	1.00	1.00	0.78	9
	Poor seed germination	1.00	1.00	1.00	1.00	4
	Gullies	1.00	1.00	1.00	1.00	2

indicators at once, whereas more than eight indicators per field occurred only on very eroded fields (class 5, with a maxim of 13 indicators per field). However, cases of highly and severely eroded fields in the ACED scheme where no or few farmers' indicators could be observed also occurred, albeit sporadically.

The presence of any farmers' indicator was positively correlated with the ACED erosion assessment classes. The correlation matrix of the farmers' indicators showed that a significant correlation (at $\alpha = 0.05$) among indicators existed, which was expected since they were all positively correlated to the erosion assessment, i.e. all indicators are related to erosion processes. This confirmed that all indicators could be considered indicators of erosion (e.g. Swete Kelly and Gomez, 1998). The highest correlation coefficients were found for *poor crop development* with (i) *absence of topsoil* (correlation coefficient = 0.33), and (ii) *patches of bare land* (correlation coefficient = 0.29). As the correlation coefficients were significant but low, no indicator was considered being a duplicate of another (redundant).

Farmers' indicators probabilities per ACED erosion class as defined in eq. (1) are reported in Table 2. The most frequent indicators were not very strong: this was expected since they were frequently observed and therefore the probability that they were observed in slightly or very slightly eroded fields was high. Among these farmers' indicators, however, the *white-soft stones* occurred mostly on highly and very eroded fields: the probability of its occurrence on fields of ACED class 4 or 5 was larger than

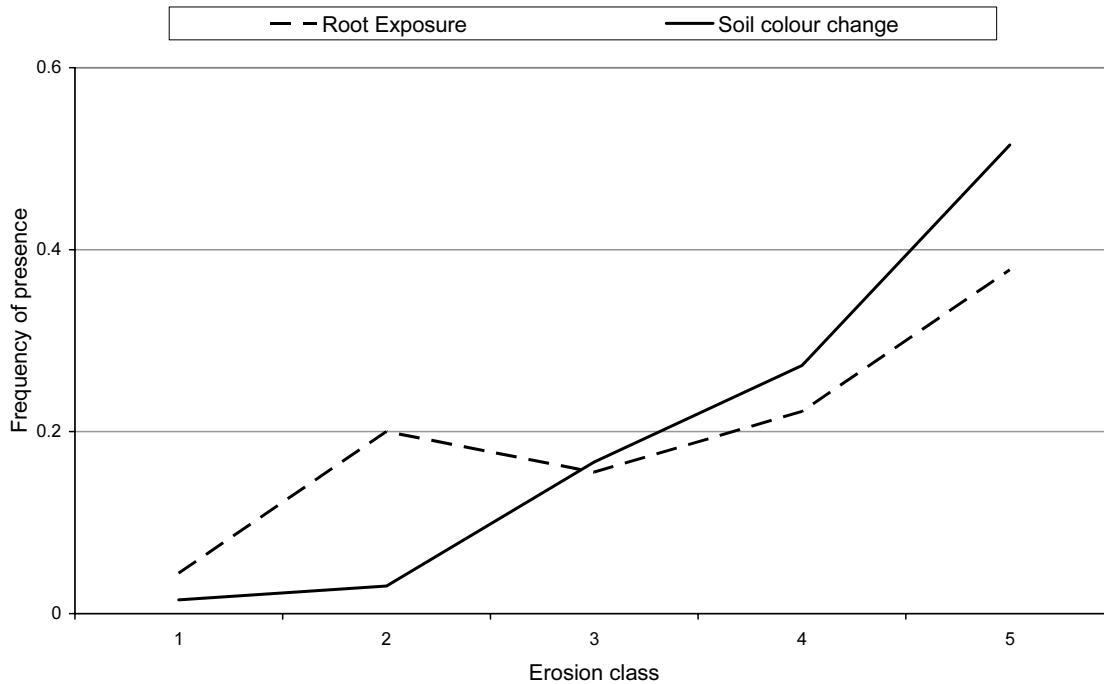


Figure 2. Comparison of a strong erosion indicators (*soil colour change*) versus a weak erosion indicators (*root exposure*). The frequency of strong indicators increased monotonically with assessed erosion. Weak indicators were more equally distributed among low or moderately eroded fields.

70 %. On the other side of the probability distribution, the sparsely occurring indicators were all associated with high and very high erosion classes. This was not surprising in the case of *gullies*, which is also a criterion of the ACED method of indicating very high erosion. Similarly, the *washing of crop and seeds* is an effect of sheet wash, which is considered as serious erosion in the ACED scheme. However, the case of *poor seed germination* is more difficult to interpret. The time during which this indicator could be observed was very limited, and it may have happened that fields where poor seed germination would not be associated with erosion had accidentally not been visited during the survey.

According to our approach, two types of indicators could be defined:

- 1) strong indicators ($p_{i4} \geq 0.70$, i.e. the probability of presence of this indicator in severely and very severely eroded fields was at least 70 %). Examples are: *rills*, *absence of topsoil*, *gullies*, *washing of crop and seeds*, and *poor seed germination* (which could be considered very strong indicators, for their probability p_{i4} were higher than 0.95); and *poor crop development*, *patches of bare land*, *soil colour change*, *deposition of soil downslope*, *rock exposure*, and *white-soft stones*.
- 2) weak indicators ($p_{i4} < 0.70$). Examples are: *Bracken fern*, *root exposure*, *slope steepness*, *root exposure*, *soil stoniness*. With the exception of *soil stoniness*, these indicators were found in more than 50 % of cases in fields that were not very severely eroded ($p_{i5} < 0.50$).

The presence of strong indicators of erosion increased from slightly to severely eroded fields in the ACED scheme, whereas weak indicators were more equally distributed among the slightly or moderately eroded fields (ACED classes 2 and 3; Fig. 2). Weak indicators probably indicate conditions

of soil degradation or soil erosion hazard more than of soil erosion *sensu strictu* (Okoba *et al.*, 2003). For instance, the presence of *Bracken fern* is an indicator of poor soil chemical fertility (Barrios *et al.*, 2001). However, in this study farmers' indicators were only tested in terms of soil erosion assessment and the relationships between weak indicators of erosion and other land degradation problems was not addressed.

Farmers' concept of soil erosion is broader than extension workers' and experts'. Our study confirms that farmers include ideas of land degradation and land fertility decline when speaking of soil erosion (Murage *et al.*, 2000). In SWC planning this difference in perception is important, because addressing only soil erosion while disregarding other land degradation problems may reduce the rate of adoption, as farmers might not perceive the benefits of the proposed actions. At the same time, it is important to distinguish between strong and weak indicators when using farmers' knowledge for assessing erosion in order to give the right advice in the right spot. Extensionists should recommend counteracting soil erosion where strong indicators are present and other measures, e.g. improving chemical fertility, where weak indicators are present.

The number of farmers' indicators and presence of strong farmers' indicators of erosion were used to build a classification tree. The data set comprised ten inputs. The first eight inputs referred to the presence (= 1) or absence (= 0) of strong indicators (*white-soft stones*, *poor crop development*, *rills*, *soil colour change*, *absence of topsoil*, *patches of bare land*, *rock exposure*, and *deposition of soils downslope*). The ninth input indicated the presence (= 1) or absence (= 0) of any of the sparsely occurring indicators (*any of gullies*, *washing of crops and seeds*, and *poor seed germination*). The tenth input was the number of indicators observed in the field (= sum of the previous entries). The classification tree is shown in Fig. 3. The tree consists of a hierarchic sequence of questions: the uppermost question must be answered first, and then the next question follows the branch stemming from the previous answer. The presence of *rills* dominates the classification tree: whenever rills are spotted, the field is classified as subject to very high erosion. This is valid for the Kwalei catchment, where most erosion occurs in the form of interrill erosion, and where rills are not frequent and gullies are rare (Vigiak *et al.*, 2005). However, it is doubtful whether such rule could be applied in other areas, where other erosion processes can be active. The presence of rills is anyway an important feature of erosion assessment survey methods (Herweg, 1996; Stocking and Murnaghan, 2001). The dominant role of rills represents therefore a point of good agreement between farmers and scientific knowledge.

The application of the classification tree to the validation set yielded 49 % of correctly classified fields. Spearman rho correlation coefficient was high (0.81) and significant (at $\alpha = 0.01$). These results were particularly satisfactory when examining the contingency table (Table 3). Most of the disagreements are in fields that were classified as slightly eroded by the ACED survey (class 2: low) and were mainly identified as very slightly eroded by the classification tree (class 1: very low). Fig. 3 shows that the classification tree never reaches the erosion class "low", i.e. the farmers' indicator classification tree mainly merged the two lower classes and could not discriminate among the two. This agrees with the way farmers perceive erosion in the area: when asked to classify fields into qualitative erosion classes, farmers defined only three classes of erosion (low, moderate or high;

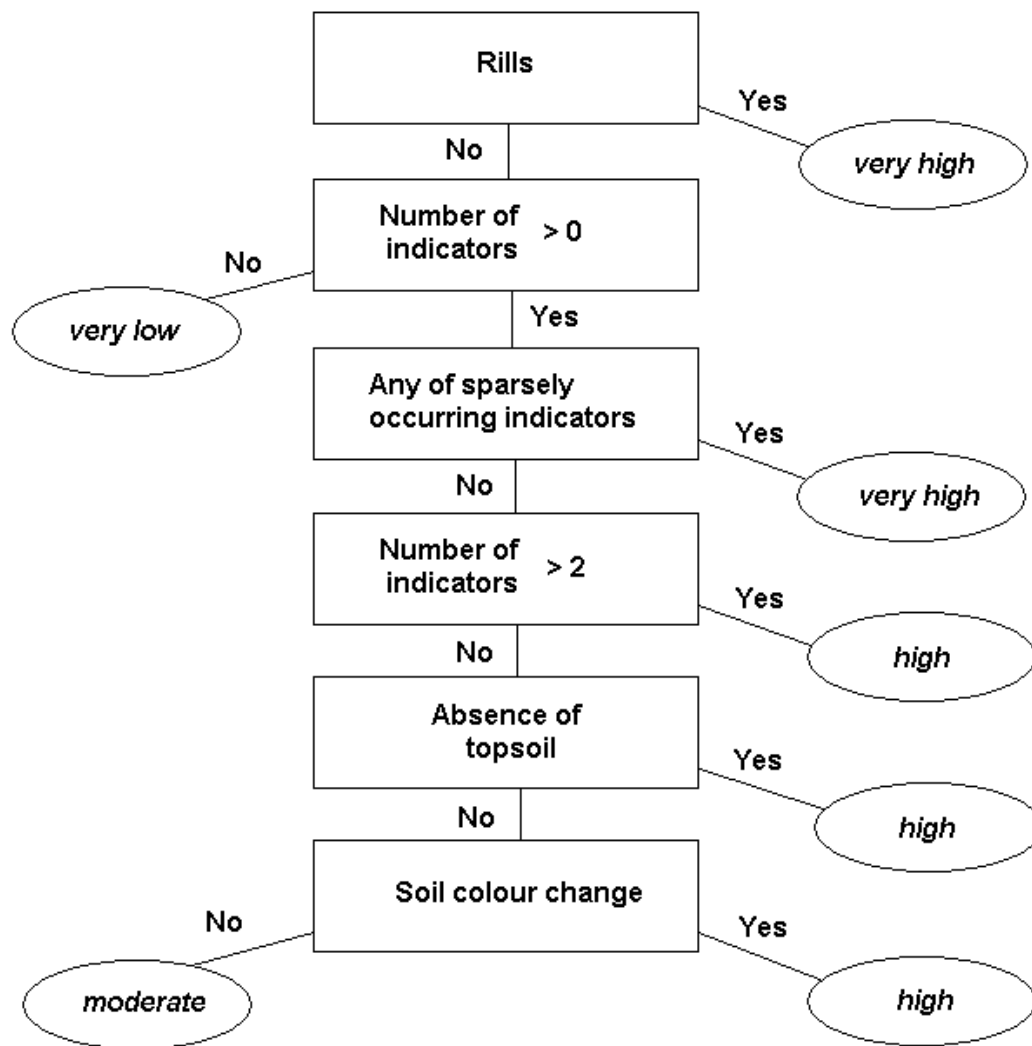


Figure 3. Classification tree for water erosion assessment using farmers' indicators of soil erosion (Sparsely occurring indicator = any of *washing away of crops and seeds, poor seed germination* or *gullies*).

Table 3. Contingency table of the validation set; columns indicate ACED erosion assessment classes; rows indicate the farmers' indicators classification tree erosion classes.

		ACED				
		Very Low	Low	Moderate	High	Very high
Classification Tree	Very low	27	29	13	3	
	Low					
	Moderate	1	7	16	8	2
	High	1		11	11	4
	Very high			1	7	30

Okoba *et al.*, 2003). Differences between classes may sometimes be subjective for the surveyor as well, and originate from comparative considerations rather than from strict rules. For instance, the boundary between very low and low erosion is gradual and less sensitive than between low and moderate classes. This drawback is not so alarming when the general aim of the survey is to identify highly eroded fields. Misjudgements also occurred among the moderately eroded fields, where 12 of the 41 moderately eroded fields of the ACED survey were classified as severely eroded by the classification tree. The very severely eroded fields were mainly classified correctly, with only six out of 36 cases of ACED class 5 fields underestimated by the classification tree. The Kappa coefficient was 0.37 (Cohen, 1968; Bonnardel, 1995), which, considering the lack of one class in the classification tree, indicates good agreement between the two sets.

The classification tree classified very severely eroded fields also when rills were absent, but the rules in the tree were weaker. The sensitivity of the presence of *rills* was checked by repeating the creation of the classification tree with the exclusion of *rills* from the set of indicators. In this case, the major factor in the classification tree was the total number of indicators, but the goodness of fit of the validation set dropped to 39 % (and the Kappa coefficient to 0.23): no other indicator was as strong as *rills*. Indeed, farmers' indicators of erosion work mainly as a 'pool': the second main feature of the classification tree is the number of indicators, and only when no farmers' indicator is present the tree yield a 'very low' erosion class.

We envisage two ways of employing the classification tree of Fig. 3 in practice. Extensionists could use it during their field visits directly to assess erosion; or, within the participatory framework of their interventions, they may ask farmers to map the key indicators, and rely on farmers' memory to assess erosion over the area. The latter use may offer the advantage that farmers recall the presence of indicators in their fields even if cultivation has already obliterated them, making the timing of the survey less critical. This may eventually lead to a considerable saving of time, better communication between experts and farmers, and, hopefully, a larger consensus on sustainable SWC activities.

Conclusions

This research demonstrated that farmers' knowledge of indicators of erosion closely matched scientific erosion assessment criteria. All indicators mentioned by farmers were positively correlated to erosion, and the number of farmers' indicators per field increased with erosion intensity (Fig. 1).

Farmers include land degradation and land fertility decline issues in their concept of soil erosion. In terms of assessment, a distinction could be made between strong indicators, interpreted as indicators of soil erosion *sensu strictu*, versus weak indicators, interpreted as more general indicators of land degradation. The link between weak indicators and land degradation issues other than soil erosion was not assessed in the present study and should be addressed in further research. The presence of weak indicators of erosion indicates that proper SWC planning should address the broader farmers' perception and include measures to improve, e.g., soil chemical fertility beside soil conservation. At the

same time, it is important to distinguish between strong and weak indicators when using farmers' knowledge for assessing erosion in order to give the right advice in the right place.

The use of farmers' indicators of erosion allowed building a simple tool for erosion assessment that worked well in the Kwalei catchment (Fig. 3). The classification tree will need further testing before expanding its use. The list of farmers' indicators was similar to other areas of the East African Highlands (Okoba *et al.*, 2003), but the importance of each indicator may differ according to the main erosion processes at work.

The classification tree is a successful example of integrating different types of knowledge for enhancing the co-operation between all the stakeholders involved in SWC activities. More research must be conducted in testing and developing further this approach. The methodology proposed in this study can be easily replicated elsewhere. Hopefully, working with farmers will again provide further insights for erosion assessment in other areas and other situations.

Acknowledgments

This research could not have been possible without the efforts of A.J. Tenge, who shared his findings on farmers' indicators in Kwalei catchment. The help of scientists and field technicians of ARI-Mlingano, AHI-Lushoto and KARI is thankfully acknowledged. The research project was funded by the Ecoregional Fund to support methodology development in ecoregional programs and the Dutch Ministry of Agriculture. We would like to thank the two reviewers for their useful comments and suggestions. Special thanks go to the main characters of our story: the farmers' of Kwalei and Gikuuri, whose kindness and cooperation has been more than generous.

References

- Admassie Y. 1992. The Catchment Approach to soil conservation in Kenya. Regional Soil Conservation Unit, Swedish International development Authority. Nairobi, Kenya. 6.
- Barrios E, Bekunda M, Delve R, Esilaba A, Mowo JG. 2001. *Identifying and classifying local indicators of soil quality. East Africa Version. Methodologies for decision making in natural resources management*. CIAT-SWCNM-TSBF-AHI, 212 pp.
- Bonnardel P. 1995. Kappa.exe.[Available online from http://kappa.chez.tiscali.fr/Kappa_cohen.htm.]
- Breiman L. 1993. *Classification and regression trees*. Chapman and Hall.
- Cohen J. 1968. Weighted kappa: nominal scale agreement with provision for scaled disagreement of partial credit. *Psychological Bulletin* **70**: 213-220.

- Ellen R, Harris H. 2000. Introduction. *Indigenous knowledge and its transformations: critical anthropological Perspectives*, R. Ellen, P. Parkers, and A. Bicker, Eds., Harwood Academic, 1-33.
- Habarurema E, Steiner KG. 1997. Soil suitability classification by farmers in southern Rwanda. *Geoderma* **75**: 75-87.
- Herweg K. 1996. *Assessment of Current Erosion damage*. Centre for Development and Environment Institute of Geography. University of Berne.
- Kamar MJ. 1998. Soil conservation implementation approaches in Kenya. *Advances in Geoecology* **31**: 1057-1064.
- Kiome R, Stocking M. 1995. Rationality of farmers perception of soil erosion - The effectiveness of soil conservation in semi-arid Kenya. *Global environmental change* **5**: 281-295.
- Kizunguto TM, Shelukindo HB. 2002. Guidelines to mobilize and support community-based Catchment Approach-Watershed management. SECAP. Lushoto, Tanzania.
- Lundgren L. 1980. Comparison of surface runoff and soil loss from runoff plots in the forest and small scale agriculture in the Usambara Mts., Tanzania. *Geografiska Annaler* **62A**: 113-148.
- Lyamchai CJ, Limo SD, Ndondi RV, Owenya MZ, Ndakidemi PA, Massawe NF. 1998. Participatory Rural Appraisal in Kwalei catchment, Lushoto district, Tanzania. SARI. Arusha, Tanzania.
- Mbaga-Semgalawe Z, Fomer H. 2000. Household adoption behaviour of improved soil conservation: the case of the North Pare and West Usambara Mountains of Tanzania. *Land Use Policy* **17**: 321-336.
- Meliyo JL, Kabushemera JW, Tenge AJ. 2001. Characterization and mapping soils of Kwalei subcatchment, Lushoto District. Mlingano Agricultural Research Institute. Tanga, Tanzania.
- Morgan RPC. 1995. *Soil erosion and conservation*. Second ed. Longman Group, 198 pp.
- Murage EW, Karanja NK, Smithson PC, Woomer PL. 2000. Diagnostic indicators of soil quality in productive and non-productive small holders' fields of Kenya's Central highlands. *Agriculture, Ecosystems and Environments* **79**: 1-8.
- Niemeijer D, Mazzuccato V. 2003. Moving beyond indigenous soil taxonomies: local theories of soils for sustainable development. *Geoderma* **111**: 403-424.
- Okoba BO, Tenge AJ, Vigiak O. 2003. Farmers' indicators for semi-quantitative erosion assessment in the East African Highlands. In: *Proceedings of the International Symposium 25 Years of Assessment of Erosion*, Ghent, Belgium, D. Gabriels and W. Cornelis (Eds).
- Ostberg W. 1995. *Land is coming up. The Burunge of Central Tanzania and their environments*. Stocolm studies in social Antropology.

-
- Payton RW, Barr JJF, Martin A, Sillitoe P, Deckers JF, Gowing JW, Hatibu N, Naseem SB, Tenywa M, Zuberi MI. 2003. Contrasting approaches to integrating indigenous knowledge about soils and scientific soil survey in East Africa and Bangladesh. *Geoderma* **111**: 355-386.
- Pretty JN, Thompson J, Kiara JK. 1995. Agricultural regeneration in Kenya: The Catchment Approach to soil and water conservation. *Ambio* **24**: 7-15.
- SPSS I. 2002. SPSS for Windows.[Available online from <http://www.spss.com/>.]
- Stocking MA, Murnaghan N. 2001. *Handbook for the field assessment of land degradation*. Earthscan Publications Ltd, 169 pp.
- Swete Kelly DE, Gomez AA. 1998. Measuring erosion as a component of sustainability. *Soil erosion at multiple scales. Principles and methods for Assessing causes and impacts*, F. Penning de Vries, F. Agus, and J. Kerr, Eds., CABI Publishing, 133-148.
- Tenge AJ, de Graaff J, Hella JP. 2004. Social and economic factors for adoption of soil and water conservation in West Usambara highlands, Tanzania. *Land Degradation & Development* **15**: 99-114.
- The MathWorks I. 2002. Matlab Statistic Toolbox.[Available online from <http://www.mathworks.com/>.]
- Van Dissel SC, de Graaff J. 1998. Differences between farmers and scientists in the perception of soil erosion: a South African case study. *Indigenous Knowledge and Development Monitor* **6**: 8-9.
- Vigiak O, Okoba BO, Sterk G, Groenenberg S. 2005. Modelling catchment-scale erosion patterns in the East African Highlands. *Earth Surface Processes and Landforms* **30**: 183-196.
- Warren A, Osbahr H, S. B, Chappell A. 2003. Indigenous views of soil erosion at Fandou Béri, southwestern Niger. *Geoderma* **111**: 439-456.
- WinklerPrins AMGA. 1999. Local soil knowledge: a tool for sustainable land management. *Society and Natural Resources* **12**: 151-161.
- WinklerPrins AMGA, Sandor JA. 2003. Local soil knowledge: insights, applications, and challenges. *Geoderma* **111**: 165-170.

Chapter 7

MODELLING SPATIAL SCALE OF WATER EROSION IN THE WEST USAMBARA MOUNTAINS

Olga Vigiak, E. Emiel van Loon, and Geert Sterk

Geomorphology. Submitted.

MODELLING SPATIAL SCALE OF WATER EROSION IN THE WEST USAMBARA MOUNTAINS

Abstract

This study aimed to assess the ability of several models to locate areas affected by severe erosion and identify the factors driving the distribution of erosion in a catchment characterised by a dynamic Hortonian hydrologic regime. The spatial patterns of severely eroded areas predicted by five erosion models were compared to the pattern of erosion observed during an extensive field survey conducted in Kwalei catchment (North-Eastern Tanzania). The actual pattern of erosion was also compared with the spatial distribution of some erosion factors: overland flow, whose distribution was simulated with a hydrologic model that accounted for overland flow reinfiltration, slope, crust, canopy cover and ground cover. The patterns of severely eroded areas varied wildly among models. The best predictions were those of (i) a classification tree built on farmers' indicators of erosion (correlation coefficient 0.75); (ii) a semi-empirical model that accounted for overland flow reinfiltration (c.c. 0.48); and (iii) a qualitative model based on slope and ground cover (c.c. 0.45). The erosion factor mostly correlated with eroded areas was crust cover (c.c. 0.57), which was also correlated to vegetation cover. Lacunarity analysis of the spatial patterns showed that erosion models could not characterise the spatial scale of eroded areas correctly. Instead, the spatial scale of erosion distribution in the catchment coincided with that of the overland flow distribution at short reinfiltration length (0.5 - 5 m), even though severely eroded areas were not spatially correlated to areas of high overland flow depth (c.c. 0.10). In conclusion, the distribution of erosion was strongly correlated to crust cover, and a simple model based on slope and ground cover performed well in locating severely eroded areas. However, in the dynamic Hortonian regime of Kwalei catchment, the travel distance of overland flow determined the spatial scale of severely eroded areas.

Keywords: *erosion modelling; spatial pattern; lacunarity analysis; dynamic Hortonian overland flow.*

Introduction

Hortonian overland flow occurs when rainfall intensity exceeds the rate of water infiltration in the soil (Horton, 1933; Kirkby, 1988). After soil ponding conditions are reached, water may at first accumulate in the micro-depressions of the soil surface. Once the storage capacity of the soil surface is filled, overland flow starts moving in the form of anastomous shallow streamlines, whose hydraulic conditions may vary from laminar to turbulent (Kirkby, 1988). Along its movement downslope, overland flow can either concentrate along preferential stream paths, such as rills, or be slowed down and disappear within areas where its movement is hampered and infiltration rates are high. In such zones, water reinfiltrates and the transported sediment is deposited. Therefore, the overland flow

generated along the slopes does not necessarily reach the streams, but the extension of the area contributing overland flow to water bodies changes dynamically according to the conditions that precede the rainfall event and the rainfall event characteristics. This hydrologic regime can be termed dynamic Hortonian (Kirkby, 1988), and is well recognized as typical of, but not restricted to, many semi-arid environments of the world (Puigdefábregas and Sanchez, 1996; Bergkamp, 1998; Ludwig *et al.*, 1999; Imeson and Prinsen, 2004). Dubruil (1985) describes many areas of humid tropical Africa where such conditions can occur.

The travel distance of overland flow at the hillslope scale depends on the magnitude of the rainfall event, the topography, and the spatial distribution of sources of overland flow, i.e. areas where overland flow generation is enhanced, and sinks of overland flow, i.e. areas where water reinfilters in the soil (e.g. Cammeraat, 2004). When the rainfall event has a high rainfall intensity peak but is of short duration, or when soil conditions are very dry, most of the overland flow generated along the slope reinfilters within the sinks present along the slope. The presence of rills and the distance to the channel may influence the amount of overland flow that reaches the streams, but such amount is especially determined by the density and the spatial organization of sources and sinks of overland flow along the slope (Bergkamp, 1998; Cammeraat, 2004). In sparsely vegetated areas, sinks may be tussocks or bands of vegetation (e.g. Bergkamp, 1998; Ludwig *et al.*, 1999), whereas in cultivated areas sinks can be field edges, small ditches, hedgerows, or vegetated strips (van Noordwijk *et al.*, 1998; Okoth, 2003). When the sinks are mostly located along the main slope direction, overland flow does not encounter obstacles and may concentrate into streamlines. When the sinks are located across the main direction, overland flow is blocked, and water can reinfilter in the soil. The effectiveness of sinks in filtering overland flow is dynamic and depends on hydrologic conditions (Bergkamp, 1998; Cammeraat, 2004).

The main mechanism of soil movement across slopes is sediment transport by overland flow. Under a dynamic Hortonian overland flow regime, the slope connectivity is interrupted. In these conditions, erosion phenomena consist of a redistribution of soil particles, and soil fertility, across the landscape, rather than soil removal from the slopes (van Noordwijk *et al.*, 1998). Hence, the sediment delivery ratio, i.e. the ratio of net erosion to gross erosion for a certain area, tends to decrease as the spatial area that is accounted for increases. The soil redistribution still yields important consequences for farmers, because the losses of fertility from the upper fields can be larger than eventual opportunities created in the downslope areas (van Noordwijk *et al.*, 1998). Soil and Water Conservation (SWC) aims at reducing sediment entrainment and removal, therefore the location of sediment sources and sinks in a landscape is an important step for an efficient SWC planning.

Distributed erosion models are potentially useful tools to predict spatial patterns of erosion (Garen *et al.*, 1999). However, the dynamics of a Hortonian hydrologic regime are not easily included in erosion models. The configuration of sinks in the landscape is often not accounted for in distributed erosion models, even if they have important consequences in the distribution of erosion in the landscape (van Noordwijk *et al.*, 1998; Takken *et al.*, 2001; Okoth, 2003). This may have important repercussions on the ability of distributed erosion models to locate the spatial patterns of erosion within a catchment.

This study aimed to assess the ability of several erosion assessment models to locate areas affected by severe erosion and to identify the key factors driving the distribution of erosion in a catchment characterised by a dynamic Hortonian hydrologic regime.

Material and methods

The study area and assessment of the actual erosion

The study was conducted in the Kwalei catchment (4°48' S, 38°26' E), situated in the West Usambara Mountains, North-East Tanzania. The catchment size is approx. 2 km², and altitude ranges from 1337 to 1820 m. The terrain is rough and highly dissected, with more than half of the hillslopes steeper than 20 %. Average annual rainfall is approximately 1000 mm, distributed in two periods, a long rainy season that stretches from the end of February to the end of May and the short, less reliable rainy season that goes from October to January (Vigiak *et al.*, 2005a). Soils on the slopes consist mainly of Humic and Haplic Acrisols (FAO-Unesco legend, FAO, 1990). They comprise porous, sandy topsoils, and clayey, deep and well-drained subsoils. Saturation may occur in the clayey and vertic Umbric Gleysols in the valley bottoms (Meliyo *et al.*, 2001). The highest part of the catchment is covered by mountain rain forest, whereas the middle and lower slopes are mainly cultivated. The main food crops are maize, bean, banana, cassava and sugarcane, whereas the main cash crops are vegetables, coffee and tea. Cultivation of annual crops is concentrated close to the settlement compounds, along the ridge shoulders. The steep slopes along the streams are generally covered by two-storey cultivation of banana and coffee.

At the catchment outlet, rainfall was measured with a tipping bucket rain gauge, discharge with a sonic water level meter; and sediment concentration with an automatic water sampler. All measurements were set to two minutes intervals (Hessel *et al.*, 2005; Vigiak *et al.*, 2005d). Six Gerlach troughs (Gerlach, 1967) were placed along two longitudinal transects in the middle and lower slopes of the catchment to measure overland flow volumes and sediment losses after each rainfall event (Vigiak *et al.*, 2005b; Vigiak *et al.*, 2005d).

The erosion status of the Kwalei catchment was assessed qualitatively with a field survey based on the Assessment of Current Erosion Damage method (ACED; Herweg, 1996). ACED consists of surveying erosion features and main causes of erosion, such as land management, surface characteristics, and run-on and run-off patterns. Five qualitative classes of erosion were defined on the basis of presence of erosion features and their intensity, from very slight (class 1), to very severe (class 5). The survey lasted from December 2002 till May 2003 and covered the whole catchment. The erosion assessment was considered to be representative for the seasonal erosion status of the fields (Vigiak *et al.*, 2005b).

Distribution of erosion factors

Kwalei catchment is characterised by dynamic Hortonian hydrologic regime: overland flow is generated by infiltration excess, but has short travel distances (Vigiak *et al.*, 2005c). The distribution of

overland flow was assessed with a hydrologic model that was built to reproduce the observed pattern of overland flow occurrence along the hillslopes (Vigiak *et al.*, 2005d). The model runs per field and uses time steps of one hour. The total field overland flow Q_{TOT} (in mm per time step) was modelled as a function of the effective rainfall (u_e , in mm), i.e. the amount of rainfall that generates discharge at the catchment outlet, the Hydrologic Response Unit, i.e. areas of homogeneous hydrology, and the field topographic connectivity (cascading sequence of run-on and run-off). Two Hydrologic Response Units were identified in the catchment: perennial crops (HRU_1: coffee and banana, forest and banana and maize fields) versus other crops (HRU_2, mainly annual crops) (Vigiak *et al.*, 2005c). The model accounted for reinfiltration along the slopes by assuming that only a fraction of the field overland flow (Q_{TOT}) would drain to the lower fields (run-off, Q_{OUT} in mm per time step). This fraction depended on the reinfiltration length L (in m), i.e. the average distance at which overland flow travels before reinfiltrating. The maximum field area generating run-off was equal to the length of the lower field border (B_F , in m) times the characteristic reinfiltration length L , i.e. the average length (m) along which the overland flow travels on the soil surface before reinfiltrating in the soil:

$$Q_{OUT} = Q_{TOT} \left[\min \left(1; \frac{B_F L}{A_F} \right) \right] \quad (1)$$

where A_F is the field area (m^2), and min indicates the minimum between the elements in brackets. The overland flow accumulation sequence was based on the flow directions observed during the ACED survey. From observations at the Gerlach troughs placed along the slopes, the average reinfiltration length in Kwalei catchment was estimated to be around 4 m (Vigiak *et al.*, 2005d). However, it is likely that reinfiltration length changes within a reasonable range of 0.1 to 10 m, depending on rainfall characteristics, soil moisture and surface conditions (e.g. Rejman, 2003; Vigiak *et al.*, 2005b). In this experiment, reinfiltration length L was set to 1 m. One-hour Q_{TOT} and Q_{OUT} of the period March-May 2003 were summed to get the total overland flow and run-off of the season.

Slope was derived from a Digital Elevation Model at 20 m pixel size and averaged per field. Crust cover (in %) was estimated during the ACED survey, and distributed using the field map created after the survey. Canopy cover (CC, in fraction, 0-1) and ground cover (GC, fraction 0-1) were estimated in the field during the ACED survey, and subsequently averaged per land use type. Also the average fraction of soil not covered by vegetation (1-CC and 1-GC) were calculated per land use type. The spatial distribution of the vegetation factors was established on the basis of the land use map (Vigiak *et al.*, 2005b).

Erosion assessment models

Several erosion assessment models were applied to the study area. The models are described in detail elsewhere: here only the main differences on the model characteristics, and methods of calibration to the study area are given.

The Morgan, Morgan and Finney model

The Morgan, Morgan and Finney model (MMF; Morgan, 2001) is an empirical, annual model that estimates erosion rates as the minimum between detachment and sediment transport rates. The model

runs per field; in the application at the Kwalei catchment, incoming run-on was added to the overland flow generated in each field to calculate overland flow detachment and transport rates. Model inputs for the application of MMF to the Kwalei conditions were partly estimated in the field and partly derived from literature (Vigiak *et al.*, 2005a). The model output consisted of field average annual net erosion rates (in $\text{kg m}^{-2} \text{y}^{-1}$), from which the seasonal estimate ($\text{kg m}^{-2} \text{s}^{-1}$) for the period March-May 2003 was derived using the ratio of actual rainfall observed in the period (330 mm) divided by the annual average rainfall (967 mm).

The Limburg Soil Erosion model

The Limburg Soil Erosion Model (LISEM; De Roo *et al.*, 1996; De Roo and Jetten, 1999) is a physics-based erosion model that runs at the event and the catchment scale. Modelled erosion processes comprise detachment by rainfall, throughfall, and overland flow, and transport by overland flow. Flow routing is modelled using a four-point finite-difference solution of the kinematic wave and Manning's equation (De Roo *et al.*, 1996). In the application for Kwalei catchment, LISEM version 2.154 was used, with a time step of 15 seconds on the basis of the DEM of 20 meter pixel size. Infiltration was modelled using the Green & Ampt equation. The model was calibrated against discharge and sediment concentration measurements at the outlet. Though it generally performed well, the model showed some problems in modelling double peaked hydrographs (Hessel *et al.*, 2005). The model output per event consisted of the pixel total erosion (in kg m^{-2}). LISEM seasonal erosion output (in $\text{kg m}^{-2} \text{s}^{-1}$) was the sum of the five largest rainfall events in the period March-May 2003.

The Vigiak model

The Vigiak model (Vigiak *et al.*, 2005b) is a semi-empirical model that runs at the catchment and event scale. Overland flow is predicted per field and per event on the basis of the hydrologic model explained above. The overland flow was used to predict field net erosion rates according to a slightly modified erosion phase of the MMF model. Soil detachability of Umbric Gleysol was calibrated versus detachment rates observed in splash cups. The reinfiltration length L of eq. (1) was optimized with a Monte Carlo (MC) experiment against spatial patterns of erosion and ranged from 0.01 to 2.5 m (average $L = 0.10$ m; Vigiak *et al.*, 2005b). The model output was the average sum of net erosion rate for the period March-May 2003 ($\text{kg m}^{-2} \text{s}^{-1}$) calculated by the behavioural MC simulations (Vigiak *et al.*, 2005b).

The Farmers' Indicators Tree

The Farmers' Indicators Tree (FIT; Vigiak *et al.*, 2005e) is a field erosion assessment method that estimates the qualitative erosion class per field and per year. It consists of a classification tree (Breiman, 1993), created on the basis of type and presence of farmers' indicators of erosion: *absence of topsoil, rills, gullies, washing of crop and seeds, poor seed germination, poor crop development, patches of bare land, soil colour change, deposition of soil downslope, rock exposure, and white-soft stones* (Vigiak *et al.*, 2005e). The presence and type of farmers' indicators of erosion were recorded at the time of the ACED survey. Calibration of the classification tree was done on half of the ACED survey dataset and validated against the other half. FIT output consists of field erosion classes, from very slight (class 1) to very severe (class 5).

Moreover, with the exception of the sparsely occurring indicators (*gullies, washing of crop and seeds, and poor seed germination*), which were considered too rare to yield meaningful spatial information, the spatial distributions of farmers' indicators of erosion, i.e. the “building blocks” of the FIT model, were studied here in more detail.

The Okoth model

Okoth (2003) proposed a simple model to locate areas exposed to high erosion risk. The model consist of a logit regression equation that was built on the basis of a field survey conducted in Kiambu District (Central Kenya). The equation uses only two input parameters:

$$\text{Logit} = 4.18 + 0.22 * \text{slope} - 0.08GC \quad (2)$$

where *slope* is the field slope (in %) and GC is the ground cover (in %). In Kiambu District, areas with the logit predictor above five are considered as subject to high erosion risk (Okoth, 2003). Okoth' study area extended over around 600 km² of Kiambu District, and encompassed different agroecological zones, from the drier livestock-sorghum zone in the South-Eastern part to the wetter Coffee-Tea zone in the North-Western part (Jaetzold and Schmidt, 1983; Okoth, 2003), which is similar to the West Usamabara Mountains for climate, geology and land use.

Analysis of spatial patterns

The first purpose of the comparison of spatial patterns was to assess the ability of erosion models to locate severely eroded areas. The model outputs were reclassified into five classes of erosion, setting the class thresholds differently for each model in order to have the same number of fields per class as in the ACED survey. The degree of agreement of model prediction maps and ACED was assessed with weighted Kappa of the contingency table (Cohen, 1968; Vigiak *et al.*, 2005a). Given a contingency table of two classification systems of n classes, in this case the five classes of erosion assessed during the ACED survey (i) or predicted by the model (j), the weighted Kappa coefficient (wK) is defined by:

$$wK = \frac{P_{o,w} - P_{e,w}}{1 - P_{e,w}} \quad (3)$$

where

$$P_{o,w} = \sum_{i=1}^n \sum_{j=1}^n w_{ij} P_{ij} \quad (4)$$

is the weighted observed distribution, and

$$P_{e,w} = \sum_{i=1}^n \sum_{j=1}^n w_{ij} P_{i.} P_{.j} \quad (5)$$

Table 1. Weights (w_{ij}) applied to the contingency table to calculate the weighted Kappa (from Vigiak *et al.*, 2005a).

		ACED map				
		Very low	Low	Moderate	High	Very High
Model output map	Very low	1	1	0.5	0.25	0
	Low	1	1	1	0.5	0.25
	Moderate	0.5	1	1	1	0.5
	High	0.25	0.5	1	1	1
	Very high	0	0.25	0.5	1	1

is the weighted chance-expected distribution, with $p_{ij} = \frac{m_{ij}}{m}$, $p_i = \frac{m_i}{m}$, $p_j = \frac{m_j}{m}$, m_{ij} is the number of fields classified in classes i and j ; m_i is the total number of fields classified in the class i ; m_j is the total number of objects classified in the class j and m is the total number of fields (Cohen, 1968).

ACED assessments depend on the field conditions at the time of the survey. Moreover, the presence of erosion features depends on the redistribution of soil in the field, which is related, but is not equal, to the net erosion losses as assessed by models. Errors of evaluation may as well be present. To account for the uncertainties in the ACED map, the weights for the class combinations were set as in Table 1: one class difference was considered acceptable (weight factors = 1), whereas for larger disagreements between the two maps, the weights were linearly dependent on the distance between classes (Vigiak *et al.*, 2005a).

Weighted Kappa values measure the general agreement between observed and modelled patterns. However, for SWC purposes, the main objective is the ability of models to identify severely eroded areas (classes 4 and 5). Therefore, the erosion maps were reclassified into binary maps: former classes 4 and 5 were classified as severe erosion (class 1), whereas former classes from 1 (very slight) to 3 (moderate erosion) were classified into low erosion (class 0). Similarly, the distribution of erosion factors was reclassified to obtain binary maps. The thresholds between high (class 1) or low (class 0) erosion factors were set to match the proportion of the ACED severely eroded areas. The forest part of the catchment, less interesting for SWC planning, was excluded. Further, to focus on areas instead of single fields, the original field vector maps were transformed into raster format. The pixel size was set to 5 m, which was small enough to maintain the general field geometry. The agreement between binary maps consisted of the correlation coefficients between ACED, model predictions, and erosion factor distributions. The elaboration of maps was done with ILWIS 3.2 Academic (Koolhoven *et al.*, 2004).

Finally, we analysed the lacunarity of the spatial patterns depicted by the binary maps. Lacunarity analysis characterises the spatial texture, i.e. the degree of aggregation, of spatial objects. Lacunarity measures the distribution of gap sizes of the object geometry, with the object being more lacunar if gaps are distributed over a larger range of sizes (Mandelbrot, 1983). The concept of lacunarity was introduced in reference to fractals, but can be applied to real objects, and has been used, for example, to

measure the spatial texture of habitats in landscape ecology studies (Plotnick *et al.*, 1993; Plotnick *et al.*, 1996). Lacunarity was calculated with the gliding box algorithm proposed by Allain and Cloitre (1991). For a binary image, the gliding box consists of a moving window of size r that moves across the image and count the mass S of the object, i.e. the number of sites (pixels) occupied by the class of interest. At the given r , lacunarity Λ_r is defined as:

$$\Lambda_r = \frac{\text{var } S_r}{(\overline{S_r})^2} + 1 \quad (6)$$

where $\text{var } S_r$ is the variance of the distribution of the mass S , and $\overline{S_r}$ is its mean.

Lacunarity depends on the fraction of the image occupied by the class of interest (the density of the class, p), the size of the window r , and the geometry of the object (Plotnick *et al.*, 1993, Plotnick *et al.*, 1996). Maximum lacunarity is at the window size r equal to the pixel size: at this point lacunarity is equal to the inverse of the density p of the binary map. As the size of the window r increases, the relative variance of the mass S decreases, so does the lacunarity. When the window size r is equal to the whole image, $\text{var } S_r$ is zero, and lacunarity is at its minimum, one. The log-log plot of the lacunarity Λ_r against the window size r gives information on the change of lacunarity across the spatial scale range. For example, in a regularly distributed class, once the window size r exceeds the size of the regular pattern, $\text{var } S_r$ drops to zero and lacunarity quickly approaches one. Lacunarity of random maps also drops quickly to one as window size r increases, because random maps are statistically invariant at larger scales. In the case of a self-similar image, instead, $\text{var } S_r$ does not change with the window size r , so the log-log plot approaches a straight line with negative slope (Plotnick *et al.*, 1996). More in general, lacunarity changes little until the point where the window size r equals to the size of the clumps, then it decreases rapidly. In this way, the lacunarity analysis can be used to detect scales: changes in slope in the log-log slope curve indicates changes in the spatial scale of the object of interest (Plotnick *et al.*, 1996). Moreover, lacunarity curves allows comparing the degree of aggregation of spatial objects: at the same window size, the higher the lacunarity, the more aggregate is the spatial object at that scale. In contrast with other landscape metrics, lacunarity analysis is not influenced by the image boundaries and is effective in detecting scale changes even when the density p is very small. In land degradation studies, lacunarity analysis proved effective in studying spatial heterogeneity of vegetation patterns in relation to geomorphologic processes (Puigdefábregas and Sanchez, 1996), hydrology (Ludwig *et al.*, 1999; Wu *et al.*, 2000) and erosion (Imeson and Prinsen, 2004). Lacunarity analysis was performed with the freeware RULE (Gardner, 1999) to detect the degree of aggregation, i.e. the spatial scale, of the binary map patterns.

Results and discussion

Table 2 shows the Kappa values resulting from the comparison of the ACED spatial pattern of erosion and the erosion assessment models predictions. The agreement between models and observations went

Table 2. Kappa values for the comparison of erosion classes as assessed in the field (ACED) and predicted by models.

	Weighted Kappa
MMF	0.27
LISEM	0.26
Vigiak	0.53
FIT	0.74
Okoth	0.45

from fair (0.20-0.40) to good (0.40-0.75; Landis and Koch, 1977). Fig. 1 shows the spatial pattern of severely eroded areas (former classes 4 and 5) of ACED and the assessment models. The North-Western corner area is predicted as subject to severe erosion by all models, but predictions differed especially in the middle and lower parts of the catchment.

Both the MMF and LISEM model scored low Kappa values. MMF mainly predicted severely eroded areas at the footslopes, whereas the ACED survey indicated serious erosion also along the slope shoulders. Model errors were attributed to the overland flow generation mechanism, which did not account for reinfiltration along the slopes (Vigiak *et al.*, 2005a). LISEM predictions were affected by difficulties in defining the spatial distribution of inputs, the low resolution of the available DEM, and structural limitations of the model, whose hydrologic component can not deal with reinfiltration along the slopes yet (Hessel *et al.*, 2005; De Roo and Jetten, 1999). LISEM predicted the high erosion in the upper part of the catchment well, but failed to locate severely eroded areas in the lower parts.

The general good performance of the semi-empirical Vigiak model was expected, because the transport capacity parameters of the model had been previously optimized in relation to the spatial distribution of the erosion in Kwalei (Vigiak *et al.*, 2005b). It is interesting to note, however, that the model could generally locate the spots of erosion in terms of number and position, but failed to capture their extent.

In contrast to the quantitative models, the qualitative erosion assessment models did not require huge amount of input data. Nonetheless, these models performed better than the quantitative models in several respects. The FIT model showed a very good agreement between observed and predicted erosion. However, it should be borne in mind that the FIT model was created using half of the spatial dataset available (Vigiak *et al.*, 2005e), so that the good performance, though promising, should be taken with caution. In particular, the model will need recalibration before being used in other areas (Vigiak *et al.*, 2005e). In contrast, Okoth two-parameter model resulted in good agreement with the ACED observations even without calibration. Okoth model was created for Kiambu District, in environmental conditions that are comparable to those of Kwalei catchment. The limits among classes set for Kwalei catchment, with severe erosion for areas with logit predictor > 7 , were different than those set for Kiambu District, with severe erosion set for areas with logit predictor > 5 (Okoth, 2003). However, the capacity of this simple model to locate erosion in qualitative terms is surprisingly

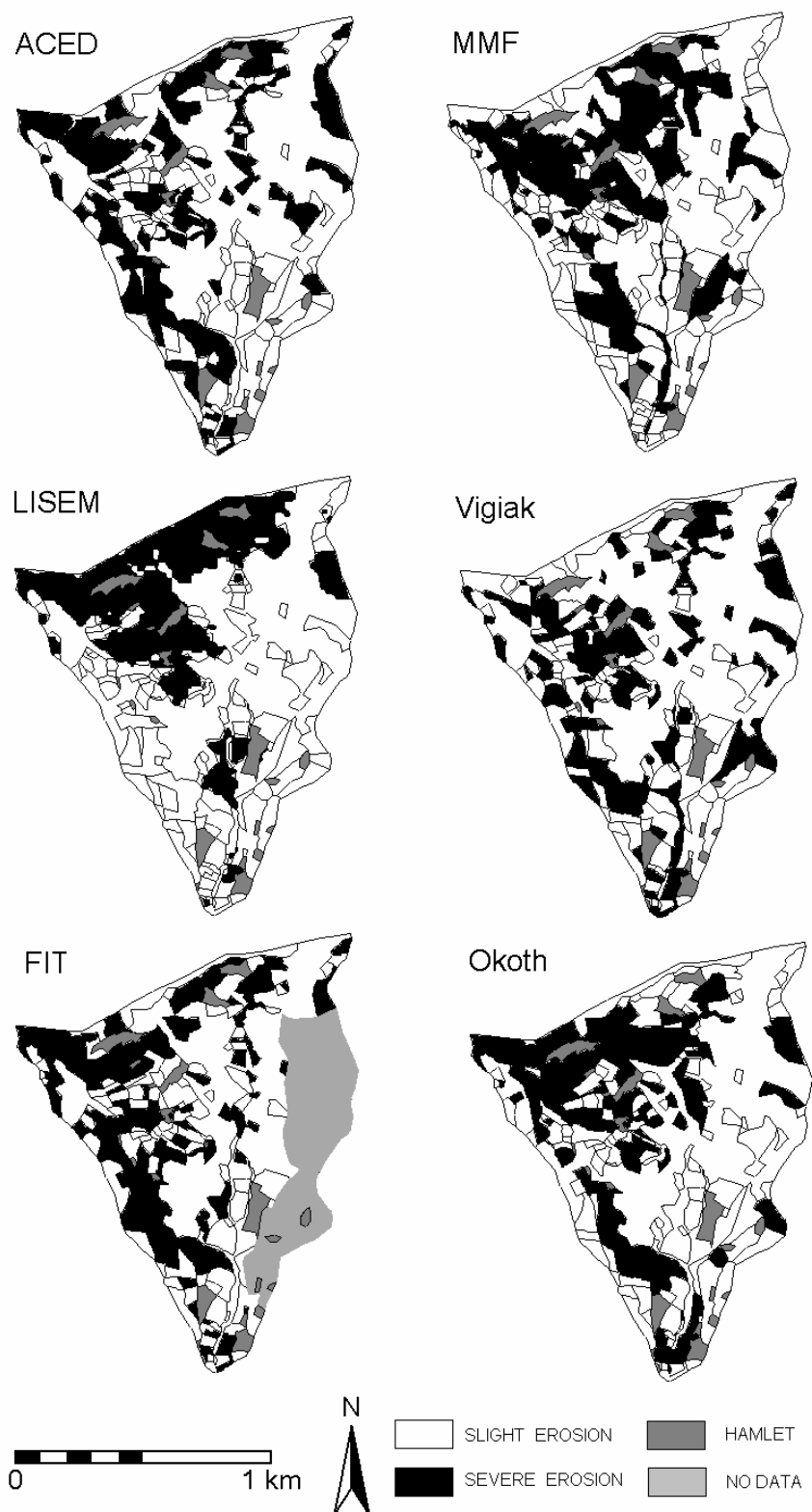


Figure 1. Comparison of severely eroded areas as assessed in the field (ACED) and predicted by five erosion assessment models, Kwalei catchment, Tanzania.

Table 3. Correlation matrix of severely eroded areas as assessed in the field (ACED) and predicted by models

	ACED	MMF	LISEM	Vigiak	FIT	Okoth
ACED	1	0.11	0.31	0.48	0.75	0.44
MMF		1	0.21	0.28	0.02	0.27
LISEM			1	0.25	0.23	0.35
Vigiak				1	0.38	0.36
FIT					1	0.35
Okoth						1

promising. The application to Kwalei condition is a first independent test of Okoth model; as the model uses easily available information, i.e. slope and ground cover, this tool may be very interesting for quick assessments of erosion in SWC planning studies in the East African Highland areas.

The location of severely eroded areas differed a lot among prediction models, as the correlation coefficients between model prediction maps show (Table 3). The correlation matrix reveals that the MMF predictions were in the least agreement with ACED and with the other models. Even if the MMF Kappa value was close to that of LISEM, the correlation coefficient for severely eroded areas was much lower, indicating that MMF had more problems in locating eroded spots. Also LISEM

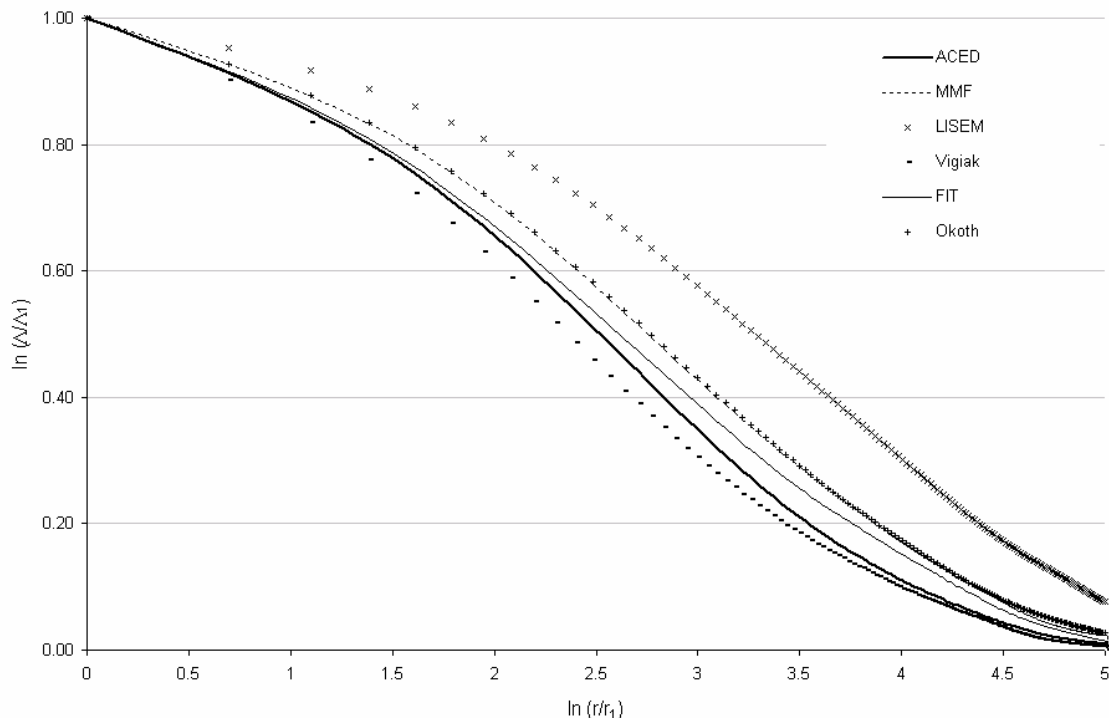


Figure 2. Standardized lacunarity curves of severely eroded areas as assessed in the field (ACED) and as predicted by erosion assessment models.

predictions differed substantially from the other models. Some correlation was found between FIT, Vigiak and Okoth models. In particular, Okoth model was the one scoring the highest correlation coefficients with all the other models, probably because the logit predictor, though empirical, has a physical basis that is common to all assessment methods.

Fig. 2 shows the log-log plot of lacunarity curves against the window size r for the binary maps of Fig. 1. To facilitate the comparison, lacunarity Λ was standardized by its highest value (Λ_I , at window $r_I = 5$ m) and the window size r was standardized by its lowest value (r_I). The window size r went from 5 m ($\ln(r/r_I) = 0$), the pixel size, to around 750 m ($\ln(r/r_I) = 5$), half of the catchment size. The ACED map shows a change in lacunarity (inflection point) at around $\ln(r/r_I) = 2$, indicating that severely eroded areas were aggregated up to a spatial scale of 40 m, slightly larger than the fields. The lacunarity of FIT model follows that of ACED closely at the beginning, but decreases at a slower rate as window size r increases, indicating that severely eroded areas predicted by FIT are spatially more aggregated than the surveyed ones. Okoth model and MMF shows exactly the same lacunarity: this suggests that MMF model prediction aggregation levels and Okoth logit predictor (eq. 2) depends ultimately on the same spatial variables, namely slope and ground cover. LISEM shows by far the highest lacunarity at all scales; indeed, LISEM basically predicts one large clump of severely eroded area. The lacunarity of the Vigiak model is the only curve being always below the ACED curve: the model is more disaggregated than ACED at all scales. Lacunarity curves revealed that no model could capture the spatial scale of severely eroded areas. Beside the Vigiak model, all models predicted a larger extent of the severely eroded clumps.

To explain the spatial scale of eroded areas, we analysed the spatial distribution of erosion factors. The ACED map showed that severely eroded areas occupied a fraction of around 30 % of the agricultural part of the Kwalei catchment. The highest 30 % of the erosion factor distributions corresponded to total overland flow depth of the hydrologic model $Q_{TOT} > 2.75$ mm; field run-off $Q_{OUT} > 0.075$ mm; slopes > 38 %; crust cover > 60 %; canopy cover < 50 % (i.e., $1-CC > 50$ %); and ground cover < 50 % (i.e., $1-GC > 50$ %). Areas above these thresholds were considered as high erosion factor (class 1), otherwise the areas were classified as low erosion factor (class 0).

Fig. 3 shows the binary maps of the erosion factors and Table 4 shows their correlation matrix. Areas of higher total overland flow depth (Q_{TOT}) did not correspond to severely eroded sites: mostly, overland flow was high along the stream line incisions, which are covered by the two-storey coffee and banana vegetation, and in the valley bottoms, where slopes are very small. These conditions assure a good protection of soil against eroding agents. Field run-off distribution (Q_{OUT}) was less correlated to the ACED map than total overland flow. In the fields, soil erosion features are created by the soil detachment, transport and deposition processes that may occur within the field area. The presence and intensity of erosion features, on which the ACED method is based, are therefore related to the total overland flow that occurs in the field (Q_{TOT}). Instead, the amount of soil that is permanently removed from the field, i.e. the field net erosion, depends on the overland flow that leaves the field (run-off, Q_{OUT}), but this may not need to coincide with the ACED map. The distribution of field run-off was not correlated to erosion factors other than the total overland flow. The amount of field run-off depends

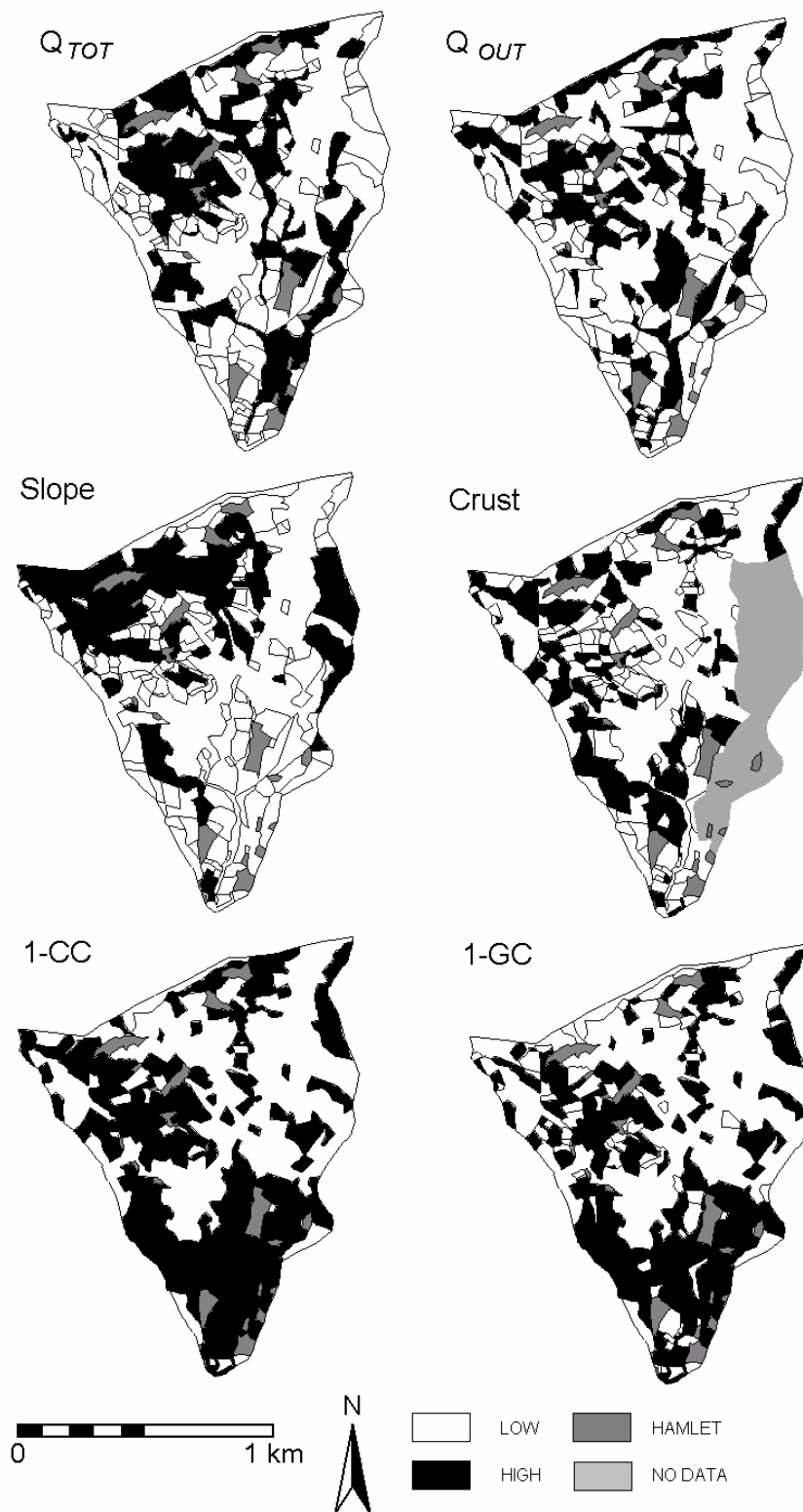


Figure 3. Spatial distribution of erosion factors in the Kwalei catchment, Tanzania.

Table 4. Correlation matrix of severely eroded areas as assessed in the field (ACED) and erosion factors.

	ACED	Q_{TOT}	Q_{OUT}	Slope	Crust	1-CC	1-GC
ACED	1	0.10	-0.02	0.20	0.57	0.51	0.44
Field overland flow (Q_{TOT}) > 2.75 mm		1	0.40	0.03	0.20	0.30	0.21
Field run-off (Q_{OUT}) > 0.075 mm			1	0.01	0.05	0.19	0.07
Slope > 38 %				1	0.11	-0.07	-0.09
Crust > 60 %					1	0.46	0.36
1 - CC > 50 %						1	0.82
1 - GC > 50 %							1

basically on total overland flow and the geometry of the field: for fields whose lower boundary is long, the relative contribution of total overland flow to run-off is relatively large (eq. 1).

Slope was better related to erosion in the upper part of the catchment than along the middle and lower parts. The good protection of vegetation along the steeper slopes, confirmed by the slightly negative correlation coefficient between slope and vegetation cover, explains the rather low correlation coefficient (0.20) between slope and severe erosion. Crust cover and poor vegetation cover were instead widespread in the middle and lower part of the catchment, where annual crops prevail. The three factors were well correlated, but crust cover had the highest correlation with severely eroded areas (c.c. 0.57). Vegetation cover protects the topsoil from the direct impact of raindrops; its removal, for example by tillage operations, exposes the soil surface to the impact of the raindrop and favour the formation of structural crusts. The presence of crust may reduce soil infiltration and enhance the occurrence of overland flow (Vigiak *et al.*, 2005c). All these conditions may result in higher erosion.

The good correlation between crust and vegetation cover on one side, and crust and erosion on the other, explains in part the good performance of Okoth model, which takes account of the ground cover, and hence of the crust distribution.

Fig. 4 shows the lacunarity curves of the erosion factors in comparison to that of severely eroded areas. Crust cover and ground cover lacunarity are quite close to that of the severely eroded areas (ACED), confirming the linkage between the two erosion factors and the location of erosion. Erosion factors are spatially more aggregated than ACED, with one, important exception: the distribution of total overland flow Q_{TOT} has exactly the same lacunarity of the severely eroded areas, even when the two patterns do not overlap.

The overland flow is the vector of soil sediment, transporting soil detached particles from sediment sources to deposition areas. In a way, it represents the ‘memory’ of the landscape, linking the field to what happens in its upper areas. This ‘memory’ can be quantified by the reinfiltration length parameter L , which determines the amount of overland flow moving across field borders (eq. 1). Fig. 5 shows the change of lacunarity in the overland flow pattern when reinfiltration length parameter L is varied in the range from 0.1 m, i.e. virtually no field run-off, till 1000 m, i.e. virtually no reinfiltration along the slopes ($L = \text{inf}$). Fig 5a shows the lacunarity of total field overland flow Q_{TOT} . At reinfiltration lengths

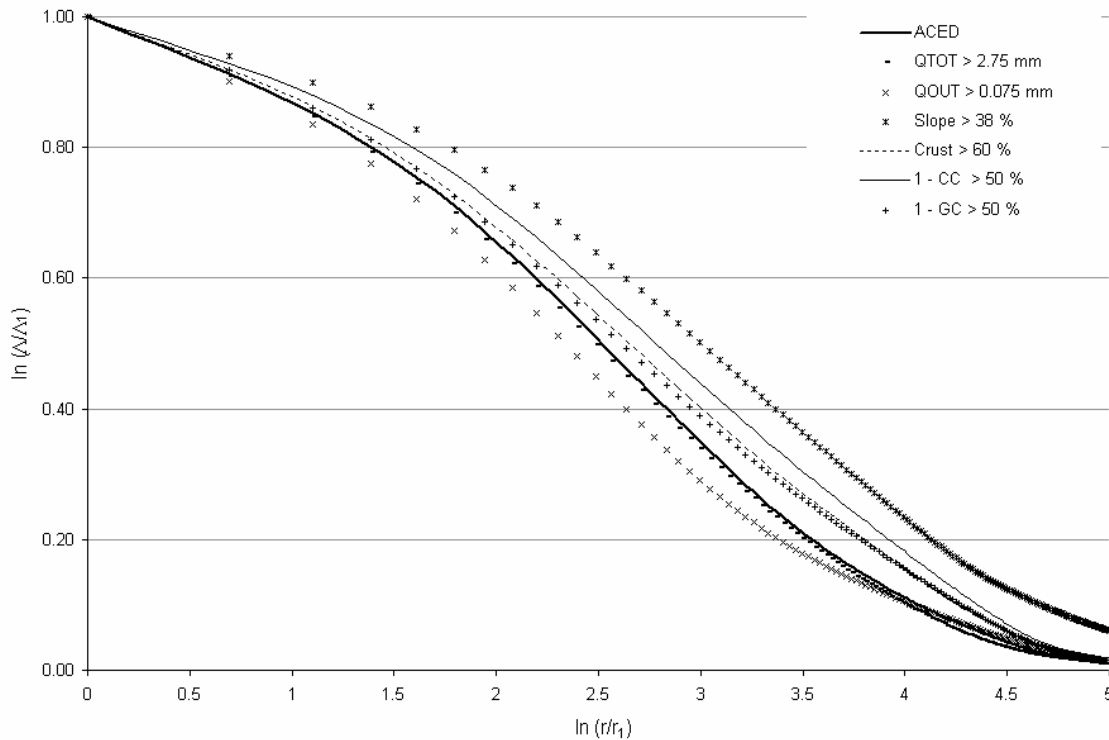


Figure 4. Standardized lacunarity curves of severely eroded areas in comparison with the erosion factors.

$L > 1$ m, the lacunarity decreases: as the field run-on increases in the lower part of the fields, the spots of high overland flow concentrate progressively in the lower segments of the slope. At first, the change is small: lacunarity curves at reinfiltration length of 2.5 and 5 m are close to that of 1 m and to that of ACED severely eroded areas. At even longer reinfiltration lengths, the lacunarity strongly decreases, especially at the hillslope scale of 100-300 m ($3 < \ln(r/r_1) < 4$), definitively diverging from that of ACED. Moreover, also at reinfiltration lengths $L < 1$ m the degree of aggregation of overland flow increases: the lacunarity curve at $L = 0.5$ m is close to that of $L = 5$ m, and that of 0.1 m is close to the lacunarity curve of total overland flow at $L = 10$ m. The distribution of overland flow according to the hydrologic model depends not only on the field topology (eq. 1) but also on the field hydrologic conditions, namely on the Hydrologic Response Unit of the field (Vigiak *et al.*, 2005d). The HRU distribution reflects the perennial (HRU_1) – annual (HRU_2) crop pattern and largely corresponds to the canopy cover pattern of Fig. 3. This explains as well the correlation between overland flow factors and canopy cover pattern (1-CC; see Table 4). Indeed, at reinfiltration length L of 0.1 m, the lacunarity of overland flow coincides to that of canopy cover (1-CC > 50 %, not shown here). When reinfiltration is practically nil, total overland flow depends exclusively on the hydrologic conditions of the field (the HRU), and ultimately on the land use. Lacunarity analysis revealed that neither an infinite reinfiltration length (classic Hortonian overland flow), nor a nil reinfiltration length (no overland flow connectivity) corresponded to the scale of the distribution of severely eroded areas. Rather, effective reinfiltration lengths in Kwalei catchment are in the range of 0.5 and 5 m.

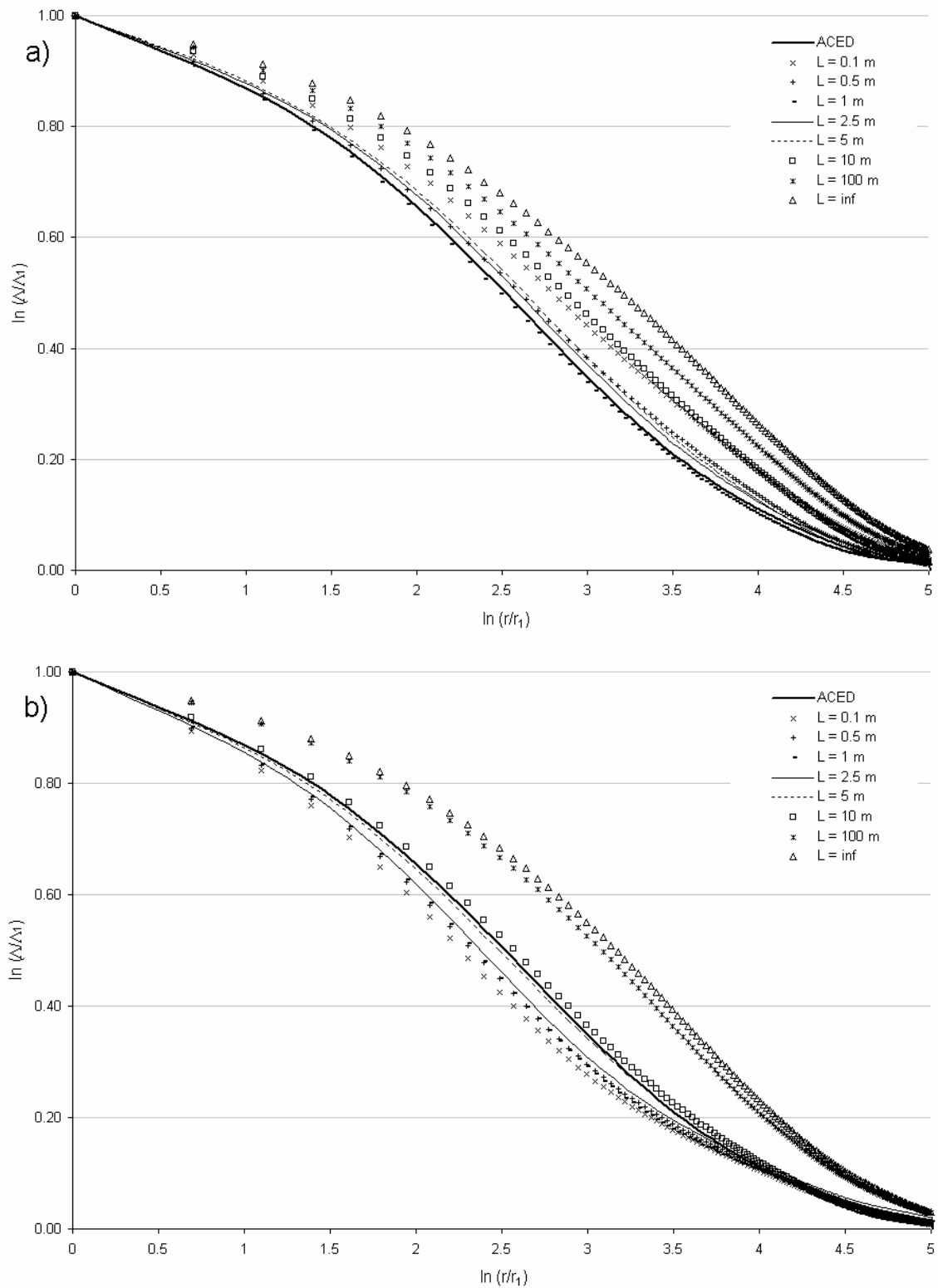


Figure 5. Standardized lacunarity curves of severely eroded areas in comparison with the highest 30 % of (a) the total overland flow (Q_{TOT}) and (b) field run-off (Q_{OUT}), at different infiltration lengths L .

Fig. 5b shows the lacunarity curves of the field run-off patterns. In this case, the increase in reinfiltration length always resulted in an increase in the aggregation of the areas with higher field run-off, which concentrate more and more downslope. Erosion features depend on total overland flow more than field run-off, but field run-off represents more properly the effect of field topology, i.e. the run-on/run-off cascade and field geometry, on the spatial distribution of overland flow. The spatial scale of field run-off that is closest to the ACED severely eroded areas occurred at reinfiltration lengths L of 5 - 10 m. This is probably the spatial scale of overland flow movement across fields, the slope 'memory' that is active in Kwalei catchment.

Fig. 5 demonstrates the importance of the travel distance of overland flow and of field geometry in the distribution of overland flow and erosion under a dynamic Hortonian hydrologic regime. The hydrologic model of Vigiak *et al.* (Vigiak *et al.*, 2005d) refers explicitly to the lower boundary of the field (eq. 1), linking the field geometry to the spatial distribution of overland flow and thus of erosion. Field boundaries, either marked by a simple vegetated strip, a line of trees or a small ridge, create obstacles that reduce the movement of water across fields, and represent landscape discontinuities where overland flow can reinfiltrate (van Noordwijk *et al.*, 1998; Okoth, 2003). When the field geometry is not accounted for, spatial distribution of physics-based models can be very wrong (Takken *et al.*, 2001): the lacunarity of a completely Hortonian overland flow ($L = \text{inf}$ in Fig. 5) is very close to that of the LISEM model. On the other hand, the curve of the Vigiak model is close to that of field run-off at reinfiltration length of 2.5 m. The Vigiak model assesses the field soil losses, i.e. the field net erosion rates, and therefore tends to underestimate erosion processes in fields where intra-field soil redistribution is important. The practical result is that the model could indicate the locations of erosion, but not their extent.

The same phenomenon is probably true also for the distribution of erosion within the field. Intra-field erosion patterns were not studied here, but it is likely that within the fields vegetation patterns create a mosaic of sources and sinks of overland flow that affects the spatial distribution of overland flow (Puigdefàbregas and Sanchez, 1996; Bergkamp, 1998; Ludwig *et al.*, 1999; Wu *et al.*, 2000; Imeson and Prinsen, 2004).

Our results are in agreement with other studies showing the importance of barriers and sinks in scaling the distribution of erosion in a landscape (e.g. Takken *et al.*, 2001; van Noordwijk *et al.*, 1998). As van Noordwijk *et al.* (1998) pointed out, lateral interactions have important consequences on erosion soil rates at the landscape scale. On wide slopes, overland flow may spread laterally; the redistribution of water and sediments can lead to a consistent reduction of the sediment delivery, as water can reinfiltrate more along the slope. Within a field, acceleration of overland flow along the slope may prevail, but at the landscape scale, the lateral interactions and the redistribution of soil usually predominate (van Noordwijk *et al.*, 1998). Eq. (1) offers a somewhat rudimental, but simple, solution to account for the effect that field geometry exerts on the spatial distribution of erosion in a landscape. As an alternative, Imeson and Prinsen (2004) suggest the use of an index of vegetation-bare soil connectivity to adjust the potential upstream area of a given site. Theirs is yet another approach to include more explicitly the vegetation pattern, in terms of spatial configuration of sources and sinks of overland flow, into the hydrologic and erosion dynamics of the landscape.

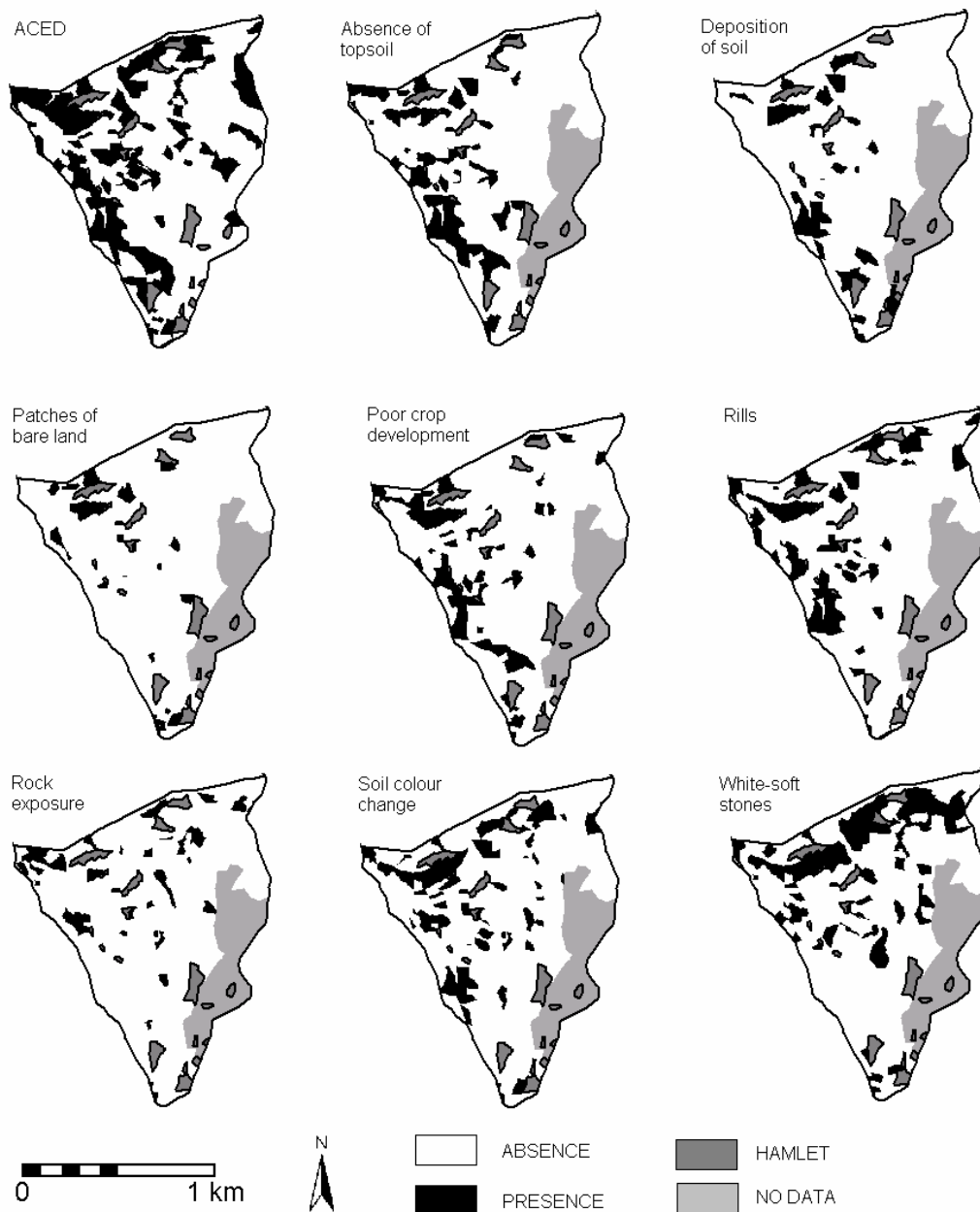


Figure 6. Distribution of severely eroded areas (ACED) and farmers' indicators of erosion.

Without doubt, hydrologic dynamics are difficult to characterise. Direct observations of overland flow occurrence and distribution require time and technical resources that are seldom available outside dedicated research activities. Given its importance, however, retrieving such information, even in general terms, may be crucial for effective assessment of erosion in a landscape. In practice, information on the spatial distribution of factors of erosion and environmental dynamics might be retrieved from the land users. The effectiveness of farmers' knowledge in locating erosion is

Table 5. Correlation coefficients matrix of farmers indicator of erosion and severely eroded areas (ACED), total overland flow (Q_{TOT}) and field run-off (Q_{OUT}) at reinfiltration length L of 1 m. The density p is the fraction (in %) of the map occupied by the class of interest.

	Absence of topsoil	Deposition soil	White-soft stones	Bare land	Poor crop develop.	Rills	Rock exposure	Soil colour change	Density p (%)
ACED	0.56	0.41	0.33	0.25	0.51	0.64	0.25	0.44	30
Q_{TOT}	0.13	0.08	-0.06	0.10	0.17	0.12	0.07	0.11	32
Q_{OUT}	-0.02	-0.16	-0.05	0.02	0	-0.06	0.07	0.01	31
Absence of topsoil	1	0.39	0.15	0.29	0.55	0.46	0.12	0.28	18
Deposition soil down.		1	0.1	0.25	0.27	0.37	-0.03	0.35	11
White-soft stones			1	0.19	0.15	0.30	0.21	0.37	24
Patches of bare land				1	0.24	0.23	0.07	0.16	6
Poor crop develop.					1	0.39	0.2	0.18	15
Rills						1	0.18	0.47	18
Rock exposure							1	0.12	8
Soil colour change								1	17

exemplified by the good performance of the FIT model. Even if the current FIT model should probably not be applied elsewhere without reparameterisation, the methodology used to develop it (Vigiak *et al.*, 2005e) can be repeated and included within the participatory appraisal activities that extension officers usually undertake when planning SWC activities (e.g. Kamar, 1998). Moreover, many indicators of erosion that were mentioned by Kwalei farmers are quite common (Swete Kelly and Gomez, 1998). Fig. 6 shows the spatial distribution of the farmers' indicators that were strongly related to erosion. Their correlation matrix is shown in Table 5, where also the density p of the area occupied by the indicators is given. Contrary to the maps shown in Figs. 1 and 3, where the density p was equivalent to that of ACED severely eroded areas (30 %), the binary maps of Fig. 6 show the actual distribution of indicators observed in the field, whose fraction thus varied. The density p affects the correlation coefficients: indicators that are less frequently observed, such as *deposition of soil downslope*, *patches of bare land* and *rock exposure* have generally lower correlation coefficients. All indicators are correlated to erosion, especially *absence of topsoil*, *rills* and *poor crop development*. The former two indicators are erosion features. *Poor crop development* can be either a consequence of erosion, i.e. erosion deplete the soil fertility and the water availability, thus crops perform poorly, or a factor of erosion, i.e. where crops are poorly developed, soil is less protected against erosion agents. All the indicators are poorly correlated with the distribution of field overland flow and field run-off.

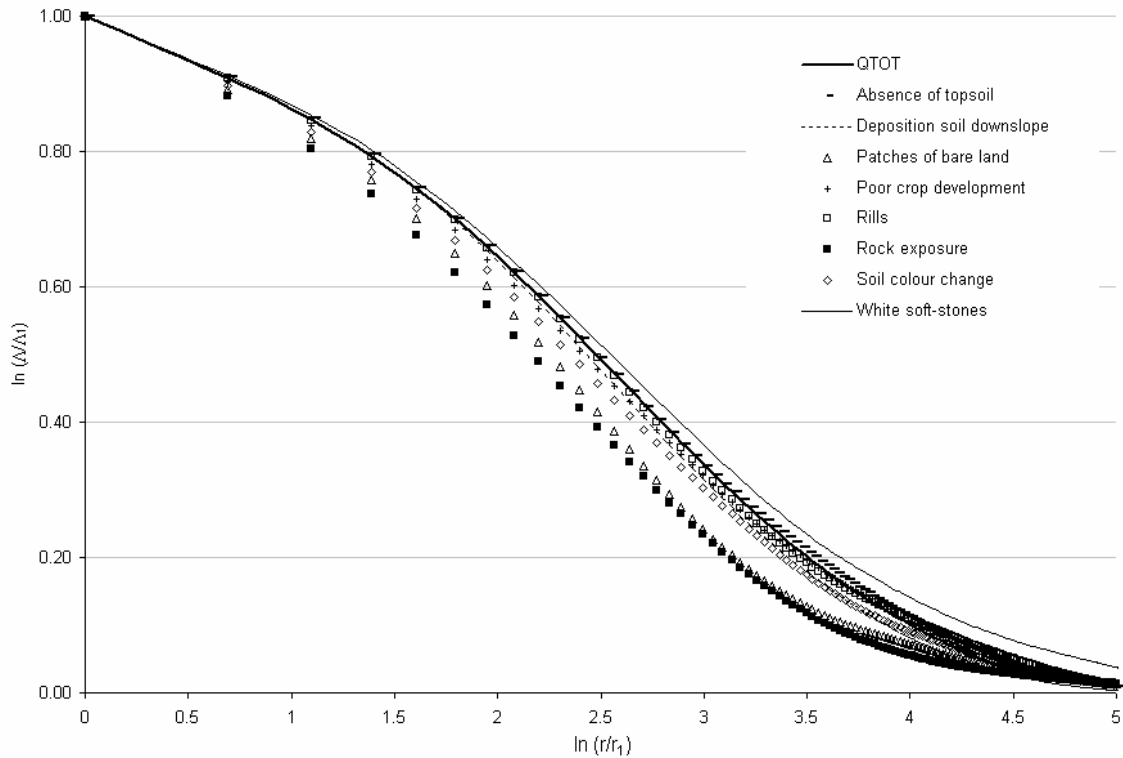


Figure 7. Standardized lacunarity curves of farmers' erosion indicators in comparison with the highest 30 % of total overland flow (Q_{TOT}) at reinfiltration length $L = 1$ m.

The density p of the binary maps of Fig. 6 has consequences on their lacunarity: sparse datasets have higher lacunarity than dense datasets (Plotnick *et al.*, 1996). However, the shape of the lacunarity curve is independent of the density p (Plotnick *et al.*, 1993, Imeson and Prinsen, 2004), thus standardized lacunarity curves of objects with different density are comparable (Fig. 7). Lacunarity of farmers' indicators is compared to the total overland flow at reinfiltration length L of 1 m, which is close to that of the severely eroded areas. *White-soft stones* are generally more aggregated: the appearance of white soft stones is indeed an effect of the removal of topsoil and the exposure of the B horizon of Humic Acrisols, so the distribution of this indicators is also related to the soil type. *Patches of bare land* and *rock exposure* appear to have a shorter spatial scale than hydrologic and erosion conditions. The lacunarity of the other indicators, instead, follow closely the curve of total overland flow: these indicators are good candidates to estimate the spatial scale of distribution of erosion and overland flow. Among these, there is little point in discussing which indicator would be the best: probably the combination of different indicators can give better ideas on the extension of erosion (Okoba and Sterk, 2005; Vigiak *et al.*, 2005e). More importantly, Fig. 7 shows that farmers have good perception of the occurrence and distribution of erosion, and this information can be used to infer the spatial scales of hydrologic and erosion conditions. Farmers' knowledge of their environment could be used as well to gather information on the intra-field variability of erosion and other relevant agronomic conditions (Dregne, 1989; van Noordwijk *et al.*, 1998; Okoba *et al.*, 2005).

In alternative to the regression-type approaches such as the one offered by the FIT model (Vigiak *et al.*, 2005e), we can see mainly two other ways of embedding farmers' knowledge into a scientific framework for modelling hydrology and erosion in a landscape. On one side, farmers' knowledge can be directly translated into expert-system models (Davis, 1993). Expert systems for land degradation and erosion have been applied with success in tropical countries (e.g. Balachandran, 1995; Suryana, 1997), as well as in temperate areas (e.g. Boardman *et al.*, 1990). These models can offer valid tools to locate erosion, and therefore can counteract the problem of data scarcity that is common to many rural areas of the tropics, but can offer little insight in the physical processes involved, and remain difficult to export to other areas.

A more innovative approach is the methodology proposed by Ferreyra (2003) for parameter optimization of crop simulation models. In precision agriculture, the retrieval of detailed information on the environment is crucial to quantify the spatio-temporal variability of inputs in crop simulation models. Ferreyra elicited farmers' and experts' knowledge of intra-field ecology in the form of nominal relationships of probabilities, i.e. "greater than", "lower than", for adjacent soil units. The resulting neighbourhood criteria sets were employed to constrain the optimization of soil-water parameters, such as saturated hydraulic conductivity, SCS curve number, soil depth and plant density. Ferreyra's methodology helps reducing the over parameterisation problems in physics-based models and improving the spatial distribution of inputs and outputs. For example, in the Kwalei case, the lacunarity of farmers' indicators of erosion could have been used to parameterise the effective infiltration length L of the hydrologic model. Given the promising results of farmers' knowledge of erosion phenomena in Kwalei catchment (Tenge *et al.*, 2005), this framework might successfully couple local knowledge to physics-based models, substantially improving the quality of spatially distributed erosion models.

Conclusions

SWC planners need reliable tools to locate the areas within a catchment that are most affected by water erosion. The development of catchment-scale distributed models concentrated on the prediction of water discharge and sediment delivery at the outlet more than on quality of spatial patterns (Jetten *et al.*, 2003). The poor quality of spatial model predictions can be attributed to the heterogeneous, nonlinear behaviour of hydrologic and erosion processes coupled with insufficient quality of spatial and temporal datasets (Merritt *et al.*, 2003; Jetten *et al.*, 2003). These shortcomings were without doubt present in the Kwalei catchment, where the accuracy of the cartographic information was lower than the usual requirements for a complex, physics-based erosion model such as LISEM (e.g. Hessel *et al.*, 2005). However, the quality of cartographic information was already better than the one usually available to SWC planners (Renschler and Harbor, 2002). Where environmental data are of poor quality and where the main objective of model predictions is the location of eroded areas, qualitative assessment tools such as the FIT model (Vigiak *et al.*, 2005e) and Okoth model (Okoth, 2003) can perform better than quantitative models. These empirical approaches would require calibration in areas

other than the ones where they were developed, but the research effort to do so would probably be more affordable than for proper calibration of more physics-based models.

The comparison of the distribution of severely eroded areas with erosion factors indicated that erosion was spatially correlated with crust cover. We could not distinguish whether crust cover was an effect rather than a cause of soil erosion: most probably it is both. The correlation of crust cover with vegetation cover also explained the good performance of the Okoth two-parameter model in locating the eroded areas of the Kwalei catchment.

Lacunarity analysis of model predictions, however, revealed a spatial scale deficiency involved in the poor performance of the erosion models. While the location of eroded area was correlated to crust cover, the spatial scale of their distribution was the same as that of the total overland flow of the fields at short infiltration lengths L (0.5 - 5 m). In the dynamic Hortonian hydrologic conditions of Kwalei catchment, where overland flow occurrence is generally easily triggered but shortly lived, erosion phenomena often consists of a redistribution of soil particles within the catchment rather than sediment delivery to water bodies.

The dynamics of overland flow along the slopes, caused by the configuration of the mosaic of sources and sinks of overland flow in a landscape, though recognized (Puigdefàbregas and Sanchez, 1996; van Noordwijk *et al.*, 1998; Imeson and Prinsen, 2004), are not sufficiently accounted for in erosion models. The semi-empirical Vigiak model embedded a mechanism to account for field geometry and infiltration along the slopes: the model could locate most spots of eroded areas, even if it failed in accounting for their extent. An alternative approach could be the use of vegetation connectivity indices to account for potential sinks of overland flow along the slopes (Puigdefàbregas and Sanchez, 1996; Imeson and Prinsen, 2004). In any case, accounting for the dynamics of the overland flow seems fundamental for predicting the spatial scale of erosion under a dynamic Hortonian regime.

Unfortunately, gathering information on the hydrology of new environments requires huge investments. In data scarce areas, farmers' knowledge represent an interesting alternative source of information. In the case of the Kwalei catchment, some indicators used by farmers to assess erosion in their fields conveyed useful information on the location of eroded areas and on the spatial scale of the erosion phenomena. It is possible to further exploit farmers' spatial knowledge of their environment, for example in the optimization of model parameters of semi-empirical and physics-based models with the methodology recently proposed by Ferreyra (2003). The combination of qualitative local knowledge in quantitative models may thus alleviate the constraints of the chronic data scarcity that affects spatially distributed environmental modelling.

References

- Allain C, Cloitre M. 1991. Characterizing the lacunarity of random and deterministic fractal sets. *Physical Review A* **44**: 3552-3557.

-
- Balachandran CS. 1995. LACONEX: a rule-based implementation to advise on plot-level land conservation in Vilathikulam, southeastern India. *Land degradation & rehabilitation* **6**: 265-283.
- Bergkamp G. 1998. A hierarchical view of the interactions of runoff and infiltration with vegetation and microtopography in semiarid shrublands. *Catena* **33**: 201-220.
- Boardman J, Evans R, Favis-Mortlock DT, Harris TM. 1990. Climate change and soil erosion on agricultural land in England and Wales. *Land degradation & rehabilitation* **2**: 95-109.
- Breiman L. 1993. *Classification and regression trees*. Chapman and Hall.
- Cammeraat ELH. 2004. Scale dependent thresholds in hydrological and erosion response of a semi-arid catchment in southeast Spain. *Agriculture, Ecosystems and Environment* **104**: 317-332.
- Cohen J. 1968. Weighted Kappa: nominal scale agreement with provision for scaled disagreement or partial credit. *Physiological Bulletin* **70**: 213-220.
- Davis JR. 1993. Expert systems and environmental modelling. *Modelling change in environmental systems*, A. J. Jakeman, M. B. Beck, and M. J. McAleer, Eds., John Wiley & Sons, 505-517.
- De Roo APJ, Wesseling CG, Ritsema CJ. 1996. LISEM: a single-event physically based hydrological and soil erosion model for drainage basins: theory, input and output. *Hydrological Processes* **10**: 1107-1117.
- De Roo APJ, Jetten VG. 1999. Calibrating and validating the LISEM model for two data sets from The Netherlands and South Africa. *Catena* **37**: 477-493.
- Dregne HE. 1989. Informed opinion: filling the soil erosion data gap. *Journal of Soil and Water Conservation* **4**: 303-305.
- Dubruil PL. 1985. Review of field observations of runoff generation in the tropics. *Journal of Hydrology* **80**: 237-264.
- FAO. 1990. *Guidelines for soil description*. Third ed. *Soil Resource Management and Conservation Service*, FAO, Land and Water Division.
- Ferreira RA. 2003. Knowledge-based techniques for parameterizing spatial biophysical models, Agricultural and biological Engineering, University of Florida, 268.
- Gardner RH. 1999. Rule: a program for the generation of random maps and the analysis of spatial patterns.[Available online from <http://www.al.umces.edu/faculty/bobgardner.html> [accessed 10.12.2004].]
- Garen G, Woodward D, Geter F. 1999. A user agency's view of hydrologic, soil erosion and water quality modelling. *Catena* **37**: 277-289.

Gerlach T. 1967. Hillslope troughs for measuring sediment movement. *Revue de geomorphologie dynamique* **17**: 173.

Herweg K. 1996. *Assessment of Current Erosion Damage*. Centre for Development and Environment Institute of Geography, University of Berne.

Hessel R, van den Bosch R, Vigiak O. 2005. Evaluation of the LISEM soil erosion model in two catchments in the East African Highlands. *Earth Surface Processes and Landforms* **subm.**

Horton RE. 1933. The role of infiltration in the hydrological cycle. *Transactions of American Geophysics Union* **14**: 446-460.

Imeson AC, Prinsen HAM. 2004. Vegetation patterns as biological indicators for identifying runoff and sediment sources and sink areas for semi-arid landscapes in Spain. *Agriculture, Ecosystems and Environment* **104**: 333-342.

Jaetzold RH, Schmidt H. 1983. *Farm management handbook of Kenya*. Vol. II/B, Central Kenya, Ministry of Agriculture.

Jetten VG, Govers G, Hessel R. 2003. Erosion models: quality of spatial predictions. *Hydrological Processes* **17**: 887-900.

Kamar MJ. 1998. Soil conservation implementation approaches in Kenya. *Advances in geoecology* **31**: 1057-1064.

Kirkby MJ. 1988. Hillslope runoff processes and models. *Journal of Hydrology* **100**: 315-339.

Koolhoven W, Hendrikse J, Nieuwenhuis W, Retsios B, Schouwenburg M, Wang L, Budde P, Nijmeijer R. 2004. ILWIS 3.2 Academic

Landis J, Koch GG. 1977. The measurement of observer agreement for categorical data. *Biometrics* **33**: 159-174.

Ludwig JA, Tongway DJ, Mardsen SG. 1999. Stripes, strands and stipples: modelling the influence of three landscape banding patterns on resource capture and productivity in semi-arid woodlands, Australia. *Catena* **37**: 257-273.

Mandelbrot BB. 1983. *The fractal geometry of nature*. W.H.Freeman.

Meliyo JL, Kabushemera JW, Tenge AJ. 2001. Characterization and mapping soils of Kwalei subcatchment, Lushoto District. Mlingano Agricultural Research Institute. Tanga, Tanzania, 34 pp.

Merritt WS, Letcher RA, Jakeman AJ. 2003. A review of erosion and sediment transport model. *Environmental modelling & software* **18**: 761-799.

- Morgan RPC. 2001. A simple approach to soil loss prediction: a revised Morgan-Morgan-Finney model. *Catena* **44**: 305-322.
- Okoba BO, Hessel R, Sterk G. 2005. Farmers' estimates of soil erosion and crop yields compared with scientific assessments in the highlands of Kenya. *Agriculture, Ecosystems and Environment* **subm.**
- Okoba BO, Sterk G. 2005. Quantification of soil erosion indicators in Gikuuri catchment in the central highlands of Kenya. *Geoderma* **subm.**
- Okoth PF. 2003. A hierarchical method for soil erosion assessment and spatial risk modelling: a case study of Kiambu District in Kenya, Geo-informatiekunde en remote sensing, Wageningen, 213.
- Plotnick RE, Gardner RH, O'Neill RV. 1993. Lacunarity indices as measures of landscape texture. *Landscape Ecology* **8**: 201-211.
- Plotnick RE, Gardner RH, Hargrove WW, Prestegard K, Perlmutter M. 1996. Lacunarity analysis: a general technique for the analysis of spatial patterns. *Physical Review E* **53**: 5461-5468.
- Puigdefábregas J, Sanchez G. 1996. Geomorphological implications of vegetation patchiness on semi-arid slopes. *Advances on hillslope processes*, M. G. Anderson and S. M. Brooks, Eds., John Wiley & Sons, 1027-1060.
- Rejman J. 2003. Dynamics of erosion based on studies of different length plots. *25 Years of Assessment of Erosion. Proceedings of International Symposium, 22-26 September 2003*, D. Gabriels and W. Cornelis, Eds., Universiteit Gent, 255.
- Renschler CS, Harbor J. 2002. Soil erosion assessment tools from point to regional scales - the role of geomorphologists in land management research and implementation. *Geoderma* **47**: 189-209.
- Suryana N. 1997. A geo-information theoretical approach to inductive erosion modelling based on terrain mapping units, Geo-informatiekunde en remote sensing, Wageningen University.
- Swete Kelly DE, Gomez AA. 1998. Measuring erosion as a component of sustainability. *Soil erosion at multiple scales: principles and methods for assessing causes and impacts*, F. W. T. Penning de Vries, F. Agus, and J. Kerr, Eds., CAB Publishing, 133-148.
- Takken I, Jetten VG, Govers G, Nachtergaele J, Steegen A. 2001. The effect of tillage-induced roughness on runoff and erosion patterns. *Geomorphology* **37**: 1-14.
- Tenge AJ, Okoba BO, Sterk G. 2005. Application of participatory soil erosion mapping and financial analysis tools in soil and water conservation planning. Part 2: case study of Kwalei catchment in West Usambara Highlands, Tanzania. *Land degradation & development* **subm.**
- van Noordwijk M, van Roode M, McCallie EL, Lusiana B. 1998. Erosion and sedimentation as multiscale, fractal processes: implications for models, experiments and the real world. *Soil erosion at*

multiple scales: principles and methods for assessing causes and impacts, F. W. T. Penning de Vries, F. Agus, and J. Kerr, Eds., CAB Publishing, 390.

Vigiak O, Okoba BO, Sterk G, Groenenberg S. 2005a. Modelling catchment-scale erosion patterns in the East African Highlands. *Earth Surface Processes and Landforms* **30**: 183-196.

Vigiak O, Sterk G, Romanowicz RJ, Beven JK. 2005b. A semi-empirical model to assess uncertainty of spatial patterns of erosion. *Catena* **subm.**

Vigiak O, van Dijck SJE, van Loon EE, Stroosnijder L. 2005c. Matching hydrologic response to measured effective hydraulic conductivity. *Hydrological Processes* **subm.**

Vigiak O, Romanowicz RJ, van Loon EE, Sterk G, Beven JK. 2005d. A disaggregating approach to describe overland flow occurrence within a catchment. *Journal of Hydrology* **subm.**

Vigiak O, Okoba BO, Sterk G, Stroosnijder L. 2005e. Water erosion assessment using farmers' indicators in the West Usambara Mountains. *Catena* **subm.**

Wu XB, Thurow TL, Whisenant SG. 2000. Fragmentation and changes in hydrologic function of tiger bush landscapes, south-west Niger. *Journal of Ecology* **88**: 790-800.

Chapter 8

SUMMARY AND CONCLUSIONS

SUMMARY AND CONCLUSIONS

Watershed management requires prompt location of sources and sinks of sediment within a catchment. Pinpointing 'hot-spots' of erosion allows concentrating limited resources in the most effective way, and positive early results of Soil and Water Conservation (SWC) plans may gain the trust and participation of the land users. In this sense, the location of severely eroded areas within the catchment of intervention can be more important than the quantification of soil losses from the catchment.

Distributed erosion models can be valuable tools for watershed planning. However, the quality of spatially distributed model predictions is seriously hampered by the natural complexity and spatial heterogeneity of the landscape system, coupled with limited availability of spatio-temporal datasets of sufficient accuracy. In practice, the environmental data that are usually available contain information to characterize only the dominant processes active in a given system, which may then be described effectively by conceptual models. In this study, conceptual (semi-empirical) approaches were considered as a good compromise between explicit inclusion of dominant physical processes and limited availability of spatio-temporal data. The general objective was to improve the quality of spatially distributed predictions of erosion modelling in data scarce environments.

Most of the research fieldwork took place in Kwalei catchment (4°48' S, 38° 26'E), located in the West Usambara Mountains of Tanzania at an average altituded of 1500 m a.s.l. The catchment has an area of around 2 km², and is roughly triangular in shape. Terrain is rough and highly dissected, with one half of hillslopes > 20 %. Drainage comprises four permanent streams running from Northwest to Southeast. Mean annual rainfall is around 1000 mm, almost half of which falls during the long rainy season, from late February until late May. A shorter and less predictable rainy season occurs from October to January. Average daily temperature is 18 °C, with diurnal temperature ranges greater than annual ranges. Soils along the slopes are well-drained, with porous and sandy topsoil and clayey subsoils. In the valley bottom, soils are vertic and may be subject to saturation. The highest part of the catchment is covered by mountain rain forest, whereas the middle and lower slopes are used for agriculture. The catchment is intensely populated and over 90 % of the catchment population depends on agriculture. The average household land size ranges from 1.2 to 1.6 ha. Food crops, mainly maize inter-cropped with banana and bean, are cultivated on the upper slopes. A two-layer cultivation of banana and coffee is frequent on the steeper slopes along the stream incisions. Irrigated vegetables are the main cash crops and are cultivated in the valley bottoms and on the lower slopes. Soil erosion is one of the major constraints to agricultural production in the area and occurs especially at the onset of the rainy season, when storms are intense and soil cover is poor.

The empirical model proposed by Morgan, Morgan and Finney (MMF) was selected as a suitable base. The model retained a physical basis in the definition of the rate of sediment detachment by rainfall and by overland flow, and the rate of sediment transport capacity by overland flow. At the same time, the model had a simple structure and required a limited amount of input parameters, which made it practical for SWC purposes. The application at catchment-scale required the introduction of a mechanism to account for incoming run-on and outgoing run-off. When tested against field

observations, however, MMF spatial predictions were fair in Kwalei catchment. Model prediction errors consisted of overestimates of erosion rates along the streamlines and underestimates of erosion along the ridges. The main cause of prediction errors was the mechanism of overland flow accumulation, which ignored the possibility of reinfiltration of overland flow along the slopes that was instead observed in the field.

Correct modelling of the hydrology of a catchment is essential for correct prediction of erosion along the slopes. Spatially distributed modelling of overland flow requires the definition of Hydrologic Response Units, i.e. areas whose hydrologic behaviour can be considered homogeneous for the purposes of the model. Infiltration measurements may guide the definition of HRUs in terms of cartographic variables, such as topography, soil and land use. Three methods of point infiltration measurements were used to infer the spatial distribution of overland flow: the constant head method, the tension infiltration method and mini-rainfall simulation method. The statistical relationship between field measurements and cartographic variables (land use, soil and topography) yielded three different HRU scenarios. The actual spatial distribution of overland flow occurrence at the hillslope scale was observed with overland flow detectors. These are simple devices that indicate whether in a certain spot overland flow has occurred (yes or no) during a rainfall event. In March-May 2002, 50 detectors were placed on a small subcatchment in the North-Western part of Kwalei catchment, and were regularly monitored after each rainfall event. The frequency of overland flow occurrence was highly variable in space. The only spatial pattern of overland flow frequency that could be recognized in terms of cartographic variables was the limit between annual crops on the upper part of the slopes, where overland flow frequency was 48 %, and the coffee and banana stands on the footslopes, where overland flow frequency was 35 %. Geostatistic analysis of the data showed no spatial autocorrelation at distances longer than 40 m. From the observation of overland flow occurrence, two main Hydrologic Response Units (HRUs) could be defined: perennial versus annual crops. Differences in rainfall interception, soil properties, especially surface sealing and porosity, and soil management explained the relatively lower occurrence of overland flow observed under perennials than in annual crops. None of the HRU patterns inferred from infiltration measurements matched the observations. Point measurements failed to account for the soil macroporosity, and for hydrology processes other than infiltration, such as canopy interception.

In March-May 2003 the detectors were placed along two longitudinal transects placed in the middle and lower slopes of Kwalei catchment. These observations largely confirmed the conclusions of the previous season. In the catchment, overland flow may be triggered by short and intense showers, but as it moves downward, it quickly reinfiltrates. The average travel distance of overland flow before reinfiltration occurs is shorter when rainfall magnitude (intensity, amount and duration) is small, canopy interception is large, and the soil is rough, porous or dry.

A consequence of such a dynamic Hortonian hydrologic regime is that large part of the overland flow that is generated along the slopes, reinfiltrates and reaches the catchment outlet as subsurface storm flow. Hourly rainfall-discharge data at the catchment outlet were modelled through a Data Based Mechanistic model that (i) defined the effective rainfall, i.e. the amount of rainfall that generated a response at the outlet; and (ii) partitioned the water discharge at the outlet into slow flow, interpreted as

ground water displacement, and quick flow, interpreted as a combination of overland flow and subsurface storm flow. The observations of overland flow occurrence at the hillslope scale were used to derive HRU probability distribution functions of overland flow in relation to the maximum one-hour effective rainfall of the event. At small effective rainfall (< 0.15 mm) annual crops contributed more to discharge, whereas at large effective rainfall (> 0.15 mm), perennial crops contributed as much as annual crops to the water discharge. These rules allowed estimating the overland flow depth per HRU and per mm of effective rainfall. Reinfiltration was accounted for in the toposequence by assuming that only the overland flow generated in the lower part of the field could drain out of it. Thus, the amount of field run-off depended on rainfall characteristics (via effective rainfall), land use (via HRU), field topology (incoming run-on), field geometry (field lower border in relation to the field area), and on the reinfiltration length, i.e. the average travel distance of overland flow. Reinfiltration length was assessed from observation of contributing area of Gerlach troughs to be around 4 m. However, overland flow travel distance is likely to change with rainfall event characteristics, HRUs, local slope and soil surface conditions.

The hydrologic model was coupled with the sediment phase of the MMF model to build a semi-empirical catchment-scale model to predict the distribution of erosion for single events. Overland flow is the main vector of sediment across slopes. This function is modelled through the sediment transport capacity rate equation, which depends on overland flow volume and local slope. In the literature, the parameterisation of the transport capacity rate equation differs according to hydraulic regime of flow, soil characteristics, and scale of observation. Thus, the choice of these parameters is uncertain, but yield important consequences in the spatial distribution of erosion. The semi-empirical model was employed to assess the uncertainties of spatially distributed predictions due to sediment transport rate parameterisation by the Generalized Likelihood Uncertainty Estimation (GLUE) method. Model simulations were evaluated against the actual pattern observed with an extensive, qualitative erosion survey conducted from December 2002 till May 2003. The survey consisted of assessing erosion status in five qualitative classes, from very slightly eroded to very severely eroded, according to the presence and intensity of erosion features. The best model simulations were at short reinfiltration length (< 1.5 m) and with the ratio of overland flow power α and local topography power γ close to 0.5. Acceptable simulations predicted correctly around 75 % of erosion pattern; model overestimations of erosion occurred mainly in vegetable plots, whereas underestimations occurred in tea, sugarcane and grassland fields. Difficulties of the parameterisation of land use inputs were considered at the basis of the model errors. The uncertainty of model predictions due to sediment transport capacity was high: depending on the transport capacity parameters, around 10 % of the fields were attributed to either slight or severe erosion class.

Beside the semi-empirical model proposed in this thesis, several quantitative and qualitative erosion models were compared for their capability of locating erosion in the Kwalei catchment. Two qualitative models performed better than the more data-demanding quantitative models. In comparison with the distribution of erosion factors, the observed pattern of severely eroded areas was highly correlated to fields with crust cover > 60 % (c.c. 0.57), which in turn was correlated to vegetation cover. Thus, a

simple regression equation based on slope and ground cover was well correlated (c.c. 0.44) to the observed pattern of severely eroded areas.

Spatial patterns convey useful geographic information about landscape processes. In Kwalei catchment, lacunarity analysis showed that severely eroded areas were aggregated up to 40 m. This spatial scale was not matched by any of the other erosion models tested in the area. All models but one resulted in clumps of eroded areas larger than the observed one. The semi-empirical model developed in this thesis could locate almost all the areas, but failed to capture their extent. The spatial scale of severely eroded areas coincided with that of the overland flow pattern predicted by the hydrologic model at infiltration length of 0.5-5 m, despite the fact that the two patterns did not overlap (c.c. 0.10). Thus, in the Kwalei catchment, the location of severely eroded areas was correlated to crust and vegetation cover more than to slope, but the spatial extent of erosion depended upon the overland flow travel distance.

Gathering environmental information requires much time and financial resources, which often are not available. However, spatially relevant, even though qualitative, information can be obtained locally from the land users. In a Participatory Rural Appraisal exercise, the farmers of Kwalei catchment were asked to list indicators they use to assess erosion in the fields. The presence of these farmers' indicators of erosion was recorded at the same time of the qualitative erosion survey. Statistical relationship between the indicators and the class of erosion assessed by the expert showed that farmers' indicators could be distinguished in strong or weak indicators. Strong indicators, i.e. those that were recorded in more than 70 % of cases in severely eroded fields, were clearly associated with erosion intensity, whereas weak indicators were more indicative of soil degradation or soil erosion hazard than of erosion *sensu strictu*. Strong indicators and number of indicators were used to create a field erosion assessment tool in the form of a classification tree (Farmers' Indicators Tree, FIT), which was calibrated against half of the fields visited. The validation of the FIT model against the other half of the dataset yielded a Spearman rho coefficient of 0.81. The FIT model was the best in locating erosion within the catchment. Moreover, the spatial scale of the distribution of some strong indicators of erosion was very close to that of eroded areas and overland flow distribution. These findings open up possibilities to integrate more effectively farmers' knowledge into hydrologic and erosion distributed modelling.

SAMENVATTING EN CONCLUSIES

Beheer van stroomgebieden vereist precieze locatie van de plekken waar bodemdeeltjes verdwijnen waar deze als sediment afgezet worden binnen het stroomgebied. Het localiseren van zogenaamde hot-spots van erosie leidt tot een effectief en geconcentreerd gebruik van beperkte middelen voor erosiebestrijding. Hierdoor leiden Bodem- en Water Conservering (BWC) plannen snel tot positieve resultaten waardoor het vertrouwen en de deelname van de landgebruikers bevordert wordt. De localisering van ernstig geërodeerde plekken binnen het stroomgebied kan belangrijker zijn dan de kwantificering van bodemverliezen uit het stroomgebied als geheel.

Ruimtelijke erosie modellen kunnen waardevolle instrumenten zijn voor de planvorming m.b.t. de inrichting van een stroomgebied. Maar de natuurlijke complexiteit en ruimtelijke heterogeniteit van het landschap, gekoppeld aan de beperkte beschikbaarheid van nauwkeurige ruimtelijke en temporele datasets, belemmeren de kwaliteit van de voorspellingen van ruimtelijke modellen. In de praktijk blijken de reeds beschikbare gegevens over het milieu de dominante actieve processen in het systeem al te kunnen karakteriseren. Deze processen kunnen vervolgens effectief beschreven worden door conceptuele modellen. In deze studie zijn zulke conceptuele (semi-empirische) benaderingen toegepast, omdat ze een goede tussenweg vormen om zowel met de dominante fysische processen als ook met de beperkte beschikbaarheid van ruimtelijke en temporele gegevens rekening te kunnen houden. De algemene doelstelling van deze studie was om, voor omstandigheden met beperkt beschikbare gegevens, de kwaliteit van ruimtelijke voorspellingen van erosie te verbeteren.

Het veldwerk vond voornamelijk plaats in het Kwalei stroomgebied, gelegen in de westelijke Usambara bergen van Tanzania, op een hoogte van 1500 meter boven zeeniveau. Het stroomgebied omvat ongeveer 2 km², en vormt ruwweg een driehoek. Het terrein is bergachtig, met de helft van de hellingen steiler dan 20%. De drainage van het stroomgebied wordt bepaald door vier permanente beken, die van noordwest naar zuidoost lopen. Jaarlijkse neerslag is ongeveer 1000 mm, waarvan de helft gedurende het lange regenseizoen (eind februari tot eind mei) valt. Een korter en moeilijk voorspelbaar regenseizoen vindt plaats van oktober tot januari. De gemiddelde dagtemperatuur is 18 °C; de temperatuurfluctuaties gedurende een etmaal zijn groter dan die gedurende het jaar. De bodems op de hellingen zijn goed gedraineerd, en bestaan uit een poreuze en zandige bovenlaag en een kleiige onderlaag. De bodems in de vallei zijn kleiig, en kunnen verzadigd raken. Het hoogst gelegen deel van het stroomgebied is bedekt met bos, en in de lagere delen vindt landbouw plaats. Het stroomgebied is dicht bevolkt, en 90% van de inwoners is afhankelijk van de landbouw. Gemiddeld heeft een huishouden 1.2 tot 1.6 ha land tot zijn beschikking. Voedselgewassen, voornamelijk maïs gecombineerd met banaan en bonen, worden op het hoger gelegen deel van de hellingen verbouwd. De combinatieteelt banaan en koffie is te vinden op de steilere hellingen naast diep ingesneden beken. Geïrrigeerde groente is het belangrijkste commerciële gewas en wordt verbouwd in de vallei en op de laaggelegen hellingen. Bodemerosie is één van grootste beperkingen van de landbouwproductie in het gebied, en gebeurt vooral aan het begin van het regenseizoen wanneer de regenintensiteit hoog is en de grondbedekking gering.

Het empirische model ontwikkeld door Morgan, Morgan en Finney (MMF) werd als geschikt uitgangspunt geselecteerd. De berekeningen in het model voor wat betreft de sedimentatie, veroorzaakt door neerslag en afstromend oppervlaktewater, en het sedimenttransportcapaciteit door afstromend oppervlaktewater, zijn gebaseerd op fysische formules. Het model heeft een eenvoudige structuur en er hoeft slechts een beperkte hoeveelheid aan parameters ingevoerd te worden, wat het geschikt maakt voor BWC doeleinden. De toepassing van het model op de schaal van een stroomgebied vereist de invoering van een mechanisme dat rekening houdt met (binnenkomend) instromend en (uitgaand) afstromend oppervlaktewater. Na toetsing met veldobservaties, blijken de ruimtelijke voorspellingen van het MMF model matig te zijn voor het Kwalei stroomgebied. Fouten in de modeluitkomsten waren voornamelijk te hoog geschatte erosie langs de beken en te laag geschatte erosie op de bergkammen. De belangrijkste oorzaak van deze fouten was het gemodelleerde mechanisme van accumulatie van afstromend oppervlaktewater wat geen rekening hield met de mogelijkheid dat afstromend oppervlaktewater lager op de helling kan infiltreren, een fenomeen wat wel waargenomen werd in het veld.

Om erosie langs de helling te kunnen voorspellen, is correcte modellering van de hydrologie essentieel. Hydrologische Respons Eenheden (HRE), gebieden waar hydrologisch gedrag homogeen is voor wat betreft de toepassing van het model, moeten bepaald worden om de ruimtelijke spreiding van afstromend oppervlaktewater te kunnen modelleren. Infiltratie metingen, gerelateerd met cartografische variabelen zoals topografie, bodem en landgebruik, kunnen nuttig zijn om HRE's te bepalen. Drie soorten infiltratiemetingen zijn gebruikt voor het bepalen van de ruimtelijke spreiding van afstromend oppervlaktewater: de 'konstante drukhoogte' methode, de 'infiltratie onder zuigspanning' methode, en de 'mini-regenvalsimulator' methode. De statistische relaties tussen de metingen en de cartografische variabelen (landgebruik, bodem en topografie) resulteerden in drie verschillende HRE scenario's.

De feitelijke ruimtelijke spreiding van afstromend oppervlaktewater werd gemeten met afstromingsdetectoren, die van boven naar beneden op een helling geplaatst werden. Deze detectoren zijn simpele instrumenten waarmee gecontroleerd kan worden of er gedurende een regenbui wel of niet afstroming heeft plaatsgevonden op de plek waar de detector is geplaatst. In de periode van maart tot mei 2002 zijn 50 detectoren geplaatst in een deelstroomgebied in het noordwesten van het Kwalei stroomgebied, en deze werden na elke regenbui gecontroleerd. De frequentie van afstromend oppervlaktewater was erg variabel in de ruimte. Het enige ruimtelijke patroon voor afstromend oppervlaktewater dat kon worden gerelateerd aan de cartografische variabelen, was de grens tussen het hoger gelegen deel van de hellingen met éénjarige gewassen (met een frequentie van afstromend oppervlaktewater van 48%), en het lager gelegen deel van de hellingen met de koffie en bananen plantages (met een frequentie van afstromend oppervlaktewater van 35%). Geo-statistische analyse gaf aan dat er geen ruimtelijke autocorrelatie bestond voor afstanden groter dan 40 meter. Verschillen in regenval interceptie, bodemeigenschappen (zoals het dichtslaan of verslempen van de bodem en de porositeit), en bodembeheer verklaren de relatieve lagere frequentie van geobserveerde afstromend oppervlaktewater onder meerjarige gewassen dan onder éénjarige gewassen. Geen van de, met infiltratiemetingen bepaalde, HRE patronen kwam overeen met de observaties. Puntmetingen slagen er

niet in om rekening te houden met de macro-porositeit van de bodem, en met hydrologische processen anders dan infiltratie, zoals de interceptie van neerslag door het bladerdek.

In de periode van maart tot mei in 2003 werden de detectoren langs twee transecten in het Kwalei stroomgebied geplaatst. De observaties bevestigden grotendeels de resultaten van het voorgaande regenseizoen. In het stroomgebied wordt afstroming veroorzaakt door korte en intensieve buien, maar afstromend water kan alsnog in lager gelegen gebieden infiltreren. De gemiddelde afstand welke door het afstromend oppervlaktewater afgelegd wordt voordat het her-infiltreert, is korter wanneer de neerslag (intensiteit, hoeveelheid en duur) lager is, de interceptie door het bladerdek groter, en de bodem ruwer, poreuzer en droger is.

Als gevolg van dit dynamische Hortonisch hydrologisch regiem, her-infiltreert het grootste deel van het afstromende oppervlaktewater dat langs de helling wordt gegenereerd. Na infiltratie vindt snelle laterale ondergrondse stroming plaats welke uiteindelijk de uitlaat van het stroomgebied bereikt. Het afvoerdebiet aan de uitlaat wordt gemodelleerd aan de hand van een mechanistisch model dat (i) de effectieve neerslag definieert, dat is, de hoeveelheid neerslag wat werkelijk afvoer in de uitlaat veroorzaakt; en (ii) de afvoer aan de uitlaat onderverdeelt in een langzame afvoer, geïnterpreteerd als grondwaterverplaatsing, en een snelle afvoer, geïnterpreteerd als een combinatie van afstromend oppervlaktewater en snelle ondergrondse stroming.

De observaties van regenbuien met afstromend oppervlaktewater, die op de schaal van een helling waren gemeten, werden gebruikt voor het afleiden van HRE kansverdelingfuncties van afstromend oppervlaktewater in relatie tot de maximale effectieve regenval per uur van een regenbui. Eénjarige gewassen dragen meer bij aan de afvoer bij lage effectieve regenval (< 0.15 mm), terwijl bij hogere effectieve regenval (> 0.15 mm) meerjarige gewassen evenveel bijdroegen als de éénjarige gewassen. Deze regel gaf de mogelijkheid om de dikte van de laag van afstromend oppervlaktewater per HRE en per mm effectieve neerslag te meten. In de topo-sequentie werd rekening gehouden met her-infiltratie door te veronderstellen dat alleen afstromend oppervlaktewater, gegenereerd in het laagste deel van het veld, weg kon stromen. De hoeveelheid afstromend water van een veld was afhankelijk van neerslagkarakteristieken (effectieve neerslag), landgebruik (HRE), veld topologie (binnenstromend regenwater), veldgeometrie (locatie van de laagst gelegen grens van het veld in relatie tot de oppervlakte van het veld) en de infiltratielengte, dat is, de gemiddelde 'reisafstand' van afstromend oppervlaktewater. De infiltratielengte werd bepaald aan de hand van observaties met Gerlach opvangbakken, die aangaven dat de lengte ongeveer 4 meter is. Maar ook de reisafstand van afstromend oppervlaktewater is afhankelijk van regenkarakteristieken, HRE, helling en de condities van de bovenste bodemlaag.

Het ontwikkelde hydrologisch model werd gekoppeld aan de erosiecomponent van het MMF model om een semi-empirisch model te bouwen voor de spreiding van erosie per regenbui op de schaal van een stroomgebied. Afstromend oppervlaktewater is de belangrijkste factor voor sedimenttransport langs de helling. Dit is gemodelleerd met een vergelijking voor transportcapaciteit van het sediment, welke afhangt van het volume van het afstromende oppervlaktewater en de lokale helling. In de literatuur verschillen de parameters voor de vergelijking voor de transportcapaciteit per stroomingstype, per bodem, en hangen af van de schaal van observatie. Met andere woorden, de keus van deze parameters

is onzeker, maar heeft belangrijke consequenties voor de resultaten wat betreft de ruimtelijke spreiding van erosie. Het ontwikkelde semi-empirische model is gebruikt om de onzekerheden in de ruimtelijke voorspellingen veroorzaakt door de keuze van de parameters voor de sedimenttransportcapaciteit, met behulp van de Generalized Likelihood Uncertainty Estimation (GLUE) methode te bepalen. Aan de hand van een uitgebreide kwalitatieve erosiekartering, uitgevoerd tussen december 2002 en mei 2003, is het werkelijke erosiepatroon waargenomen, waarmee de modelsimulaties zijn geëvalueerd. Deze kartering bestond uit het vaststellen van de erosietoestand, onderverdeeld in vijf kwalitatieve klassen variërende van erg licht geërodeerd tot zeer zwaar geërodeerd. Hierbij werd gekeken naar de aanwezigheid en intensiteit van erosie kenmerken. Model simulaties presteerden het beste voor een korte her-infiltratielengte (<1.5 m) en met de verhouding tussen de macht α voor afstromend oppervlaktewater en de macht γ voor de lokale topografie in de buurt van 0.5. Simulaties voorspelden ongeveer 75% van de erosie patroon juist. Voor de groentevelden waren de schattingen van erosie door het model te hoog, terwijl te lage hoeveelheden geschat werden voor velden met thee, suikerriet en gras. De fouten in het model worden veroorzaakt doordat de parameters voor het landgebruik moeilijk te bepalen zijn. De onzekerheid van de modeluitkomsten op basis van de sedimenttransportcapaciteit was groot: afhankelijk van welke parameters voor transportcapaciteit werden geselecteerd, werden ongeveer 10% van de velden toebedeeld aan of de lichte of de zwaar geërodeerde klasse.

Naast het semi-empirische model, zoals voorgesteld in deze dissertatie, werden verscheidene kwantitatieve en kwalitatieve erosiemodellen vergeleken op hun capaciteit om erosie in het Kwalei stroomgebied te lokaliseren. Twee kwalitatieve modellen presteerden beter dan de kwantitatieve modellen die veel inputgegevens vereisen. Van de spreiding van alle erosie factoren, was het geobserveerde patroon van zwaar geërodeerde plekken het sterkst gecorreleerd met velden met een korstbedekking hoger dan 60 % (c.c. 0.57), wat weer correleert met de vegetatiebedekking. Een simpele regressievergelijking gebaseerd op helling en bodembedekking was goed gecorreleerd (c.c. 0.44) met het geobserveerde patroon van de zwaar geërodeerde gebieden.

Ruimtelijke patronen bevatten nuttige geografische informatie over landschapsprocessen. Lacunaire analyse (lacunarity analysis) toonde aan dat zwaar geërodeerde gebieden tot eenheden van 40 meter bijeengevoegd kunnen worden in het Kwalei stroomgebied. Deze ruimtelijke schaal kwam niet overeen met de erosiemodellen die voor dit gebied getest werden. Op één na, resulteerden alle modellen in clusters van geërodeerde gebieden die groter waren dan de geobserveerde gebieden. Het ontwikkelde semi-empirische model kon bijna alle gebieden lokaliseren, maar faalde in het vaststellen van de afmetingen ervan. De ruimtelijke schaal van de zwaar geërodeerde gebieden kwam overeen met het door het hydrologische model voorspelde patroon van het afstromende oppervlaktewater voor een her-infiltratielengte tussen de 0.5 en 5 meter, ondanks dat de twee patronen niet met elkaar overlappen (c.c. 0.10). Dus, de locatie van zwaar geërodeerde gebieden was sterker gecorreleerd met de korst en vegetatiebedekking dan met de helling, maar de ruimtelijke dimensie van erosie was afhankelijk van de reisafstand van het afstromend oppervlaktewater.

Het verzamelen van informatie van de natuurlijke omgeving vraagt veel tijd en geld, welke vaak niet beschikbaar zijn. Maar ruimtelijk relevante informatie, hoewel kwalitatief, kan bij de landgebruikers verkregen worden. Gebruik makend van participatieve methodes, werden de boeren in het Kwalei

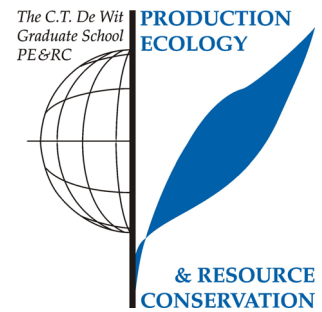
stroomgebied gevraagd om indicatoren te benoemen, die zij gebruiken voor het vaststellen van erosie in hun velden. Deze boerenindicatoren voor erosie werden tegelijkertijd met de kwalitatieve erosiekartering vastgelegd. Statistische relaties tussen deze indicatoren en de erosieklassen gedefinieerd door experts toonden aan dat de boerenindicatoren konden worden opgedeeld in sterke en zwakke indicatoren. Sterke indicatoren, welke aan meer dan 70% van de zwaar geërodeerde gebieden werden toebedeeld, waren duidelijk geassocieerd met erosie-intensiteit, terwijl de zwakke indicatoren aangaven welke gebieden vatbaar waren voor bodemdegradatie of bodemerosie maar waar erosie niet noodzakelijk ook daadwerkelijk plaatsvond. Er is een instrument, in de vorm van een classificatie boom (Farmers' Indicators Tree, FIT), voor erosie-evaluatie op veldschaal ontworpen dat gebruik maakt van de aanwezigheid en de hoeveelheid van de sterke indicatoren. Dit instrument isgeijkt met gegevens van de helft van de bezochte velden. De validatie van het FIT model gebeurde met gegevens van de andere helft van de velden, en gaf een Spearman rho coefficient van 0.81. Het FIT model presteerde het beste in de lokalisering van erosie binnen het stroomgebied. Bovendien kwam de schaal van de ruimtelijke spreiding van sommige sterke indicatoren redelijk overeen met de schaal van de geërodeerde gebieden en van het afstromende oppervlaktewater. Deze resultaten creëren mogelijkheden om op effectievere wijze boerenkennis te integreren met ruimtelijke hydrologische en erosiemodellen.

Curriculum vitae

Olga Vigiak was born in Vercelli, Italy, on the 8th of April 1971. After finishing her Secondary School studies in her hometown, in 1990 she moved to Florence to attend the course in Tropical and Subtropical Agricultural Sciences (Scienze Agrarie Tropicali e Subtropicali), during which she visited Tunisia and Eritrea. She graduated cum laude in 1996 discussing her thesis on the evaluation of soil degradation processes active in the Eritrean Highlands. After graduating, she returned to Vercelli, where she started working as a ranger in a regional park. In the meantime, she attended the post-graduate course in Rural development and co-operation in Developing Countries, at the University of Padua (Italy). From 1998 to 2000, she attended the MSc course in Soil and Water, Erosion and Soil and Water Conservation specialisation, at Wageningen University, The Netherlands. Her MSc thesis work focused on a Geographic Information System application to model the reduction of wind speed by windbreaks in East Anglia, U.K, in collaboration with the University College of London. Her work was awarded as best MSc dissertation in Land and Water subjects (scriptieprijs Land en watergebruik 2000). In 2000, she started her PhD at the Erosion and Soil and Water Conservation Group of Wageningen University on spatially distributed water erosion modelling in the West Usambara Mountains of Tanzania. In 2004 she was awarded the Storm-van der Chijs stipend, which she spent visiting the World Agroforestry Centre (ICRAF) activities in Western Kenya. In the near future, she will move to Lao PDR for a post-doc fellowship offered by the International Water Management Institute (IWMI) on landscape ecology in the upper catchments of the Mekong river. The research will focus on the effect of riverside vegetation on reducing the sediment delivery ratio to the river and improving the water quality of the river.

PE&RC PhD Education Statement Form

With the educational activities listed below the PhD candidate has complied with the educational requirements set by the C.T. de Wit Graduate School for Production Ecology and Resource Conservation (PE&RC) which comprises of a minimum total of 32 ECTS (= 22 weeks of activities)



Review of literature (ECTS 4)

- Methodology development of catchment-scale erosion modelling

Writing of project proposal (ECTS 5)

- Methodology development of catchment-scale erosion modelling

Post-Graduate Courses (ECTS 5)

- Spatial modelling in ecology (2002)
- Wind and water erosion: modelling and measurements (2003)
- FORM_OSE Living with hydro-geological risk: from theory to practice (2004)
- Multivariate analysis (2004)

Deficiency, Refresh, Brush-up and General Courses (ECTS 2)

- Scientific writing (2001)
- Career orientation for PhD students (2004)

PhD discussion groups (ECTS 5)

- Sustainable land use and resource management (2001-2004)
- Statistics, maths and modelling in production ecology and resource conservation (2001-2004)

PE&RC annual meetings, seminars and introduction days (ECTS 1.5)

- Methodology and technology seminars (2001)
- Seminar Kalman filtering and data assimilation (2001)
- International workshop in catchment-scale hydrological modelling and data assimilation (2001)
- ASA-SSA workshop 'The use of risk assessment tools in comprehensive nutrient management plan (CNMP) development (2004)

International symposia, workshops and conferences (ECTS 3)

- COST 623 Soil erosion patterns: evolution, spatio-temporal dynamics and connectivity (ESSC, Muncheberg, 2002)
- International symposium 25 years of assessment of erosion (Ghent University, 2003)
- ASA-CSSA-SSSA Meeting (Seattle, USA, 2004)

Laboratory training and working visits (ECTS 2)

- Lancaster University. Hydrological modelling (2003)
- Indian Institute for Remote Sensing. Erosion assessment with remote sensing in Hymalayan range (2004)